
THE UNIVERSITY *of* EDINBURGH

# Role for *Gli3* in the formation of the major axonal tracts in the telencephalon

Dario Magnani

Thesis submitted for the degree of doctor of philosophy at the

University of Edinburgh

2009

*...e chi ha avuto, ha avuto, e chi ha rat, ha rat*

## Disclaimer

I (Dario Magnani) performed all of the experiments presented in this thesis unless otherwise clearly stated in the text. No part o this work has been or is being submitted for any other degree of qualification.

Signed:

Date:

## Acknowledgements

I would like to thank my supervisors Thomas Theil and David Price for their precious guidance and help throughout the course of my PhD studies.

I am also thankful in particularly to Chris Conway, Vassiliki Fotaki, Kerstin Hasenpusch-Theil, Hayden Selvadurai, Melanie White, Arianna Rinaldi for their comments on my scientific work, especially during process of writing up this thesis.

Kerstin Hasenpusch-Theil, Vassiliki Fotaki, Chris Conway, (K, V and C: hey guys I am thanking you twice… but 100 times would not be enough!), Osmany Larralde-Diaz, Tom Pratt, Petrina Georgala, Martine Manuel, Natasha Tian, Katy Gillies, Mark Barnett, Sally Till, Lasani Wijetunge, Aoife MacMahon and Alison Murray for helping me, not only offering their time in the lab, but also in the every days hard life of a PhD student. Thank you also to John Mason, Peter Kind and Norah Spears for their help and guidance in several aspects of the lab life. Trudi Gillespie helped a lot with confocal imaging. Tom Pratt kindly provided me with the *τ-GFP* animals, and Erin C. Jacobs and Anthony T. Campagnoni with the *Golli τ-GFP* animals.

A big thank you goes to Manuel Valiente Cortés, Oscar Marín Parra and Guillermina López Bendito for teaching me the slice culture technique and for several useful advises on my research (and also for the nice break in the sunny Spain).

Finally, obviously, thank you to my father Enzo and my mother Tania… but no words would be able to describe my gratitude to them (especially because they do not

understand English!), and to my sister Irene. Also, thank you to Sophie, her support has been *incroyable*… and I hope she will continue in “helping” for long time.

# Table of contents

**Disclaimer** ..... **3**
**Acknowledgements** ..... **4**
**Table of contents** ..... **6**
**Abstract** ..... **9**
**Abbreviations** ..... **12**
**Chapter 1: Introduction** ..... **14**
1.1 First anatomical subdivisions in early telencephalic development ..... 15
1.2 Three signalling centres control the regionalization process in the telencephalon ..... 20
1.3 Several transcription factors are involved in patterning the different telencephalic regions ..... 26
1.4 Cellular and molecular mechanisms in the development of ventral telencephalon ..... 30
1.5 Cellular and molecular mechanisms in the development of the cerebral cortex ..... 35
1.6 Development of the corpus callosum ..... 38
1.7 Formation of the corticothalamic and thalamocortical tracts ..... 43
1.8 *Gli3* is a key regulator of forebrain development ..... 53
1.9 Different *Gli3* mutations cause several human syndromes ..... 53
1.10 Different mouse models are available for the study of *Gli3 in vivo* ..... 56
1.11 *Gli3* in forebrain development ..... 59
1.12 Gli3 is involved in the Shh signalling pathway ..... 62
1.13 *Gli3* and *Shh* counteract each other in patterning the ventral telencephalon ..... 65
**1.14 Aims of the thesis** ..... **67**
**Chapter 2: Materials and Methods** ..... **69**
2.1 Animals ..... 69
2.1.1 Animal husbandry ..... 69
2.1.2 Preparation of embryos ..... 69
2.1.3 Brain/heads preparation ..... 70
2.2 PCR ..... 71
2.2.1 Mouse genotyping ..... 71
2.2.2 Quantitative RT-PCR ..... 73
2.3 Histology ..... 75
2.3.1 Cresyl violet staining ..... 75

2.3.2 Immunofluorescence on vibratome sections ... 75
2.3.3 Immunofluorescence on cryostat-sections ... 77
2.3.4 Imunohistochemistry on wax sections ... 78
2.3.5 In situ hybridization on wax sections ... 79
2.3.5.1 Generation of DIG-labelled riboprobes ... 79
2.3.5.2 In situ Hybridisation ... 81
2.3.6 BrdU and IdU-labelling of S-phase nuclei for cell cycle kinetic analysis ... 82
2.3.7 Enumeration of BrdU- and IdU-labelled nuclei for cell cycle kinetic analysis ... 82
2.3.8 Statistical analyses and graph plotting ... 83
2.4 Microscopy ... 83
2.4.1 Light microscopy ... 83
2.4.2 Fluorescence microscopy ... 83
2.5 Axon tracing with DiI and/or DiA ... 84
2.6 Organotypic co-cultures ... 85
**Chapter 3: Axon guidance defects in the forebrain of Pdn mutants ... 88**
**3.1 Introduction ... 88**
3.2 Cresyl violet and NF stainings reveal defects in the major axonal tracts in newborn *Pdn/Pdn* mutant brains ... 90
3.3 DiI injections in newborn brains show absence of the corpus callosum and guidance mistakes in thalamocortical and corticothalamic tracts of *Pdn/Pdn* mutants ... 98
3.4 DiI injections and NF staining reveal guidance mistakes at early stages of thalamocortical and corticothalamic tract development in *Pdn/Pdn* mutant brains ... 107
3.5 Pdn/Pdn Golli tau-GFP mice display guidance mistakes in early projecting corticothalamic axons ... 113
**3.6 Discussion ... 126**
**Chapter 4: The *Pdn* ventral telencephalon fails to guide thalamic axons towards the cortex ... 135**
**4.1 Introduction ... 135**
4.2 *Gli3* expression pattern in the developing forebrain ... 137
4.3 The *Pdn* mutation does not alter the molecular identity of different thalamic territories at early phases of diencephalic patterning ... 141
4.4 The formation of the *Isl1*$^{+}$ permissive corridor is affected in the *Pdn/Pdn* ventral telencephalon ... 147
4.5 *Pdn/Pdn* ventral telencephalon is not able to guide thalamocortical axons towards the developing cortex ... 155
**4.6 Discussion ... 162**

**Chapter 5: Patterning defects in *Pdn* mutants correlate with the failure of corticofugal axons to enter the ventral telencephalon ..... 169**

**5.1 Introduction ..... 169**

5.2 Cortical lamination is not affected in newborn *Pdn/Pdn* mutant brains ..... 171

5.3 LGE pioneer neurons are missing in the *Pdn/Pdn* ventral telencephalon ..... 175

5.4 The *Pdn/Pdn* ventral telencephalon displays regionalization defects within the ventral telencephalon and at the PSPB at early stages of brain development ..... 178

5.5 The *Pdn/Pdn* LGE displays a reduced number of neurons and an elongation of the S phase and of the cell cycle at E10.5 ..... 188

5.6 *Shh* signalling is up-regulated within the ventral telencephalon of *Pdn/Pdn* mutants at early stages of brain development ..... 202

**5.7 Discussion ..... 209**

5.7.1 Cortical layer specification is not affected in *Pdn* mutants ..... 210

5.7.2 *Gli3* counteracts *Shh* expression and Shh signalling in the ventral telencephalon ..... 212

5.7.3 The *Pdn* mutation causes regionalization defects in the ventral telencephalon and at the PSPB ..... 215

5.7.4 *Pdn* mutation causes growth defects in ventral telencephalon ..... 218

5.7.5 LGE pioneer neurons defects may be causing thalamocortical tract abnormalities in *Pdn/Pdn* brains ..... 221

**Chapter 6: General discussion and future work ..... 225**

6.1 The *Pdn* mutation does not result in severe defects in the developing cortex and thalamus ..... 225

6.2 Ventral telencephalic patterning defects in *Pdn* mutants correlate with defects of LGE pioneer neurons, and failure of cortical axons in entering the ventral telencephalon ..... 228

6.3 Thalamocortical tract defects in *Pdn* mutants are caused by abnormalities in ventral telencephalic guidance cues ..... 233

**6.4 Synopsis ..... 239**

**Bibliography ..... 243**

# Abstract

In the adult brain, the thalamocortical tract conveys sensory information from the external environment to the cortex. The cortex analyzes and integrates this information and sends neural responses back to the thalamus through the corticothalamic tract. To reach their final target both thalamocortical and corticothalamic axons have to cover long distances during embryogenesis, changing direction several times and passing through different brain territories. The ventral telencephalon plays a major role in the early development of these tracts. At least three main axon guidance mechanisms act in the ventral telencephalon. First, two different populations of pioneer neurons in the lateral ganglionic eminence (LGE) (LGE pioneer neurons) and medial ganglionic eminence (MGE) (MGE pioneer neurons) provide scaffolds which allow growing corticothalamic and thalamocortical axons to cross the pallium sub pallium boundary (PSPB) and the diencephalic telencephalic boundary (DTB), respectively. Second, the ventral telencephalon forms a permissive corridor for thalamic axons by tangential migration of *Isl1* and *Ebf1* expressing cells from the LGE into the MGE. Finally, thalamortical and corticothalamic axons guide each other once they have met in the ventral telencephalon ("handshake hypothesis").

The *Gli3* transcription factor has been shown to be essential for normal early embryonic regionalization of the mammalian forebrain, although roles of *Gli3* in later aspects of forebrain development, like the formation of axonal connections, have not been

investigated previously. Here, I present the analysis of axonal tract development in the forebrain of the *Gli3* hypomorphic mutant mouse *Polydactyly Nagoja (Pdn)*. These animals lack the major axonal commissures of the forebrain: the corpus callosum, the hippocampal commissure, the anterior commissure and the fimbria. In addition, DiI injections and neurofilament (NF) staining showed defects in the formation of the corticothalamic and thalamocortical tracts. Although the *Pdn/Pdn* cortex forms early coticofugal neurons and their axons, these axons do not penetrate the LGE and instead run along the PSPB. Later in development, although a thick bundle of *Pdn/Pdn* cortical axons is still observed to project along the PSPB, some *Pdn/Pdn* cortical axons eventually enter the ventral telencephalon navigating along several abnormal routes until they reach thalamic regions. In contrast, *Pdn/Pdn* thalamic axons penetrate into the ventral telencephalon at early stages of thalamic tract development. However, rostrally they deviate from their normal trajectory, leaving the internal capsule prematurely and only few of them reach the developing cortex. Caudally, an ectopic *Pdn/Pdn* dorsal thalamic axon tract projects ventrally in the ventral telencephalon not entering the internal capsule at all. These defects are still observed in newborn *Pdn/Pdn* mutant mice.

Next, I investigated the developmental mechanisms causing these pathfindings defects. No obvious defects are present in *Pdn/Pdn* cortical laminae formation and in the patterning of the *Pdn/Pdn* dorsal thalamus. In addition, *Pdn/Pdn* thalamocortical axons are able to respond to ventral telencephalic guidance cues when transplanted into wild type brain sections. However, these axonal pathfinding defects correlate with patterning defects of the *Pdn/Pdn* LGE. This region is partially ventralized and displays a reduction in the number of postmitotic neurons in the mantle zone due to an elongated cell cycle

length of LGE progenitor cells. Finally, *Pdn/Pdn* mutant display an upregulation of *Shh* expression and Shh signalling in the ventral telencephalon. Interestingly, these patterning defects lead to the absence of DiI back-labelled LGE pioneer neurons, which correlates with the failure of corticothalamic axons to penetrate the ventral telencephalon. In addition, ventral telencephalic thalamocortical guidance mistakes happen at the same time of abnormal formation of the corridor cells.

Taken together these data reveal a novel role for *Gli3* in the formation of ventral telencephalic intermediate cues important for the development of the thalamocortical and corticothalamic connections. Indeed, *Pdn* animals are the first known mutants with defective development of the LGE pioneer neurons, and their study provides a link between early patterning defects and axon pathfinding in the developing telencephalon.

# Abbreviations

**ANR** -- anterior neural ridge

**AC** -- anterior commissure

**CC** -- corpus callosum

**CgC** -- cingulated cortex

**CGE** -- caudal ganglionic eminence

**Cp** -- choroid plexus

**CR** -- Cajal-Retzius cells

**Ctx** -- cortex

**DG** -- dentate gyrus

**dLGN** -- dorsal lateral geniculate nucleus

**dt** -- dorsal thalamus

**DTB** -- diencephalic telencephalic boundary

**dTH** -- dorsal thalamus

**f** -- fornix

**fi** -- fimbria

**GP** -- globus pallidus

**GW** -- glia wedge

**HC** -- hippocampal commissure

**hem** -- cortical hem

**hip** -- hippocampus

**ht** -- hypothalamus

**ic** -- internal capsule

**IGG** -- indusium griseum

**iz** -- intermediate zona

**LGE** -- lateral ganglionic eminence

**LV** -- lateral ventricol

**MGE** -- medial ganglionic eminence

**MZG** -- midline zipper glia

**Ncx** -- neocortex

**opt** -- optic tract

**Pb** -- probst bundle

**PFP** -- perforating pathway

**PoA** -- preoptic area

**PSPB** -- pallium subpallium boundary

**Str** -- striatum

**TH** -- dorsal thalamus

**VB** -- ventral basal

**vt** -- ventral telencephalon

# Chapter 1: Introduction

The embryonic telencephalon gives rise to the cerebral cortex, the hippocampus and the basal ganglia. It is within these structures that conscious thought takes place in human beings. Telencephalic function is dependent on the interconnections of different telencephalic structures, such as the olfactory bulbs and the two cortical hemispheres and on its connection with other brain structures, such as the thalamus and the hypothalamus. Thanks to these connections, these different structures work together as one, collecting and transmitting sensory information, integrating and memorising them, creating behavioural responses. Despite its functional complexity in adulthood, the basic organization of the CNS is remarkably conserved when compared with other vertebrates. This conservation validates the use of a wide range of organisms from frogs to chickens and mice to study the mechanisms underlying CNS development.

Insight into the developmental mechanisms underlying forebrain development may also help in the molecular and cellular understanding of several developmental, congenital and neurodegenerative disorders affecting a number of human beings with devastating consequences. The use of model organisms is essential to this purpose and it may help to design new strategies for the prevention and treatment of neurological disorders. In addition it could also help to better comprehend how complicated neural networks develop and work.

## 1.1 First anatomical subdivisions in early telencephalic development

During vertebrate embryonic development the brain originates from the rostral part of the neural tube. In the first embryonic brain partition, the rostral part of the neural tube divides into three brain vesicles: the forebrain, the midbrain and the hindbrain. Afterwards these three primary vesicles will further subdivide: the forebrain will give rise to the telencephalon and the diencephalon, the hindbrain to the metencephalon and the myelencephalon. The midbrain will become the mesencephalon without any further subdivision. The telencephalic primordium is specified in mouse approximately at E8.5.

The first division to happen within the telencephalon is between the dorsal and the ventral telencephalon. The dorsal region of the telencephalon gives rise to the pallium or dorsal telencephalon, while the ventral region generates the sub-pallium or ventral telencephalon. The pallium eventually forms the neocortex from its anterior and lateral regions, while from its posterior and medial region the hippocampus, the cortical hem and the choroid plexus will develop. The subpallium instead is further subdivided into the medial ganglionic eminence (MGE), derived from its medial domain, and into the lateral and caudal ganglionic eminences (LGE and CGE), derived form its lateral and posterior regions and the anterior entopeduncular area/preoptic area (AEP/POa), derived from its ventromedial regions (Fig 1.1).

The following sections will describe how the main signalling centres control morphogenesis of the telencephalon, affecting differential expression of several

transcription factors. Great focus will be given to the role of *Shh*, as it is the up-stream effector of *Gli3,* the gene of my interest. Subsequently, it will be described how the different telencephalic structures develop and diversify form each other, but also how they interconnect and connect with other brain structures through the major telencephalic axonal tracts. Finally, the latest knowledge on the role of *Gli3* in the development of the telencephalon will be summarized.

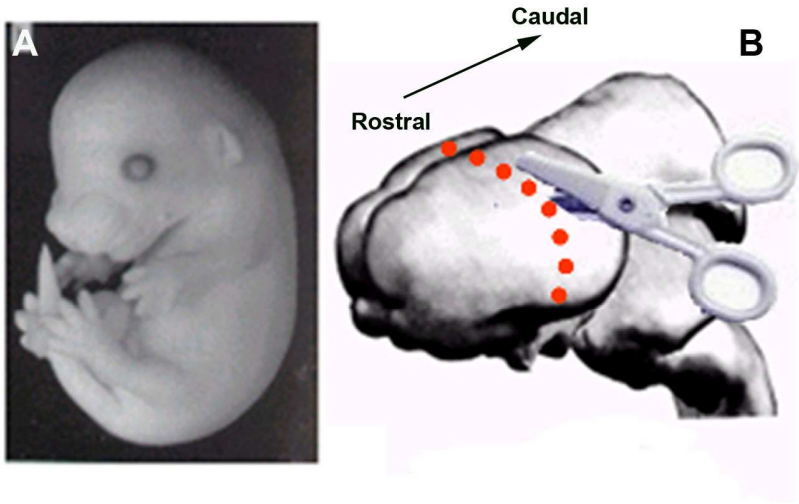
A
B
Caudal
Rostral

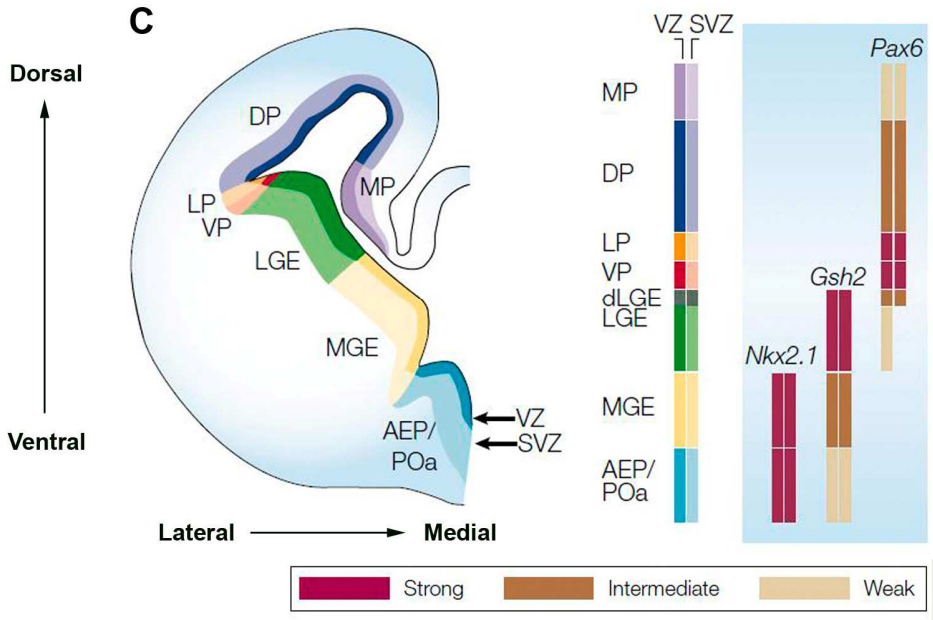
C
Dorsal
Ventral
Lateral
Medial
DP
MP
LP
VP
LGE
MGE
AEP/
POa
VZ
SVZ
VZ SVZ
MP
DP
LP
VP
dLGE
LGE
MGE
AEP/
POa
Pax6
Gsh2
Nkx2.1
Strong
Intermediate
Weak

**Figure 1.1.**

**First anatomical subdivisions in early telencephalic development**

Embryonic mouse (A) and brain indicating plane of coronal section (B) at stage E13.5. Schematic representation of coronal telencephalic half section of E12.5/E13.5 embryos (C adapted form …). In C it is possible to observe the regional subdivisions of the telencephalon. The dorsal region of the telencephalon gives rise to the pallium or dorsal telencephalon, which is further subdivided in medial pallium (MP), dorsal pallium (DP), lateral pallium (LP) and ventral pallium (VP); while the ventral region generates the basal ganglia or ventral telencephalon. The pallium eventually forms the neocortex from its anterior and lateral regions, while from its posterior and medial region the hippocampus, the cortical hem and the choroid plexus will develop. The subpallium instead is further subdivided into the medial ganglionic eminence (MGE), derived from its medial domain, and into the lateral and caudal ganglionic eminences (LGE and CGE), derived form its lateral and posterior regions and the anterior entopeduncular area/preoptic area (AEP/POa), derived from its ventromedial regions. Different colours show the distinct progenitor cell domains of the telencephalon: subventricular zone (SVZ) and ventricular zone (VZ). Long arrow indicating the lateral/medial axe. During development the differential expression of transcription factors instructs the different telencephalic regions to acquire different identities, such as *Pax6* in the dorsal telencephalon, *Gsh2* in the LGE and *Nkx2.1* in the MGE and AEP/Poa.

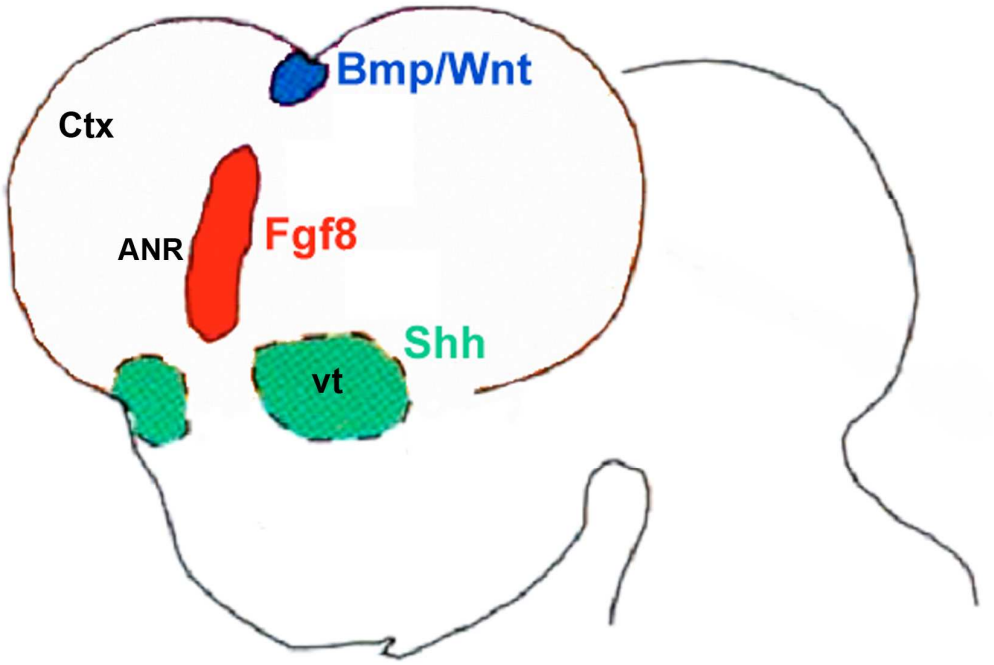


**Figure 1.2.**

**Three signalling centres control the regionalization process in the telencephalon**

Schematic representation of an E12.5 mouse brain showing the position of the signalling centres within the forebrain. *Fgf8* and other *Fgf* family members including *Fgf17* and *Fgf18* are expressed in the anterior neural ridge (ANR) (in red). Several *Wnt* and *Bmp* genes are expressed in the dorso-madial telencephalon (in blue) and *Shh* is expressed in the ventral telencephalon (in green). Arrows indicating the dorso/ventral and rosto/caudal axes. Abbreviations: Ctx, cortex; vt, ventral telencephalon; ANR, anterior neural ridge.

## 1.2 Three signalling centres control the regionalization process in the telencephalon

Regionalization is the process that subdivides the telencephalon into its subregions. This process is mainly controlled by discrete groups of cells known as signalling centres. Three signalling centres are sufficient to influence the fate of the surrounding telencephalic territories by expressing **(i) *Bmp/Wnt* genes** in the dorso-medial telencephalon, **(ii) *Fgf8*** in the rostro-medial telencephalon or anterior neural ridge, and **(iii) *Shh*** in the ventral telencephalon (Fig 1.2).

**(i) *Bmps* and *Wnts***

An important source of signalling molecules necessary to pattern the dorsal telecephalon is the dorsomedial cortex, which gives rise to the cortical hem, the choroid plexus and later to the hippocampus. This region expresses two families of secreted molecules: Bmps and Wnts. These molecules are important to induce dorsomedial telencephalic structures (Lee and Jessell, 1999; Monuki et al., 2001). *Bmp* signalling can induce dorsal midline features both in vitro and in vivo. Indeed beads soaked with Bmp can induce dorsal midline characteristics in cortical explants, such as apoptosis and *Msx1* expression, but also suppress cortico-lateral fate, showed by inhibition of *Foxg1* expression (Furuta et al., 1997). In addition, upregulation of *Bmp* signalling, with the use of an activated Bmp receptor, induces expansion of the dorsal midline at the expense of the cortex (Panchision et al., 2001). In the absence of *Bmp2* and *Bmp4* and of the *Bmp*

receptors the choroid plexus and cortical hem are missing while dorsal and ventral telencephalon are normal (Fernandes et al., 2007; Hebert et al., 2002). The roof plate in the dorso-medial telencephalon disappears together with *Wnt2b* expression (Monuki et al., 2001). This suggests that *Wnt* genes collaborate with Bmp genes in organizing the dorsomedial telencephalon. Indeed, one of the most important *Wnt* signalling sources is the cortical hem adjacent to the hippocampus primordium. *Wnt* signals are mediated through several intracellular pathways, including the β-catenin-mediated canonical pathway, which is the one present in the hippocampal primordium (Grove et al., 1998). The absence of *Wnt3a* results in the failure of hippocampal formation (Lee et al., 2000). In addition, ectopic activation of *Wnt* signalling in areas that would normally give rise to lateral cortical tissues result in ecpotic formation of hippocampal tissue (Machon et al., 2007). Furthermore, several Wnt genes are also expressed throughout the cortical ventricular zone from early stages of telencephalic development (Grove et al., 1998; Parr et al., 1993). It is not known yet whether they have a broader role in patterning the dorsal telencephalon.

In the absence of *Gli3* the dorsomedial telencephalon fails to invaginate leading to the absence of dorsomedial structures like the cortical hem, the choroid plexus and dorsomedial cortex. This is probably caused by the absence of *Bmp* and *Wnt* gene expression (Grove et al., 1998; Kuschel et al., 2003; Theil et al., 1999b; Tole et al., 2000a).

***(ii) Fgf***

Another important source of signalling important to pattern the telecephalon is the anterior neural ridge, which is a source of *Fgfs*. *Fgfs* are important for patterning the dorso-rostral telencephalon. A reduction of *Fgf8* levels in *Fgf8* hypomorphic mutants or a reduction of *Fgf8* signaling due to an overexpression of a dominant negative receptor result in a size reduction of the rostral cortex and an expansion of the caudal cortex (Fukuchi-Shimogori and Grove, 2001a; Garel et al., 2003). *Fgf8*$^{-/-}$ mutants also display defects in the formation of rosto-ventral telencephalic structures (Gutin et al., 2006; Storm et al., 2006). In recent studies it has been shown that mice mutant for the two *Fgf* receptors Fgfr1 and Fgfr2 fail to form the ventral telencephalon from a very early stage of brain development (Gutin et al., 2006), and lack the expression of *Nkx2.1* and *Gsh2* expression, which are important for the formation of the MGE (Sussel et al., 1999) and the LGE (Toresson et al., 2000a; Yun et al., 2003), respectively. In addition, *Fgf8* hypomorphic mutants display a reduction of ventral telencephalic markers including *Nkx2.1* (Storm et al., 2006). Further information comes from a recent study which demonstrates the general importance of *Fgf* signalling in promoting whole telencephalic character. Peak et al. (2009) effectively abolished *Fgf* signalling from the telencephalon with the use of triple mutants for three out of four *Fgf* receptors: *Fgfr1, Fgfr2* and *Fgfr3.* These mutants completely lack the telencephalon except for the dorsal-caudal midline (Paek et al., 2009). This work suggests that the different Fgf ligands and receptors act in concert in specifying and organizing the whole telencephalon, rather then working independently patterning different areas.

*Fgf* signalling acts in a positive feedback loop with *Shh* in specifying ventral identity in the telencephalon. This is demonstrated by the fact that that *Shh* is necessary to maintain

*Fgf3, Fgf*8, *Fgf*15, *Fgf*17, and *Fgf*18 expression and that *Fgf* receptors are necessary for the ventralizing effect of Shh (Aoto et al., 2002; Gutin et al., 2006; Ohkubo et al., 2002; Rash and Grove, 2007). In addition, an in vitro study demonstrated that ectopic *Fgf8* expression induces ventral fate within the dorsal telencephalon when *Shh* signalling is interrupted (Kuschel et al., 2003). However, *Shh* controls *Fgf* gene expression indirectly. This is shown by the fact that *Fgf8* expression expands in *Gli3* mutants (Aoto et al., 2002; Kuschel et al., 2003; Theil et al., 1999b). *Fgf8* expansion is not recovered in *Shh* and *Gli3* double null mutants (Rallu et al., 2002; Rash and Grove, 2007). This is probably due to the fact that in normal conditions *Shh* inhibits *Gli3,* which inhibits *Fgfs*, therefore *Shh* promotes *Fgf* signalling by indirectly reducing *GliR* activity.

***(iii) Shh***

A crucial molecule involved in patterning the ventral telencephalon is *Shh*. In *Shh* null mutant mice the telencephalon is severely hypoplastic and it is not possible to identify ventral telencephalic structures anatomically (Chiang et al., 1996; Ericson et al., 1995; Ishibashi and McMahon, 2002; Ishibashi et al., 2005; Ohkubo et al., 2002). This leads to the absence of ventral telencephalic markers such as *Nkx2.1, Gsh1, Olig2,* and *Lhx6* (Corbin et al., 2000; Corbin et al., 2003). Nearly the whole remaining telencephalic tissue is positive for dorsal telencephalic markers, such as *Emx1* and *Pax6* (Chiang et al., 1996; Ohkubo et al., 2002). Importantly, not all ventral telencephalic structures are lost. This is shown by the reduced expression of dLGE markers, such as *Gsh2* and *ER81*. The ventral telencephalic identity of these territories is also confirmed by the expression of *Dlx2* (Corbin et al., 2003; Fuccillo et al., 2006a).

The best-known role of *Shh* in forebrain development is its function as a morphogen. Shh protein is cleaved in two smaller sub-units: the C-terminal is a protease while the N-terminal is the part that mediates the signalling activities (Bumcrot et al., 1995; Hammerschmidt et al., 1997). The diffusion of Shh protein in the extracellular matrix can control cell fate depending on its concentration over long distances (Briscoe and Ericson, 1999; Jacob and Briscoe, 2003). For example, in the neural tube progenitor cells immediately adjacent to a Shh source, the floorplate (short-range morphogen), acquire a different fate to those that are over 10-15 cell diameters away (long-range morphogen) (Briscoe and Ericson, 1999). There are different sources of Shh within the developing embryo that control neural development: initially the notochord immediately underneath the neural tube, and subsequently the floorplate in the ventral neural tube and the prechordal plate immediately rostral to the notochord and ventrally to the forming brain (Fuccillo et al., 2006a). Once forebrain starts to form it contains itself additional sources of Shh: the mantle of the MGE, the preoptic area, the amygdala in the telencephalon, and the hypothalamus and the zona limitans intrathalamica in the diencephalon. Interestingly, the expression of the ventral telencephalic marker *Nkx2.1* in the ventral telencephalon precedes *Shh* expression (Shimamura et al., 1995). This implies that the specification of the ventral telencephalon relies on an extra telencephalic and non-neural source of Shh, probably coming from the prechordal plate. The later ventral telencephalic expression of Shh, after the ventral telencephalon has been specified, is necessary for the maintenance of ventral identity. This was shown by abolishing *Shh* expression after the initial ventral telencephalic patterning has been completed, leading to a reduction of *Nkx2.1* expression in the ventral telencephalon (Xu

et al., 2005). The timing of exposure to Shh also seems to be important for the specification of MGE identity versus LGE identity (Kohtz et al., 1998). The temporal window in which *Shh* specifies ventral telencephalic identity seems to be between E9.5 and E12.5. This is demonstrated by experiments on *Smo* conditional knockouts. *Smo* is a *Shh* co-receptor necessary for the activation of intracellular *Shh* signalling (see chapter 1.12). Machold et al. (2003) used a $Smo^{flox}$ $Nestin^{Cre}$ line that completely removes *Smo* in the ventral telencephalon after E12.5: the ventral telencephalon was specified in these mutant mice. Fucillo et al. (2004) instead combined the $Smo^{flox}$ allele with a $Foxg1^{Cre}$ allele that completely removes *Smo* from the telencephalon by E9.5. These embryos displayed reduction of the ventral telencephalon and an expansion of dorsal telencephalic markers. These experiments reveal the temporal competence of telencephalic cells to respond to Shh.

Upregulation of *Shh* and *Shh* signalling in the telencephalon also showed that different telencephalic regions are differentially competent to respond to *Shh* (Rallu et al., 2002). Indeed, in embryos infected with viruses expressing an activated form of Smo or full Shh protein, lateral telencephalic regions, such as LGE, lateral cortex and the septum can upregulate the MGE marker *Nkx2.1*. However, more dorsal and medial regions, such as the dorsal and medial cortex can only up regulate the pan-ventral genes *Gsh2* and *Dlx2* (Rallu et al., 2002). The upregulation of these genes also depended on the antero-posterior axis beeing more prominent rostrally (Rallu et al., 2002). This also suggested that an intrinsic pattern of competence to Shh had been already established in the telencephalon by E9.5, the earliest time of viral infection in this work.

## 1.3 Several transcription factors are involved in patterning the different telencephalic regions

How these signalling molecules exert their action on the morphogenesis of the telencephalon is still poorly understood. However, an intermediate requirement is their influence on the activation of transcription factors. During development the differential expression of these regulatory genes instructs the different telencephalic regions to acquire different identities.

The beginning of telencephalic development is coincident with the expression of the forkhead transcription factor gene *Foxg1* (Shimamura et al., 1997; Shimamura and Rubenstein, 1997; Tao and Lai, 1992). Subsequently to *Foxg1* expression the telencephalic primordium will divide further into more distinct territories, which differ from each other in their gene expression patterns but also in their anatomical structures and in growth characteristics.

However, *Foxg1* expression does not seem to be the first step for telencephalic induction. Indeed, surgical removal of the anterior neural ridge prior to *Foxg1* expression leads to the failure of *Foxg1* induction (Shimamura and Rubenstein, 1997). Shimamura and Rubenstein (1997) also showed that Fgf8-soaked beads are able to induce *Foxg1* expression in anterior neural ridge explants. In addition, reduction of *Foxg1* in *Fgf8* null mutants also indicates that *Fgf8* may positively regulate *Foxg1*

(Storm et al., 2006). This may suggest that the anterior neural ridge is already competent to respond to *Fgf8* by inducing *Foxg1* expression.

*Foxg1* probably plays a more direct role in inducing ventral telencephalic fate. In *Foxg1* null mice the ventral telencephalon is absent (Martynoga et al., 2005; Xuan et al., 1995). *Foxg1* induces ventral telencephalic fate, acting in cooperation with *Fgfs*. Indeed it induces *Fgf8* expression. This also suggests that *Fgf8* and *Foxg1* influence each other in a positive feedback, at least during ventral telencephalic development (Martynoga et al., 2005).

*Foxg1* expression is also indirectly dependent on *Shh* expression. In $Shh^{-/-}$ mutant mice *Foxg1* expression is lost. However, this is probably due to an increase in *Gli3R* activity (Rash and Grove, 2007). Indeed, in double $Foxg1^{-/-}$ $Gli3^{-/-}$ mutants the whole telencephalon is lost suggesting an essential requirement for *Gli3* and *Foxg1* in maintaining telencephalic structures (Hanashima et al., 2007).

*Foxg1* is also important for cortical development and might cooperate with *Fgf8* in patterning the dorsal telencephalon. In *Foxg1* knockout mice the two cerebral hemispheres are reduced in size (Xuan et al., 1995) and the remaining cortex is caudalized (Hanashima et al., 2007; Martynoga et al., 2005; Muzio and Mallamaci, 2005).

It has been shown that *Foxg1* also has a role in confining the development of the dorsal midline region. The dorsal telencephalon is split into two domains: the dorso-medial midline not expressing *Foxg1,* and the cerebral cortex expressing *Foxg1*. $Foxg1^{-/-}$ mutants display an expansion of dorsal midline regions and its marker genes *Bmp4* (Dou et al., 1999; Martynoga et al., 2005) and Wnt3a (Muzio and Mallamaci, 2005). In

addition, Bmp4 and Bmp2 repress *Foxg1* expression in telencephalic explants (Panchision et al., 2001).

Another gene important in the discrimination of these two regions is *the Lhx2* homeobox gene, which is cell autonomously required to repress dorsomedial fate in the developing cortex, as shown by *Lhx2* chimeras and *Lhx2* null mutants, which both display a reduction of cortical fields and a great expansion of the cortical hem and choroid plexus (Mangale et al., 2008; Monuki et al., 2001). *Lhx2* seems to be important for cortical fate specification not only repressing dorso-medial fate, but also repressing ventral pallium expansion (Assimacopoulos et al., 2003).

Another key gene in the early patterning of the cerebral cortex is *Pax6*. *Pax6* is expressed in the dorsal telencephalon, in a complementary manner to *Nkx2.1*. After E9.5 *Nkx2.1* and *Pax6* expression domains are separated by *Gsh2* expression (Corbin et al., 2000). *Pax6* and *Gsh2* cooperate in specifying the boundary between the pallium and the subpallium (PSPB) (Corbin et al., 2000; Stoykova et al., 2000; Toresson et al., 2000b; Yun et al., 2001). *Pax6*$^{sey/sey}$ mutants (small eye mutants) revealed the role of Pax6 in patterning the dorsal telencephalon (Hill et al., 1989; Stoykova et al., 2000). Indeed, *Pax6*$^{sey/sey}$ displays a dorsal expansion of ventral markers, such as *Dlx1* and *Vax1* (Stoykova et al., 1996), a phenotype opposite to *Shh*$^{-/-}$ mutants. Interestingly, removal of Pax6 in *Shh*$^{-/-}$ mutants partially compensates for *Shh* loss (Fuccillo et al., 2006b). This may suggest that *Gli3* and *Pax6* cooperate in specifying the dorsal thelencephalon. Indeed, while *Gli3* is not necessary for *Pax6* expression at early stages of development, it is indirectly required to maintain its high rostro-lateral to low caudo-medial telencephalic gradient (Aoto et al., 2002; Kuschel et al., 2003).

The gene that could link *Pax6* and *Gli3* functions within the developing cortex is probably *Emx2,* expression of which is strongly reduced in *Gli3* mutants (Theil et al., 1999b; Theil et al., 2002; Tole et al., 2000a). *Emx2*, together with *Emx1*, is involved in the patterning of the dorsal telencephalon (Yoshida et al., 1997). They show a nested pattern of expression in the dorsal thelencephalon and the absence of one is partially compensated by the other (Yoshida et al., 1997). However, *Emx2*$^{-/-}$ mutants display a stronger phenotype that *Emx1*$^{-/-}$ mutants. *Emx1*$^{-/-}$ mutants are viable even if they lack the corpus callosum and display a reduction in the thickness of the cerebral cortex and of the size of the hippocampus (reviewed in(Zaki et al., 2003). In contrast, the *Emx2*$^{-/-}$ mutants die shortly after birth displaying a strong size reduction of cortical hemispheres and olfactory bulbs. In addition, several other abnormalities have been observed in *Emx2*$^{-/-}$ mutants, including defects in several cortical axonal connections, such as the corpus callosum, fimbria and fornix, a heterotrophic choroid plexus, disorganized cortical layers and an abnormally broad cortical ventricular zone; the cortical hem expands at early steps of development although its size is reduced at later stages (reviewed in(Zaki et al., 2003). Interestingly, *Pax6* is upregulated in *Emx2*$^{-/-}$ mutants. Indeed, *Pax6* and *Emx2* antagonize each other in patterning the cortical neural epithelium (Bishop et al., 2003; Bishop et al., 2000; Mallamaci et al., 2000; Muzio and Mallamaci, 2003). *Emx2* is expressed in a high dorso-medial to low rostro-lateral gradient, which is opposite to the *Pax6* expression pattern. *Pax6* and *Emx2* mutants also display opposite cortical phenotypes: in the *Emx2*$^{-/-}$ mutants the caudal and medial cortex is lost resulting in a caudal and medial shift in rostral and lateral identities. Conversely, in *Pax6*$^{-/-}$ mutants rostro-lateral cortical identity is lost resulting in a rostro-medial shift of caudal and

medial areas (Bishop et al., 2000). In addition, both *Pax6* and *Gli3* double mutants and *Pax6* and *Emx2* double mutants display a reduction of the cortex and an expansion of the cortical hem and sub-pallial regions (Fuccillo et al., 2006b; Muzio et al., 2002). Therefore *Gli3* may indirectly affect *Pax6* expression by affecting the expression of its antagonist *Emx2* in the cerebral cortex.

Once dorsal and ventral telencephalon are specified several other genetic and morphological mechanisms further increase the complexity of these structures.

## 1.4 Cellular and molecular mechanisms in the development of ventral telencephalon

The ventral telencephalon has been anatomically defined as follows:

(i) The LGE is the bulge that forms between the cortex and MGE.

(ii) The MGE is the bulge that forms between the LGE and the septum while the CGE is the caudal part of the LGE. However, there are no clear anatomical landmarks that allow the discrimination between these two regions.

(iii) The POa is the region immediately in front of the optic recess, at the border between the telencephalon and the diencephalon.

Although most of these definitions are based on anatomical landmarks, such as sulci and bulges, they are very imprecise. Indeed, these anatomical limits are based on morphological criteria that continuously change during the development of the brain. In addition, these structures are transient (Marin and Rubenstein, 2001). Moreover,

anatomical boundaries do not necessarily coincide with molecular landmarks. For example, the ventral pallium (VP), which is positive for pallial markers, is located slightly ventral to the sulcus that anatomically defines the boundary between the pallium and subpallium. Consequently, pallial markers are expressed in the region that would be defined anatomically as the LGE (Puelles et al., 2000; Stenman et al., 2003b).

More recent studies divide the subpallial regions into different progenitor domains according to their gene expression profiles. For example, the progenitor region of the subpallium is precisely delineated by the expression of *Dlx2* and *Mash1* (Bulfone et al., 1993; Puelles et al., 2000). The expression of these genes starts around E9.5. The LGE and MGE can be further discriminated by the absence of *Nkx2.1* and the presence of *Gsh2* expression in the LGE (Puelles et al., 2000). The LGE itself can be further subdivided in more molecular sub-domains: the dorsal LGE (dLGE) and ventral LGE (vLGE); the dLGE is delimited by the expression of *Er81* and high levels of Gsh2 expression (Yun et al., 2001). The dorsal-most part of the LGE abuts with the ventral pallium (VP), which is characterized by co-expression of *Pax6* and *Gsh2* before E 11.5. At E9.5 *Pax6* is strongly expressed in the pallium (Stoykova et al., 1996; Stoykova et al., 1997) while *Gsh2* is expressed in subpallial progenitors (Hsieh-Li et al., 1995). These two genes play important complementary roles in patterning the progenitor cells flanking the pallial- subpallial boundary (PSB) (Yun et al., 2001). In *Pax6*$^{-/-}$ single mutants the most ventral area of the developing cortex acquire LGE identity, while in *Gsh2*$^{-/-}$ mutants the dLGE is transformed into cortical (Corbin et al., 2000; Stoykova et al., 2000; Toresson et al., 2000b; Yun et al., 2001). In *Gsh2*$^{-/-}$ and *Pax6*$^{-/-}$ double mutants the PSPB is partially restored (Toresson et al., 2000a), suggesting additional

mechanisms in maintaining and positioning this boundary and the specification of the VP. By E11.5 in the mouse, the gene expression domain of the VP is distinct: the expression domain of *Dbx1* overlaps with those of *Tbr2* and *Ngn2* and fills the gap between *Emx1* in the dorsal telencephalon and *Gsh2* in the ventral telencephalon (Yun et al., 2001). Therefore, although the VP is positioned in a region that anatomically would be defined as ventral telencephalon, its origin is not entirely ventral telencephalic; indeed it is negative for *Dlx2* expression (Puelles et al., 2000; Yun et al., 2001). This anatomical and genetical complexity also demonstrates how difficult it is to clearly define brain regions based only on anatomical observations. However, these analyses only begin to point out the heterogeneity of the different progenitor cell types in the ventral telencephalon. A recent study identified at least four different progenitor domains (pLGE1 to pLGE4) in the developing LGE, five progenitor regions in the MGE (pMGE1 to pMGE5) and two progenitor regions in the POa at E13.5, characterized by a complicated code of differential gene expression (Flames et al., 2007).

This complex scheme of differential gene expression in various regions of the ventral telecephalon reflects the multiple roles played by this region in several aspects of forebrain development. The ventral telencephalon gives rise to multiple neuronal types that form the basal ganglia and part of the amygdala and septum, but also to several different types of olfactory and cortical interneurons, also contributing to dorsal telencephalic development (Marin and Rubenstein, 2001; Pleasure et al., 2000).

It has been shown that tangential migrations contribute substantially to neural diversity within distinct telencephalic regions (Anderson et al., 2001). Neurons originating in

restricted regions of the developing ventral telencephalon migrate over long distances to populate different telencephalic regions.

A large number of different neurons originating in the MGE preferentially migrate up to the cortex (Anderson et al., 2001; Wichterle et al., 1999; Wichterle et al., 2001). Indeed *Nkx2.1* mutant mice display a reduction of 50% of GABA-ergic interneurons when compared to wild type (Sussel et al., 1999). Two different types of interneurons arise from the MGE, one containing parvalbumin and another containing somatostatin (Butts et al., 2005; Wichterle et al., 2001). These two different populations together contribute 60% of cortical interneurons (Gonchar and Burkhalter, 1997; Kawaguchi, 1997). Another source of interneurons is the CGE. The route that CGE-derived interneurons take to colonize the cortex is not clear yet, although it seems quite clear that a proportion of CGE interneurons express calretinin (Lopez-Bendito et al., 2004a; Lopez-Bendito et al., 2004b), while another proportion also express parvalbumin and somatostatin but not calretinin (Nery et al., 2002). Therefore the CGE produces a more heterogeneous set of cortical interneurons than the MGE. This is also in accordance with the molecular identity of the CGE, which displays *Nkx2.1* expression in its ventral region and *Gsh2* and *ER81* in its dorsal domain, acquiring molecular characteristics of both the MGE and the LGE. The contribution of cortical interneurons from the LGE is thought to be much more modest compared with the MGE (Anderson et al., 2001; Wichterle et al., 1999; Wichterle et al., 2001). However it still does produces cortical GABA-ergic interneurons (Anderson et al., 2001), and almost all the GABA-ergic interneurons in the hippocampus originate from the LGE (Pleasure et al., 2000).

In contrast to the vast wave of dorsally migrating neurons originating in the ventral telencephalon, cells of the lateral cortical stream migrate from the dLGE (which corresponds molecularly to the cortico-striatal border) to more ventral region of the ventral telencephalon (reviewed in(Corbin et al., 2001; Molnar and Butler, 2002). These cells colonise the basal telencephalic limbic system including the amygdala and the piriform cortex (Stoykova et al., 2000; Toresson et al., 2000a; Yun et al., 2001). (Carney et al., 2006) analyzed in more detail the mechanism of their ventral migration and their cell composition, showing that most of these neurons are *Pax6*$^{+}$. In addition, they also show a genetic requirement for *Gsh2* in their formation, emphasizing the interactive role of *Pax6* and *Gsh2* at the corticostriatal boundary.

It is known that calretinin expressing neurons generated in different regions of the LGE colonize the striatum and the olfactory bulbs (Stenman et al., 2003a). Studies from Jan Stenman and Campbell (2003) provide more interesting evidence of how different progenitor pools contribute differentially to the colonization of particular areas of the telencephalon. They demonstrated that the dLGE (*Dlx2*$^{+}$ *ER81*$^{+}$*)* gives rise to olfactory interneurons, while the vLGE (*Dlx2*$^{+}$ *Isl1*$^{+}$ *ER81*$^{-}$*)* gives rise to striatal neurons.

The ganglionic eminences also play an important role in the guidance of the corticothalamic and thalamocortical axonal projections, but this will be discussed at a later stage of this introduction (chapter 1.7).

## 1.5 Cellular and molecular mechanisms in the development of the cerebral cortex

Neurogenesis in the dorsal telencephalon happens later than in the ventral telencephalon. The first post-mitotic neurons in the developing cortex are seen at E10.5, originating from the cortical ventricular zone and forming the preplate. Subsequently the preplate is split into the marginal zone on the surface and the subplate just above the intermediate zone. The cortical plate starts to develop in between these two layers. Within the cortical plate the later born neurons, coming from the progenitor region of the ventricular zone, migrate over the early born neurons forming a layered structure in an inside-out fashion. Therefore, the deepest cortical layer VI forms first and the upper layer II last (reviewed in (Molyneaux et al., 2007). Eventually the cerebral cortex is composed of 6 neural layers. The process of formation of these different cortical layers is known as cortical lamination. The only layer that escapes this inside-out process is the marginal zone, or layer I, which is the first one to form. Layer I itself is important for the lamination process, as it contains Cajal-Retzius cells secreting the reelin glycoprotein that directs cortical lamination (Tissir and Goffinet, 2003). Indeed, the inside-out layer organization is lost in the *Reeler* mutant mouse and cortical layers are inverted (Curran and D'Arcangelo, 1998; D'Arcangelo et al., 1995; Ogawa et al., 1995). The formation of the different cortical layers can be investigated thanks to the identification of different lamina markers, such us *Cux1* (layer II/III), *Tbr1* (layer VI, Cajal-Retzius cells and at

low levels in layers II/III), *Ror-β* (layer IV), Sox5 (layers VI and V), CTIP2 (layer V, corticospinal neurons) and Satb2 (strong expression in layer II/III and low expression in layers IV and V, callosal neurons) (reviewed in Molyneaux et al. 2007).

Different types of progenitor cells give rise to the complex structure of the laminated cortex. So far, 3 different types have been identified: (i) **neuroepithelial cells**, (ii) **radial glia cells** and (iii) **basal progenitors** (Gotz and Huttner, 2005; Molyneaux et al., 2007).

(i) **Neuroepithelial** cells are the first progenitors to appear in the developing cortex and they will divide symmetrically to give rise to new progenitors and asymmetrically to produce the first post mitotic neurons in the preplate (Gotz and Huttner, 2005; Smart, 1973).

(ii) As neurogenesis progresses neuroepithelial progenitors become **radial glia cells** (Hartfuss et al., 2001; Malatesta et al., 2003). Radial glia cells extend a long process towards the pia surface and a short one anchors them at the ventricular surface. These cells progress through the cell cycle maintaining their cell bodies within the ventricular zone and they divide asymmetrically at the ventricular surface producing another radial glia cell and a post mitotic neuron or an intermediate progenitor (see next paragraph). Postmitotic neurons and intermediate progenitors subsequently use the long radial glial processes to migrate radially outside the ventricular zone. Therefore, radial glia cells, thanks to their processes, also support radial migration of differentiating neurons during the process of cortical lamination (Rakic, 1972; Rakic, 2003a; Rakic, 2003b). Recently another type of progenitor has

been identified as a subtype of radial glia cells. This sub-population was called **"short progenitor",** because although they are positive for radial glia specific markers such us RC2 and Glast, they do not have radial processes (Gal et al., 2006).

(iii) Eventually the last type of progenitors to form are the **intermediate progenitors** found in the cortical subventricular zone. In vitro studies reveal that radial glial cells not only form a post-mitotic neuron and a new radial glial progenitor by asymmetric cell division, but they also produce in alternate divisions intermediate progenitors (Mo et al., 2007). The intermediate progenitor migrates into the subventricular zone before going on to further divide and produce two post-mitotic neurons (Gotz and Huttner, 2005; Molyneaux et al., 2007). Contrarily to radial glia cells, they do not have long processes and divide away from the ventricular surface, hence their name. Indeed the subventricular zone significantly contributes to the number of post-mitotic neurons in more superficial cortical layers at later stages of cortical development (Bayer et al., 1991; Smart, 1973).

However, to date it is still not possible to link the different progenitors to the different post-mitotic neurons within the different layers. An interesting example is *Cux1,* which is a marker for upper layer cortical neurons. *Cux1* is also expressed in intermediate progenitors in the subventricular zone when the formation of the last cortical layers is taking place (Nieto et al., 2004; Tarabykin et al., 2001; Zimmer et al., 2004). However, *Cux1* expression in the ventricular zone already starts at E11.5, suggesting that the

specification of the later forming neurons may already be taking place as early as E11.5. However, further studies are still needed to investigate these possibilities.

Cortical lamination is also important for the formation of the major axonal tracts. Indeed, neurons located in different cortical layers connect their axons to different targets. For example, only neurons within layer VI, with a small population in layer V, project axons towards the thalamus, while neurons in layers II/III, V and VI connect the two cerebral hemisphere extending axons across the corpus callosum.

## 1.6 Development of the corpus callosum

In the adult brain, the corpus callosum is the major commissural tract, which connects the two cortical hemispheres. This axonal tract has the function to integrate and exchange information between the two sides of the cortex. The development of the corpus callosum does not stop at birth and it continues to grow postnatally (Richards et al., 2004). To reach their final target area, callosal axons follow a complicated course with several changes of direction. Callosal neurons project their axons ventrally from the cortical layers II/III, V and VI into the intermediate zone. Afterwards callosal axons make a sharp turn projecting medially towards the contralateral cortex. They pass over the midline region making another sharp turn, and eventually reach their final target through the same number of changes of direction within the contralateral cortex (Richards, 2002). It has been proposed that the guidance molecule Sema3a repels callosal axons from the marginal zone pushing them in the direction of the intermediate

zone (Polleux et al., 1998). However, it is still not clear what makes callosal axons project medially or laterally within the cortical intermediate zone. Indeed, the molecular mechanisms controlling the development of distinct subtypes of neocortical projecting neurons are only starting to emerge. For example, *SABT2* null callosal neurons project subcortically instead of projecting their axons medially within the cortex (Alcamo et al., 2008). In addition, in *Sox5*$^{-/-}$ mutants the production of corticofugal neurons is accelerated leading to abnormal cortical innervation of different subcerebral targets (Lai et al., 2008).

Once they reach the midline, callosal axons are guided to the contralateral side by a number of intermediate targets: (i) **the glial sling** (Silver et al., 1982), (ii) **pioneer neurons** originating from the cingulate cortex (Rash and Richards, 2001) and (iii) the **midline glial populations** (Richards, 2002; Shu and Richards, 2001) and (Fig 1.3).

(i) The **glial sling** is located immediately ventrally to the corpus callosum and provides a substrate on which callosal axons navigate to cross the midline (Silver et al., 1982). Although it has been previously described as a glial structure, hence its name, it has been subsequently demonstrated that cells within the glial sling are neurons (Shu et al., 2003).

(ii) The first cortical axons to project across the midline are those from **pioneer neurons** of the cingulate cortex. These axons intimately interact with later arriving callosal axons and have been proposed to make the route to the contralateral side (Rash and Richards, 2001).

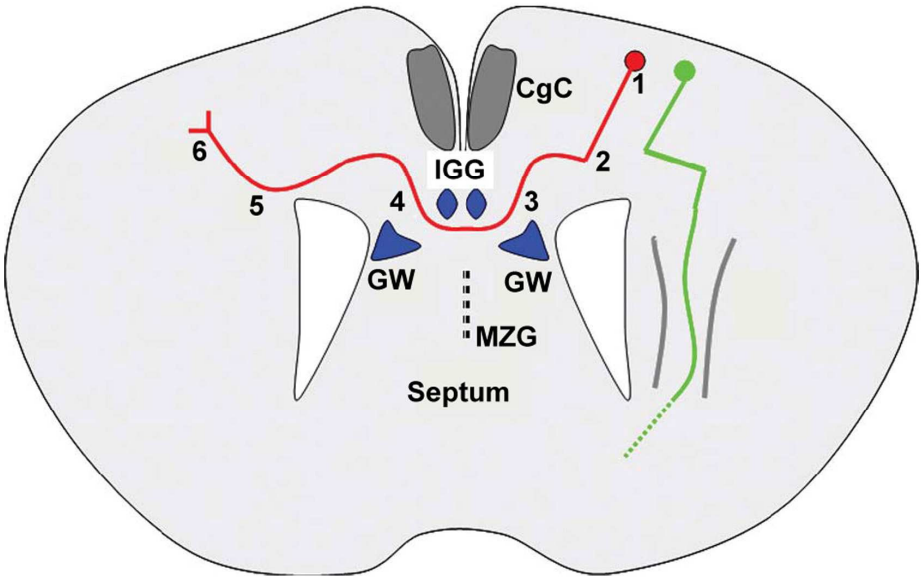


**Figure 1.3.**

**Schematic representation of a coronal brain section of an E18.5 embryo showing the developmental stages in corpus callosum formation.**

In red a callosal neuron is shown, in green a cortical neuron projecting laterally. 1, 2, 3, 4, 5 and 6 are decision points for callosal axons. To reach their final target area, callosal axons follow a complicated course with several changes of directions (1-6). During this course, growing callosal axons are guided to the controlateral cortex by several intermediate intermediated targets, which are the midline glial populations and pioneer neurons originating from the cingulate cortex. Abbreviations: CgC, cingulated cortex; IGG, indusium griseum; GW, glia wedge; MZG, midline zipper glia.

(iii) **Midline glial populations**, such as the **indusium griseum** and the **glial wedge** express the repulsive guidance molecules *Slit1/2* and channel cortical axons through the midline (Richards, 2002; Shu and Richards, 2001). Cortical neurons expressing the Robo receptors are repelled from the glial wedge and do not project into the septum but progress to the contralateral side. (Richards, 2002; Shu and Richards, 2001).

A necessary requirement for callosal axons to cross the midline is the fusion of the dorsal midline. A failure in this process will result in the absence of the territories in which callosal axons navigate (reviewed in (Paul et al., 2007). It is still largely unknown how this process happens, but it has been proposed that another midline glial population is necessary for this process: the **midline zipper glia** (Richards, 2002; Shu and Richards, 2001).

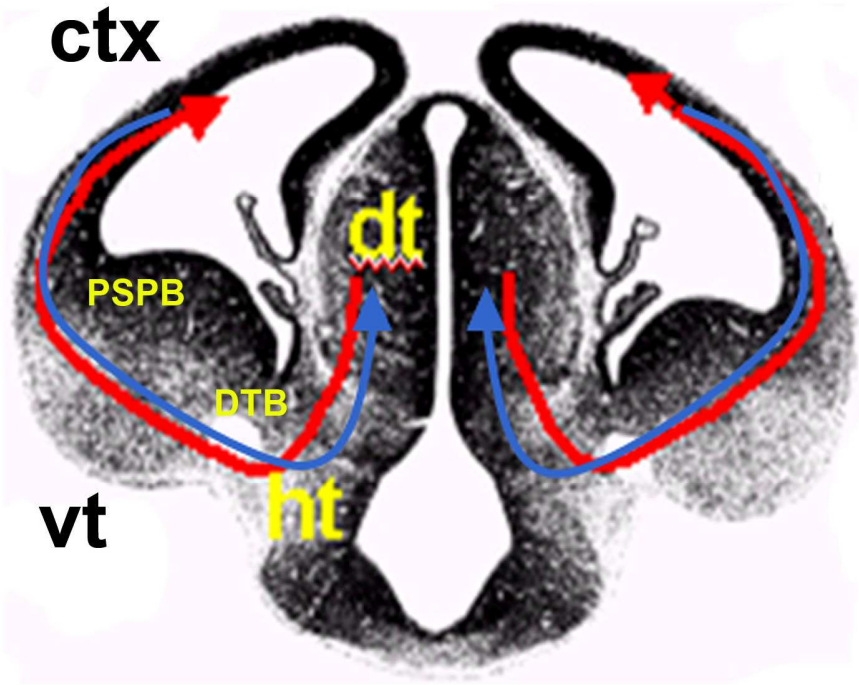


**Figure 1.4.**

**Schematic representation of a coronal brain section of E14.5 embryo, showing the complex course that both thalamocortical and corticothalamic (in blue) axons have to cover to reach their final target areas.**

Thalamocortical neurons (red) send their axons ventrally from the dorsal thalamus to the DTB where they change direction to penetrate the ventral telencephalon (VT). Afterwards, thalamocortical axons navigate until they reach the PSPB where they change direction a second time to invade the cortical region. Axons from cortical neurons (blue) follow a reciprocal pathway to the dorsal thalamus, growing through the same territories as thalamocortical axons but in the opposite direction. Abbreviations: PSPB, pallium subpallium boundary; DTB, diencephalic telencephalic boundary; ht, hypothalamus; dt, dorsal thalamus.

## 1.7 Formation of the corticothalamic and thalamocortical tracts

The corticothalamic and thalamocortical tracts are prominent tracts within the forebrain. In the adult brain, the thalamocortical tract conveys sensory information from the external environment to the cortex. The cortex analyzes and integrates this information and sends neural responses back to the thalamus through the corticothalamic tract. During embryonic development, neurons in the thalamus and cortex connect with one another by sending out axons in a coordinated manner. For example, neurons in the caudal cortex (the visual cortex) connect with dorsolateral regions of the thalamus (called the dorsal lateral geniculate nuclei, dLGN); neurons from the medial cortex (the somatosensory cortex) connect with the mediolateral region of the thalamus (called the ventral basal, VB); finally axons coming from the frontal cortex connect with ventromedial regions of the thalamus (called the medial basal, MB) (Lopez-Bendito and Molnar, 2003; Price et al., 2006).

The complex function of these two tracts is reflected in their intricate developmental program: both thalamocortical and corticothalamic axons have to cover large distances, changing direction several times and passing through different brain territories. Thalamocortical neurons send their axons ventrally from the dorsal thalamus to the DTB where they change direction, to penetrate the ventral telencephalon (VT). Afterwards, thalamocortical axons navigate until they reach the PSPB where they change direction a second time to invade the cortical region. They finally migrate through the "intermediate" zone of the developing cortex until they innervate target neurons in

cortical layer 4. Axons from cortical neurons follow a reciprocal pathway to the dorsal thalamus, growing through the same territories as thalamocortical axons but in the opposite direction (Fig 1.4). A detailed analysis of the timing of progression of corticothalamic axons from the cortex until their final target has been achieved with the use of a *Golli tau-green fluorescent protein* mouse line (Jacobs et al., 2007). In this study it is shown how corticothalamic axons progress over the pallium-sub-pallium boundary and the diencephalic-telencephalic boundary in a multi step fashion, pausing at different points along their path at different stages of development.

The ventral telencephalon is an important structure that thalamocortical and corticothalamic axons have to navigate through in order to meet each other and connect to their final target (Garel and Rubenstein, 2004; Seibt et al., 2003). At least three main axon guidance mechanisms have been proposed to exist in the VT, which guide thalamocortical and corticothalamic axons at different time points during embryonic brain development: (i) **Pioneer axons** within the VT provide scaffolds for growing thalamocortical and corticothalamic axons (Metin and Godement, 1996)**.** (ii) The VT forms a **permissive corridor** important for thalamocortical axon pathfinding (Lopez-Bendito et al., 2006)**.** (iii) Thalamortical and corticothalamic axons guide each other once they have met **"handshake hypothesis"** (Molnar and Blakemore, 1995) (Fig 1.5)**.**

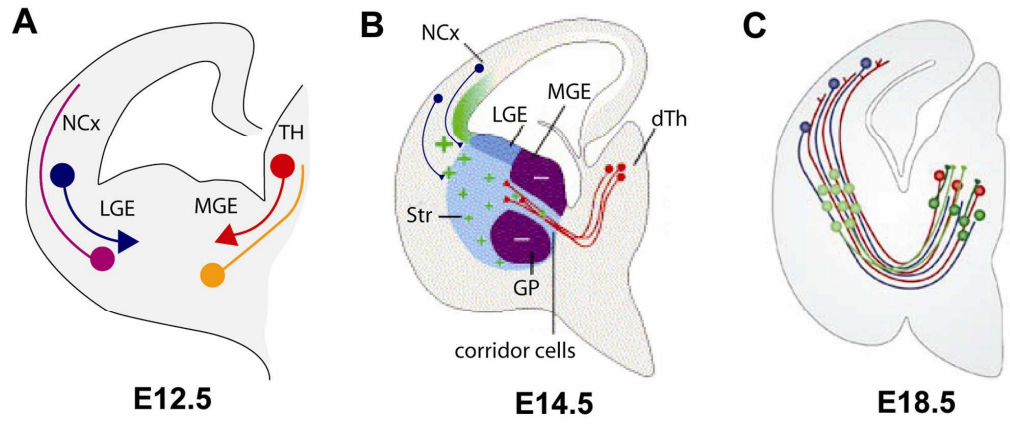


**Figure 1.5.**

**Schematic representation of ventral telencephalic intermediate cues required to guide thalamocortical and corticothalmic axons towards their final target areas.**

At least three main axon guidance mechanisms have been proposed to exist in the VT that guide thalamocortical and corticothalamic axons at different time points during embryonic brain development. (A) **Pioneer axons** within the VT provide scaffolds for growing thalamocortical (in red) and corticothalamic (in blue) axons**.** Two different populations of pioneer neurons are present in the ganglionic eminences, one in the LGE (in purple) and one in the MGE (in yellow). (B) The VT forms a **permissive corridor,** which is important for thalamocortical axon pathfinding**.** The MGE is normally repulsive for the growth of thalamic axons. The permissive corridor in the MGE is derived from cells migrating tangentially from the LGE into the MGE. Corridor cells, LGE and cortex express attractive guidance molecules for thalamocortical axons. (C) Thalamortical and corticothalamic axons guide each other once they have met, as described by the **"handshake hypothesis".** Once thalamocortical axons and corticothalamic axons meet, they interact strongly and connect intimately. This interaction has been hypothesized to be required for both sets of axons to reach their final target. Abbreviations: Ncx, neocortex; LGE, lateral ganglionic eminence; MGE, medial ganglionic eminence; Str, striatum; GP globus pallidum; dTH and TH, dorsal thalamus.

### (i) Pioneer axons

The first known axonal cues that thalamocortical and corticothalamic axons meet before they penetrate the VT are two different populations of pioneer neurons in the ganglionic eminences (GEs) (Metin and Godement, 1996). At embryonic day E13.5, corticofugal axons make a pause just after passing over the pallial-subpallial boundary in the LGE (Jacobs et al., 2007) while thalamocortical axons have already navigated through the MGE. At this age, corticofugal and thalamocortical axons have not yet made contact with one another. It has been proposed that they follow pathways formed by early projecting axons in order to reach their later targets (Metin and Godement, 1996; Molnar et al., 1998; Tuttle et al., 1999). These early projecting axons are defined as pioneer neurons; they only rely on messages (i.e. secreted guidance molecules) from neighbouring territories to extend axons in the target area. Later-arriving cortical and thalamic axons can use pioneer axons to orientate their direction of growth in the invading regions. The VT-Pioneer neurons are transient populations, which appear at E12.5 in the embryonic mouse brain (Tuttle et al., 1999).

The MGE pioneer neurons provide a scaffold that orientates growing thalamic axons across the diencephalic-telencephalic boundary (DTB). They are located in the ventral MGE and project axons from the telencephalon to the diencephalon (Tuttle et al., 1999). In contrast, the LGE pioneer neurons, which are located in the LGE, provide an axonal scaffold for cortical axons to pass over the PSPB (Metin and Godement, 1996).

Not much is known about these populations: there are no markers available to distinguish them, they can only be identified by DiI injections into the cortex and

thalamus at early stages of thalamocortical and corticothalamic development (E12.5) when thalamic and cortical axons have not reached the VT yet. At this embryonic stage, groups of neurons along the thalamocortical and cotircothalamic pathway project their axons to the developing thalamus and cortex and they are transiently associated with later growing thalamic and cortical axons (Metin and Godement, 1996).

Evidence that pioneer neurons are probably important for corticofugal axon guidance and orientation came from work on embryonic hamster and mouse brains (Metin and Godement, 1996). These experiments involved cultivating cortical explants together with VT (LGE plus MGE), in the absence of reciprocal thalamocortical axons. In these experiments the authors show that the LGE is capable of orientating cortical axons. In these cultures cortical axons tend to converge on a small region in the MGE, growing through the whole LGE in an ordered fashion. They also co-cultured explants from the cortex with different regions of the VT (the LGE alone and the MGE alone) and with the brainstem. They showed that this orientating effect is only maintained when cortical explants are co-cultured with LGE explants: cortical axons grow through the LGE orientating their axons to the end of the explants (the ventral region of the LGE). In contrast, co-culture of the cortex together with MGE or brainstem fail to support long distance growth and to orientate corticofugal axons. Indeed, once cortical axons have penetrated the MGE they immediately converge on a point in the middle of the explants. Instead, cortical axons are repelled by the brainstem, which preferentially directs cortical axons along the edge of the explants. This means that only the LGE is able to support an orientated growth of corticofugal axons towards the MGE. Metin and Godement suggest that this is due to the presence of pioneer neurons in the LGE. However, so far there is

no evidence in vivo that the absence of LGE pioneer neurons results in a failure of corticofugal axons in projecting their axons towards the ventral telencephalon.

Metin and Godement also hypothesized that the VT plays the same role in the guidance of early projecting thalamocortical axons across the diencephalic-telencephalic-boundary. The best evidence of a guidance role for MGE pioneer neurons comes from the analysis of *Lhx2* knockout and *Mash1*-deficient mice (Lakhina et al., 2007). In these mice, thalamic axons do not penetrate the ventral telencephalon. This effect correlates well with the absence of DiI back-labeled MGE pioneer neurons. In these mutant mice only few thalamocortical axons appear to enter the ventral thalamus, thalamic axons instead run along the diencephalic-telencephalic-boundary.

(ii) **Permissive corridor cells**

After E12.5 thalamocortical axons penetrate into the ventral telencephalon, passing over the DTB. Subsequently, they have to change direction projecting dorsally into the MGE channeling through the internal capsule (IC) and then navigating into the LGE, until they reach the PSPB and eventually the cortex. In an elegant study, Lopez-Bendito et al. (2006) demonstrated that thalamocortical axons are guided through the ventral telencephalon by a permissive channel in the MGE, which otherwise would be repulsive for the growth of thalamic axons. This channel is positive for *Isl1* and *Ebf1*, but surprisingly is negative for *Nkx2.1* expression, which normally characterizes the surrounding MGE (see chapter 3). Indeed, the *lsl*1$^{+}$ channel in the MGE is derived from cells migrating tangentially from the *lsl*1$^{+}$ region in the LGE. The authors demonstrated that blocking this tangential migration and the subsequent formation of the *lsl*1$^{+}$ channel resulted in failure of the thalamocortical tract to correctly navigate through the ventral

telencephalon. The important finding that the *lsl*1$^{+}$ corridor cells guides thalamocortical projections through the ventral telencephalon also linked together different aspects of telencephalic development, such as tangential migration and axon guidance. In addition, the discovery of the permissive corridor in guiding thalamocortical axons is starting to partially explain the thalamocortical phenotypes of mutants mice in which the development of this tract is effected, such as in *Pax6*$^{-/-}$ mutants (Simpson et al., 2009).

**(iii) Handshake hypothesis**

Between E14.5 and E15.5, thalamocortical axons and corticothalamic axons meet for the first time in the VT (Lopez-Bendito and Molnar, 2003; Molnar and Blakemore, 1995). It has been observed that once they reach one other they interact strongly and connect intimately. This interaction has been hypothesized to be required for both sets of axons to reach their final target. This hypothesis is known as the "handshake hypothesis" (Molnar and Blakemore, 1995), indicating that thalamic projections are introduced to cortical axons in ventral telencephalon. After they have "shaken hands"/growth-cones (which is the distal tip sensitive to guidance molecules at the end of the axons, responsible for axonal navigation) they use each other to innervate the reciprocal target area. This idea comes from the observation that thalamocortical and corticothalamic projections are closely opposed inside the internal capsule and they do not occupy separate compartments. Good evidence supporting this hypothesis comes from the study on (**i)** ***Tbr1*****, (ii)** ***Gbx1*** **and (iii)** ***Pax6*** mutant mice (Hevner et al., 2002).

**(i)** ***Tbr1*** is expressed in the cortex but not in the dorsal thalamus. Therefore mice mutant for *Tbr1* should display defects in cortical development and cortical axons, but not in thalamic axons. Indeed, *Tbr1* knock-out mice have defects in cortical

neurons and consequently in descending corticothalamic fibers: at E14.5 cortical axons have not reached the IC, but they deviate dorsally within the LGE and at later stages (E16.5) they never cross the diencephalic telencephalic boundary (DTB). In these mutants, thalamocortical axons are also not able to reach the cortex and they deviate laterally through the IC and never reach the PSPB growing into the external capsule instead.

**(ii)** ***Gbx2***, in contrast, is expressed specifically in the dorsal thalamus and not in the cortex. The absence of this gene affects the development of neurons within the dorsal thalamus and consequently the thalamocortical projection. The number of thalamic axons and their growth is severely reduced at E14.5; at later stages (E16.5) few thalamic axons enter the subpallium, not progressing further dorsally than the boundary between LGE and MGE. However, in the absence of the thalamocortical tract, *Gbx2*$^{-/-}$ cortical axons also fail to reach the dorsal thalamus (DT). Interestingly, *Gbx2*$^{-/-}$ cortical axons grow out normally from the cortex at E14.5 into subpallial region and they reach the IC, but then very few penetrate the diencephalon, entering instead the cerebral peduncle.

**(iii)** ***Pax6*** is expressed in the cortex, in the VT and in the dorsal thalamus. This implies that *Pax6*$^{sey/sey}$ mice might not only display defects in the brain territories from which cortical and thalamic neurons originate but also defects in territories along which axons have to navigate. In *Pax6* mutant mice most of the thalamocortical axons grow towards the hypothalamus at E16.5 and only very few thalamic axons cross the DTB at later stage of embryonic development (E18.5), but most of these axons in the VT are deflected towards the amygdaloid region.

No *Pax6*$^{sey/sey}$ thalamic axons ever reach the cortex (Pratt et al., 2000b). Reciprocally, *Pax6*$^{sey/sey}$ corticothalamic axons do not reach the thalamus, but interestingly they make similar innervation mistakes as thalamic axons avoiding the IC and growing along the edge of the striatum towards the amygdaloid region. This suggests that even misrouted thalamic and cortical axons may still interact.

The limitation of these analyses is the fact that it is not possible yet to completely exclude defects in cortical axons in *Gbx2*$^{-/-}$ mutants and/or thalamic axons in *Tbr1*$^{-/-}$ mutants. Moreover, some ventral telencephalic defects independently affect thalamocortical and corticothalamic axons in *Pax6*$^{sey/sey}$ mutants. The use of conditional knockouts would help in these respects. However, following this line, the comparative analyses of other mutant mice further corroborate the handshake hypothesis. Indeed, *Emx2, Mash1, Fezl* and *Nkx2.1* mutant mice (Hevner et al., 2002; Jones et al., 2002; Komuta et al., 2007; Lopez-Bendito et al., 2002; Pratt et al., 2000b; Tuttle et al., 1999) all display defects in the reciprocal axonal connections between cortex and thalamus. The majority of these mistakes happen in the ventral telencephalon before thalamic and cortical axons reach their final target. Though not proving the handshake hypothesis, these findings suggest at least that those tracts do not develop independently from each other.

In this complex scenario a number of guidance molecules have been shown to guide thalamocortical and corticothalmic axons to their final targets, attracting or repelling axons at different points along their path. Netrin1 has been shown to attract rostro-medial thalamocortical axons and to repel caudo-lateral thalamocortical axons, topographically sorting them within the internal capsule (Powell et al., 2008).

Accordingly, the loss of Netrin1 results in failure of thalamocortical axons to reach the cortex (Braisted et al., 2000). Ephrins also have a role in sorting thalamocortical axons in the internal capsule during their journey to the cortex (Bolz et al., 2004; Cang et al., 2005; Torii and Levitt, 2005). Slit and Robo interactions that result in repulsion of the growth cone, also seem to push thalamocortical axons away from the hypothalamus into the telencephalon, and corticothalamic axons posteriorly into the CGE in the direction of the incoming thalamocortical tract (Bagri et al., 2002; Lopez-Bendito et al., 2007). Netrin-1 is also required to guide thalamocortical axons towards the cortex and to promote the growth of thalamocortical axons (Braisted et al., 2000; Metin et al., 1997). However, its guidance effects on thalamocortical axons have only been demonstrated in vitro. In vitro studies also show Semaphorin isoform D acts as chemorepellent and inhibits axonal branching of corticothalamic axons Bagnard 1998. In the same study, it has also been shown that another isoform Semaphorin E is attractive for corticothalamic axons, showing multiple guidance roles for Semaphorin family of guidance molecules (Bagnard et al., 1998). A recent study also showed defects in a subset of thalamocortical axons (coming from the dLGN) in reaching their cortical target in Semaphorin6a$^{-/-}$ mutants (Little et al., 2009).

## 1.8 *Gli3* is a key regulator of forebrain development

*GLI3* encodes a zinc finger transcription factor, expression of which starts early (around E7.5) in embryonic development Hui 1994. It is located on chromosome 17p13 in humans and its murine homologue is located on chromosome 13 (Vortkamp et al., 1991). There are other *GLI* genes in human and other mammals: *GLI1* and *GLI2*. *GLI2* and *GLI3* have been identified thanks to their sequence similarity to *GLI1*. All *GLI* genes have a high degree of homology with the *cubitus interruptus* (*ci*) gene in *Drosophila* (Orenic et al., 1990), and act in the *sonic hedgehog* (*Shh*) and Hh pathway in vertebrates and Drosophila, respectively (Ingham and McMahon, 2001; Litingtung and Chiang, 2000a; Litingtung and Chiang, 2000b; Ruppert et al., 1990; Wang et al., 2000). *GLI3* operates at different time points during development and in different organ systems. The best-characterised sites of *GLI3* expression and function are the central nervous system (CNS) and the limb bud. Indeed several *GLI3* mutations are associated with head and limb defects in humans.

## 1.9 Different *Gli3* mutations cause several human syndromes

*GLI*3 is mutated in the following human syndromes: Greig Cephalopolysyndactyly Syndrome (GCPS) (Biesecker, 2006; Johnston et al., 2003; Vortkamp et al., 1991; Wild et al., 1997), Acrocallosal Syndrome (ACS) (Elson et al., 2002), Pallister-Hall Syndrome

(PHS) (Biesecker, 2006; Bose et al., 2002; McCann et al., 2006) (Biesecker, 2006; Biesecker and Johnston, 2005), Polydactylysyndromes (PAP-A, PAP-A/B, PPD-IV) and Crossed Polydactyly Type I (Cheng et al., 2006).

GCPS and ACS patients display similar defects. Indeed, both GCPS and ACS patients display pre- and postaxial polydactyly and craniofacial abnormalities, manifested as macrocephaly and hypertelorism with an enlarged nasal bridge (Elson et al., 2002; Johnston et al., 2003). However, patients with ACS lack the corpus callosum and are severely mentally retarded (Elson et al., 2002), while patients with GCPS prevalently display a normal intellectual development, even if, sometimes, cases of mental retardation have been reported in GCPS patients (Bonatz et al., 1997). GCPS and ACS are often caused by deletions of the *GLI3* gene that involve the zinc finger coding region, but also frameshift, nonsense, splice site and translocation mutations have been found (Biesecker, 2006; Johnston et al., 2003; Vortkamp et al., 1992; Vortkamp et al., 1991; Wild et al., 1997). However, it has been suggested that mutations in ACS patients could also involve other genes flanking the *GLI3* coding region, explaining the differences between ACS and GCPS patients (Johnston et al., 2003). Otherwise, it could be that these two syndromes are different manifestations of the same disorder. Recently, an ACS patient has been shown to have a point mutation in the *GLI3* gene (Elson et al., 2002). This mutation affects a conserved amino acid resulting from a G to C substitution, but how this affects the proprieties of the Gli3 protein is still unclear. However, because of their similarities these syndromes are sometimes confused and a patient classified with ACS could instead be a GCPS patient and vice-versa.

In contrast, the clinical features of PHS have only limited similarities with those of ACS

and GCPS (Biesecker, 2006; Bose et al., 2002; Kang et al., 1997). These patients display central or postaxial polydactyly, hypothalamic hamartoma, bifid epiglottis, pulmonary segmentation anomalies and imperforate anus. PHS is normally caused by nonsense and frameshift mutations in the 3' region of the gene that lead to truncation mutations (Biesecker, 2006). These kinds of mutations are supposed to interfere with the posttranslational modification of *GLI3*.

Polydactyly syndromes (PAP-A, PAP-A/B, PPD-IV) are characterized by a postaxial extra finger and toe in the hands and in the feet, respectively. These mutations are caused by deletions in the *GLI3* gene that lead to frameshift mutations and the formation of truncated proteins (Biesecker, 2006; Biesecker and Johnston, 2005).

Crossed Polydactyly Type I (CP Type I) is also characterized by polydactyly, but in these patients postaxial polydactyly of the hand is combined with preaxial polydactyly of the feet (Cheng et al., 2006). A recent report shows the presence of a point mutation in 28 members of a Chinese family affected by CP Type I. This mutation is supposed to lead to a truncated GLI3 protein. Moreover, this finding enlarges the spectrum of different malformation caused by mutations in the *GLI3* gene (Cheng et al., 2006). However, it is still unclear how all these different *GLI3* isoforms caused by all these different mutations produce such a large spectrum of phenotypes.

## 1.10 Different mouse models are available for the study of *Gli3 in vivo*

To gain insight into the role of *GLI3* in vivo, several mutant mice for *Gli3* have been used. The best characterized *Gli3* mouse mutant to date is the *extra-toes* ($Xt^J$) mutant (Johnson, 1967a). $Xt^J$ mutants have a deletion of 51.5 Kb that includes part of the zinc finger coding domain of the *Gli3* gene and the complete 3' coding region (Maynard et al., 2002). These mutants completely lack *Gli3* function.

A second *Gli3* mutation ($Xt^H$) is known that results in loss of part of the promoter and 5' coding region (Schimmang et al., 1992; Schimmang et al., 1993; Vortkamp et al., 1991). This mutation does not lead to any functional transcript and the $Xt^H$ has an almost identical phenotype to $Xt^J$. Both these mutants, $Xt^J$ and $Xt^H$, are considered as a model of GCPS (Hui and Joyner, 1993).

A third allelic mutation is known for *Gli3* in mouse that is called *Polydactyly Nagoja* (*Pdn*) (Hayasaka et al., 1980), which is caused by the integration of a retrotransposon into the third intron of the *Gli3* gene and which results in a reduced level of wild-type *Gli3* transcripts and in the formation of two classes of novel transcrips by alternative splicing (Thien and Rüther, 1999) and (Fig 1.6). Class I transcripts contain out of frame insertion, which lead to three truncated proteins that do not contain the zinc finger domain, and therefore should not maintain any transcriptional activity (Fig 1.6). Class II transcripts contain in-frame insertion that lead to two longer proteins containing the zinc finger domain (Fig 1.6). However, it is unknown whether these longer isoforms maintain

any transcriptional activity. Due to the reduction of *Gli3* wild type transcripts and to the qualitatively similar but quantitatively weaker phenotypes compared to $Xt^J/Xt^J$ mutants the *Pdn* allele is regarded as hypomorphyc allele (Thien and Ruther, 1999).

A fourth mutation is known to exist for the *Gli3* gene in mouse: the *add* allele was generated by the insertion of a transgene in the promoter region that leads to a reduction of *Gli3* gene expression (Schimmang et al., 1993). The phenotype of this mutant is weaker in comparison with the others.

It is possible to generate an allelic series of *Gli3* mutants by crossing $Xt^J/+$ and *Pdn*/+ mutants. The result is the production of mutants qualitatively similar but with increasingly weaker phenotype, with $Xt^J/Xt^J$ having the strongest and *Pdn*/*Pdn* the weakest phenotype (Kuschel et al., 2003).

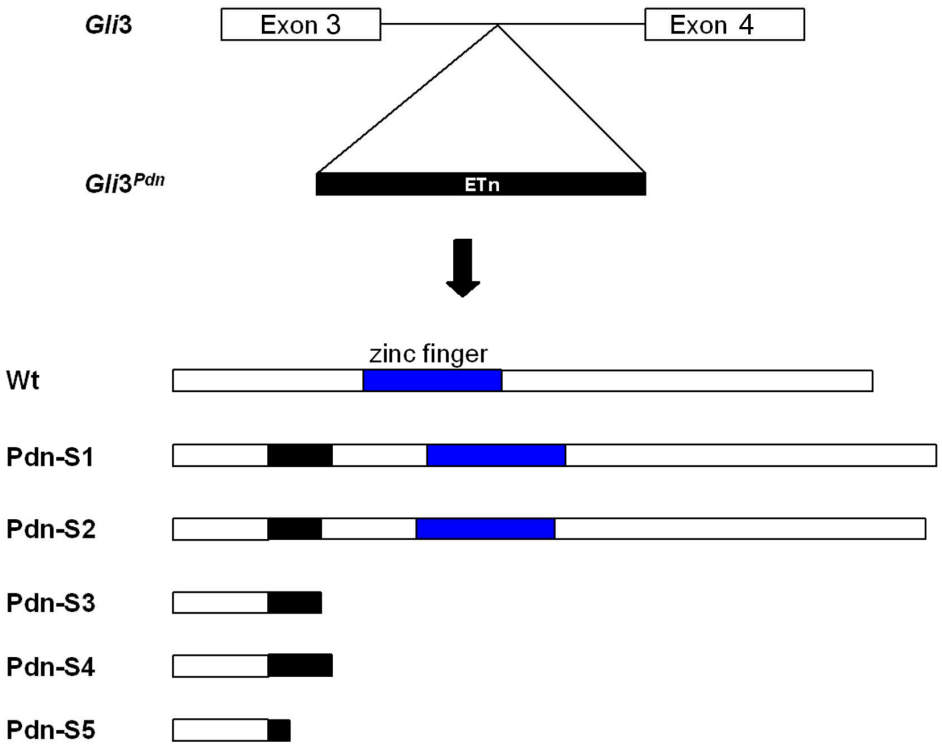


**Figure 1.6.**

**The *Polydactyly Nagoya* (*Pdn*) mutation is caused by retrotransposal integration into the *Gli3* gene**

The *Pdn* mutation is caused by the integration of a retrotransposon into the third intron of the *Gli3*, gene which leads to alternative spicing and a reduction in the wild-type *Gli3* transcript level. In addition, novel classes of transcripts are produced (*Pdn-S1* to *Pdn-S5*). The first type is predicted to produce truncated proteins that are non-functional, because they lack the zinc finger domain (*Pdn-S3* to *Pdn-S5)*. The second type of transcript encodes longer proteins with an insertion of 56 or 61 amino acids in the N-terminal domain (*Pdn-S1* and *Pdn-S2)*; these isoforms contain the zinc finger domain (in blue) and could act as transcriptional regulators.

## 1.11 *Gli3* in forebrain development

Great progress in the clarification of the role of *Gli3* in brain development has been achieved by the analysis of $Xt^J/Xt^J$ mutants (Johnson, 1967b). However, these studies are limited to the embryonic stages of $Xt^J$ mutants because these mice die perinatally. Moreover, these studies are also complicated by the fact that these mutants show a high level of exencephaly, a failure to close the neural tube in the most rostral regions of the brain (Grove et al., 1998) where the neural tissue starts to over-grow abnormally. This defect has a high correlation with the genetic background of the mice.

In mutant mice that do not display exencephaly the strongest and most evident defect is the failure to invaginate the dorso-medial telencephalon leading to the absence of the hippocampus, the choroid plexus and the cortical hem. The olfactory bulbs are also missing (Theil et al., 1999b). The use of $Xt^J/Xt^J$ mutants mice has revealed that *Gli3* plays an important role in the regionalization of the dorsal telencephalon, by controlling the establishment and the maintenance of two of the three telencephalic signalling centres expressing *Bmp/Wnt, Fgf8*.

The cortical hem is an important site of *Wnt* and *Bmp* gene expression in the forebrain. It is also important for the development of the hippocampus (Grove et al., 1998) and a source of Cajal Retzius cells (Meyer et al., 2002). $Xt^J/Xt^J$ mutants display an absence of the expression of *Wnt2b, 3a and 5a* (Tole et al., 2000b) which are expressed in the territories corresponding to the cortical hem (Grove et al., 1998). *Wnt8b and Wnt7b* are still (also if abnormally and weekly) expressed in the dorsal telencephalon of $Xt^J/Xt^J$

mutants, but expression of *conductin*, which is a direct target of *Wnt* canonical signalling, is absent from the dorsal $Xt^J/Xt^J$ telenecphalon suggesting the absence of canonical *Wnt* signalling (Theil, 2005). $Xt^J/Xt^J$ mutant also lack the expression of *Bmp2, 4, 6* and *7*. These genes are normally expressed in the choroid plexus and cortical hem of wild type embryos, which are also missing in $Xt^J/Xt^J$ mutant (Theil et al., 1999b; Tole et al., 2000b).

The $Xt^J/Xt^J$ dorsal telencephalon displays ectopic *Fgf8* expression (Theil et al., 1999b). Starting from E 8.5 *Fgf8* and its direct target gene *Sprouty2* are expressed at the rostal end of the telencephalon in the anterior neural ridge (Aoto et al., 2002; Theil et al., 1999b). In $Xt^J/Xt^J$ mutants *Fgf8* and *Sprouty2* expression is expanded in the dorso-medially telencephalon from E9.5 (Aoto et al., 2002; Kuschel et al., 2003; Theil et al., 1999b).

Dorso-ventral patterning in the telencephalon is also affected in $Xt^J/Xt^J$ mutants. *Gli3* mutants display a ventralization of the dorsal telencephalon (Kuschel et al., 2003; Tole et al., 2000b). Several genes such as *Mash1, Dlx2, Dlx5* and *Isl1*, whose expression is normally restricted to the ventral telencephalon are ectopically expressed in dorsal telencephalon of $Xt^J/Xt^J$ mutants. This effect is particularly dramatic in the rostral region of the telencephalon, spatially and temporally coinciding with Fgf8 up-regulation (Aoto et al., 2002; Kuschel et al., 2003; Tole et al., 2000b). Interestingly, at least until E12.5, *Shh* expression is restricted to the ventral telencephalon (Aoto et al., 2002; Theil et al., 1999b; Tole et al., 2000b). Also, at E9.5 expression of *Shh* target gene *Patched1 (Ptc1)* remains restricted to the ventral telenecphalon (Theil et al., 1999b; Tole et al., 2000b).

In addition, in $Xt^J/Xt^J$ mutants the boundary between the dorso-medial telencephalon and the diencephalon is compromised (Theil et al., 1999a) leading to the mixing of di- and telencephalic cells (Fotaki et al., 2006). The use of $Gli3^{-/-}$ chimeric mice has recently demonstrate that *Gli3* is required cell-autonomously to repress diencephalic or ventral-telencephalic fate for dorsal telencephalic cells to acquire cortical identity (Quinn et al., 2009). The $Xt^J/Xt^J$ dorsal telencephalon displays a strong reduction of *Emx2* expression in the dorsal thelencephalon from E8.5 (Theil et al., 1999b; Tole et al., 2000b). *Emx1* expression instead is completely lacking from the $Xt^J/Xt^J$ dorsal telencephalon (Theil et al., 1999b; Tole et al., 2000b). The $Xt^J/Xt^J$ dorsal telencephalon also displays a disruption of the *Pax6* high dorso-lateral and low dorso-medial gradient (Aoto et al., 2002; Kuschel et al., 2003) and a slight reduction of *Otx1* (Theil et al., 1999b). Previous studies on $Xt^j/Xt^j$ mutants also started to investigate the role of *Gli3* in the ventral telencephalon (Yu et al., 2009a). In this work it has been shown that $Xt^j/Xt^j$ mutants display an increase in ventral telencephalic neural differentiation and apoptosis at E10.5, leading to abnormal growth of the ventral telencephalon and consequently anatomical distortions of the telencephalon.

Several studies have reported severe defects in the process that leads to the layered structure of the cerebral cortex in *Gli3* mutant mice (Fotaki et al., 2006; Friedrichs et al., 2008; Kuschel et al., 2003; Theil, 2005; Theil et al., 1999b). $Xt^J/Xt^J$ mutants display defects in the early steps of cortical lamination, which involve the organization of the marginal zone, the cortical plate and the early subplate. The $Xt^J/Xt^J$ developing cortex does not form layers but cortical progenitors are arranged in clusters losing their apical-basal cell polarity (Theil, 2005). In this study, these defects correlate with a reduction in

number and an organization into clusters of Cajal-Retzius cells. However, the size of the $Xt^J/Xt^J$ cerebral cortex is strongly reduced in size and completely degenerates in newborn mice. These defects are too severe to allow investigation into the role of *Gli3* in later aspects of brain development including the formation of the different cortical layers. The hypomorphic mutant *Pdn* is more appropriate for studying the role of *Gli3* in cortical lamination. As mentioned before, by crossing $Xt^J$/+ and *Pdn*/+ mutants it is possible to generate an allelic series of *Gli3* mutants. In $Xt^J/Pdn$ embryos, dorso-ventral telencephalic patterning and ventralization of the dorsal telencephalon are not as severely affected as in $Xt^J/Xt^J$ (Kuschel et al., 2003). For example $Xt^J/Pdn$ mutants do not diplay mixing of diencephalic and telencephalic cells, forming molecular separation between the dorsal telencephalon and the diencephalon (Friedrichs et al., 2008). However, *Wnt2b* expression in the cortical hem is still missing in these mutants while *Bmp4* expression is strongly reduced (Kuschel et al., 2003). $Xt^J/Pdn$ mutants display severe defects in cortical lamination with abnormal distribution of *Sox5*, *Tbr1*, *Cux1*, *Ror-*$\beta$ expressing neurons, which remain in the cortical ventricular zone Friedrichs 2008. The early developing $Xt^J/Pdn$ cortex also displays clusters of Cajal-Retzius cells and of radial glial fibres (Friedrichs et al., 2008).

## 1.12 Gli3 is involved in the Shh signalling pathway

*Gli3* together with *Gli1* and *Gli2* is a downstream effector of the *Shh* signalling pathway (Murone et al., 1999). In the presence of *Shh* all three *Gli* genes act as transcriptional

activators, activating transcription of *Shh* target genes (Ruiz i Altaba, 1998; Sasaki et al., 1999). Interestingly, *Gli3* also works as a transcriptional repressor in the absence of *Shh*, repressing *Shh* target genes (Persson et al., 2002; Ruiz i Altaba, 1998).

Different regions of the *Gli3* protein encode different transcriptional activities, with the N-terminal region encoding transcriptional repressor activity, while the activator activity resides in the C-terminus (Aza-Blanc et al., 2000; Ingham and McMahon, 2001). Proteolytic cleavage, which occurs in the absence of *Shh* and which removes the Gli3 C-terminal activator domain, controls the transition between the *Gli3* transcriptional activator form and the repressor form (Marigo et al., 1996; Wang et al., 2000). Gli3 repressor is most prominent in the dorsal telencephalon where *Shh* signalling is absent, while Gli3 activator is more abundant in the ventral telencephalon (Fotaki et al., 2006). Therefore, it is probably the ratio between these two forms that is important in patterning the dorso-ventral telencephalon. To ultimately activate *Gli* genes, *Shh* has to bind to the membrane receptor Ptc1 (Goodrich et al., 1996). This binding relieves the repression that Ptc1 has on the associated receptor smoothened (Smo), activating the signal cascade that result in *Gli* activation and nuclear translocation (Murone et al., 1999; Taipale et al., 2002; Zhang et al., 2001).

Several studies link cilia with *Shh* signalling (Han et al., 2008; Huangfu and Anderson, 2005; Liu et al., 2005). Cilia are microtubule-based subcellular organelles, which have recently been implicated in a wide variety of developmental functions, such as left-right asymmetry and limb, kidney, pancreas, and skeleton formation (Bisgrove and Yost, 2006). In addition, in the developing nervous system, mutant embryos with aberrant cilia formation display defects in neural patterning and in closure of the neural tube (Caspary

et al., 2007; Houde et al., 2006; Huangfu and Anderson, 2005; Huangfu et al., 2003; Liu et al., 2005; May et al., 2005; Murcia et al., 2000; Willaredt et al., 2008). Interestingly, Smo receptor localizes on the cilia in response to Shh pathway stimulation Corbit K C 2005. In addition, the three *Gli* proteins are also localized at the distal tip of cilia (Haycraft C J 2005; Chen M-H, Chuang P-T 2009). Indeed, mutant embryos in which cilia formation is affected photocopies the telencephalic defects of the $Xt^J/Xt^J$ mutant embryos (Willaredt et al., 2008). Also, the cleavage that transforms *Gli3* activator into *Gli3* repressor has been suggested to occur within the cilia. Taken together, these studies suggest a role for these structures in detecting *Shh* molecules in the environment and transducing its signal in central nervous system (Whitfield, 2004; Willaredt et al., 2008).

Although all three *Gli* genes function downstream of *Shh, Gli3* appears to be the major player in dorsal telencephalic development for progenitor cells responding to low levels of Shh signalling. *Gli1* is probably redundant with the other *Gli* genes, because *Gli1* mutants do not show any obvious forebrain phenotype (Park et al., 2000). On the contrary, the role of *Gli2* is necessary for the formation of the floor plate throughout the CNS, in regions responding to high levels of Shh signalling, including the ventral telencephalon, but *Gli2* mutants mice do not have any dorsal telencephalic phenotypes (Ding et al., 1998; Matise et al., 1998; Park et al., 2000; Yu et al., 2009b). In addition, the importance of *Gli3* in dorsal telencephalic cells is shown by the severity of dorsal telencephalic defects of $Xt^J/Xt^J$ mutants, where none of the other *Gli* genes can compensate for its absence (Theil et al., 1999b; Tole et al., 2000b).

$Xt^J/Xt^J$ mutants do not seem to display severe defects in the patterning of the ventral telencephalon. However, until a very recent work by Yu et al. (2009) it was not even

known whether Gli activators are required for patterning the ventral telecephalon. This work showed that in the absence of *Gli1* and *Gli2* the ventral telencephalon lacks *Nkx2.1* and *Nkx6.2* expression in two subgroups of progenitors on both sides of the sulcus separating LGE and MGE (Yu et al., 2009b). In addition, the PSPB of *Gli2/3* double mutants displays a dorsal expansion of *Gsh2* and *Dlx2* expression into the lateral cortex, while the *Gli2/3-/-* ventral telencephalon displays a reduction of ventral telencephalic markers, including *Lhx6, Ebf1* and *GAD67* (Rallu et al., 2002; Yu et al., 2009b). It is therefore likely that in $Xt^{J}/Xt^{J}$ mutants *Gli2* can compensate for the loss of the Gli3 activator form during ventral telencephalic development and vice versa Gli3 activator form compensates for the loss of Gli2 in *Gli2* mutants, as it happens in the spinal cord (Park et al., 2000). Interestingly, this study also shows the importance of *Shh* signalling, which is completely abolished in *Gli2/3* double mutants, for patterning different sub-regions of the ventral telencephalon (Yu et al., 2009b).

## 1.13 *Gli3* and *Shh* counteract each other in patterning the ventral telencephalon

Importantly, several studies have shown an antagonizing role of *Shh* and *Gli3* in different organ systems, for example in the spinal cord and limb bud. Indeed, removal of one copy of *Gli3* in *Shh* null mutants rescues many of the ventral defects in the $Shh^{-/-}$ spinal cord (Litingtung and Chiang, 2000b; Park et al., 2000). A similar rescue was also observed in the limb bud (Litingtung et al., 2002). Removal of *Gli3* in $Shh^{-/-}$ mutants and

*Smo*$^{-/-}$ mutants largely restores the ventral telencephalic patterning, confirming that *Gli3* and *Shh* antagonize each others effects in patterning the ventral telencephalon (Rallu et al., 2002). This result also shows that a mechanism working in parallel to *Shh* could be important in patterning the ventral telencephalon. A candidate molecule that mediates this alternative patterning process could be *Fgf8* (Gutin et al., 2006; Kuschel et al., 2003). However, *Fgf8* also is indirectly regulated by *Shh* through *Gli3* repressor form (in fact Fgf8 is up regulated in *Gli3* mutants). In this scenario it is probable that while *Fgf8* directly promotes ventral telencephalic fate, *Shh* indirectly promotes ventral telencephalic fate by restricting Gli3R activity.

In both *Gli3* and *Shh* mutants the dorsomedial telencephalon fails to develop (Chiang et al., 1996; Grove et al., 1998; Theil et al., 1999b). However, the dorsomedial telencephalon is not rescued in *Gli3* and *Shh* double mutants, as a dorsal expansion of several *Fgfs*, such us *Fgf15* and *Fgf8,* persists (Rash and Grove, 2007). These data point away from an involvement of *Shh* in dorsomedial telencephalic defects suggesting Gli3 repressor and Fgf signalling as better candidates in patterning this region. In addition, removal of *Pax6* from *Shh* null mutant seems to rescue *Wnt8b* and *Bmp4* expression in the dorsomedial telencephalon, suggesting that *Pax6* upregulation may be partially responsible for the dorsomedial phenotype in *Shh* null mutants (Fuccillo et al., 2006b).

## 1.14 Aims of the thesis

The role of *Gli3* in the regionalization of the telencephalon is well known, thanks to the use of the *Gli3* null mutants $Xt^J$. However, defects in $Xt^J/Xt^J$ mutants are too severe to allow the analysis of later roles of *Gli3* in forebrain development, like the development of the major axon tracts in the forebrain. In addition, mutations in the *GLI3* gene have been found in human patients with ACS. These patients lack the corpus callosum and are severely mentally retarded (Elson et al., 2002). This suggests that G*LI3* may be involved in the formation of the corpus callosum and potentially in the formation of other axonal tracts projecting from or connecting to the cerebral cortex. For these reasons I started to study telencephalic development in the *Gli3* hypomorphic mutant *Pdn*. Such an analysis may also provide additional insights into the pathomechanisms of ACS.

The first aim of the work presented here is to analyze the formation of the major axonal tracts in the forebrain of the *Pdn/Pdn* hypomorphic mutants. Indeed, evaral experiments revealed, together with the absence of the corpus callosum, several axonal guidance mistakes of thalamocortical and corticothalamic axons. In the following two parts, I addressed the possible molecular and cellular mechanisms leading to defects in the *Pdn/Pdn* thalamococtical and corticothalamic tracts. To do that I investigated the correct formation of the *Pdn/Pdn* cortex and thalamus from which cortical and thalamic axons originate, respectively. No major defects in the development of the *Pdn/Pdn* cortex and thalamus were found. In contrast, abnormalities were found in the formation of some

ventral telencephalic axon guidance cues. I therefore characterized patterning of the *Pdn/Pdn* ventral telencephalon, defects in which may explain abnormalities in the formation of these intermediate targets. I could identify growth and regionalization defects in the *Pdn/Pdn* LGE. Finally, these patterning defects correlated with an upregulation of Shh signalling in the ventral telencephalon of *Pdn* mutants.

# Chapter 2: Materials and Methods

## 2.1 Animals

### 2.1.1 Animal husbandry

*Pdn* heterozygous animals were kept on a C3H/He background and were interbred. Heterozygous and wild-type embryos did not show qualitatively different phenotypes and were indiscriminately used as control embryos designated as *Pdn*/+ unless otherwise stated. In case of quantitative analyses, wild-type and *Pdn*/*Pdn* embryos were compared to have a more accurate quantification of potentially subtle defects. For each marker and each stage, 3-5 different, non-exencephalic embryos were analysed at rostral, medial and caudal levels of the developing forebrain. *Golli-tau-GFP* (Jacobs et al., 2007) and *tau-GFP* mice (Pratt et al., 2000a) were crossed with *Pdn* heterozygous animals and kept on a mixed background.

### 2.1.2 Preparation of embryos

For the isolation of staged embryos, embryonic (E) day 0.5 was assumed to start at midday of the day of vaginal plug discovery. On the day at which embryos were required, pregnant females were sacrified by cervical dislocation and the uteri removed from the abdomen. Embryos were dissected out of their deciduas into cold PBS using forceps. For retrospective genotyping embryo tails were placed in a separate 1.5 ml tube for genomic DNA extraction (see 2.2.1). Embryos were fixed in 4% Paraformaldehyde

(PFA) for two hours on a tumbler to ensure even fixation. Alternatively, embryonic tissue was transferred into liquid $N_2$ and stored at -80°C until further preparation (e.g. RNA isolation).

All mouse experiments were performed in accordance with Home Office guidelines on animal welfare.

### 2.1.3 Brain/heads preparation

Whole embryonic heads (until E14.5) or brains were dissected away from their skulls (from E16.5 to P0) and were placed in 4% PFA/PBS overnight at 4°C and then prepared according to the requirement of the technique of sectioning.

For **vibratome sectioning**, fixed samples were washed several times in PBS with shaking at room temperature and then positioned in molten 4% low melting agarose/dd$H_2O$ and allowed to set on ice. Either 100 µm or 200 µm thin sections were cut coronally using a VT 1000S vibratome (Leica).

For **cryostat sectioning,** fixed samples were washed once in PBS at room temperature and then placed in a 30% sucrose/PBS solution overnight at 4°C. The day after, samples were embedded in OCT (sigma) and then frozen in liquid nitrogen. OCT embedded heads were sectioned at 15-25 µm using a CM3050S cryostat (Leica). Sections were collected onto Superfrost Plus (VWR International) slides and allowed to dry over night at 4°C.

For **microtome sectioning**, fixed samples were washed once in PBS at room temperature and then placed in 70% ethanol (EtOH)/dd$H_20$ solution overnight at 4°C.

Subsequently, samples were embedded in paraffin wax using an automated tissue processor (Tissue-Tek, VIP, Sakura). Wax embedded heads were sectioned coronally in 12.5 µm using a microtome (Reichert, Jung 2050). Sections were floated (from a water bath at 55°C) onto Superfrost Plus (VWR International) slides and allowed to dry over night at 37°C.

## 2.2 PCR

### 2.2.1 Mouse genotyping

Mouse ear clips or embryo tails were digested in 100 µl of DirectPCR Lysis Reagent (Tail) from Viagen containing 200 µg/ml proteinase K at 55°C for 2 hours in an thermomixer (Eppendorf) at 1400 rpm. To heat inactivate proteinase K, this solution was incubated at 85°C for 45 minutes. 1µl of this solution was directly used in PCR reactions.

All PCR reactions were performed in a total volume of 25 µl containing 1µl 10mM dNTPs, 5 µl 5X Green GoTaq Reaction Buffer (which includes 1.5 mM of $MgCl_2$), 0.25 µl GoTaq DNA polymerase (5 u/µl) from Promega, 16.5 µl sterile $ddH_2O$, and 0.5µl of each primer at a concentration 10 µM (Table 2.2).

For ***Pdn*** genotyping the thermal cycling conditions were as follows: hot start at 95°C for 3 minutes, followed by a 30 cycle reaction with 1 minute denaturing at 94°C, 1 minute annealing at 55°C, and 1 minute extension at 72°C, plus 7 minutes at 72°C.

For ***Golli tau GFP*** genotyping the PCR conditions were as follows: hot start at 95°C for 3 minutes, followed by a 30 cycle reaction with 30 seconds denaturing at 94°C, 30 seconds annealing at 60°C, and 30 seconds extension at 72°C, plus 7 minutes at 72°C. This analysis did not allow discrimination between wild-type and heterozygous animals and embryos.

The PCR products were loaded on 2% agarose gels containing 1X TAE buffer including SYBR Safe (Invitrogen). After 30 minutes electrophoresis at 110V products were visualized under ultraviolet light.

**Table 2.1 PCR Primers for genotyping**

| **Allele** | **Primer** | **Sequence** | **Band size bp** |
|---|---|---|---|
| ***Gli3*** | F5<br>PdnR6 | 5'-GTTCAAGTTCGTGCATAGCTACCAGGTTCC-3'<br>5'-TGTTTCCCATTGTCCAACCCTACCC-3' | 214 |
| ***Pdn*** | Pdn Etn 11F<br>PdnR6 | 5'-TTGAGCCTTGATCAGAGTAACTGTC-3'<br>5'-TGTTTCCCATTGTCCAACCCTACCC-3' | 180 |
| ***Golli τ-GFP*** | GFP 3119<br>TAU 2070 | 5'-GTCGGCCATGATATAGACGTT-3'<br>5'-GAGAGGTGAATCTGGGAAATC-3' | 1100 |

***Tau-GFP*** mice and embryos were genotyped by direct observation of the mouse ear clips and embryonic brains under a fluorescent microscope. All the genotyped *GFP* animals and embryos were heterozygous because homozygous embryos dies at gastrulation (MacKay et al., 2005).

### 2.2.2 Quantitative RT-PCR

Embryonic brain tissue was dissected from the ventral telencephalon of E12.5 +/+ and *Pdn/Pdn* embryos including LGE and MGE. Total RNA was extracted using an RNAeasy Micro kit (Qiagen, Valencia, CA) according to the manufacturer's instructions. The RNA concentraction was measured using a NanoDrop (Thermo Scientific) Using ImProm-II Reverse Transcriptase (Promega) to generate cDNA, 500 ng of RNA was reverse transcribed with oligo (dT)-15 primers (Promega, Madison, WI) according to the manufacturer's instructions.

To quantify specific gene expression, I used quantitative RT-PCR (qRT-PCR) on ventral telencephalic cDNA from wild-type and *Pdn/Pdn* mutants. qRT-PCR was done using Qiagen Quantitect SYBR Green PCR Kit as described by the manufacturer's instructions and a DNA Engine Opticon Continuous Fluorescence Detector (Genetic Research Instrumentation, Essex, UK). Target cDNA was normalized to the control house keeping gene glyceraldehyde-3-phosphate-dehydrogenase (*GAPDH)* (Table 2.2) and expression levels were calculated from standard curves generated from a concentration series of cDNAs isolated from the ventral telencephalon of wild-type brains. The PCR was as follows: hot start at 95°C for 15 minutes, followed by a 40-45 cycles reaction

with 15 seconds denaturing at 94°C, 30 seconds annealing at 60°C, and 30 seconds extension at 72°C.

**Table 2.2 qRT-PCR primers.**

| Gene | RefSeq NCBI | Sequence | Transcript region |
|---|---|---|---|
| ***Gli1*** | NM_010296.2 | For: 5-'GTTATGGAGCAGCCAGAGAG-3'<br>Rev: 5'-GAGTTGATGAAAGCCACCAG-3' | 316-505 |
| ***Ptch1*** | NM_008957.2 | For: 5'-GCATTCTGGCCCTAGCAATA-3'<br>Rev: 5'-CAACAGTCACCGAAGCAGAA-3' | 3945-4096 |
| ***Shh*** | NM_009170.2 | For: 5'-ATTTTGTGAGGCCAAGCAAC-3'<br>Rev: 5'-CAGGAGCATAGCAGGAGAGG-3' | 2037-2140 |
| ***GAPDH*** | XM_001476723.1 | For: 5'-AGGTTGTCTCCTGCGACTTCA-3'<br>Rev: 5'-CCAGGAAATGAAGCTTGACAAAG-3' | 747-891 |

## 2.3 Histology

### 2.3.1 Cresyl violet staining

Heads were prepared and processed as outlined in section 2.1.3. Paraffin sections were de-waxed in xylene with 2 washes of 15 minutes and rehydrated through an alcohol series in $ddH_2O$ (100% EtOH, 96% EtOH, 90% EtOH, 70% EtOH, 50% EtOH, $ddH_2O$ 1 minute each). Sections were washed in Potassium Sulfit (50% Potassium Sulfit in $ddH_2O$) for 15 minutes at room temperature, then in $ddH_2O$ 2 times for 1 minute. Sections were immerged in Cresyl violet solution (1.5% Cresyl violet in acetate buffer: 245ml $H_2O$ + 2.5ml 1M sodium acetate + 2.5ml 1M acetic acid) for 20 minute at room temperature, then washed 2 times in acetate buffer for 1 minute. Differentiation reaction was performed to eliminate the excess of Cresyl violet form the sections in differentiation solution ($ddH_2O$ with few drops of glacial acetic acid) for 30-40 seconds and repeated if necessary. Sections were then dehydrated through an alcohol series (50% EtOH, 70% EtOH, 90% EtOH, 100% EtOH 1 minute each, and xylene 2 times for 10 minutes) and mounted in DPX.

### 2.3.2 Immunofluorescence on vibratome sections

Heads were prepared and processed as outlined in section 2.1.3. 100 µm vibratome sections were blocked using blocking solution (PBS/0.5% TritonX-100 + 20% sheep serum) for 1hour at room temperature. Primary antibodies diluted (Table 2.3) in blocking solution were added to the sections and then stored overnight at room

temperature. Sections were washed 3 times for 10 minutes in PBS and then Cy2- and/or Cy3-conjugated secondary antibodies diluted (Table 2.4) in blocking solution + 0.2 µM TOPRO3 were added and stored 2 to 4 hours at room temperature. The sections were washed 3 times in PBS for 10 minutes and subsequently mounted in Mowiol (polyvinyl alcohol 4-88) (Fluca) plus some crystals of 1,4-diazabicyclo 2.2.2 octane (Dabco) to avoid bleaching.

**Table 2.3 Primary antibodies used in this thesis**

| Antibody | Origin | Dilution on vibratome sections | Dilution on cryo sections | Dilution on paraffin sections | Company |
|---|---|---|---|---|---|
| Neurofilament (2H3) | Mouse | 1:10 | 1:10 | 1:3 | DSHB |
| GFP | Rabbit | 1:1000 | 1:1000 | - | ABCAM |
| Glast | Guinea Pig | 1:5000 | 1:5000 | - | CHEMICON |
| Islet1/2 (39.45) | Mouse | 1:200 | 1:100 | 1:200 | DSHB |
| reelin | Mouse | - | - | 1:2000 | Provided by Andre M. Goffinet |
| Tbr1 | Rabbit | 1:2500 | 1:2500 | 1:2500 | CHEMICON |
| Gsh2 | Rabbit | 1:2000 | 1:2000 | 1:2000 | Provided by Kenneth Campbell |
| Pax6 | Mouse | 1:200 | 1:200 | 1:200 | DSHB |
| Tuj1 | Mouse | 1:1000 | 1:1000 | 1:500 | Sigma |
| pHH3 | Rabbit | 1:200 | 1:200 | 1:200 | Upstrate |
| BrdU | Rat | - | 1:50 | 1:50 | ABCAM |
| IdU/BrdU | Mouse | - | 1:50 | 1:50 | BD bioscience |

**Table 2.4 Secondary antibodies used in this thesis**

| Antigen | Conjugated with | Origin | Dilution on cryo, paraffin and vibratome sections | Company |
|---|---|---|---|---|
| Rabbit IgG | Alexa647 | goat | 1:200 | Molecular Probes |
| Mouse IgG | Alexa647 | goat | 1:200 | Molecular Probes |
| Rabbit IgG | Biotin | goat | 1:400 only on wax | DAKO |
| Mouse IgG | Biotin | goat | 1:400 only on wax | DAKO |
| Rabbit IgG | Cy2 | donkey | 1:100 | Jackson/Dianova |
| Mouse IgG | Cy2 | donkey | 1:100 | Jackson/Dianova |
| Rabbit IgG | Cy3 | donkey | 1:100 | Jackson/Dianova |
| Mouse IgG | Cy3 | donkey | 1:100 | Jackson/Dianova |
| Guinea pig IgG | Cy3 | donkey | 1:100 | Jackson/Dianova |
| Mouse IgM | Cy3 | donkey | 1:100 | Jackson/Dianova |
| Rat IgG | Cy3 | donkey | 1:100 | Jackson/Dianova |
| DIG | Alkaline Phosphatase | Sheep | 1:1000 only for in situ hybridization | Roche |

### 2.3.3 Immunofluorescence on cryostat-sections

Heads were prepared and processed as outlined in section 2.1.3. Slides were washed three times in PBS, incubated with 10% sheep/PBS serum for 1 hour. Subsequently, slides were incubated with primary antibodies (Table 2.3) diluted in 10% sheep serum in PBS overnight at room temperature. Slides were then washed 3 times in PBST and the Cy2- and/or Cy3-conjugated secondary antibodies (Table 2.4) were applied for 4 h at room temperature in PBS + 1% sheep serum. Slides were washed once in PBS. Sections were incubated with 0.2 µM TOPRO3 in PBS for 1 to 3 minutes. The sections were

washed 3 to 5 times in PBS and mounted in Mowiol (polyvinyl alcohol 4-88) (Fluca) plus some crystals of 1,4-diazabicyclo 2.2.2 octane (Dabco) to avoid bleaching.

Fluorescence imaging was carried out on a Leica TCS NT confocal microscope. Images were processed and mounted using Photoshop 6.0 (Adobe). For double antibody staining, to avoid cross-reactivity of secondary antibodies, primary antibodies from two different species were selected.

### 2.3.4 Imunohistochemistry on wax sections

Heads were prepared and processed as outlined in section 2.1.3. Sections were de-waxed with 3 washes in xylene of 7 minute each and rehydrated through an alcohol series (100% EtOH 2 times for 2 minutes and then 96% EtOH, 90% EtOH, 70% EtOH, 50% EtOH, dd$H_2O$ 1 minute each). Sections were microwaved for 10 min in 10mM sodium citrate buffer (pH 6). Subsequently, endogenous peroxidase activity was blocked using 3% hydrogen peroxide in methanol.

Sections were encircled with an ImmEdge fat pen (Vector laboratories), incubated in blocking buffer (20% sheep serum in PBS) for 1 hour and followed by incubation with primary antibody (Table 2.3) diluted in blocking buffer at room temperature overnight. Slides were washed 3 times in PBS and were then incubated in secondary biotinylated antibody (Table 2.4) diluted in 1% sheep serum in PBS for 1 to 4 hours, followed by Avidin and Biotinylated horseradish peroxidase macromolecular Complex (ABC) (Vector Laboratories) for 30 minutes. Slides were washed 3 times in PBS and were then stained with 3, 3'-diaminobenzidine (DAB) (Sigma Fast DAB tablets) (Sigma). The

reaction was stopped in $H_2O$. Sections were dehydrated through an alcohol series (50% EtOH, 70% EtOH, 90% EtOH, 100% EtOH 1 minute each, and xylene 2 times for 10 minutes) and mounted in DPX.

### 2.3.5 In situ hybridization on wax sections

#### 2.3.5.1 Generation of DIG-labelled riboprobes

DIG-labelled antisense RNA riboprobes were generated as follows; 1 µl of 1 µg/µl of the linearized plasmid was mixed with 1 µl 10x transcription buffer (Roche, Germany), 1µl DIG RNA Labelling Mix (Roche, Germany), 0.25 µl RNAsin (40 U/ µl) (Promega) and 1 µl of either T3, T7, or Sp6 (20 U/µl) polymerase (Roche) to a final volume of 10 µl. The reaction mix was incubated for 4 hours to overnight at 37°C.

RNA riboprobes were precipitated over night at -20°C using 5 µl 10M $NH_4Ac$ and 40µl 100% EtOH. The precipitation mixes were centrifuged at 13200 rpm for 30 minutes at 4°C and the supernatant discarded. The RNA riboprobes pellets were then washed in 100 µl of 70% EtOH and centrifuged at 13,000 rpm for 1 minute, the supernatant discarded, and the RNA riboprobes were re-suspended in 25µl of Solution I (50% formamide/2x SSC, pH 4.5) and stored at -20°C for several months.

**Table 2.5 In situ hybridization probes used in this thesis**

| Gene | RNA polymerase | Linearization | Plasmid reference | Brain regions marked |
|---|---|---|---|---|
| *Gli3* | T7 | NotI | T. Theil lab | Telencephalic ventricular zone (vz) |
| *Gbx2* | T7 | HindIII | (Wassarman et al., 1997) | Thalamus mantle zone (mz) |
| *Ngn2* | T7 | BamHI | (Gradwohl et al., 1996) | Thalamic and dorsal-telencephalic vz + thalamus mz |
| *Lhx2* | SP6 | SalI | EST2101448 | telencephalic vz + thalamus mz |
| *Emx2* | T7 | EcoRI | (Simeone et al., 1992) | dorsal-telencephalic vz |
| *Dlx2* | T3 | HindIII | (Bulfone et al., 1993) | Ventral telencephalon |
| *Ebf1* | SP6 | XhoI | (Lopez-Bendito et al., 2006) | LGE mz |
| *Nkx2.1* | T3 | BamHI | (Lazzaro et al., 1991) | MGE |
| *Ngr IG* | T7 | NotI | (Lopez-Bendito et al., 2006) | Dorsal-telencephalic vz |
| *Ror-β* | T3 | XhoI | (Hevner et al., 2003) | Cortex, layer IV |
| *Cux2* | T3 | NotI | (Zimmer et al., 2004) | Cortex, layers IV II/III |
| *Six3* | T7 | XbaI | (Oliver et al., 1995) | Ventral telencephalic vz + lateral cortical stream |
| *Dbx1* | T3 | EcoRI | (Yun et al., 2001) | Ventral pallium |
| *Nkx6.2* | T7 | BamHI | (Flames et al., 2007) | Ventricular zone between LGE and MGE |
| *Gsh1* | SP6 | EcoRI | (Valerius et al., 1995) | MGE vz |
| *Shh* | T3 | HindIII | (Echelard et al., 1993) | MGE mz |
| *Gli1* | T7 | HindIII | (Hui et al., 1994) | vz between LGE and MGE |
| *Ptc1* | SP6 | SphI | (Goodrich et al., 1996) | MGE vz |

### 2.3.5.2 In situ Hybridisation

Heads were prepared and processed as outlined in section 2.1.3. Sections were de-waxed with 3 washes in xylene of 7 minute each and rehydrated through an alcohol series in dd$H_2O$ (50% xylene/50% EtOH 2 times for 2 minutes, 100% EtOH 2 times for 2 minutes and 96% EtOH, 90% EtOH, 70% EtOH, 50% EtOH, 1 minute each), then washed twice in PBS for 5 minutes. Slides were then placed in 20µg/ml Proteinase K/PBS for 5 minutes at 37°C. To inactivate Proteinase K, slides were placed in 0.2% glycine/PBS for 5 minutes and washed for 5 minutes 2 times in PBS. Sections were post-fixed in 4% PFA/PBS + 0.2% Gluteraldehyde for 20 minutes and again washed for 5 minutes twice in PBS. Sections were encircled with an ImmEdge fat pen (Vector laboratories) and pre-hybridizaded with 50-80 µl hybridization buffer (50% formamide/2x SSC, pH 4.5 supplemented with 100µg Boehringer Block, 100µl 0,5M EDTA, 100 µl 10% Tween20, 100 µl CHAPS, 200µl 50mg/ml tRNA, and 4 µl 50mg/ml heparin) for 2 hours at 70°C in a humidified chamber containing 50% formamide in dd$H_2O$. RNA riboprobes (Table2.5) were diluted in hybridization buffer, denatured for 5 minutes at 95°C and then placed on ice for 1 minute, before adding onto the sections (5 to 7.5 µl per brain section). Sections were then hybridized in the same humidified chamber overnight at 70°C.

Post-hybridization washes consisted of 2 incubation in Solution I (50% formamide/5x SSC, pH 4.5) for 15 minute at 65°C, and washed 3 times in PBS + 0.1% Tween20

(PBT) at room temperature for 10 minutes each. Sections were incubated for 1 hr in 20µg/ml Boehringer Block in PBT/10% sheep serum (B-Block) at room temperature and then incubated in anti-digoxigenin-antibody (Table 2.4) diluited in B-Block at 37°C for 2 hours. Slides were washed 3 times for 5 minute in PBT and once for 10 minutes in NTM (100 mM NaCl, 100 mM Tris-HCl pH 9.5, 50 mM $MgCl_2$) at room temperature. For the detection of the DIG-labelled RNA's NBT/BCIP stock solution (Roche) was diluted 1/50 in NTM and sections were incubated with this staining solution until adequate colour development was observed. The colour reaction was stopped using several washes in PBS, and slides were mounted in aquatex mounting agent (Merck) before imaging.

### 2.3.6 BrdU and IdU-labelling of S-phase nuclei for cell cycle kinetic analysis

For IdU and BrdU double labelling, pregnant females were intraperitonally injected with 200µl of IdU solution (100 µg/ml in 0.9% NaCl), and after 1.5 hours later with 200µl of BrdU solution (100 µg/ml in 0.9% NaCl). Females were sacrificed 30 minute subsequently to the second injection.

### 2.3.7 Enumeration of BrdU- and IdU-labelled nuclei for cell cycle kinetic analysis

Evenly spaced sections throughout antero-posterior dimension of the embryonic telencephalon were immunofluorescently stained (see 2.3.4) and imaged with a confocal microscope. For each section images were acquired in three channels (appearing red for BrdU labelling, green for BrdU + IdU labelling, and blue for TOPRO-3 staining in all

the figures) as separated files. These images were then staked with Photoshop software and used for the enumeration of the labelled cells as described in Chapter 5.

### 2.3.8 Statistical analyses and graph plotting

Data were statistically analysed and graph plotted with the two computer applications Excel (Microsoft) and SPSS (SPSS software).

## 2.4 Microscopy

### 2.4.1 Light microscopy

Slides were viewed using a Leica DMLB upright compound microscope (Leica, Nussloch, Germany). Images were taken using an attached Leica DSC480 digital camera and the images processed using Leica IM50 image management software.

### 2.4.2 Fluorescence microscopy

Fluorescent staining was observed using a Leica DMRE compound microscope associated with the Leica TCS NT Confocal system using Leica “Lite” software to take images. Alternatively, fluorescent staining was viewed using epifluorescence on a Leica DMLB upright compound microscope with a TRITC filter. Images were taken using an attached Leica DSC480 digital camera and the images processed using Leica IM50 image management software. DiI=red, DiA=green, TOPRO3=blue, Cy2=green, Cy3=red, Alexa-fluor 647=red.

## 2.5 Axon tracing with DiI and/or DiA

Different methods were used to label the thalamocortical and corticothalamic tracts, depending on whether the crystals were injected into the dorsal thalamus or the cortex. Heads were fixed as described in section 2.1.3. 1,1'-dioctadecyl-3,3,3',3'-tetramethyl-indocarbocyanine perchlorate (DiI) crystals and/or 4-(4-dihexadecylamino)styryl-N-methylpyridinium iodide (DiA) crystals were placed in locations that would contact and label axons.

For cortical injections, single crystals of the lipophilic tracer DiI were injected into the cortex of whole brains left intact at three or four symmetrical positions along the rostrocaudal extent of the cortex. For DiI/DiA double labelling only two crystals were injected into each cerebral hemisphere: one of DiI into the caudal cortex and one of DiA into the medial cortex.

For thalamic injections, caudal parts of the brains were removed with a coronal cut to expose the caudal surface of the dorsal thalamus. Injections of single crystals were made at one to three positions along the dorsoventral extent of the dorsal thalamus, depending of the size of the brain.

For callosal axons labelling, rostral parts of the brains were removed with a coronal cut to expose the cortical laminae, crystals were focally injected into the coronally sectioned cortex, above the ventricular zone.

All injections were made by picking up single DiI crystals with pulled glass capillaries and lancing the tissue at each desired location to deposit the crystal. Dyes were allowed to diffuse at room temperature for 4 (for E12.5 brains) to 8 (for E14.5 to P0 brains)

weeks in 4% PFA in PBS at room temperature for cortical and thalamic injections or for 8 days at 37°C for labelling of callosal axons. After DiI and/or DiA diffusion, heads were placed in 4% agarose and 100 µm thin sections were cut at the VT 1000S vibratome (Leica). Sections were cleared in 1:1 glycerol:PBS solution overnight at 4°C, and then further cleared in 9:1 glycerol:PBS solution containing the nuclear counter-stain TOPRO3 (0.2 µM) overnight at 4°C. Subsequently, sections were mounted in 9:1 glycerol:PBS solution on glass slides and sealed with nail polish. Allowed to dry O/N at RT and stored at 4°C.

## 2.6 Organotypic co-cultures

E13.5 embryonic brains were dissected and were washed in Krebs solution (supplemented with 0.5ml Hepes, 0.5ml Pen-Strep, 0.1ml Gentamicin) in a Petri dish at 4°C before positioning them in molten (at 43°C) 4% low melting agarose/PBS (Sea Plaque Agarose) (Lonza) and allowed to set on ice. 300µm thin sections were cut coronally using a VT 1000S vibratome (Leika). Brain slices were cultured on polycarbonate culture membranes (8µm pore size; Corning Costar) in organ tissue dishes (BD Bioscience, Falcon Organ culture dishes) containing 1 ml of medium (Neurobasal/B-27 supplemented with 0.5% Glucose, 10µl Pen-Strep and 10µl Glutamine) (Gibco). Explants were removed from donor tissue with the use of surgical knifes, and transplanted on recipient slices directly on polycarbonate culture membranes. Slices were cultured for 72 hours, fixed with 4% PFA 2 hours at 4°C, vibratome

sectioned (80 µm) using the VT 1000S vibratome (Leika) and processed for anti-GFP immunofluorescence as described in section 2.3.2.

**Table 2.6 Common solutions used in this thesis**

| Solution | Preparation |
|---|---|
| **10x PBS** (pH7.4) | A 2-liter stock can be prepared by dissolving 160 g NaCl, 4 g KCl, 28.8 g $Na_2HPO_4$ and 5.4 g $KH_2PO_4$ in distilled water and topping up to 2 liter. The pH is ~6.8, but when diluted to 1x PBS it should change to 7.4. Check pH of 1x solution before using. |
| **4% PFA** | Pour 100ml of 1x PBS into a conical flask containing 4g of paraformaldehyde. Place flask on top of the hotplate/stirrer inside the fume cupboard and set the heat control to highest temperature with moderate stirring. Allow the PFA to dissolve. When cooled, transfer the PFA solution to 4°C (store 1 week) or to -20°C (store several months). |
| **50% TAE** (pH7.6-7.8) | A 1-liter stock can be prepared by dissolving 242g Tris, 100mL of 0.5M EDTA pH 8.0, 57.1ml Glacial Acetic Acid and enough water to dissolve solids. pH can be adjusted with 1M HCl to 7.6-7.8, then top up to 1 liter. |
| **Mowiol** | Pour 20ml of 1x PBS into a conical flask containing 5g of Mowiol and stir overnight at room temperature. Then add 10ml of Glycerol and stir overnight at room temperature. Centrifuge Mowiol solution for 15 minute at 12000 rpm and aliquot supernatant in 2 ml Eppendorf tubes and freeze at -20°C (store several months). |
| **20x SSC** (pH4.5) | A 1-liter stock can be prepared by dissolving in 800ml of distilled water 175.3g of NaCl and 88.2g of sodium citrate. pH can be adjusted with 1M Citric acid to 4.5, then top up to 1 liter. |
| **10x Krebs** | A 1-liter stock can be prepared by dissolving 73.6g NaCl, 1.87g KCl, 1.66g $NaH_2PO_4$ (monobasic), 2.44g $MgCl_2$, 3.68g, then top up to 1 liter. Sterilize by autoclaving. Store 1 month at 4°C. |

# Chapter 3: Axon guidance defects in the forebrain of Pdn mutants

## 3.1 Introduction

Despite the well-known role of *Gli3* in the regionalization of the telencephalon, it is not fully known whether *Gli3* may also play a role in later aspects of brain development including the formation of axonal connections. However, the defects in $Xt^J/Xt^J$ mutant are too severe to allow such an analysis.

For this reason, I have started analyzing the general morphology and axonal tract formation in the forebrain of the *Gli3* hypomorphic mutant mouse *Polydactyly Nagoja* (*Pdn*) (Hayasaka et al., 1980). The general morphology and regionalization processes in *Pdn/Pdn* mutant brains are not as severely affected as in $Xt^J/Xt^J$ mutant brains (Kuschel et al., 2003; Naruse et al., 1990). Therefore, *Pdn/Pdn* mutants allow the study of later aspects of forebrain development, like the formation of the major axonal tracts. Previous studies have already revealed the absence of the corpus callosum in these mutants (Naruse et al., 1990). However, it is completely unknown whether *Gli3* is involved in the development of other axonal tracts within the forebrain.

In this chapter strong evidence is provided for a role of *Gli3* in the development of commissural, corticothalamic and thalamocortical axonal connections. First, the general brain morphology of *Pdn/Pdn* newborn (P0) brains was revealed with the use of cresyl

violet staining. Secondly, investigation of the developmental timing and trajectories of the major axonal tracts in *Pdn/Pdn* brains was carried out with the use of neurofilament (NF) immunostaining and DiI axonal tracing techniques. Finally, the development of the corticothalamic tract was analyzed with the use of *Golli tau-green fluorescent protein* (*tau-GFP*) transgenic mice, which express tau-GFP protein within early projecting cortical neurons and their axons (Jacobs et al., 2007).

These experiments reported agenesis of the corpus callosum, as well as of the anterior commissure and the hippocampal commissure at later stages of *Pdn/Pdn* brain development.

Moreover, these analyses showed that although the *Pdn/Pdn* cortex forms early projecting neurons and their axons at E14.5, during the first steps of corticothalamic tract formation some cortical axons do not penetrate the lateral ganglionic eminence (LGE) and instead run along the pallial-subpallial boundary (PSPB). Later in development, a thick bundle of *Pdn/Pdn* P0 cortical axons is still observed to project along the PSPB in the direction of the amygdaloid region. In addition, some *Pdn/Pdn* cortical axons eventually enter the ventral telencephalon navigating until the diencephalic-telencephalic boundary (DTB) and reaching thalamic regions. However, once in the ventral telencephalon these other axons project through several abnormal routes within the striatal region and ventral to the internal capsule.

In addition, at E14.5, rostrally, *Pdn/Pdn* thalamic axons also deviate from their normal trajectory along their path within the medial ganglionic eminence (MGE) and do not reach the developing cortex yet. Caudally, an ectopic axon tract projects ventrally within the ventral telencephalon not entering the internal capsule at all. At P0, the *Pdn/Pdn*

thalamocortical tract displays several guidance mistakes within the ventral telencephalon. A thick axon bundle is still observed to project ventrally in more caudal regions. Also several axons diverge from the internal capsule describing abnormal trajectories. However, in newborn *Pdn/Pdn* brains it is possible to observe a partial recovery of these axon tracts abnormalities resulting in the appropriate connections between different *Pdn/Pdn* cortical and thalamic areas.

## 3.2 Cresyl violet and NF stainings reveal defects in the major axonal tracts in newborn *Pdn/Pdn* mutant brains

Investigations into the general anatomy of P0 wild type and *Pdn/Pdn* brains were carried out with the use of cresyl violet and neurofilament staining (Fig. 3.1). Cresyl violet is a cationic dye that binds to negatively charged molecules, such as DNA and RNA on ribosomes in the cytoplasm. On brain sections cresyl violet staining reveals general brain morphology by labelling cell bodies and showing their distribution within the tissue. With this method it is also possible to reveal indirectly the major fibre tracts, which will remain pale due to the low cell body density within these structures.

Based on the observations that the gross anatomical morphology of *Pdn/+* brains is identical to wild type brains, in the following experiments both genotypes were used as controls, unless specifically stated otherwise.

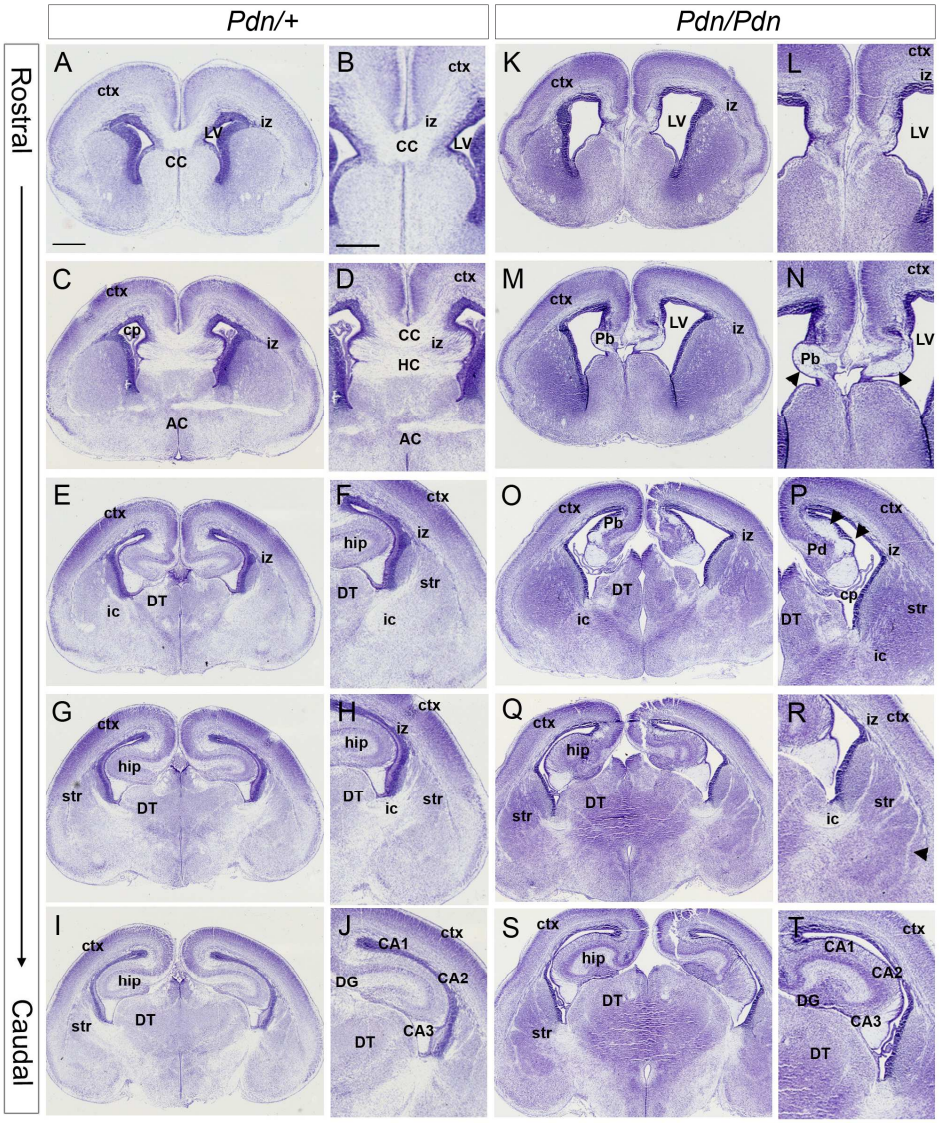
Pdn/+
Pdn/Pdn
Rostral
Caudal
A
ctx
LV
iz
CC
B
ctx
iz
CC
LV
K
ctx
LV
iz
L
ctx
iz
LV
C
ctx
cp
iz
AC
D
ctx
CC
iz
HC
AC
M
ctx
Pb
LV
iz
N
ctx
LV
Pb
E
ctx
iz
DT
ic
F
ctx
iz
hip
DT
str
ic
O
ctx
Pb
iz
DT
ic
P
ctx
Pd
iz
cp
DT
str
ic
G
ctx
hip
str
DT
H
ctx
iz
hip
DT
ic
str
Q
ctx
hip
str
DT
R
iz
ctx
ic
str
I
ctx
hip
str
DT
J
CA1
ctx
DG
CA2
DT
CA3
S
ctx
hip
DT
str
T
ctx
CA1
CA2
DG
CA3
DT

**Figure 3.1.**

**Cresyl violet staining showing the structures of the P0 wild type (A-J) and *Pdn*/*Pdn* (K-T) brain.** B, D, F, H, J are higher magnifications of A, C, E, G, I, respectively; L, N, P, R, T are higher magnifications of K, M, O, Q, S, respectively. From A and B to I and J and from K and L to S and T are serial sections organized form rostral to caudal (see also figures 1.1). *Pdn*/+ brain coronal sections show a thick cerebral cortex, comprised of layers of densely organized cell bodies, lying on axon fibres running within the intermediate zone (A to J). In more rostral sections the corpus callosum is crossing the midline connecting the two cerebral hemispheres (A-D). In medial sections it is possible to observe the choroid plexus, the anterior commissure and the hippocampal commissure (C, D). Caudal sections show the hippocampus (E-J), with the different hippocampal fields CA1, CA2, CA3 and the dentate gyrus (H, J). Caudal sections also reveal the internal capsule and the striatum (E-J). *Pdn/Pdn* mutant coronal sections reveal a general disorganization of brain morphology (K-T). The cerebral cortex appears thinner, particularly in more caudal sections, while the lateral ventricles are enlarged (O-T). However, the dense cell body layers lying on the intermediate zone can still be discriminated (O-T). In medial regions the choroid plexus appears hypertrophic and dysmorphic (O-T). The hippocampal and the anterior commissure are missing (K-P). The hippocampal architecture is disrupted (O-T). The corpus callosum is also absent and cortical fibres never cross the midline (K-P), but instead form large Probst bundles (arrowheads in N, P). The internal capsule is abnormally broad and the striatum disorganized containing thick fibre bundles (Q, R), with a prominent bundle also running along the PSPB (arrowhead in R) (n=4) (Scale bar in A 250 μm; applays to C, E, G, I, K, M, O, Q, S) (Scale bar in B 250 μm; applays to D, F, H, J, N, L, P, R, T).

Abbreviations: CC, corpus callosum; Ctx, cortex; LV, lateral ventricol; iz, intermediate zona; Cp, choroid plexus; AC, anterior commissure; DT, dorsal thalamus; ic, internal capsule; hip, hippocampus; Str, striatum; HC, hippocampal commissure; DG, dentate gyrus; Pb, probst bundle.

Observations of cresyl violet stained coronal sections of *Pdn/+* brains show the general anatomy at P0 (Fig. 3.1; A-L). It is possible to observe a thick cerebral cortex, comprised of layers of densely organized cell bodies, lying on axon fibres running within the intermediate zone (Fig. 3.1; A-F). In more rostral sections the corpus callosum is crossing the midline connecting the two cerebral hemispheres (Fig. 3.1; A-D). The ventricles are quite tight and the striatal region bulges out. In mid-rostrocaudal sections it is also possible to observe the choroid plexus, the anterior commissure and the hippocampal commissure (Fig. 3.1; C, D). Finally, in more caudal sections the hippocampus is clearly visible lying between the thalamus and the cortex (Fig. 3.1; G-L). The different hippocampal fields CA1, CA2, CA3 and the dentate gyrus are already formed in *Pdn/+* newborn mouse brains (Fig. 3.1; L). At caudal levels it is also possible to observe quite clearly the internal capsule and the striatum (Fig. 1; E-L). Overall, from rostral to caudal, the midline invagination has taken place and the two cerebral hemispheres are tightly fused in the dorso-medial-most regions of the cerebral cortex.

In P0 *Pdn/Pdn* mutant mouse brains, cresyl violet staining revealed a disorganization of brain morphology (Fig. 3.1; M-V). The *Pdn/Pdn* cerebral cortex appears thinner, in particular in more caudal sections, (Fig. 3.1; S-V) and the lateral ventricles are enlarged (Fig. 3.1; M-R). The dense cell body layers lying on the intermediate zone can still be discriminated (Fig. 3.1; M-T). In mid-rostrocaudal regions the choroid plexus appeared hypertrophic and dysmorphic (Fig. 3.1; Q-T). Moreover, the hippocampal and the anterior commissure are missing. Finally, the hippocampal architecture looks abnormal, although the hippocampal fields start to form and the dentate gyrus is present (Fig. 3.1;

V). In addition, the corpus callosum is absent and cortical fibres never cross the midline (Fig. 3.1; M-P), but instead form large Probst bundles at the midline particularly evident in mid-rostrocaudal and caudal sections (Fig. 3.1; O-R). Probst bundles are axonal bundles longitudinally orientated that indent dorso-medial regions of the cortex, often observed when the corpus callosum is absent (Babcock, 1984).

This analysis also revealed an abnormally broad internal capsule and a disorganized striatum containing thick fibre bundles. A prominent bundle also runs along the PSPB (Fig. 3.1; S-T). All these general abnormalities are accompanied by midline fusion defects.

Overall cresyl violet staining revealed an abnormal morphology of *Pdn/Pdn* mutant brains, particularly in the formation of the major axon tracts. Therefore, further analyses were focused on the investigation on these axonal tract defects. NF immuno-staining was performed on P0 *Pdn/+* and *Pdn/Pdn* brains (Fig. 3.2). The NF antibody exclusively labels axons revealing their organization within the tissue. This method provides the advantage of directly staining the axonal tracts, which were only indirectly revealed with cresyl violet.

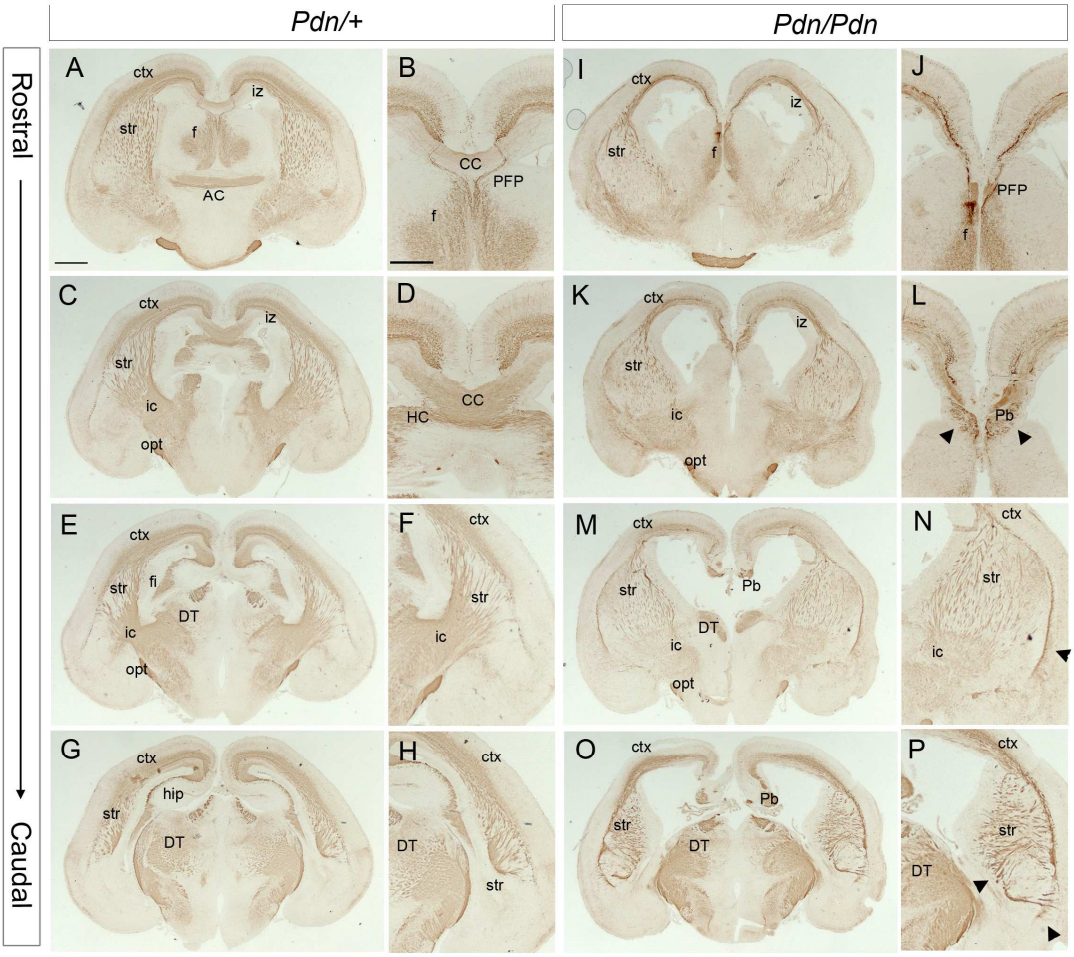
Pdn/+
Pdn/Pdn
Rostral
Caudal
A
ctx
iz
str
f
AC
B
CC
PFP
f
I
ctx
iz
str
f
J
PFP
f
C
ctx
iz
str
ic
opt
D
CC
HC
K
ctx
iz
str
ic
opt
L
Pb
E
ctx
str
fi
DT
ic
opt
F
ctx
str
ic
M
ctx
str
Pb
DT
ic
opt
N
ctx
str
ic
G
ctx
hip
str
DT
H
ctx
DT
str
O
ctx
Pb
str
DT
P
ctx
str
DT

**Figure 3.2.**

**Neurofilament staining showing the major axonal tracts of the P0 wild type (A-H) and *Pdn*/*Pdn* (I-P) brain.** B, D, F, H are higher magnifications of A, C, E, G respectively; J, L, N, P are higher magnifications of I, K, M, O respectively. From A and B to G and H and from I and J to O and P are serial sections organized form rostral to caudal.

*Pdn*/+ coronal brain sections show the presence axons within each side of the cerebral cortex that project medially to form the corpus callosum (A-D) and laterally to form the thalamocortical and corticothalamic tracts (C-F). Thalamocortical and corticothalamic axons run within the ventral telencephalon loosely organized within the striatum, but more densely packed within the internal capsule (C-F). In medial sections, it is possible to observe corticothalamic and thalamocortical axons making a second sharp turn at the DTB, entering the diencephalon (C-F). Rostral and medial sections also show the presence of the anterior commissure, the fimbria and the hippocampal commissure (A-F).

*Pdn/Pdn* mutant coronal brain sections reveal agenesis of the corpus callusum (I-N). Cortical axons are running within the intermediate zone of the *Pdn/Pdn* cerebral cortex in the direction of the midline, but do not project to the contralateral side (J, L), resulting in Probst bundles in more caudal sections (arrowheads in L). The anterior and the hippocampal commissures are also missing (I-P). Corticothalamic and thalamocortical connections are present (I-P). However, fewer axons are running within the striatum (K-N), and a thick axon bundle runs along the PSPB (arrowhead in N). The internal capsule is abnormally broad and the striatum appears disorganized, with axons running in several abnormal directions (arrowheads in P). (n=5) (Scale bar in A 250 μm; applays to C, E, G, I, K, M, O) (Scale bar in B 250 μm; applays to D, F, H, J, N, L, P)

Abbreviations: opt, optic tract; PFP, perforating pathway.

Coronal sections of *Pdn/+* brains immunostained for NF revealed the major axonal tracts at P0 (Fig. 3.2; A-H). In rostral sections, axons within each side of the cerebral cortex project within the intermediate zone in the direction of the dorsal midline and pass over to the contralateral side via the corpus callosum (Fig. 3.2; A-D). The same sections also show the presence of the anterior commissure, the fimbria and the hippocampal commissure (Fig. 3.2; A-F). Laterally in mid-rostrocaudal to caudal sections axons are running within the intermediate zone and projecting through the striatum making a sharp turn from the dorsal to the ventral telencephalon (Fig. 3.2; C-F). Thalamocortical and corticothalamic axons are running within the ventral telencephalon loosely organized within the striatum, but more densely packed within the internal capsule (Fig. 3.2; C-F). In mid-rostrocaudal sections, it is possible to observe corticothalamic and thalamocortical axons making a second sharp turn at the DTB, entering the diencephalon (Fig. 3.2; C-F).

NF immunohistochemical analyses of P0 *Pdn/Pdn* mutant brains reveal agenesis of the corpus callusum, as shown by cresyl violet staining (Fig. 3.2; I-P). Cortical axons are running within the intermediate zone of the *Pdn/Pdn* cerebral cortex in the direction of the midline, but do not project to the contralateral side (Fig. 3.2; L, N), resulting in Probst bundles in more caudal sections (Fig. 3.2; N).

In addition to callosal defects, NF immunostaining shows the absence of the anterior and the hippocampal commissures, which were never labelled within the *Pdn/Pdn* P0 brains in accordance with cresyl violet staining (Fig. 3.2; I-P).

Interestingly, NF staining also revealed defects in *Pdn/Pdn* corticothalamic and thalamocortical connections. Although these tracts appeared to be present, there are fewer axons within the striatum making a sharp turn from the cortical intermediate zone towards the ventral telencephalon (Fig. 3.2; I, M, O-P); moreover a thick axon bundle runs along the PSPB (Fig. 3.2; P). The internal capsule is abnormally broad and the striatum appears disorganized with axons running in several abnormal directions (Fig. 3.2; T). However, the dorsal thalamus shows a relatively normal innervation pattern (Fig. 3.2; R).

Taken together, these analyses revealed several axonal connection abnormalities within the newborn (P0) brains of *Pdn/Pdn* mutant animals. In particular, commissural connections comprising the corpus callosum, the anterior and the hippocampal commissure are absent. The connections between the cortex and the thalamus also appear severely impaired at the internal capsule and within the striatal region, with ectopic axon bundles running along the PSPB.

## 3.3 DiI injections in newborn brains show absence of the corpus callosum and guidance mistakes in thalamocortical and corticothalamic tracts of *Pdn/Pdn* mutants

Although NF and cresyl violet stainings revealed the general morphology and the pattern of the major axon tracts within the brain, these methods do not allow investigation of the trajectory of isolated axon tracts. Further investigations were aimed to reveal the

trajectory defects observed in the corpus callosum as well as the thalamocortical and corticothalamic tracts. To characterize abnormalities of these axon tracts DiI injections were performed within the cortex and thalamus of *Pdn/+* and *Pdn/Pdn* P0 brains (Fig. 3.3). DiI is a lipophilic and fluorescent dye, which diffuses along the cellular membranes of cells including their axonal processes. Injected into a specific part of the brain, the DiI stains the cellular membrane of the neurons and diffuses along the axons showing their trajectory in the brain.

DiI injections within the *Pdn/+* cerebral cortex revealed the corpus callosum of P0 coronal brain sections (Fig. 3.3; A-B). DiI injected into one of the cerebral hemispheres diffuses along callosal axons until the contralateral hemisphere, showing that in newborn brains callosal axons have formed and already cross the dorsal midline, where they strongly fasciculate forming one of the largest axonal tract within the brain (Fig. 3.3; A-B).

DiI injections in *Pdn/Pdn* brains show the absence of the corpus callosum. *Pdn/Pdn* cortical axons normally project towards the midline, but they are unable to cross it and remain ipsilateral (Fig. 3.3; C-F). Instead, *Pdn/Pdn* callosal axons project caudally within dorso-medial regions of the cerebral cortex, forming Probst bundles already visible with NF and cresyl violet staining (Fig. 3.3; E-F).

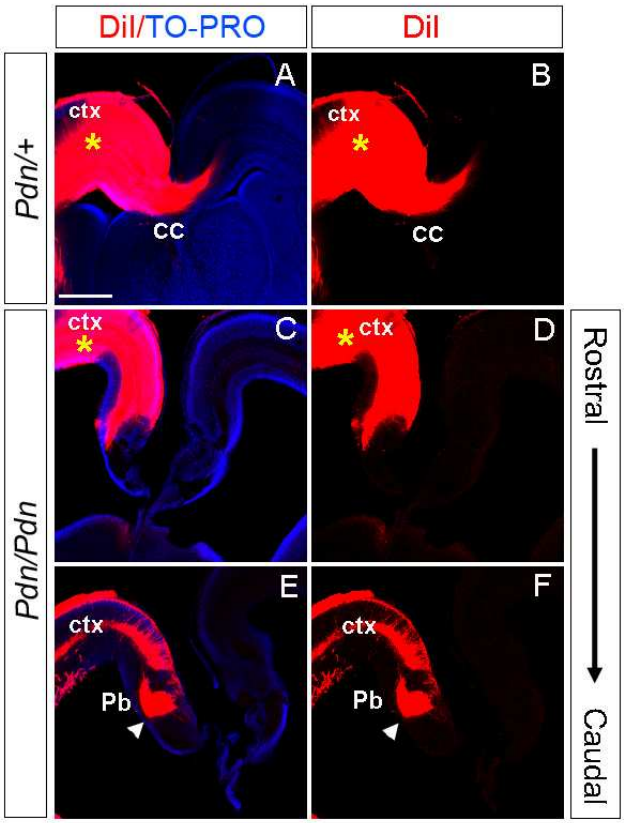


**Figure 3.3.**

**DiI injections showing medially projecting callosal axons in *Pdn/+* (A-B) and *Pdn/Pdn* (C-F) P0 brains.** A, C and E coronal brain sections are contrastained with TO-PRO. B, D and F display only DiI labelled axons without contrastaining. C, D and E, F are serial sections organized form rostral to caudal. DiI was injected in the dorso-rostral cortex (asterisk in A) of the *Pdn/+* brain revealing the corpus callosum (A-B). DiI injections in *Pdn/Pdn* brains show the absence of the corpus callosum (C-D). DiI injected in the *Pdn/Pdn* dorso-rostral cortex (asterisk in C) reveals that cortical axons normally project towards the midline, but they are unable to cross it and remain ipsilateral (C-D). In addition, *Pdn/Pdn* callosal axons project caudally within dorso-medial regions of the cerebral cortex, forming Probst bundles (arrowheads in E and F). (n=4) (Scale bar in A 200 μm; applays to all pannels).

In newborn *Pdn/+* brains thalamocortical and corticothalamic axons have entirely completed their journey to their final targets. Cortical axons have navigated until the dorsal thalamus; they have passed over the PSPB making a sharp turn to enter the striatal region, channelled through the internal capsule, passed over the DTB making a second change of direction, and eventually navigated into the dorsal thalamus. Also thalamic axons, from opposite directions, have covered the same distances with several changes of directions, and reached their final target area in the developing cortex (reviewed in (Lopez-Bendito and Molnar, 2003). Therefore, in P0 *Pdn/+* brains, cortical DiI injections anterogradely label the corticothalamic tract and retrogradely label the thalamocortical tract (Fig. 3.4; A), while dorso-thalamic injections anterogradely label the thalamocortical tract and retrogradely label the corticothalamic tract (Fig. 3.4; B-C). Coronal sections of *Pdn/+* P0 brains reveal labelling of both the entire corticothalamic and thalamocortical tracts, nicely showing parallel-organized fibres within the striatum and highly fasciculated axons within the internal capsule (Fig. 3.4; A-C). However with this method is not possible to discriminate between thalamocortical and corticothalamic tracts.

Coronal section of cortical and thalamic DiI injected P0 *Pdn/Pdn* mutant brains reveal several abnormalities (Fig. 3.4; D-F). Although DiI injected in the cortex diffuses into the dorsal thalamus, showing that some *Pdn/Pdn* cortical and thalamic axons undertake the normal route within the ventral telencephalon until the diencephalon, fewer axons are labelled within the striatum, the internal capsule and the diencephalon (Fig. 3.4; D).

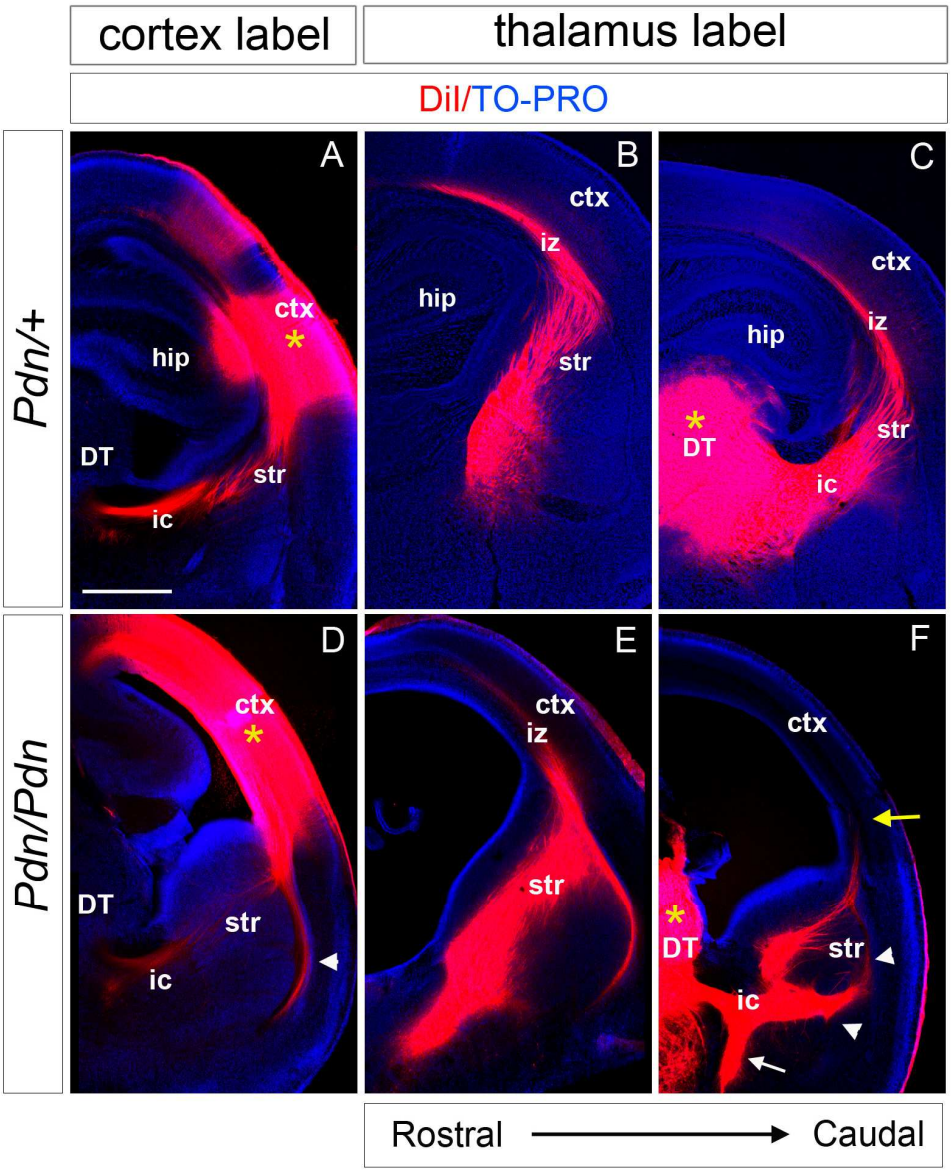
cortex label
thalamus label
DiI/TO-PRO
Pdn/+
Pdn/Pdn
A
B
C
D
E
F
ctx
hip
DT
str
ic
iz
Rostral
Caudal

**Figure 3.4.**

**DiI labelling of thalamocortical and corticothalamic tracts in P0 *Pdn/+* (A-C) and *Pdn/Pdn* brains (D-F)**. B, E and C, F are serial sections organized from rostral to caudal.

DiI is injected in the lateral cortex (asterisk in A) of the *Pdn/+* brains reveals thalamocortical and corticothalamic axons over the PSPB making a sharp turn between the striatal region and cortex, channelling through the internal capsule and making another sharp turn at the DTB between the thelencephalon and diencephalon (A). DiI is injected in the *Pdn/+* dorsal thalamus (asterisk in C) reveals parallel-organized cortical and thalamic fibres within the striatum and the cortical intermediate zone (B, C) and highly fasciculated axons within the internal capsule (C).

DiI injected in the lateral cortex (asterisk in D) of the *Pdn/Pdn* brains reveals several axonal abnormalities (D). Although DiI injected in the cortex diffuses into the dorsal thalamus, fewer axons than in *Pdn/+* are labelled within the striatum, the internal capsule and the diencephalon (D). Most of the *Pdn/Pdn* DiI labelled axons ectopically runs along the PSPB (arrowhead D). DiI injected in the *Pdn/Pdn* dorsal thalamus (asterisk in F) reveals several axonal abnormalities (E-F). DiI diffuses along the axons from the dorsal thalamus through the DTB to the ventral telencephalon and the striatum (E-F). However, a number of axons leave the internal capsule and project ventrally bifurcating in thick fascicles along the tracts projecting directly toward the PSPB rather than dorsally toward the cortex (arrowheads in F). Dorsal thalamic injections also reveal an ectopic bundle running along the PSPB (E). In more caudal sections, a thick bundle of axons projects ventrally growing through the globus pallidus in the direction of the amygdala (white arrow in F). Finally, very little DiI labeled axon fibres are present in the dorsal most region of the cortex; this defect is more severe caudally (yellow arrow in F). (n=6) (Scale bar in A 200 μm; applays to all pannels).

Unlike in *Pdn/+* sections, most of the *Pdn/Pdn* DiI labelled axons do not turn within the striatal region and a thick axon bundle runs along the PSPB (Fig. 3.4; D).

In *Pdn/Pdn* P0 mutant brains, the DiI injected into the thalamus also reveals dramatic axon guidance mistakes (Fig. 3.4; E-F). The dye diffuses along the axons from the dorsal thalamus through the DTB reaching the ventral telencephalon. In rostral sections, axons channel through the internal capsule (Fig. 3.4; F), but once axons penetrate the ventral telencephalon, DiI labelling reveals several bifurcations. A number of axons leave the internal capsule and project ventrally bifurcating in thick fascicles along the tracts. More dorsally within the striatum several axons project directly toward the PSPB rather than dorsally toward the cortex (Fig. 3.4; F). Dorsal thalamic injections also reveal an ectopic bundle running along the PSPB (Fig. 3.4; E). In more caudal sections, a thick bundle of axons projects ventrally growing through the globus pallidus in the direction of the amygdala, never channelling through the internal capsule (Fig. 3.4; F). Finally, very little DiI labels axon fibres in the dorsal most region of the cortex; this defect is even more severe caudally, where only few labelled axons are detected behind the PSPB (Fig. 3.4; F).

Cortex and thalamus innervate each other in a precise time-dependent and stereotypical pattern. During development, different cortical areas innervate different thalamic nuclei. For instance, cortical axons located in the caudal cortex (the visual cortex) connect with neurons located in a dorso-lateral area within the dorsal thalamus, the geninculate nucleus (dLGN). More rostral regions within the cortex (the somatosensory cortex)

connect with a more ventro-medial neuronal area within the dorsal thalamus, the ventral basal nucleus (VB) (reviewed in (Lopez-Bendito and Molnar, 2003; Price et al., 2006). Injections of the differently coloured fluorescent dyes DiI and DiA, which fluoresce red and green respectively, into the putative visual and somatosensory cortex, aimed to clarify whether the abnormalities in the axonal connections between cortex and thalamus in *Pdn/Pdn* mutant brains are the result of a subset of cortical and thalamic neurons being unable to connect with each other.

By injecting small crystals of DiI and DiA into different regions of the *Pdn/+* P0 cortex, it was possible to trace putative cortico-visual axons connecting with the dLGN and putative somatosensory axons connecting with the VB on the same brain section (Fig. 3.5; A-D). DiI injected in the *Pdn/+* putative visual cortex revealed axons connecting within the dLGN (Fig. 3.5; A, C-D), and DiA injected in the *Pdn/+* putative somatosensory cortex labels axons connecting within the VB (Fig. 3.5; B, C-D). The same experiment performed on *Pdn/Pdn* mutant brains shows that the different cortical areas connect with the appropriate target areas within dorsal-thalamic regions (Fig. 3.5; E-H). However, a difference is found in the size of the labelled thalamic nuclei. *Pdn/Pdn* brains display a reduction in the size of labelled regions within the thalamus (Fig. 3.5; E-H). Specifically, the VB and the dLGN labelled by DiA and DiI, respectively, show fewer axons connecting cortex and thalamus in P0 *Pdn/Pdn* brains, when compared to P0 *Pdn/+* brains (Fig. 3.5; D, H). In addition, the *Pdn/Pdn* dLGN was particularly small in comparison to the *Pdn/+* dLGN (Fig. 3.5; D, F). This result was in accordance with previous analyses that revealed corticothalamic and thalamocortical guidance mistakes are more severe caudally than rostrally in *Pdn/Pdn* mutants.

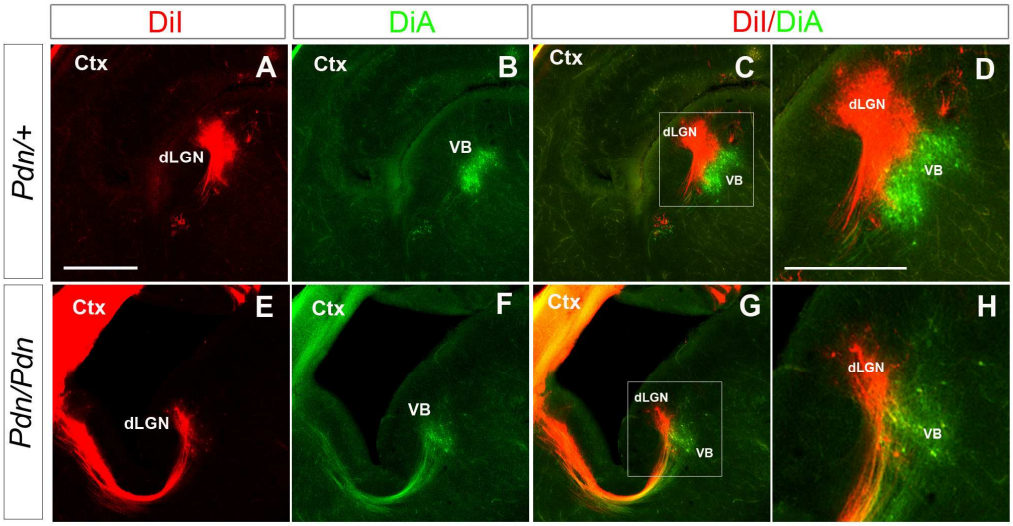


**Figure 3.5.**

**Visualization of the pattern of innervations between dorsal thalamus and cortex by double DiI and DiA injections into different regions of the *Pdn/+* and *Pdn/Pdn* P0 cortex.** A and E show DiI injections in the visual (caudal) cortex diffusing until the dLGN. B and F show DiA injections in the somatosensory (medial) cortex diffusing until the VB. C and G merged picture of A, B and E, F, respectively. D and H are higher magnification of C and G, respectively.

DiI injected in the *Pdn/+* visual cortex revealed axons connecting within the dLGN (A, C-D), and DiA injected in the *Pdn/+* somatosensory cortex labels axons connecting within the VB (B-D).

DiI injected in the *Pdn/Pdn* visual cortex revealed axons connecting within the dLGN (E, G-H), and DiA injected in the *Pdn/Pdn* somatosensory cortex labels axons connecting within the VB (F-H), revealing that *Pdn/Pdn* mutant brains show a correct pattern of innervations between cortex and thalamus. However, *Pdn/Pdn* thalamus displays a reduction in the size of labelled VB and the dLGN labelled by DiA and DiI, respectively (compare D with H). Abbreviations: dLGN, dorsal lateral geniculate nucleus; VB, ventral basal (n=3) (Scale bar in A 200 μm; applays to B, C, E, F, G) (Scale bar in D 200 μm; applays to H).

Altogether, these analyses show that P0 *Pdn/Pdn* mutants display severe abnormalities within the connections between cortex and thalamus. The most severe guidance defects are actually observed during their navigation within the ventral telencephalon and at the PSPB. Several corticothalamic and thalamocortical axons deviate from their normal path, running along the PSPB. Others project ventrally and laterally within the ventral telencephalon deviating form the internal capsule and form the striatal region. However, the DiI/DiA injections showed that P0 *Pdn/Pdn* cortical and thalamic tissues maintain or eventually recover their capacity to connect to each other.

## 3.4 DiI injections and NF staining reveal guidance mistakes at early stages of thalamocortical and corticothalamic tract development in *Pdn/Pdn* mutant brains

*Gli3* may play an important role in the establishment of corticothalamic and thalamocortical connections within the developing brain, in this case abnormalities in these tracts should be observed early during development.

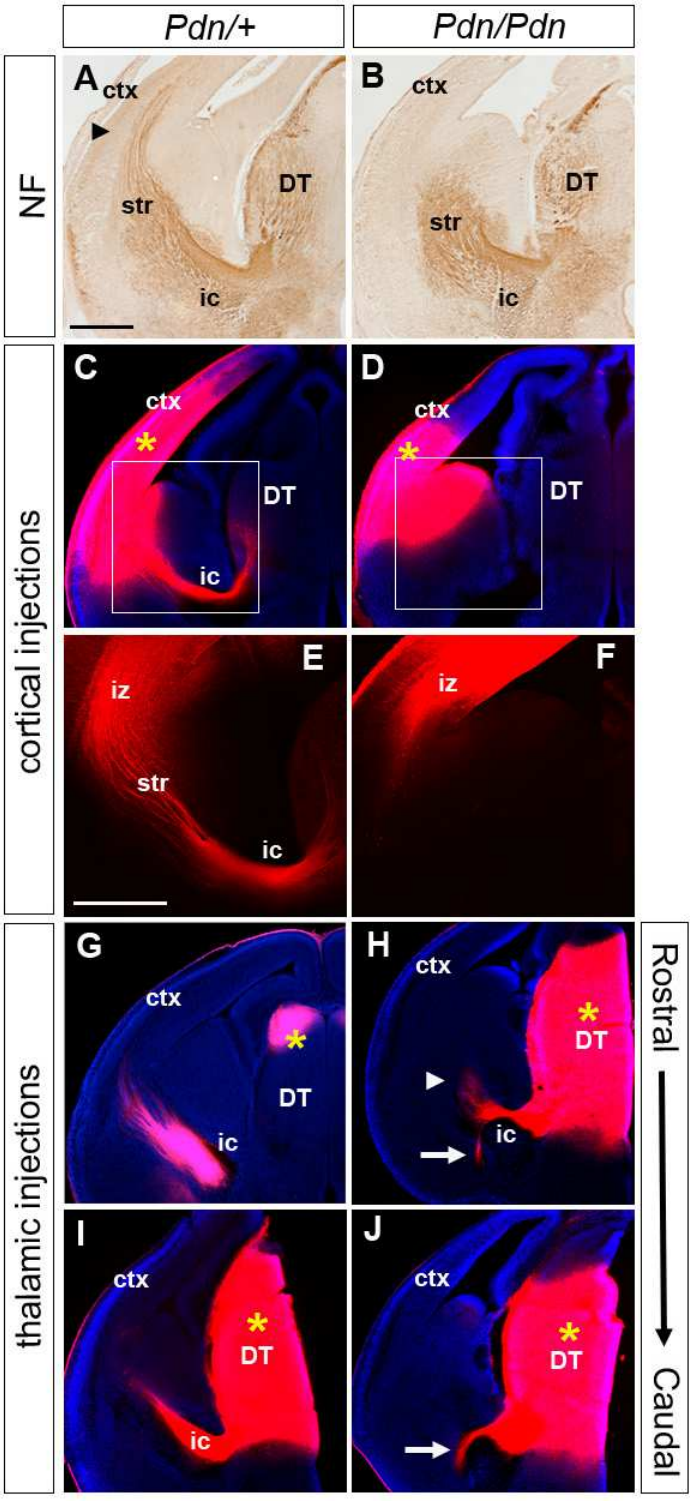
Pdn/+
Pdn/Pdn
NF
cortical injections
thalamic injections
A
ctx
str
DT
ic
B
ctx
DT
str
ic
C
ctx
DT
ic
D
ctx
DT
E
iz
str
ic
F
iz
G
ctx
DT
ic
H
ctx
DT
ic
I
ctx
DT
ic
J
ctx
DT
Rostral
Caudal

**Figure 3.6.**

**NF staining (A-B) and DiI injections (C-J) revealing the developing thalamocortical and corticothalamic tracts in *Pdn/+* and *Pdn/Pdn* brains.** E and F are higher magnification of C and D, respectively. G, H and I, J are serial sections organized form rostral to caudal.

NF staining on coronal sections of E14.5 *Pdn/+* embryos reveals NF+ axons in the developing thalamus, ventral telencphalon and cortex (arrowhead in A). Also, the internal capsule within the ventral telencephalon, which contains a high density of NF+ axons, and the striatum with more loosely organized axons (A). E14.5 *Pdn/Pdn* coronal brain sections show NF+ axons within the thalamus and ventral telencephalon (B). However, the internal capsule is broader and axons run in a more disorganized manner within the striatum (B). Interestingly, in *Pdn/Pdn* mutants it is not possible to detect any NF+ axons within the developing cortex (B).

DiI injections in the E14.5 *Pdn/+* developing cortex (asterisk in C) show that cortical axons have entered the intermediate zone and project towards the ventral telencephalon (C and E). Cortical DiI injections into E14.5 *Pdn/Pdn* mutant cortex (asterisk in D) show that no cortical axons have entered the ventral telencephalon (D, F); DiI injections in the E14.5 *Pdn/+* thalamus (asterisks in G and I) show that thalamic axons have penetrated the MGE, passed over the DTB, navigated through the internal capsule and the LGE and started to enter the cortex (G, I). DiI injections in the E14.5 *Pdn/Pdn* thalamus (asterisks in H and J) show thalamic axons passing over the DTB (H and J). However, as soon as thalamic axons enter the ventral telencephalon several guidance mistakes are clear. Rostrally, axons funnel through the internal capsule, but subsequently defasciculate projecting in more lateral directions, but not towards the cortex (arrowhead in H). In more medial and caudal regions, axons project ventrally, not entering the internal capsule, but going towards the amygdaloid region in the opposite direction of their natural route to the cortex (arrows in H and J). (n=6) (Scale bar in A 100 μm; applays to B-D and G-J) (Scale bar in E 100 μm; applays to F).

The following experiments were aimed to verify whether the first steps of *Pdn/Pdn* cortical and thalamic axonal navigation were affected or whether only later arriving axons were not able to innervate the appropriate target area.

To reveal the major axonal tracts at an early stage of development NF staining was performed on coronal sections of E14.5 *Pdn/+* and *Pdn/Pdn* brains (Fig. 3.6). $NF^+$ axons were present in the developing thalamus, ventral telencephalon and cortex of *Pdn/+* embryos. This analysis also revealed the internal capsule within the ventral telencephalon, which contains a high density of NF+ axons, and the striatum with more loosely organized axons (Fig. 3.6; A).

*Pdn/Pdn* coronal brain sections also show NF+ axons within the thalamus and ventral telencephalon (Fig. 3.6; B). Although these axons show a similar pattern, the striatum and internal capsule are broader and axons seem to run in a more disorganized manner within more dorsal regions of the LGE (Fig. 3.6; B). Interestingly, in *Pdn/Pdn* mutants it was not possible to detect any NF+ axons within the developing cortical regions, NF+ axons within the ventral telencephalon stop before the PSPB with no axons coming from or arriving at the E14.5 *Pdn/Pdn* cortex (Fig. 3.6; B).

Although NF staining showed the general pattern of the developing axon tracts within the E14.5 *Pdn/+* and *Pdn/Pdn* brains, this method did not allow the investigation of the trajectory of the first-projecting thalamocortical and corticothalamic axons. During embryonic mouse development, thalamocortical and corticothalamic axons start navigating within the ventral telencephalon at around E13.5/E14.5 (Lopez-Bendito and Molnar, 2003). To reveal the trajectories of these early navigating axons DiI injections were performed in E14.5 developing cortex and thalamus of *Pdn/+* and *Pdn/Pdn* brains

(Fig. 3.6; C-L). At this stage in *Pdn/+* brains, cortical axons have entered the intermediate zone and project towards the ventral telencephalon, just starting to cross the PSPB, having covered approximately only one third of the total distance to their final target, the dorsal thalamus. *Pdn/+* thalamic axons instead of coming through from the ventral side of the dorsal thalamus, have penetrated the MGE passing over the DTB, channelled through the internal capsule, navigated up to dorsal regions of the LGE and started to enter the developing cortex. Therefore, cortical DiI injections into *Pdn/+* E14.5 brains anterogradely label the corticothalamic tract and retrogradely label the thalamocortical tract (Fig. 3.6; C, E). The DiI diffused along axons from the cortex to the ventral telencephalon revealing a sharp change of direction of cortical and thalamic axons at the PSPB. In sub-pallial regions it is possible to observe the striatum and highly fasciculated axons within the internal capsule. At the DTB, axons make another sharp turn towards dorsal thalamic territories (Fig. 3.6; C, E).

Dorsal thalamic DiI injections into *Pdn/+* E14.5 brains, instead, preferentially reveal anterogradely labelled thalamocortical axons, because cortical axons have not reached the dorsal thalamus yet (Fig. 3.6; G; I). DiI labelled thalamic axons coming from the site of injections make a sharp turn at the DTB. Subsequently highly fasciculated thalamic axons are funnelled through a narrow internal capsule and navigate towards the developing cortex (Fig. 3.6; G, I). In dorsolateral regions of the developing cortex, it is possible to observe a few DiI labelled axons fibres, quite probably thalamocortical axons, which have already reached the cortex (Fig. 3.6; E, G).

Interestingly, cortical DiI injections into E14.5 *Pdn* mutant brains showed that no cortical axons had entered the ventral telencephalon yet (Fig. 3.6; D, F); this analysis

revealed cortical axons navigating through the intermediate zone and projecting along the PSPB towards the amygdaloid region instead of entering the LGE (Fig. 3.6; F). The fact that it was not possible to retrogradely label the thalamocortical tract also suggested that corticothalamic axons and thalamocortical axons have not met yet in the ventral telencephalon and/or that thalamic axons have not reached the cortex yet. This was also confirmed by thalamic injections of DiI (Fig. 3.6; H, L). In *Pdn/Pdn* mutant brains the DiI diffused from the dorsal thalamus to the ventral telencephalon, revealing thalamic axons passing over the DTB and making a sharp turn (Fig. 3.6; H). However, as soon as thalamic axons enter the ventral telencephalon several guidance mistakes happen (Fig. 3.6; H). In more caudal regions, axons project ventrally, not entering the internal capsule, but going towards the amygdaloid region in the opposite direction to what was observed in *Pdn/+* thalamic axons (Fig. 3.6; H-L). More rostrally, axons funnel through the internal capsule, but subsequently defasciculate projecting in more lateral directions, but not towards the cortex (Fig. 3.6; H). No DiI positive fibres were actually found in the *Pdn/Pdn* E14.5 cerebral cortex, indicating that no thalamic axons are entering the cortex yet.

In conclusion, these data reveal strong abnormalities in thalamocortical and corticothalamic tract development at the early stages of their navigation in the *Pdn* mutants. Surprisingly, the earliest projecting *Pdn/Pdn* cortical axons are not able to penetrate the ventral telencephalon, but project instead along the PSPB. *Pdn/Pdn* thalamic axons penetrate the MGE, but in caudal regions they miss project ventrally towards the amygdaloid region. In more rostral sections, thalamocortical axons are first

channelled through the IC, but they subsequently defasciculate and do not reach the cortex. These data also suggest that *Pdn/Pdn* cortical and thalamic axons have not met yet within the ventral telencephalon, where in normal circumstances they are supposed to interact in order to guide each other.

Interestingly, NF immuno-staining also shows the absence of $NF^+$ fibres within the *Pdn/Pdn* cortex. This may suggest that cortical neurons are delayed in the production of axons or the in production of NF within their axons. It is also possible that a delay occurs in the production of early cortical projecting neurons.

However, the methods used so far did not allow the investigation of the formation of *Pdn/Pdn* early cortical projecting neurons and their axons. Moreover, it was still not possible to completely discriminate between guidance defects of the corticothalamic and thalamocortical tracts within the *Pdn/Pdn* developing brain.

## 3.5 Pdn/Pdn Golli tau-GFP mice display guidance mistakes in early projecting corticothalamic axons

As mentioned above, NF staining and DiI injections are not selective for either the thalamocortical or corticothalamic tracts. P0 cortical DiI injections, indeed, revealed that cortical and thalamic axons intermingle and/or that thalamic axons have reached the cortex, but the behaviour of corticothalamic axons alone was still unknown in *Pdn* mutants. For these reasons, further investigation needed to be done in order to discriminate corticothalamic from thalamocortical defects within the *Pdn/Pdn*

developing brain. The next experiment aimed to reveal *Pdn/Pdn* corticothalamic axonal trajectories at later stages of development and to discover whether cortical axons are part of the ectopic bundles running along the PSPB. It was still unknown whether *Pdn/Pdn* cortical axons were eventually able to penetrate the ventral telencephalon and project in the direction of the diencephalon. In addition, it was unclear whether *Pdn/Pdn* mutants were affected in the formation of early projecting subplate and cortical plate neurons and their axons. Such a clarification could provide an understanding of whether axon guidance mistakes observed in corticothalamic and thalamocortical tract formation are the result of defects in the neural development of the *Pdn/Pdn* developing cortex, affecting corticothalamic axonal outgrowth and/or thalamocortical axonal ingrowth.

To visualize exclusively corticothalamic axons in *Pdn/+* and *Pdn/Pdn* brains, the *Golli tau-green fluorescent protein* (*tau-GFP*) mouse line was used. In these animals, the *golli* promoter element of the myelin basic protein gene drives the expression of a tau-GFP fusion protein, which labels cell bodies and axons of the earliest projecting cortical axons within the subplate and cortical plate (Jacobs et al., 2007). A *Pdn/Pdn Golli tau-GFP* mouse line was produced by crossing *Pdn/+* animals with *Golli tau-GFP* homozygous transgenic mice (Jacobs et al., 2007).

GFP expression in P0 *Pdn/+ Golli tau-GFP* brains was detected with the use of a GFP antibody on 100 μm thick coronal vibratome sections (Fig. 3.7; A-C). Coronal sections of these brains showed GFP expression in the cell bodies of cortical neurons (Fig. 3.7; A-C), in particular within layers 5 and 6 and within subplate neurons (Jacobs et al., 2007). Corticofugal $GFP^+$ axons navigate across the PSPB revealing the striatum and the

internal capsule. They also pass over the DTB reaching the dorsal thalamus, entirely completing their trip to their final target (Fig. 3.7; C).

Coronal sections of *Pdn/Pdn Golli tau-GFP* embryos showed the presence of GFP positive neurons within lower layers and the subplate of the cortex of P0 brains (Fig. 3.7; D-F). The GFP antibody also stained *Pdn/Pdn* cortical-cortical projecting axons, confirming results from work described earlier on the absence of the corpus callosum (Fig. 3.7; D-F), with GFP positive callosal fibres forming Probst bundles in dorso-medial regions of the cortex (Fig. 3.7; E). Laterally, cortical axons start to project along the anterior commissure, but they never reach the contralateral side, again confirming NF and cresyl violet staining (data not shown). In addition, the cerebral cortex appeared to be thinner especially in more caudal sections (Fig. 3.7; E-F).

Some *Pdn/Pdn* GFP positive corticothalamic axons extended towards the thalamus. Indeed, they grow through the PSPB, the striatum and the internal capsule until they cross the DTB and enter the diencephalon (Fig. 3.7; D-F). However, cortical axons do not reach the dorsal-most regions of the dorsal thalamus, unlike in *Pdn/+ Golli tau-GFP* P0 brains (Fig. 3.7; F). However, several corticofugal axons make several guidance mistakes within the ventral telencephalon (Fig. 3.7; E-F). Only a small number of GPF positive axons make a sharp turn within the striatum and several corticofugal axons result in ectopic bundles running along the PSPB (Fig. 3.7; E). Some of them eventually enter the ventral telencephalon from more ventral points, after they have projected in the direction of the amygdaloid region.

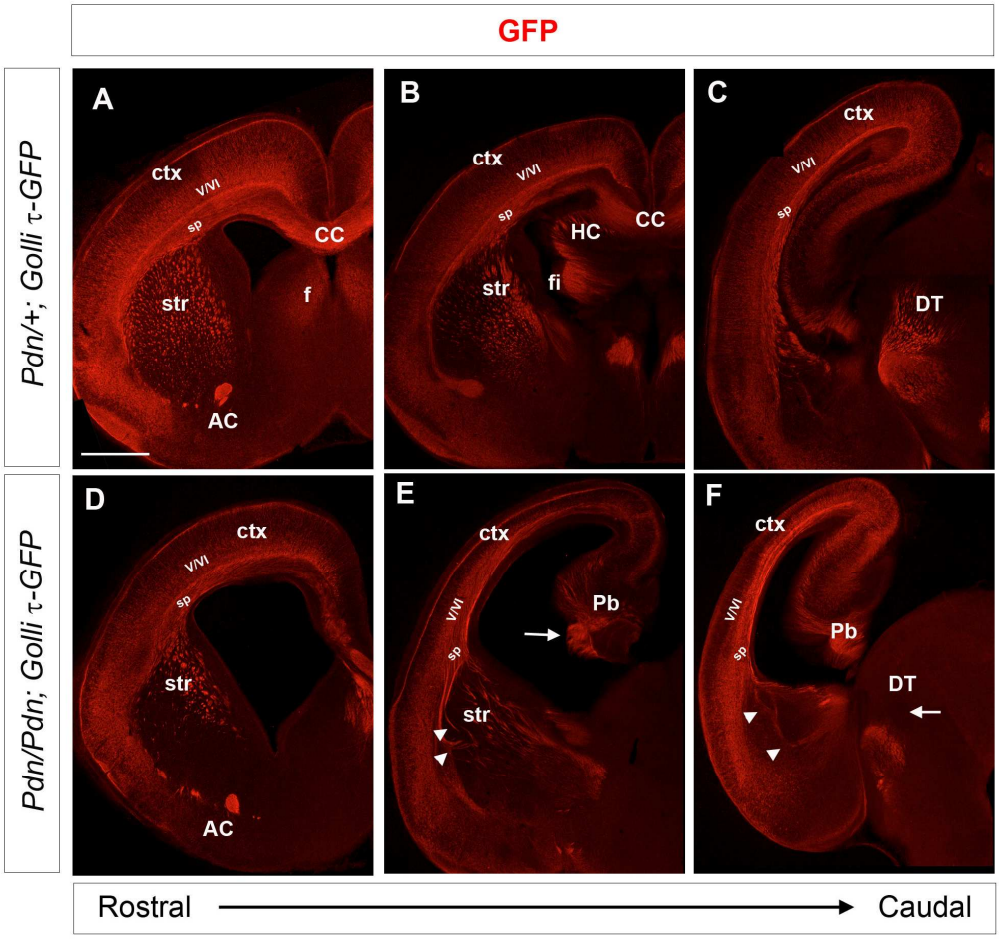
GFP
Pdn/+; Golli τ-GFP
Pdn/Pdn; Golli τ-GFP
A
B
C
D
E
F
ctx
VVI
sp
CC
HC
f
fi
str
AC
DT
Pb
Rostral
Caudal

**Figure 3.7.**

**GFP staining on coronal sections of P0 *Pdn/+ Golli tau-GFP* (A-C) and *Pdn/Pdn Golli tau-GFP* (D-F) brains.** From A to C and D to F are serial sections organized form rostral to caudal.

In both *Pdn/+ Golli tau-GFP* and *Pdn/Pdn Golli tau-GFP* brains GFP+ cortical neurons are present (A-F). These neurons are located in cortical layers 5 and 6 and in the cortical subplate. However, the *Pdn/Pdn Golli tau-GFP* cerebral cortex appeared to be thinner, especially in more caudal sections (campare E and F with B and C).

GFP staining also reveals *Pdn/+ Golli tau-GFP* GFP+ corpus callosum, anterior commissure and fimbria (A, B). In *Pdn/Pdn Golli tau-GFP* brains the corpus callosum and fimbria are absent (D-E), with GFP positive fibres forming Probst bundles in caudal regions of the dorso-medial cortex (arrow in E, F).

*In Pdn/+ Golli tau-GFP* brains $GFP^+$ corticofugal axons have navigated across the PSPB revealing the striatum and the internal capsule (A-B), and passed over the DTB reaching the dorsal thalamus (C). In *Pdn/Pdn Golli tau-GFP* brains GFP+ corticothalamic axons extended through the PSPB, the striatum and the internal capsule until they cross the DTB and enter the diencephalon (D-F). However, cortical axons do not reach the dorsal-most regions of the dorsal thalamus (arrow in F). In addition, fewer GPF+ axons enter the striatum, but they navigate through several abnormal routes (arrowheads in F). Several corticofugal axons result in ectopic bundles running along the PSPB (E). Some ventrally projecting GPF+ axons eventually enter the ventral telencephalon from more ventral points (arrowheads in E). (n=4) (Scale bar in A 200 μm; applays to all pannels). Abbreviations: f, fornix; fi, fimbria; V/VI, layers V/VI; sp, subplate.

This also results in fewer and more disorganized fibres entering the striatum, especially in more caudal regions where cortical axons navigate in the direction of the diencephalon through the ventral telencephalon using several abnormal routes (Fig. 3.7; F).

To check the first steps of corticothalamic tract formation, GFP staining was also performed on coronal sections of E14.5 *Golli tau-GFP* and *Pdn/Pdn Golli tau-GFP* mouse brains (Fig. 3.8). At this embryonic stage GFP is expressed within the cell bodies and axons of the first projecting neurons within the subplate and cortical plate (Jacobs et al., 2007) (Fig. 3.8; A-F). In controls, GFP immunostaining shows that corticothalamic axons have just passed over the PSPB and started to penetrate the ventral telencephalon (Fig. 3.8; D, F). To visualize the boundary between the dorsal and the ventral telencephalon the glial fibres delimiting the PSPB were stained with an antibody against Glast (Fig. 3.8; B, E, H, K). Indeed several GFP positive cortical axons were observed to grow across the $Glast^{+}$ fibres extending within the LGE (Fig. 3.8; F).

Coronal sections of E14.5 *Pdn/Pdn Golli tau-GFP* brains reveal the presence of GFP positive neurons and their axons within the subplate and cortical plate of these embryonic brains (Fig. 3.8; D, F, L, N). Although $GFP^{+}$ cortical neurons are normally forming within *Pdn/Pdn Golli tau-GFP* developing cortex, it was not possible to detect any GFP positive corticofugal axons projecting over the PSPB, labelled by Glast-positive glial fibres (Fig. 3.8; I, L), and entering the LGE (Fig. 3.8; L), confirming the DiI data. In addition a long branch of GFP+ cortical axons extended ventrally along the PSPB, toward the amygdaloid region (Fig. 3.8; I).

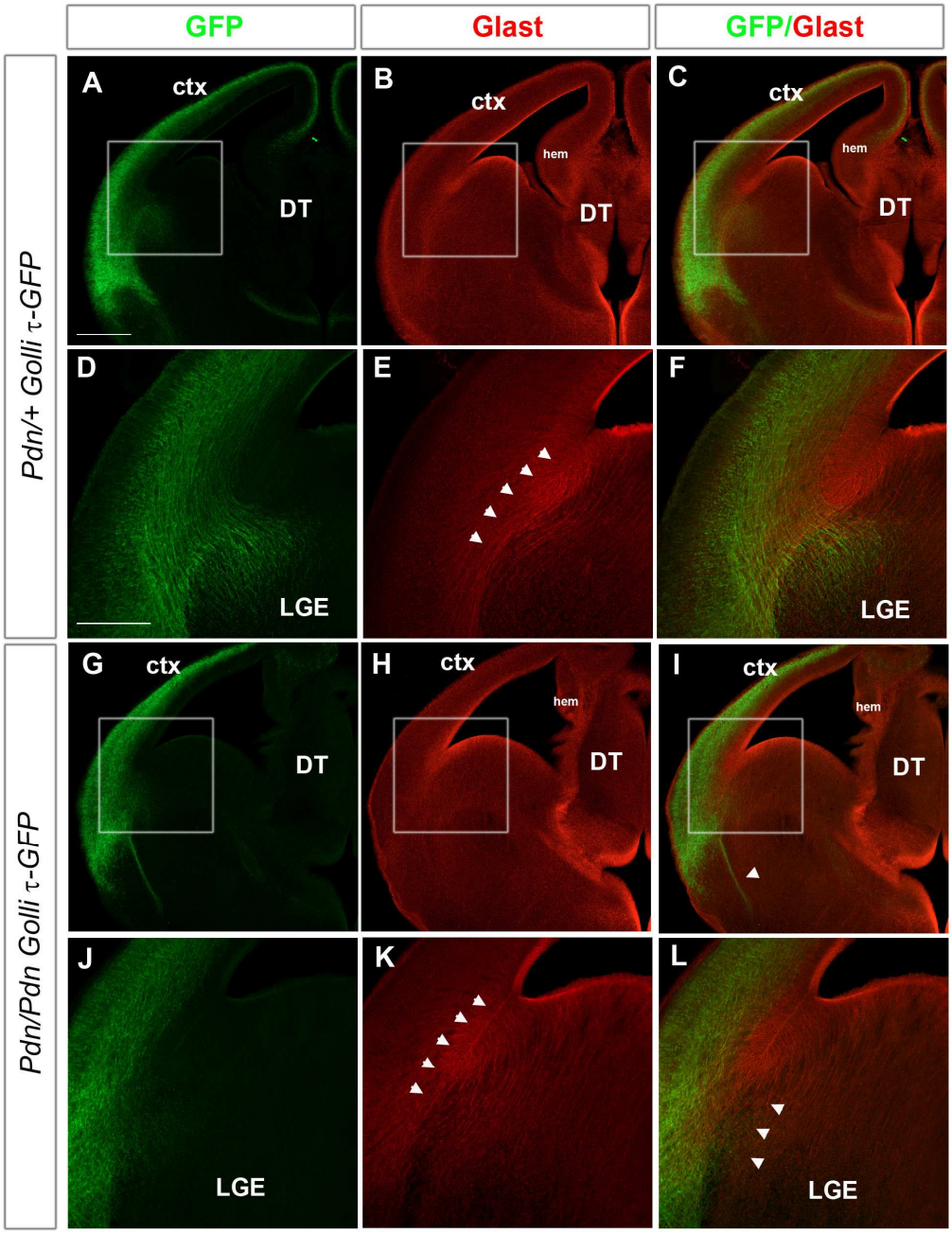
GFP
Glast
GFP/Glast
Pdn/+ Golli τ-GFP
Pdn/Pdn Golli τ-GFP
A
B
C
D
E
F
G
H
I
J
K
L
ctx
hem
DT
LGE

**Figure 3.8.**

**GFP staining on coronal sections of E14.5 *Pdn/+ Golli tau-GFP* (A-F) and *Pdn/Pdn Golli tau-GFP* (G-L) brains.** A, D, G, J are sections revealing GFP staining only. B, E, H, K are sections revealing glast staining only. C and F are merged picture of A, B and E, F, respectively. I and L are merged picture of G, H and J, K, respectively. D, E, F and L, K, L are higher magnification pictures of A, B, C and G, H, I, respectively.

GFP staining reveals the presence of GFP positive neurons and their axons within the subplate and cortical plate of *Pdn/+ Golli tau-GFP* and *Pdn/Pdn Golli tau-GFP* brains (A, C, D, F, G, I, J, L).

In both *Pdn/+ Golli tau-GFP* and *Pdn/Pdn Golli tau-GFP* the boundary of glial fibres delimiting the PSPB was stained with glast antibody (B, E, H, K and arrowheads in E and K). GFP immunostaining shows that *Pdn/+ Golli tau-GFP* corticothalamic axons have just passed over the PSPB and started to penetrate the ventral telencephalon (D, F). Several GFP positive cortical axons are observed to grow across the glast$^{+}$ fibres extending within the LGE (F). On the contrary, it was not possible to detect any GFP+ *Pdn/Pdn Golli tau-GFP* corticofugal axons projecting over the PSPB (G J), labelled by glast-positive glial fibres entering the ventral telencephalon (I and arrowheads in L). In addition a long branch of GFP+ cortical axons extended ventrally along the PSPB, toward the amygdaloid region (arrowhead in I). (n=3) (Scale bar in A 100 μm; applays to B-C and G-I) (Scale bar in D 100 μm; applays to E-F and J-L).

Abbreviations: hem, cortical hem; LGE lateral ganglionic eminence.

After E15.5, *Pdn/+* cortical axons progress through the internal capsule until they reach the DTB. Indeed, they will stop here until E17.5 when they will progress over the DTB (Jacobs et al., 2007).

To check at which stage *Pdn/Pdn* cortical axons penetrat the ventral telencephalon for the first time, GFP antibody staining was performed on E16.5 *Pdn/+ Golli tau-GFP* and *Pdn/Pdn Golli tau-GFP* brain coronal sections (Fig. 3.9). At this embryonic stage, *Pdn/+ Golli tau-GFP* axons reach the DTB through the internal capsule (Fig. 3.9; D, F); again the PSPB was labelled by Glast antibody staining (Fig. 3.9; B, E). In addition, at this age it is already possible to reveal the anterior commissure and corpus callosum axons positive for GFP immunostaining (Fig. 3.9; A, C).

E16.5 *Pdn/Pdn Golli tau-GFP* brain coronal sections do not have any GFP positive axons entering the ventral telencephalon and channelling through the internal capsule (Fig. 3.9; L, N); instead cortical axons run along the PSPB, delimited by Glast positive glial fibres (Fig. 3.9; H, M), not entering the ventral telencephalon yet (Fig. 3.9; I, N). Only one out of three analyzed E16.5 *Pdn/Pdn* brains show the presence of a few axons just starting to penetrate the LGE in the most rostral sections, but these axons do not grow far within the ventral telencephalon. A thick bundle of GFP+ cortical axons run ectopically along the PSPB towards the amygdaloid region (Fig. 3.9; I).

Taken together, these experiments showed in great detail the timing and patterning of the axonal processes of *Pdn/Pdn* early projecting cortical neurons. The *Pdn* homozygous mutant cortex is able to produce early projecting neurons and their axons within the cortical sub-plate and cortical plate. At E14.5 *Pdn/Pdn* corticothalamic axons are not

able to penetrate the ventral telencephalon, but rather they grow along the PSPB confirming the DiI data. At E16.5 *Pdn/Pdn* cortical axons have not reached the DTB yet, and only in one of three analyzed brains it is possible to observe some axons entering the LGE in rostral sections. Interestingly, at P0 the axonal phenotype is partially recovered, as observed with DiI injections, showing cortical axons having reached the thalamus in the diencephalon. However, several guidance mistakes are still observed in the *Pdn/Pdn* ventral telencephalon. High numbers of axons run along the PSPB and do not enter the LGE. Moreover, the cortical fibres entering the ventral telencephalon project towards the thalamus, following abnormal routes.

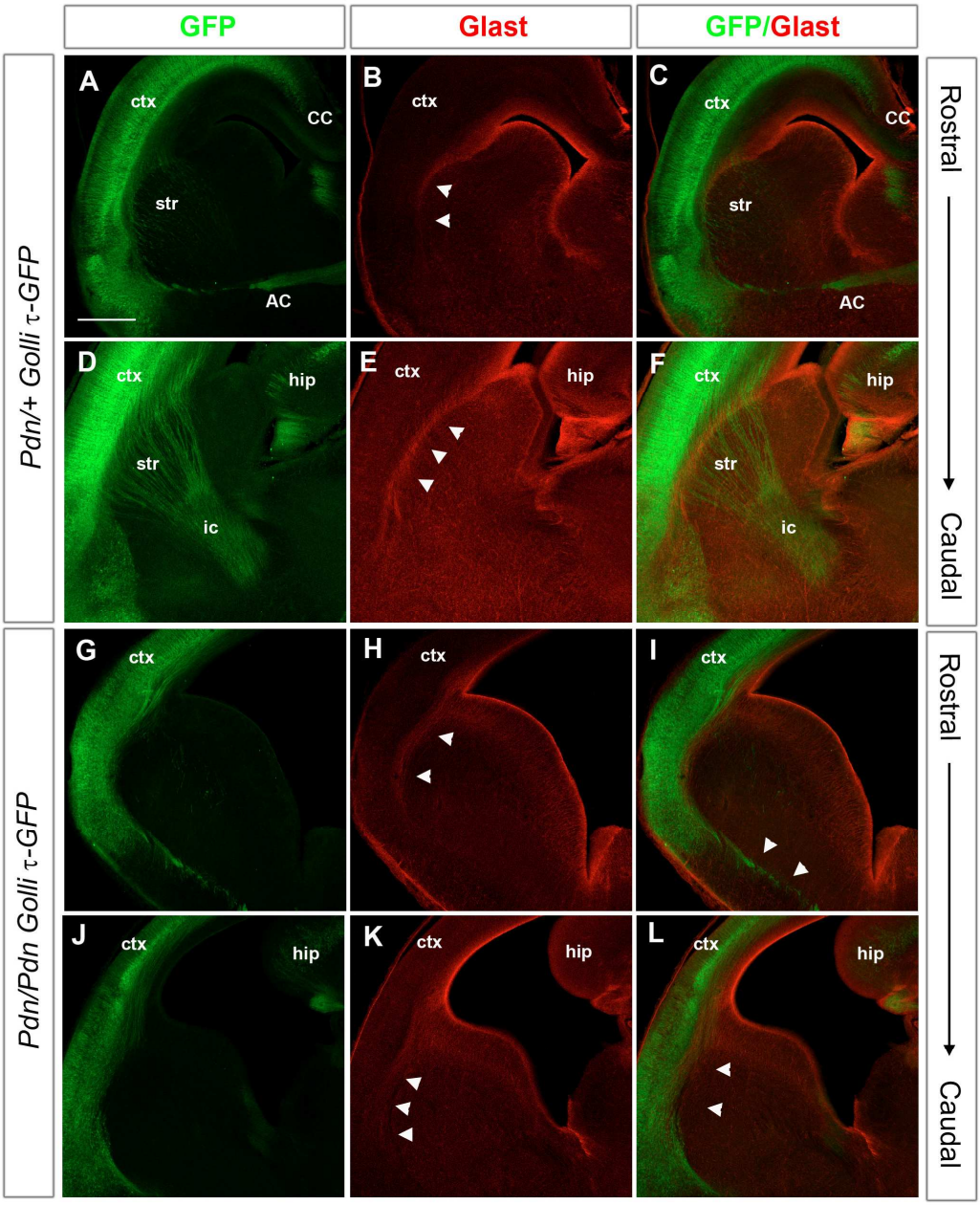
GFP
Glast
GFP/Glast
Pdn/+ Golli τ-GFP
Pdn/Pdn Golli τ-GFP
Rostral
Caudal
A
B
C
D
E
F
G
H
I
J
K
L
ctx
CC
str
AC
hip
ic

**Figure 3.9.**

**GFP staining on coronal sections of E16.5 *Pdn/+ Golli tau-GFP* (A-F) and *Pdn/Pdn Golli tau-GFP* (G-L) brains.** A and C are serial sections organized form rostral to caudal; as well as B and E, C and F, G and J, H and K, I and L. A, D, G, J are sections revealing GFP staining only. B, E, H, K are sections revealing glast staining only. C and F are merged pictures of A, B and E, F, respectively. I and L are merged pictures of G, H and J, K, respectively.

GFP staining reveals the presence of GFP positive neurons and their axons within the subplate and cortical plate of on *Pdn/+ Golli tau-GFP* and *Pdn/Pdn Golli tau-GFP* brains (A, C, D, F, G, I, J, L).

At this embryonic age it is already possible to observe the formation of the GFP+ anterior commissure and corpus callosum in *Pdn/+ Golli tau-GFP* brains (A, C). No corpus callosum and no anterior commisure are present in *Pdn/Pdn Golli tau-GFP* brains (G, I).

In both *Pdn/+ Golli tau-GFP* and *Pdn/Pdn Golli tau-GFP* brains the glial fibre boundary delimiting the PSPB was stained with glast antibody (arrowheads in B, E, H, K). *Pdn/+ Golli tau-GFP* axons reach the DTB passing through the striatum (A, C) and in more caudal section the internal capsule (D, F). No GFP+ *Pdn/Pdn Golli tau-GFP* axons enter the ventral telencephalon passing over the PSPB (arrowheads in L) channelling through the internal capsule (G, J, I, L). In addition a thick bundle of GFP+ cortical axons run ectopically along the PSPB towards the amygdaloid region (arrowheads I). (n=4) (Scale bar in A 100 μm; applays to all pannels).

**Table 3.1**

**Different axon defects observed in *Pdn/Pdn* mutans at different embryonic stages**

| **Fibre tracts in *Pdn/Pdn* mutans** | **E14.5** | **E16.5** | **P0** |
|---|---|---|---|
| **Corpus callosum** | - | Absent | Absent (resulting in probst bondles in caudal sections) |
| **Anterior commissure** | - | Absent | Absent |
| **Hippocampal commissure** | - | Absent | Absent |
| **Corticothalamic tract** | Not entering the VT | Not entering the VT | Reaching the DTB |
| **Thalamocortical tract (rostral)** | Prematurely leaving the ic and not reaching the cortex | - | Guidance mistakes int eh striatum, reching the cortex |
| **Thalamocortical tract (caudal)** | Projecting ventrally toward the amigloid region | - | Projecting ventrally toward the amigloid region |

## 3.6 Discussion

In this chapter I reveal several axon abnormalities in the *Gli3* hypomorphic mutant *Pdn/Pdn* (also see table 3.1). All the major axonal commisures of the telencephalon are missing in *Pdn/Pdn* newborn brains, including the corpus callosum, the anterior commissure and the hippocampal commissure. Interestingly, callosal axons are present and navigate in the intermediate zone of the *Pdn/Pdn* cerebral cortex in the direction of the midline, but do not project to the contralateral side and form Probst bundles in more caudal sections. Therefore, although the *Pdn/Pdn* cerebral cortex produces cortical axons, all of the tracts connecting the two cerebral hemispheres are missing.

Several guidance mistakes also happen during the development of the thalamocortical and corticothalamic tracts. Although these tracts appeared to be present in newborn *Pdn/Pdn* brains, fewer axons are navigating through the striatum and the internal capsule appears disorganized in the ventral telencephalon, with axons running in several abnormal directions. In addition, a thick axon bundle runs along the PSPB. At E14.5, cortical axons have not entered the mutant ventral telencephalon yet, but they run instead along the PSPB. *Pdn/Pdn* thalamic axons, once they have entered the ventral telencephalon, display two main axonal defects: caudally, they project ventrally, not entering the internal capsule at all, while in more rostral regions they leave the internal capsule prematurely and defasciculate within the LGE, failing to reach the cortex.

At P0 *Pdn/Pdn* mutants also display several anatomical brain abnormalities. Although the dense cell body layers lying in the intermediate zone can still be discriminated, the

*Pdn/Pdn* cerebral cortex is thinner, particularly in more caudal sections, and the lateral ventricles are enlarged. In medial regions the choroid plexus appeared hypertrophic and dysmorphic. Finally, the hippocampal architecture is also disrupted. Importantly, the dorso-medial cortex does not invaginate properly leading to the absence of the fusion of the medial cortex. This last defect seems to be the major cause of callosal abnormalities. Indeed, DiI injections, cresyl violet and NF stainings all reveal that cortical axons are present and project in the direction of the dorsal midline. However, here the lack of midline fusion virtually creates the absence of the tissue in which callosal axons have to navigate through in order to reach the contralateral cortex. It has been proposed that the midline zipper glia are necessary for this process (Richards, 2002; Shu and Richards, 2001). However, the cellular and the molecular mechanisms leading to midline fusion are poorly understood (reviewed in (Paul et al., 2007). This makes it difficult to analyze the causes of midline fusion defects in *Pdn/Pdn* mutants. Nevertheless, the causes of the absence of the corpus callosum in *Pdn/Pdn* mutants probably needs to be researched in the context of causes that determine midline fusion defects. Indeed, preliminary data showed that in P0 *Pdn/Pdn* mutants the indusium griseum glia are absent and that the midline zipper glia are ectopically expanded ventrally (unpublished data from our lab). These data are based upon immunostaining on P0 *Pdn/+* and *Pdn/Pdn* coronal brains section for the intermediate filament glial fibrillary acidic protein (GFAP), which labels the three midline glia populations comprising in the indusium griseum glia, the glial wedge and the midline zipper glia (Shu and Richards, 2001; Silver et al., 1993; Silver et al., 1982). The correct morphogenesis of these glial populations along the midline is thought to be crucial for guiding the axons of the developing corpus callosum (Shu and

Richards, 2001; Shu et al., 2002; Silver et al., 1993; Silver et al., 1982). Interestingly, *Pdn/Pdn* mutants display ectopic *Fgf8* expression and its direct target gene *Sprouty2* in the anterior neural ridge (Kuschel et al., 2003), which is the region where dorsal midline invagination starts to take place. A recent report has shown the importance of *Fgf* signalling in the formation of the corpus callosum, by controlling the process of midline radial glia translocation, which consist in radial migration of glial cells from the glial wedge at the ventricular zone to the pial surface, generating the indusium griseum glia. In this study it was revealed that conditionally inactivating *Fgfr1* gene in radial glial cells or knocking down *Fgfr1* by RNAi in vivo resulted in absence of the corpus callosum as a consequence of a failure of indusium griseum glia translocation (Smith et al., 2006). It is therefore possible that anatomical defects and change in *Fgf8* expression could probably be the primary cause of the failure of *Pdn/Pdn* callosal axons to cross the midline. This aspect of the *Pdn/Pdn* brain development will need more attention in the future, because it could bring new insights into the development of the corpus callosum in the context of midline fusion and midline glia populations' development. In addition, understanding the role of *Gli3* in callosal axon pathfinding defects may also be relevant for the pathogenesis in ACS patients.

In this thesis I decided to focus on the study of the causes leading to defects of the thalamocortical and corticothalamic tracts. DiI/DiA injections in the P0 *Pdn/Pdn* cortex and thalamus allowed a detailed analysis of the guidance mistakes of these two tracts. However, the major limitation of DiI/DiA injections is the impossibility to discriminate between cortical axons and thalamic axons. Indeed, cortical DiI/DiA injections anterogradely label the corticothalamic tract and retrogradely label the thalamocortical

tract, while dorso-thalamic injections anterogradely label the thalamocortical tract and retrogradely label the corticothalamic tract.

Nevertheless, this technique provides an exhaustive description of the axonal path of these two tracts, and in some cases, with due prudence, it is possible to speculate on the discrimination between thalamocortical and corticothalamic axonal mistakes. Interestingly, cortical and thalamic DiI injections show that some *Pdn/Pdn* cortical and thalamic axons undertake the normal route until their final target navigating through the striatum, the internal capsule, showing that cortex and thalamus eventually connect to each other, at least in part. However, most of the *Pdn/Pdn* DiI labelled axons run ectopically in a thick axon bundle along the PSPB, as revealed by both thalamic and cortical DiI injections. However, with thalamic DiI injections, in more caudal sections, it is possible to observe some axon bundles not entering the internal capsule but projecting ventrally in the direction of the amygdaloid region. More rostrally and dorsally, DiI labelled axons bifurcate several times in thick fascicles along the tracts, with several axons projecting directly towards the PSPB rather than dorsally towards the cortex. The fact that these later results are only observed with dorso-thalamic DiI injections suggests that these ectopic axonal fascicles are predominantly composed of thalamic axons. This is also confirmed by DiI injections at E14.5. Indeed, in *Pdn/+* brains, DiI injections in cortex and thalamus are not able to discriminate between these two tracts, because cortical and thalamic axons have met within the ventral telencephalon and/or because thalamic axons have already reached the developing cortex. On the contrary, in the *Pdn/Pdn* mutants, cortical and thalamic injections reveal that at E14.5 thalamocortical and corticothalamic tracts have not yet met in the ventral telencephalon and that

thalamic axons have not reached the cortex. Therefore, cortical DiI injections only revealed *Pdn/Pdn* cortical axons, showing that no cortical axons had entered the ventral telencephalon, while thalamic injections only revealed thalamocortical axons showing that no *Pdn/Pdn* thalamic axons had navigated as far as cortical territories. In addition, in more rostral sections thalamic axons project dorsally forming a broader internal capsule and subsequently defasciculate projecting in more lateral directions, but not towards the cortex. However, in more caudal sections a thick bundle of thalamic axons projects ventrally within the MGE and does not channel through the internal capsule.

The *golli τ-GFP* mouse line crossed with *Pdn* animals allowed the visualization of corticofugal axons in *Pdn/Pdn* brains. This analysis not only confirmed the *Pdn/Pdn* cortical axons mistakes, but also helps to extrapolate the *Pdn/Pdn* thalamocortical phenotype from DiI injections, which indiscriminately label the thalamocortical and the corticothalamic tracts at P0. Indeed, by selectively labelling *Pdn/Pdn* cortical axons it was possible to observe that while *Pdn/Pdn* thalamic axons project ventrally towards the amygdaloid region as soon they enter the ventral telenephalon, *Pdn/Pdn* cortical axons take this path after they have projected along the PSPB and reached the amygdale, entering the ventral telencephalon from more ventral regions.

The caudal part of the internal capsule is composed of the first axons to enter the ventral telencephalon. These axons are coming from thalamic neurons of the dLGN and connect with the visual cortex (Price et al., 2006). It would be interesting to know whether in *Pdn/Pdn* mutants these ectopic ventrally projecting thalamic axons are actually coming from the dLGN or whether they are a miscellaneous group of other types of dorsal

thalamic axons. A reasonably easy way to check this would be to inject DiI within the amygdaloid region at P0, retrogradely labelling the cell bodies of these ectopically projecting axons. However, some indications on their identity could come from the double DiI/DiA injection experiment. The injections of small crystals of DiI and DiA into different cortical regions allowed the visualization of putative cortico-visual axons connecting with the dLGN and putative somatosensory axons connecting with the VB. This showed that although the different *Pdn/Pdn* cortical areas connect with the appropriate target areas within *Pdn/Pdn* dorsal thalamic regions, differences were found in the size of the labelled thalamic nuclei. *Pdn/Pdn* brains display a reduction in the size of the VB and the dLGN labelled by DiA and DiI, respectively. This correlates very well with the observation of several axons making mistakes in the ventral telencephalon. Although only some of the thalamic and cortical axons appropriately connect the *Pdn/Pdn* cortex and thalamus, several others axons are lost along the way and they never reach their final targets.

Interestingly, the *Pdn/Pdn* dLGN contained less back-labelled neurons in comparison to the *Pdn/+* dLGN, while the *Pdn/Pdn* VB seemed to be less affected in the number of back-labelled neurons. Together with the fact that corticothalamic and thalamocortical guidance mistakes are more severe caudally than rostrally in *Pdn/Pdn* mutants, the dramatic size reduction of the back-labelled dLGN suggests that most of the axons coming from the dLGE are lost in the ventral telencephalon and do not reach their final target. Although the causes of these mistakes are unknown it is tempting to speculate on few possibilities. The *Pdn/Pdn* caudal cortex is thinner than rostral and medial cortical regions. In addition, although very little DiI injected into the dorsal thalamus labels axon

fibres in the dorsal most region of the P0 *Pdn/Pdn* cortex, this defect is particularly extreme in caudal *Pdn/Pdn* cortex, where only few labelled axons are detected behind the PSPB. For this reason the *Pdn* mutation may more severely affect cortical axons coming form the caudal cortex and therefore the incoming thalamic axons form the dLGN. This could be either because thalamic axons do not find the reciprocal corticothalamic axons to guide them to their final target, or alternatively because their final target territories are the most affected. However, this cannot explain the thalamocortical tract defects observed at early stages of *Pdn/Pdn* thalamocortical tract development. E14.5 *Pdn/Pdn* thalamic axons project ventrally immediately after they have entered the ventral telencephalon, much earlier than they have the possibility to interact with the reciprocal cortical tract. It could be possible, therefore, that some ventral telencephalic intermediate cues may selectively affect incoming thalamocortical axons, making some of them project away form the cortex. In addition, ventral telencephalic intermediate cues guiding cortical axons could also be affected in *Pdn/Pdn* mutants. Indeed, no *Pdn/Pdn* cortical axons enter the ventral telencephalon at all and this also happens before they have the possibility to interact with incoming *Pdn/Pdn* thalamocorical axons.

In some aspects the thalamocortical defects observed in *Pdn/Pdn* mouse brains are very similar to those observed in *Ebf1, Dlx1/2* and *Sema6a* mutant mice (Garel et al., 2002; Leighton et al., 2001; Little et al., 2009). However, this will be discussed in the final discussion (chapter 6.), because the possible causes of these similarities are more comprehensible in the contest of the results showed in the following chapters of this thesis.

Interestingly, only several days later, after E16.5, it is possible to observe some *Pdn/Pdn* cortical axons entering the ventral telencephalon. This may suggest that thalamocortical axons may eventually reach the cortex without the guidance of corticothalamic axons, and subsequently guide corticothalamic axons to enter the ventral telencephalon. Indeed, at P0 several corticofugal axons enter the ventral telencephalon from more ventral positions, after they have projected in the direction of the amygdaloid region, which is the region where several *Pdn/Pdn* thalamic axons are abnormally directed. To verify this idea it would be extremely helpful to use a reporter mouse line in which thalamocortical axons are selectively labelled and to observe the behaviour of thalamocortical axons in the *Pdn/Pdn* background, or even better in *Pdn/Pdn Golli tau-GFP* background.

NF staining at E14.5 also reveals the absence of $NF^+$ axons in the *Pdn/Pdn* cortex. This may suggest that the *Pdn/Pdn* cortex may be delayed in the production of $NF^+$ axons. Alternatively, it could also be possible that $NF^+$ axons in the *Pdn/+* cortex are indeed thalamic axons that have already reached it. Therefore, the fact that *Pdn/Pdn* thalamic axons have not reached the *Pdn/Pdn* cortex at E14.5, as shown by DiI injections, could be the reason why it is not possible to detect $NF^+$ fibres in the *Pdn/Pdn* cortex. In agreement with this hypothesis is the fact that *Pdn/Pdn Golli tau-GFP* embryos show *Pdn/Pdn* brains normally forming early projecting cortical neurons and their axons in lower *Pdn/Pdn* layers and the *Pdn/Pdn* subplate, as early as E14.5. This suggests that the formation of cortical projecting neurons and their axons is not affected in *Pdn/Pdn* mutants. In addition, the whole P0 *Pdn/Pdn* cortex is positive for neurofilament staining. However, again to check these hypotheses it would be necessary to unequivocally label thalamocortical axons in *Pdn/Pdn* brains.

Nevertheless, the results in this chapter show that several axons guidance defects are happening once *Pdn/Pdn* thalamic and cortical axons are interacting with the *Pdn/Pdn* ventral telencephalon. The cellular and molecular mechanisms underling these defects are the subject of the experimental work shown in the following sections of this thesis.

# Chapter 4: The *Pdn* ventral telencephalon fails to guide thalamic axons towards the cortex

## 4.1 Introduction

In the previous chapter, axon guidance mistakes of the thalamocortical and corticothalamic tracts were shown in the ventral telencephalon of *Pdn/Pdn* mutants. E14.5 and E16.5 *Pdn/Pdn* corticothalamic axons do not enter the LGE but project along the PSPB. Only at P0 do some *Pdn/Pdn* cortical axons eventually project towards the diencephalon. Contrarily, *Pdn/Pdn* thalamic axons do enter the MGE, but subsequently display several guidance mistakes. Caudally, they immediately project ventrally, while rostrally they do enter the internal capsule, but the tract subsequently bifurcates several times and only a few thalamic axons reach the developing cortex. These defects are still evident at P0. However, these analyses did not allow discrimination of whether (1) the defects within the formation of *Pnd/Pdn* thalamocortical and corticothalamic tracts were caused by thalamic and cortical axons not being able to respond appropriately to guidance cues along their path (cell-autonomous defects), or (2) defects in the formation of these guidance cues along the path of thalamocortical and corticothalamic axons in the *Pdn/Pdn* telencephalon could affect the capacity of these axons to reach their final target (non-cell-autonomous defects). The following experiments aimed to investigate to

which extent cell-autonomous and non-cell-autonomous defects contribute to the observed axonal phenotype in *Pdn/Pdn* mutant mice.

In this chapter defects in *Pdn/Pdn* thalamocortical tract formation are investigated first, while the defects observed in corticothalamic tract formation are analyzed in the next chapter. The following experiments were focused on characterizing early steps of *Pdn/Pdn* dorsal thalamus patterning, and also analyzing the formation of intermediate cues within the *Pdn/Pdn* ventral telencephalon important for thalamocortical axon progression. First, the expression pattern of *Gli3* was studied in detail to correlate expression with the phenotypic defects observed in Pdn mutants. Secondly, in situ hybridization for several genes that are important for the formation of different thalamic nuclei showed that the *Pdn/Pdn* mutation does not affect the expression pattern of these genes in different regions of the developing *Pdn/Pdn* thalamus. Subsequently, DiI injections, in situ hybridizations and immunostaining techniques were used to reveal the presence and the correct spatial distribution of different axon guidance cues within the *Pdn/Pdn* ventral telencephalon. In situ hybridizations also aimed to reveal the presence of attractive guidance molecules for thalamocortical axons within the *Pdn/Pdn* cortex. These analyses showed that the *Pdn/Pdn* ventral telencephalon displays abnormalities in the formation of the "corridor cell" population necessary to channel thalamic axons through the MGE (Lopez-Bendito et al., 2006). Finally, the capacity of *Pdn/Pdn* thalamic axons to navigate within the ventral telencephalon was tested in an in vitro assay transplanting *Pdn/Pdn* thalamic tissue into the *Pdn/+* ventral telencephalon. This experiment showed no major abnormalities in the growth pattern of *Pdn/Pdn*

thalamocortical axons and, therefore, their ability to respond correctly to *Pdn/+* ventral telencephalic intermediate targets.

In contrast, transplantation of *Pdn/+* thalamic tissue into the *Pdn/Pdn* ventral telencephalon showed that the *Pdn/Pdn* ventral telencephalon has lost the ability to guide *Pdn/+* thalamocortical axons and direct them towards the cortex. Altogether these data show that the *Pdn* mutation seems to preferentially affect thalamocortical intermediate guidance cues within the ventral telencephalon rather than the dorsal thalamic axons themselves in their capacity to respond to these cues.

## 4.2 *Gli3* expression pattern in the developing forebrain

Although previous studies have already published *Gli3* expression pattern within the developing mouse telencephalon and diencephalons (Fotaki et al., 2006; Hui and Joyner, 1993), these studies did not focus on its expression within different telencephalic and diencephalic territories at different ages of early embryonic development, during the formation of thalamocortical and corticathalamic connections and of their intermediate guidance cues. Therefore, I decided to systematically reveal the spatial expression of *Gli3* within the telencephalon and diencephalon of mouse embryos between E10.5 and E14.5 (Fig. 4.1).

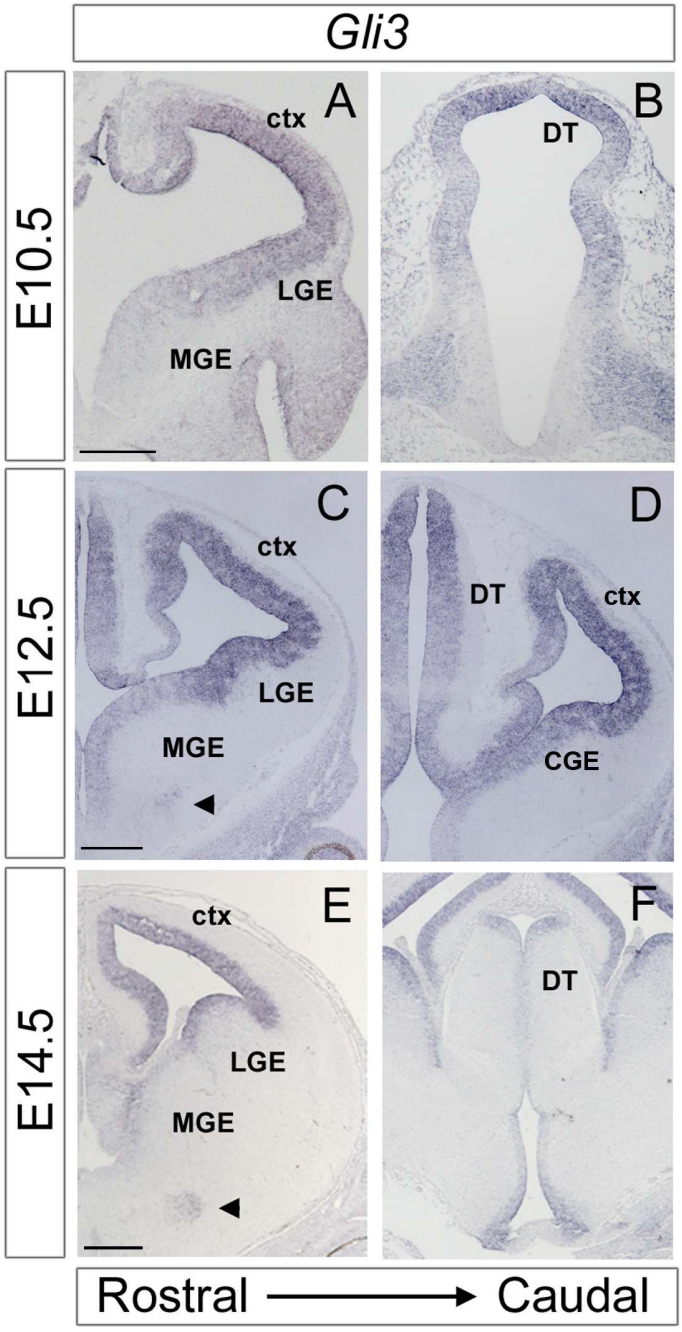
Gli3
E10.5
E12.5
E14.5
A
ctx
LGE
MGE
B
DT
C
ctx
LGE
MGE
D
DT
ctx
CGE
E
ctx
LGE
MGE
F
DT
Rostral
Caudal

**Figure 4.1.**
**In situ hybridizations revealing *Gli3* mRNA expression in *Pdn*/+ E10.5 (A, B), E12.5 (C, D) and E14.5 (E, F) coronal brain sections.** A and B are serial sections organized from rostral to caudal, as well as C and D, E and F.

*Gli3* is expressed in progenitor cells within the ventricular zones of the developing cortex, ventral telencephalon and dorsal thalamus at E10.5 (A, B), E12.5 (C, D) and E14.5 (E, F), but not in neurons. In rostral sections *Gli3* expression seems to follow a gradient high-dorsal to low-ventral within the telencephalon, with the MGE more lightly stained than cortex and LGE (A, C, E). By E14.5, *Gli3* expression in the dorsal thalamus seems to be drastically reduced if compared with *Gli3* thalamic expression at E10.5 and E11.5 (compare B and D with F). In addition, at E12.5 and E14.5 *Gli3* expression is also observed in a small group of cells within the mantle zone of the MGE, which probably correspond to globus pallidum (arrowheads in C and E). Abbreviations: VT, ventral thalamus. (Scale bars in A-B, C-D and E-F 100 μm).

In situ hybridizations reveal *Gli3* mRNA within the ventricular zones of the developing cortex and dorsal thalamus, but not in neurons (Fig. 4.1). *Gli3* is expressed within the dorsal thalamus and cerebral cortex before (E10.5 and E12.5) and at the time (E14.5) when the thalamocortical and corticothalamic tracts start to display abnormalities. Its expression coincides with the birth of thalamic and cortical projecting neurons, and with the formation of guidance cues within the ventral telencephalon (Fig. 4.1; B, D, F). In addition, between E12.5 and E14.5 several cortical and thalamic projecting neurons are born and start to project their axons towards their final targets. *Gli3* is also expressed between E10.5 and E14.5 within the ventricular zone of the LGE at high levels and the MGE at lower levels when several intermediate guidance cues within the ventral telencephalon are forming (Fig. 4.1). In addition, at E12.5 and E14.5, in situ hybridizations also showed *Gli3* expression in a small group of cells within the mantle zone of the MGE, which has not been previously described (Fig. 4.1; C, E). Therefore, the *Pdn* mutation may affect the ability of projecting axons to navigate towards their target territories within the cortex and thalamus, or the formation of thalamocortical and/or corticothalamic intermediate guidance cues. However, because *Gli3* is not expressed in neurons, but in progenitor cells, its effects on the development of the thalamocortical and corticothalamic tracts and their intermediate guidance cues are more likely to be indirect.

## 4.3 The *Pdn* mutation does not alter the molecular identity of different thalamic territories at early phases of diencephalic patterning

Most of the dorsal thalamic projecting neurons are born in the thalamus between E12.5 and E18.5 (reviewed in (Lopez-Bendito and Molnar, 2003; Price et al., 2006). Defects in patterning the dorsal thalamus may be the primary cause of the guidance defects observed in *Pdn/Pdn* thalamocortical connections. For this reason, the expression patterns of several genes important for thalamus development were analyzed in the *Pdn/Pdn* mutant diencephalon by in situ hybridization.

In situ hybridization was performed for the following markers on E14.5 *Pdn/+* and *Pdn/Pdn* brains: *Gbx2, Ngn2, Dlx2, Emx2 and Lhx2* expression was analyzed on coronal E12.5 brain sections. The expression pattern of these genes within the diencephalons has been previously established (Lopez-Bendito and Molnar, 2003; Nakagawa and O'Leary, 2001). In addition, mice mutants for these genes display defects in thalamocortical tract formation and within their reciprocal corticothalamic innervations. Moreover, some of these genes have been shown to change their expression pattern in the telencephalon of *Gli3* mutants. Here I only focus on their expression patterns within the thalamus and other diencephalic territories. The decision to focus on these embryonic ages was made because at E12.5 and at E14.5 several early projecting thalamic neurons are specified. In addition, E14.5 *Pdn/Pdn* mutant brains show thalamocortical tract defects. Differences in the expression pattern of these genes would suggest patterning and differentiation defects within the developing dorsal thalamus of *Pdn/Pdn* mutant brains.

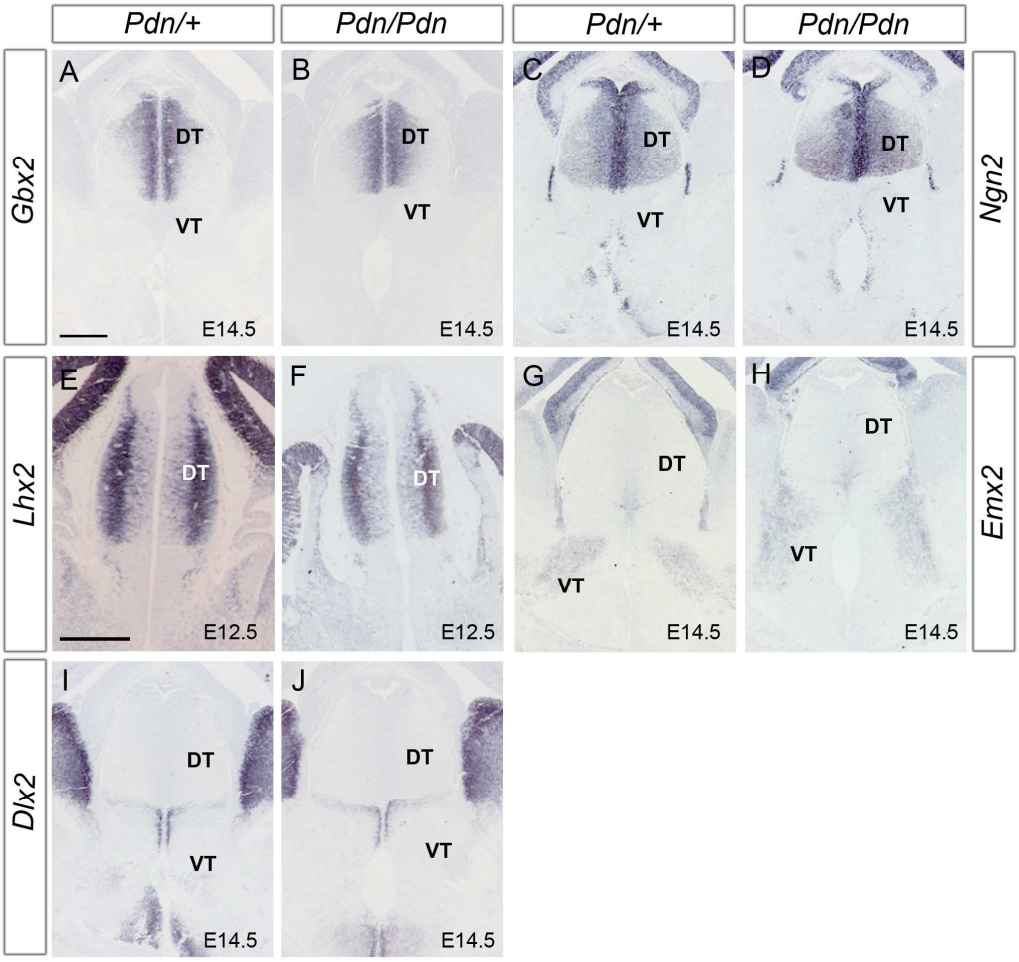
Pdn/+
Pdn/Pdn
Pdn/+
Pdn/Pdn
Gbx2
Ngn2
Lhx2
Emx2
Dlx2
A
B
C
D
E
F
G
H
I
J
DT
VT
E14.5
E12.5

**Figure 4.2.**

**In situ hybridization on *Pdn/+* and *Pdn/Pdn* coronal brain sections revealing the diencephalic expression patterns of *Gbx2* (A, B), *Ngn2* (C, D), *Emx2* (G, H) *and Dlx2* (I, J) at E14.5 and of *Lhx2* (E, F) at E12.5.**

In *Pdn/+* brains, *Gbx2* is expressed within the ventricular zone of the dorsal thalamus, but also in the dorsal most region of the dorso-thalamic mantle (A). *Ngn2* is expressed at high levels within the ventricular zone of the dorsal thalamus, with a sharp expression boundary at the zona limitans intrathalamica (C). It is also expressed within the mantle zone in a high ventral to low dorsal gradient (C). *Lhx2* is expressed in the ventricular zone of the developing dorsal thalamus in a "salt and pepper" fashion and at high level within the dorso-thalamic mantle zone (E). *Emx2* is expressed in a diffuse fashion at the border between the diencephalon and the telencephalon (G). It is also expressed within the ventral thalamic until the boundary between dorsal and ventral thalamus (G). *Dlx2* diencephalic expression is limited to the ventral thalamic ventricular zone and the zona limitans intrathalamica (I). It was not possible to detect any difference in the expression patterns of these genes within the diencephalon of *Pdn/Pdn* mutant brains (compare A with B, C with D, E with F, G with H and I with L). (n=3) (Scale bar in A 100 μm; applays to B-D and G-J) (Scale bar in E 100 μm; applays to F).

In *Pdn/+* brains the homeobox transcription factor *Gbx2* is expressed at E14.5 within the dorsal thalamus and it has been shown to be required for the formation of different thalamic nuclei (Chen et al., 2009; Miyashita-Lin et al., 1999). Indeed *Gbx2* null mutants display defects in the production of dorsal thalamic post-mitotic cells at early steps of thalamic formation (E14.5). This leads to the near absence of the dLGN and a drastic reduction of the size of the VB later in development (P0), resulting in thalamocortical tract defects with little production of projecting thalamocortical axons (Miyashita-Lin et al., 1999). The *Gbx2*$^{-/-}$ dorsal thalamic axons, which are still produced, fail to reach the developing cortex, stopping within the subpallial regions and the reciprocal corticothalamic axons do not enter the diencephalon even though there are no cortical developmental defects (Hevner et al., 2002). The formation of several other thalamic nuclei, not connecting with the cortex, is also affected, like the ventral lateral geniculate and the mentromedial and poster nuclei (Miyashita-Lin et al., 1999). At E14.5 *Gbx2* is expressed within the VZ of the DT, but also in the dorsal most region of the dorso-thalamic mantle (Fig.4.2; A).

*Neurogenin2 (Ngn2)* is a bHLH transcription factor expression of which is strikingly regionalized within the dorsal thalamus (Nakagawa and O'Leary, 2001). *Ngn2* is expressed in dorsal thalamic neurons mainly projecting to rostral cortical areas, within a gradient of high ventro-rostral to low lateral-dorsal (Seibt et al., 2003). *Ngn2* is required cell-autonomously for thalamic axons to reach the frontal cortex, specifying the responsiveness of thalamic axons to respond to guidance cues within the ventral telencephalon (Seibt et al., 2003). At E14.5 in *Pdn/+* diencephalon, *Ngn2* is expressed at

high levels within the ventricular zone of the dorsal thalamus, with a sharp expression boundary at the zona limitans intrathalamica. It is also expressed within the mantle zone in a high ventral to low dorsal gradient (Fig. 4.2; C).

*Lhx2* is a LIM-homeodomain transcription factor, whose regionalized expression in dorsal thalamus has been suggested to play a role in the formation of the identity of dorsal thalamic nuclei in combination with other transcription factors, such as *Ngn2* and *Gbx2* (Bachy et al., 2002; Nakagawa and O'Leary, 2001). *Lhx2* is involved in the establishment of the axonal connections from the caudal dorsal thalamus to the cortex (Lakhina et al., 2007). *Lhx2* null mutants also display defects in thalamocortical tract formation with thalamocortical axons not being able to enter the ventral telencephalon because of the absence of MGE pioneer neurons (Lakhina et al., 2007). At E12.5, *Lhx2* is expressed in the ventricular zone of the developing dorsal thalamus and within the mantle zone (Fig. 4.2; E).

*Emx2* knockout mice display severe defects in cortical development: the cortical hemispheres are reduced in size and cortical lamination is affected (Mallamaci et al., 2000; Yoshida et al., 1997). *Emx2* absence also leads to a shift of cortical area identity and to altered distribution of thalamocortical projections within the cortex (Bishop et al., 2003). *Emx2* knockout mice also display early thalamocortical guidance mistakes with several thalamic axons projecting ventrally along the DTB and not entering the ventral telencephalon at E14.5. This is due to a misplacement of primitive internal capsule neurons within the *Emx2*$^{-/-}$ ventral telencephalon (Lai et al., 2008; Lopez-Bendito et al., 2002). In situ hybridization shows that *Emx2* is expressed in a diffuse fashion at the

border between the diencephalon and the telencephalon. Its ventral thalamic expression extends nearly to the boundary of the dorsal thalamus (Fig. 4.2; G).

*Dlx2* null mutants also show guidance mistakes in thalamocortical axonal connections within the developing ventral telencephalon. Several *Dlx2*$^{-/-}$ thalamocortical axons project ventrally once they have entered the ventral telencephalon. Moreover *Dlx2*$^{-/-}$ mutants also display defects in the topography of the connections between cortex and thalamus, with a ventral shift of dorsal thalamic nuclei connecting with the cortex. These data also show the importance of ventral telencephalic guidance cues in sorting thalamocortical axons before they connect with the cerebral cortex (Garel et al., 2002). In situ hybridization on coronal sections of E14.5 *Pdn/+* brains show that *Dlx2* expression in the diencephalon is limited to the ventral thalamus, ventral to the zona limitans intrathalamica (Fig. 4.2; I).

It was not possible to detect any difference in the expression patterns of these genes within the diencephalon of *Pdn/Pdn* mutant brains. Interestingly, previous reports showed a down-regulation of *Emx2* and an up-regulation of *Dlx2* within the developing cortex of *Pdn/Pdn* mutant brains mutants (Kuschel et al., 2003). However, these alterations are specific for the telencephalon (Fig. 4.2; B, D, F, H and J).

These analyses revealed that the *Pdn* mutation does not alter the molecular identity of different thalamic territories. Although we cannot exclude primary defects in developing thalamic neurons, these results suggest that the severe guidance mistakes of early *Pdn/Pdn* projecting thalamocortical axons are more likely to be caused by defects in ventral telencephalic intermediate guidance cues.

## 4.4 The formation of the *Isl1*$^{+}$ permissive corridor is affected in the *Pdn/Pdn* ventral telencephalon

During their navigation thalamocortical axons rely on a number of intermediate guidance targets within the MGE and LGE to progress towards the cortex. The following experiments focused on the identification of these cues within the *Pdn/Pdn* ventral telencephalon.

At around E13.5 thalamic axons reach the ventral telencephalon. At this point they have to make a sharp turn and enter the MGE passing over the DTB. A population of neurons located within the MGE, close to the DTB, has been shown to play an important role in guiding dorsal thalamic axons across this boundary by projecting pioneer axons from the MGE towards the dorsal thalamus. *Lhx2* mutant embryos display a dramatic reduction of these pioneer neurons and thalamic axons fail to enter the *Lhx2*$^{-/-}$ MGE (Lakhina et al., 2007). However, the investigation of these neurons is complicated by the fact that no definitive markers have been identified to reveal them. So far, the only way to detect these pioneers is to retrogradely label these cells by injecting DiI into the developing thalamus. Using this method it was possible to identify a substantial population of back-labelled cells within the MGE of E12.5 *Pdn/+* brains (Fig. 4.3; A, B).

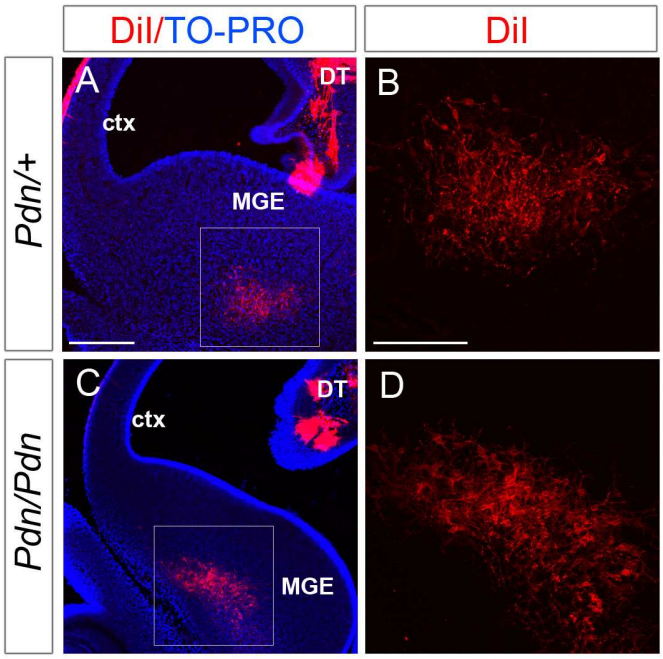


**Figure 4.3.**

**Dorsal thalamic DiI injections showing MGE pioneer neurons on *Pdn*/+ and *Pdn*/*Pdn* E12.5 coronal brain sections (A-D).** B and D are higher magnifications of A and C, respectively. A, C coronal brain sections are contrastained with TO-PRO.

DiI injected into the *Pdn*/+ developing thalamus diffuses until the ventral telencephalon revealing a substantial population of back-labelled cells within the MGE (A, B). Higher magnification reveals a conspicuous number of DiI back-labelled neural cell bodies (B). The same experiment on E12.5 *Pdn/Pdn* brains showed no obvious differences between *Pdn/Pdn* mutant and *Pdn*/+ control brains (C, D). (n=4) (Scale bar in A 100 μm; applays to C) (Scale bar in B 50 μm; applays to D).

The same experiment on E12.5 *Pdn/Pdn* brains showed no obvious differences between *Pdn* homozygous mutant and control brains (Fig. 4.3; C, D), suggesting that *Pdn/Pdn* MGE pioneer neurons can normally guide thalamocortical axons through the DTB within the ventral telencephalon.

Once thalamocortical axons enter the MGE they face a non-permissive environment. A permissive corridor of neurons guides projecting fibres towards the cortex and allows thalamocortical axons to progress through the MGE (Lopez-Bendito et al., 2006). The corridor forming cells originate within the LGE and migrate tangentially to the MGE. Indeed, they are positive for the expression of markers characteristic of the LGE mantle, such as *Ebf1* and *Isl1*, but they are negative for markers characteristic of the MGE, such us *Nkx2.1*. Failure in the tangential migration of the corridor cells from the LGE to the MGE results in the failure of thalamocortical axon to grow within the ventral telencephalon, *in vivo* as well as *in vitro* (Lopez-Bendito et al., 2006). In the following experiment, the expression of corridor cell markers was examined within the developing ventral telencephalon of *Pdn/+* and *Pdn/Pdn* embryos (Fig. 4.4; E-H).

The early formation of corridor cells was investigated by the use of in situ hybridization for *Ebf1*. In *Pdn/+* coronal brain sections, *Efb1* expression labels the presumptive corridor neurons within the mantle of the LGE at E11.5 and E12.5 (Fig. 4.4; A, C). At E11.5 *Ebf1* expressing cells start to migrate from the LGE into the MGE with only a few *Ebf1* expressing cells entering the MGE (Fig. 4.4; A). Subsequently, at E12.5, *Ebf1* in situ hybridization staining expands within the mantle of the LGE and progressively more *Ebf1* expressing cells invade the mantle region of the dorsal MGE (Fig. 4.4; C).

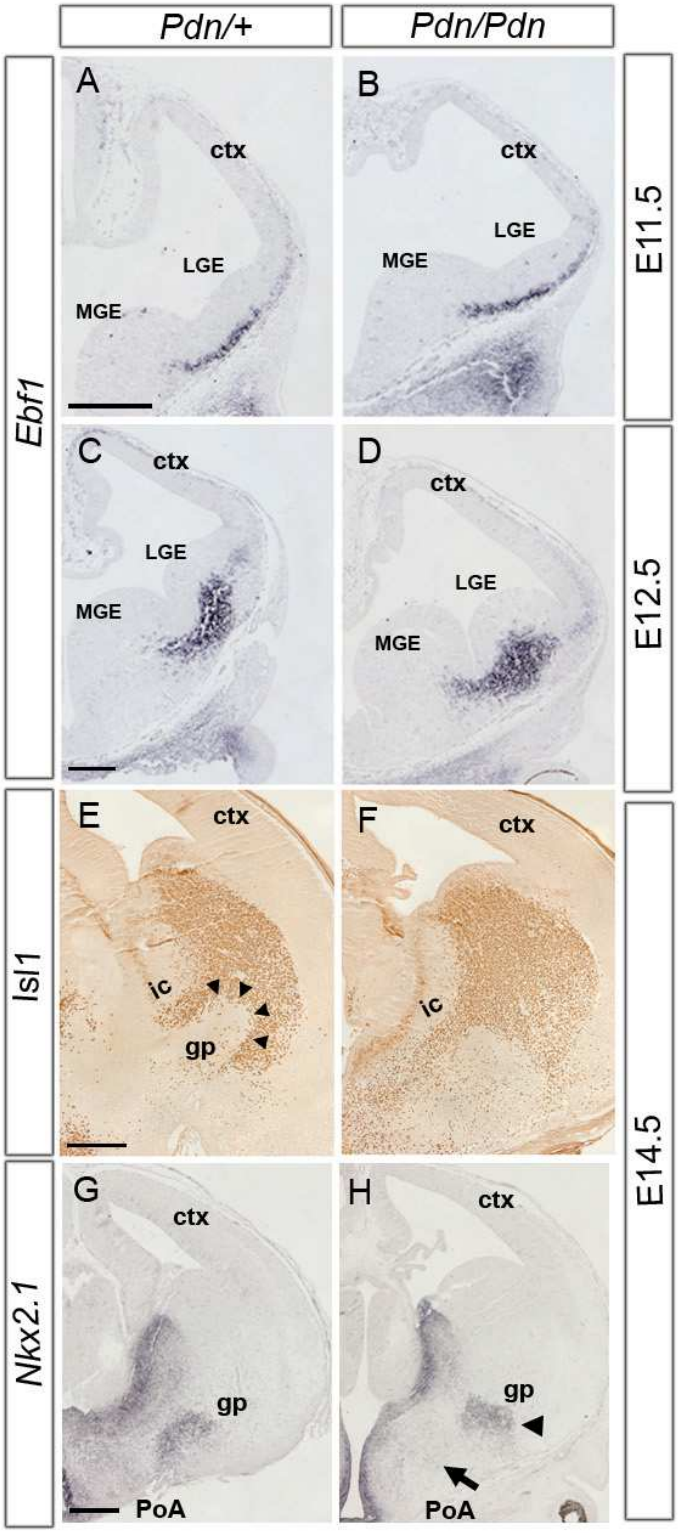
Pdn/+
Pdn/Pdn
Ebf1
Isl1
Nkx2.1
E11.5
E12.5
E14.5
A
B
C
D
E
F
G
H
ctx
LGE
MGE
ic
gp
PoA

**Figure 4.4.**

**Investigation of the formation of corridor permissive to thalamocortical axons in the ventral telencephalon of E12.5 *Pdn/+* and *Pdn/Pdn* brains (A-H).**

In *Pdn/+* coronal brain sections, *Efb1* expression labels the presumptive corridor neurons within the mantle of the LGE at E11.5 (A) and E12.5 (C). At E11.5 *Ebf1* expressing cells start to migrate from the LGE into the MGE and only a few *Ebf1* expressing have entered the MGE (A). At E12.5, more LGE mantle cells express *Ebf1* and more *Ebf1* expressing cells invade the mantle region of the dorsal MGE (C). At these stages no difference was found in *Ebf1* expression between *Pdn/+* and *Pdn/Pdn* mutant brains (B, D). *Isl1* immunohistochemistry on *Pdn/+* coronal brains sections at E14.5 labels the LGE and LGE derived corridor cells migrating within the MGE (E). The mantle region of the LGE uniformly expresses Isl1 (E). Dorsally within the LGE, Isl1 expression stops sharply at the PSPB (E). Ventrally, $Isl1^{+}$ migrating cells avoid the globus pallidus and form a characteristic "horseshoe" shape around it (arrowheads in E). *Pdn/Pdn* LGE mantle cells are positive for Isl1 and show no difference to control brain sections (F). Also, dorsally Isl1 expression stopped at the PSPB (F). However, Isl1+ ventrally migrating cells display an altered distribution within the *Pdn/Pdn* MGE, losing the "horseshoe" shaped organization (F). The upper branch, forming the internal capsule, is not as well defined as in *Pdn/+* ventral telencephalon, while the lower branch and the globus pallidus are not discernible (F). The E14.5 *Pdn/+* ventricular zone and the mantle zone of the MGE express *Nkx2.1*, as revealed by in situ hybridization, showing a complementary pattern to Isl1 (G). However, the MGE corridor cells are negative for *Nkx2.1* (G). In *Pdn/Pdn* brains, *Nkx2.1* expression was reduced within the MGE (H). The *Nkx2.1*- corridor region is larger (H). Moreover, the *Nkx2.1* expressing *Pdn/Pdn* MGE mantle region was smaller compared to control brains, resulting in a different shape and in a size reduction of the globus pallidus (arrowhead in H). *Nkx2.1* is also expressed in a diffuse manner within the region of the preoptic area (G), but its expression is drastically reduced in the *Pdn/Pdn* preoptic area (arrow in H).Abbreviations: gp, globus pallidum; PoA, preoptic area. (Scale bars in A-B, C-D, E-F ans G-H 100 μm).

At these stages no difference was found in *Ebf1* expression between *Pdn/+* and *Pdn/Pdn* mutant brains (Fig. 4.4; B, D).

*Isl1* is a marker for LGE derived corridor cells migrating within the MGE. Isl1 expression was detected by immunohistochemistry on coronal sections of E14.5 *Pdn/+* and *Pdn/Pdn* brains. The mantle region of the LGE uniformly expresses Isl1. Dorsally within the LGE, Isl1 expression stops sharply at the PSPB in *Pdn/+* coronal brains sections. Ventrally, $Isl1^{+}$ migrating cells avoid the globus pallidus and form a characteristic "horseshoe" shape around it (Fig. 4.4; E), with thalamocortical axons growing through the upper branch of this horseshoe structure (Lopez-Bendito et al., 2006).

*Pdn/Pdn* LGE mantle cells were positive for Isl1 showing no difference between *Pdn/Pdn* mutant and control brains sections (Fig. 4.4; F). Dorsally Isl1 expression stopped at the PSPB (Fig. 4.4; F). However, the expression pattern of Isl1 in ventrally migrating cells was different. Although $Isl1^{+}$ cells are still migrating ventrally they display an altered distribution within the MGE, losing the horseshoe shaped organization. The upper branch, forming the internal capsule, is not as well defined as in *Pdn/+* ventral telencephalon, while the lower branch and the globus pallidus are not discernible (Fig. 4.4; F). In addition, contrarily to *Pdn/+*, within the *Pdn/Pdn* preoptic area region it is possible to observe a sparse number of cells positive for $Isl1^{+}$ (Fig. 4.4; F).

The ventricular zone and the mantle zone of the MGE express *Nkx2.1*, as revealed by in situ hybridization on coronal sections of E14.5 *Pdn/+* brains, showing a complementary pattern to Isl1 (Fig. 4.4; G). The corridor cells are negative for *Nkx2.1* within the *Pdn/+*

MGE (Fig. 4.4; G). *Nkx2.1* is also expressed in a diffuse manner within the region of the preoptic area (Fig. 4.4; G). In *Pdn/Pdn* brains, *Nkx2.1* expression was reduced within the MGE. The gap of *Nkx2.1* expression between the globus pallidus and the MGE ventricular zone, which corresponds to the corridor region, was larger. Moreover, the *Nkx2.1* expressing *Pdn/Pdn* MGE mantle region was smaller compared to control brains, resulting in a different shape and in a size reduction of the globus pallidus (Fig. 4.4; H). From these data, it appears that the corridor cells are migrating ventrally forming the internal capsule, but the $Isl1^{+}$ area is enlarged, while the globus pallidus is smaller.

Once thalamocortical axons have navigated through the permissive channel and through the LGE, they reach the cortex passing over the PSPB. The developing cortex attracts thalamocortical axons from the ventral telencephalon. In particular, the developing cortex expresses the Ig form of Neuregulin1 (Nrg1-Ig), which attracts thalamocortical axons towards the cortex. Indeed, ablation of Nrg1-Ig affects the navigation of thalamocortical axons stopping them from passing over the PSPB into the cortex (Lopez-Bendito et al., 2006). In situ hybridization performed on E14.5 *Pdn/+* brains showed Nrg1-Ig expression in the ventricular zone of the developing cortex (Fig. 4.5; A, C). The same experiments on *Pdn/Pdn* brains did not reveal obvious differences in the expression of Nrg1-Ig within the cortex (Fig. 4.5; B, D). These data show that the *Pdn/Pdn* developing cortex contains some of the information required to attract thalamocortical axons towards their final targets.

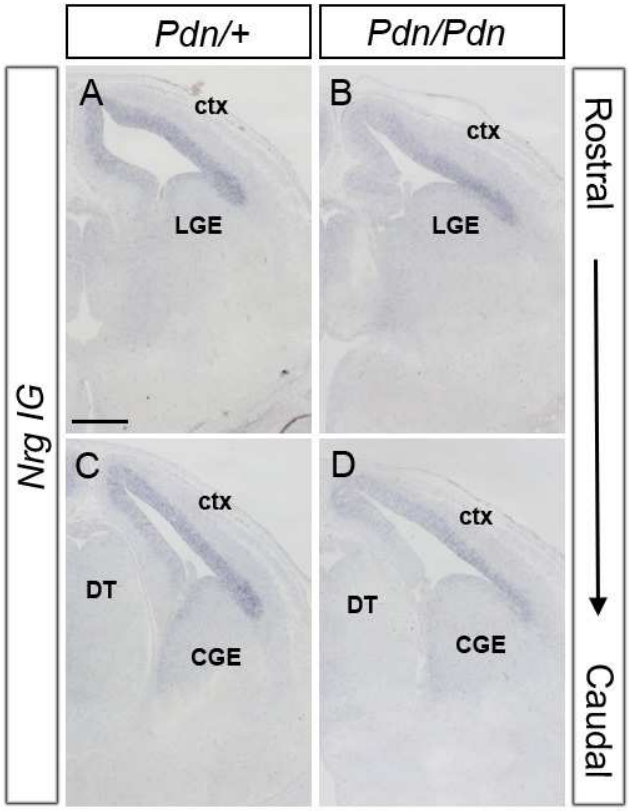


**Figure 4.5.**

**In situ hybridization performed on E14.5 *Pdn/+* and *Pdn/Pdn* coronal brain sections to reveal *Nrg1-Ig* expression (A-D).** A and C are serial sections organized from rostral to caudal, as well as B and D.

*Nrg1-Ig* is expressed in the ventricular zone of *Pdn/+* developing cortex in a gradient high ventro-lateral to low doro-medial (A, C). Low *Nrg1-Ig* expression is also detected in the ventricular zone of the LGE (A) and CGE (C). The same experiments on *Pdn/Pdn* brains did not reveal obvious differences in the expression of *Nrg1-Ig* if compared to *Pdn/+* (B, D). (n=3) (Scale bar in A 100 μm; applays to all pannels).

Taken together, these data reveal that the thalamocortical axon phenotype observed in *Pdn/Pdn* brains correlates with defects in formation of thalamocortical guidance cues within the ventral telencephalon of these animals. The *Pdn/Pdn* ventral telencephalon shows abnormalities in the formation of the permissive $Isl1^+$ corridor cells. *Ebf1* in situ hybridization and Isl1 immunostaining show that the corridor cells do form and do migrate ventrally from the LGE to the MGE. However, the distribution of these ventrally migrating cells is affected. $Isl1^+$ cells form a broader corridor and show a more diffuse distribution pattern within the *Pdn/Pdn* MGE mantle and preoptic area. This is also confirmed by *Nkx2.1* expression, which is drastically reduced within the *Pdn/Pdn* MGE mantle. These defects may result in an expansion of territories permissive to thalamocortical axons in the *Pdn/Pdn* MGE. This hypothesis was tested with an in vitro assay described in the following section.

## 4.5 *Pdn/Pdn* ventral telencephalon is not able to guide thalamocortical axons towards the developing cortex

Although obvious patterning abnormalities were not found within the dorsal thalamus of *Pdn/Pdn* mutant brains it could be possible that thalamocortical axons are compromised in their ability to respond to guidance cues in the ventral telencephalon. The capacity of *Pdn/Pdn* thalamocortical axons to navigate within the ventral telencephalon was tested with an in vitro culture assay. To distinguish the donor tissue from the recipient tissue in

these culture assays, *Pdn* mice were crossed with τ-GFP expressing mice. In these animals, a τ-GFP fusion protein is ubiquitously expressed. The τ tag tethers the GFP to microtubules and thus, labels axonal projections and cell bodies (Pratt et al., 2000a).

E13.5 GFP negative brains were sliced coronally in 300μm thick sections on a vibratome. These sections were used as recipient tissue. Subsequently, the preoptic area was removed from recipient slices. The GFP-expressing E13.5 brains were also sliced coronally, the dorsal thalamus was dissected from these sections and used as donor tissue replacing the recipient preoptic area. After 72 hours of culture, the transplants were fixed and GFP immunostaining revealed the trajectory of GFP positive thalamic axons within the recipient section. This slice culture method provides the advantage of maintaining the brain morphology within the slices allowing thalamic axons to grow within the telencephalic tissue in a pattern similar to the *in vivo* situation (Fig. 4.6).

E13.5 *Pdn/+ GFP*$^{+}$ thalamic explants were transplanted into E13.5 *Pdn/+* coronal slices for control experiments. In 8 of 9 control experiments, the *Pdn/+ τ-GFP*$^{+}$ thalamic axons projected towards the *Pdn/+* cerebral cortex. Within the *Pdn/+* ventral telencephalon, GFP$^{+}$ thalamic axons are channeled through the internal capsule similar to the *in vivo* situation. Notably, axons avoid the globus pallidus (Fig. 4.6; A, B). In 4 out of 9 cases, some axons also grew along the ventral border of the globus pallidus (Fig. 4.6; A, B and Table 4.1). However, this result is not surprising because the removal of the preoptic area in some sections result in a direct contact of the thalamic explants with the striatal regions.

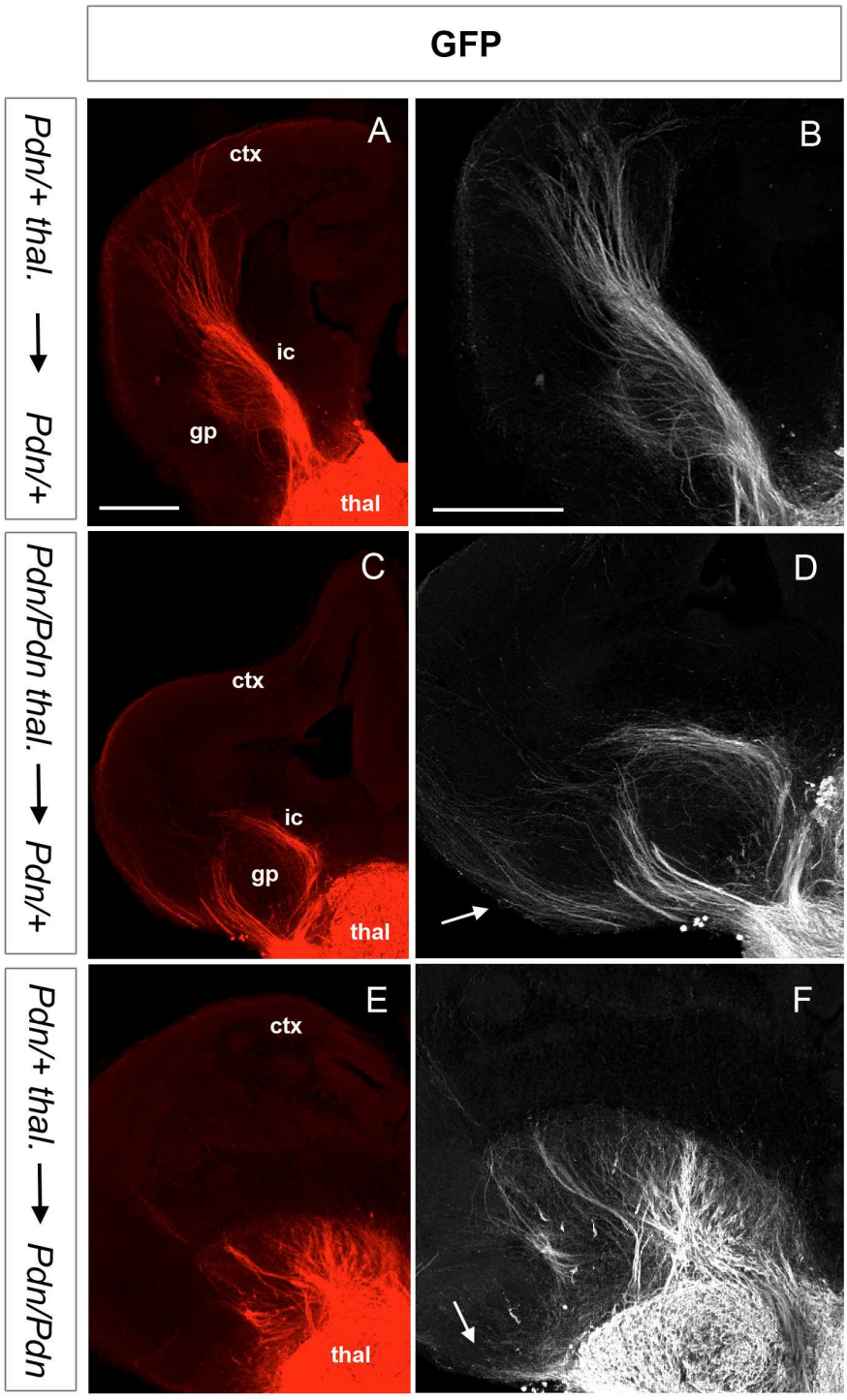
GFP
Pdn/+ thal. → Pdn/+
Pdn/Pdn thal. → Pdn/+
Pdn/+ thal. → Pdn/Pdn
A
B
C
D
E
F
ctx
ic
gp
thal

**Figure 4.6.**

**GFP staining on organotypic co-culture experiments in which E13.5 *Pdn/+* and *Pdn/Pdn τ-GFP*$^+$ dorsal thalamic explants were transplanted into E13.5 *Pdn/+* and *Pdn/Pdn* ventral telencephalon of coronal brains slice.** A, B *Pdn/+ GFP*$^+$ thalamic explants were transplanted into *Pdn/+* coronal slices. C, D *Pdn/Pdn τ-GFP+* thalamic explants were transplanted into *Pdn/+* coronal slices. E, F *Pdn/+* GFP$^+$ thalamic explants were transplanted *Pdn/Pdn* coronal sections. B, D and F are higher magnifications of A, C and D, respectively.

*Pdn/+ τ-GFP*$^+$ thalamic axons projected towards the *Pdn/+* cerebral cortex (A, B). Within the *Pdn/+* ventral telencephalon, thalamic axons channeled through the internal capsule similar to the *in vivo* situation, mainly avoiding the globus pallidus (A, B). Some of the axons also grew along the ventral border of the globus pallidum (more clear in B). *Pdn/Pdn* GFP$^+$ thalamic axons display a very similar behaviour to *Pdn/+* GPF$^+$ axons (C, D). *Pdn/Pdn* thalamic axons grew into the internal capsule of *Pdn/+* sections avoiding the globus pallidus (C, D). Some axons also grew along the ventral edge of the globus pallidum (more clear in D). However, contrary to the above experiment, some of the *Pdn/Pdn* GFP$^+$ thalamic axons grew along the edge of the *Pdn/+* slice (arrow in D). *Pdn/+* GFP$^+$ thalamic axons appear to grow in a disorganized manner within the *Pdn/Pdn* MGE of the host slice (E, F). *Pdn/+* thalamic axons abnormally penetrated the whole *Pdn/Pdn* MGE mantle zone never channelling through the *Pdn/Pdn* internal capsule (E, F). In addition, it is also possible to observe some of the *Pdn/+* thalamic axons growing along the edge of the *Pdn/Pdn* section in a similar pattern observed for *Pdn/Pdn* thalamic explants transplanted into *Pdn/+* ventral telencephalon (arrow in F). Abbreviations: thal, thalamic explants. (Scale bar in A 200 μm; applays to C, E) (Scale bar in B 200 μm; applays to D, F).

This region is positive for *Isl1* and is therefore permissive to the growth of thalamic axons (Lopez-Bendito et al., 2006). A similar pattern of growth has been observed in previous transplantation experiments (Lopez-Bendito et al., 2006).

Thus, this in vitro assay efficiently reproduces the in vivo behaviour of thalamocortical axons in the developing brain. Axons preferentially fasciculate and grow within the internal and the striatal territories, avoiding MGE territories such as the globus pallidus and the MGE ventricular zone.

Testing the ability of *Pdn/Pdn* thalamocortical axons to navigate into the *Pdn/+* ventral telencephalon under these culture conditions involved the transplantation of *Pdn/Pdn τ-GFP+* thalamic explants into *Pdn/+* coronal slices (Fig. 4.6; C, D). In 7 out of 9 cultures, the *Pdn/Pdn* $GFP^+$ thalamic axons displayed a very similar behaviour to *Pdn/+* $GPF^+$ axons (Fig. 4.6; C, D). *Pdn/Pdn* thalamic axons were growing within the internal capsule of *Pdn/+* sections avoiding the globus pallidus and the ventricular zone of the MGE (Fig. 4.6; C, D). In addition, in 3 out of 9 explants several axons were also found to grow along the ventral edge of the globus pallidus (Fig. 4.6; C, D). However, in 4 out of 9 experiments some *Pdn/Pdn* $GFP^+$ thalamic axons were observed to grow along the edge of the *Pdn/+* slice (Fig. 4.6; C, D and Table 4.1). This behaviour was not observed in the control experiments.

Other variations from the described pattern of growth of thalamic axons were observed in 2 out of 9 *Pdn/+* and 2 out of 9 *Pdn/Pdn* GFP+ thalamic explants transplanted in Pdn/+ sections (Table 1). These differences were likely to be caused by the use of either

too caudal or too rostral recipient sections. Alternatively sometimes too dorsal cuts removed, together with the preoptic area, most of the axonal repulsive regions of the MGE, such as the globus pallidus.

Overall, these experiments suggest that *Pdn/Pdn* thalamic axons generally responded normally to ventral telencephalic guidance cues *in vitro*, being able to navigate within *Pdn/+* ventral telencephalon.

Finally, to test the guidance propriety of the *Pdn/Pdn* ventral telencephalon on *Pdn/+* thalamic axons, *Pdn/+* $GFP^+$ thalamus was transplanted into *Pdn/Pdn* coronal brain sections. In this culture experiment, GFP immunostaining revealed that *Pdn/+* $GFP^+$ thalamic axons appeared to grow in a disorganized manner within the *Pdn/Pdn* MGE of the host slice (Fig. 4.6; E, F). In 10 out of 10 culture experiments, *Pdn/+* thalamic axons were penetrating the whole recipient *Pdn/Pdn* MGE mantle zone and never channelling through the *Pdn/Pdn* internal capsule. Interestingly, in 6 transplant experiments it was possible to observe *Pdn/+* thalamic axons growing along the edge of the *Pdn/Pdn* section in a similar pattern observed for *Pdn/Pdn* thalamic explants transplanted into *Pdn/+* ventral telencephalon (Table 1).

In conclusion, these culture experiments show that *Pdn/Pdn* thalamic axons, as well as *Pdn/+* thalamic axons are generally able to respond to *Pdn/+* ventral telencephalic guidance cues. They are able to grow through the internal capsule towards the cortex, and to avoid the globus pallidus and the MGE ventricular zone. Only a small subset of *Pdn/Pdn* thalamic axons fail to respond properly to repulsive guidance cues within the *Pdn/+* environment, growing along the edge of the *Pdn/+* sections. In contrast, the *Pdn/Pdn* ventral telencephalon is not able to guide *Pdn/+* thalamic axons towards the

cortex, instead allowing them to grow in several different directions and within regions of the *Pdn/Pdn* MGE normally repulsive to thalamocortical axons.

**Table 4.1**

**Different patterns of axon growth observed when *Pdn*/+ and *Pdn/Pdn* thalamic explants were transplanted in *Pdn*/+ and *Pdn/Pdn* living coronal brain sections**

| **Different patterns of thalamic axon growth** | ***Pdn*/+ thalamus transplanted in *Pdn*/+ slices** | ***Pdn/Pdn* thalamus transplanted in *Pdn*/+ slices** | ***Pdn*/+ thalamus transplanted in *Pdn/Pdn* slices** |
|---|---|---|---|
| **1)** Axons growing in the internal capsule | **8** | **7** | **-** |
| **2)** Axons growing in the external capsule | 4 | 3 | - |
| **3)** Axons growing in the MGE mantle | 2 | 2 | **10** |
| **4)** Axons growing along the edge of the section | - | 4 | 6 |
| 5) Total number of successful transplants performed | **9** | **9** | **10** |

## 4.6 Discussion

In the previous chapter defects in the thalamocortical tract of *Pdn/Pdn* mutants were shown. *Pdn/Pdn* thalamocortical axons do penetrate the ventral telencephalon. However, soon afterwards thalamic axons display several different guidance mistakes along their way to the cortex. In the caudal part of the tract, thalamic axons do not enter the internal capsule, projecting ventrally. Rostrally, once thalamic axons have entered the internal capsule they defasciculate and do not project towards the cortex. In this chapter, it is first shown that *Gli3* is expressed in different telencephalic and diencephalic territories at E10.5, E12.5 and E14.5. *Gli3* is expressed in the dorsal thalamus and cortex during the formation of thalamocortical and corticothalamic connections, respectively, and in the ventral telencephalon during the formation of thalamocortical and corticothalamic intermediate guidance cues. Interestingly, from this analysis it was also possible to observe a new *Gli3* expression domain in the mantle region of the MGE, containing post-mitotic neurons. Therefore the *Pdn* mutation might actually affect the development of all these three structures of the forebrain. Subsequently, the experiments in this chapter were aimed at understanding to what extent *Pdn/Pdn* thalamocortical mistakes are caused by cell-autonomous defects in thalamic neurons and/or by defects in the development of *Pdn/Pdn* ventral telencephalic intermediate cues. First, the expression patterns of several genes important for thalamus development are not affected in the *Pdn/Pdn* mutant diencephalon. Also, MGE pioneer neurons that allow thalamocortical axons to enter the ventral telencephalon are not affected in *Pdn/Pdn* mutants. However,

the navigation of thalamic axons within the ventral telencephalon is not supported by the normal formation of corridor cells in the *Pdn/Pdn* ventral telencephalon. In addition, although *Pdn/Pdn* thalamic axons normally respond to guidance cues in the wild type ventral telencphalon, the *Pdn/Pdn* ventral telencephalon fails to guide wild type thalamic axons towards the cortex in a transplantation essay.

*Gli3* is expressed in the diencephalic ventricular zone before (E10.5 and E12.5) and at the time (E14.5) when the thalamocortical neurons form and start to project their axons, suggesting a possible role for *Gli3* in the regionalization of dorsal thalamus. However, no changes were observed in the expression pattern of several genes important for dorsal thalamic patterning in the *Pdn/Pdn* mutant brains, such as *Gbx2, Ngn2, Dlx2, Emx2 and Lhx2*. This suggests no major defects in the patterning of the developing *Pdn/Pdn* dorsal thalamus. Interestingly, it was not even possible to detect changes in the diencephalic expression patterns of genes whose expression change in the dorsal telencephalon of *Pdn/Pdn* mutants. Indeed, it has been previously reported that there is a down-regulation of *Emx2* and an up-regulation of *Dlx2* within the developing cortex of *Pdn/Pdn* mutant brains (Kuschel et al., 2003). However, these alterations only affect the telencephalon of *Pdn/Pdn* mutants. Once thalamic neurons are formed, they also have to correctly express a variety of guidance receptors and transcriptional factors that enable their axons to respond correctly to guidance cues and ultimately reach the cortex (reviewed in (Lopez-Bendito and Molnar, 2003; Price et al., 2006). Therefore, it was not possible to completely exclude primary defects in *Pdn/Pdn* developing thalamic neurons and their axons. To check the cell autonomous capacity of *Pdn/Pdn* thalamocortical axons to respond to ventral telencephalic intermediate cues an *in vitro* culture essay was

performed, in which thalamic axons are transplanted into the preoptic area of living-sectioned coronal brain sections. The use of living coronal brain sections as recipient tissues provides the advantage of maintaining the brain morphology of the slices, allowing thalamic axons to grow within the telencephalic tissue in a pattern similar to the *in vivo* situation. Thalamic axons are channelled through the internal capsule, and most axons avoid the globus pallidus. Thus, this *in vitro* assay is a way to reproduce the *in vivo* behaviour of thalamocortical axons in the ventral telencephalon. This technique also avoids the time consuming and expensive use of conditional knockouts, in which for example *Gli3* would be selectively abolished in the thalamus. One limitation of this method is the variability that affects the patterns of growth of thalamic axons in the ventral telencephalon. Indeed, the growth pattern of thalamic axons in the slice is subject to how the surgical cut which removes the preoptic area is done. The variations observed in these experiments are sumarized in table 4.1. In several cases, some thalamic axons also grew along the ventral border of the globus pallidus. This result is not surprising because the removal of the preoptic area in some sections results in a direct contact of the thalamic explants with the external capsule, which is as permissive to the growth of thalamic axons as the internal capsule (Lopez-Bendito et al., 2006). Therefore, if the excision of the preoptic area exposes more the internal capsule region, thalamic axons will preferentially grow along the internal capsule (row 1 in table 4.1). On the contrary, if removal of the preoptic area exposes more the external capsule thalamic axons will preferentially grow in this region rather that in the internal capsule (row 2 in table 4.1). Exposure of both of these regions results in thalamic axons entering both the internal and external capsule (row 1 and 2 in table 4.1). In other cases the cutting not only

removed the preoptic area but also part of the MGE. The remaining MGE tissue was not sufficient to repel all thalamic axons, allowing some of them to grow straight towards the LGE (row 3 in table 4.1). Finally, when the preoptic area region, which is repulsive to thalamocortical axon growth, was not completely removed, thalamic axons did not grow at all in the ventral telencephalon. These later cases were taken out from the analyses and considered as failed experiments. To circumvent these problems the slice culture experiments were repeated several times. Nevertheless, the different thalamic axonal growth patterns, observed in the slice cultures, only vary between a limited number of possibilities, giving a realistic idea of how thalamocortical axons respond to ventral telencephalic guidance cues. Similar patterns of axon migration have also been observed in transplantation experiments performed previously (Lopez-Bendito et al., 2006).

These growth patterns were also observed when *Pdn/Pdn* thalamic explants were transplanted into control sections. This suggested that the great majority of *Pdn/Pdn* thalamic axons are in general able to respond to guidance cues present in the wild-type ventral telencephalon. Interestingly, in some explant experiments, a small population of *Pdn/Pdn* thalamic axons was observed to grow along the edge of the wild-type slices (row 4 in table 4.1). This behaviour was not observed in control experiments, and may indicate that the *Pdn* mutation may affect a small sub-population of thalamic neurons, in their ability to correctly project their axons in the ventral telencephalon.

These results suggested that the severe guidance mistakes of early *Pdn/Pdn* projecting thalamocortical axons are more likely to be caused by defects in ventral telencephalic intermediate guidance cues, rather then defects in *Pdn/Pdn* thalamic neurons and axons

themselves. Indeed, when wild type thalamic explants were transplanted into *Pdn/Pdn* sections, thalamic axons penetrated the whole *Pdn/Pdn* MGE mantle zone and never formed the internal capsule. This showed that the *Pdn/Pdn* ventral telencephalon has completely lost any ability to guide thalamic axons. Interestingly, in some transplant experiments it was possible to observe wild-type thalamic axons growing along the edge of the *Pdn/Pdn* section in a similar pattern observed for *Pdn/Pdn* thalamic explants transplanted into wild-type ventral telencephalon. This may suggest that *Gli3* may control some factor that normally prevents this growth pattern. Further research would need to be carried out to test this hypothesis.

The outcome provided by the transplant experiment correlates well with the analyses of ventral telencephalic intermediate cues in *Pdn/Pdn* brains. *Pdn/Pdn* thalamic axons are able to penetrate the ventral telencephalon, in accordance with the fact that in the *Pdn/Pdn* MGE pioneer neurons are normally present and project their axons in the *Pdn/Pdn* thalamus, guiding thalamic axons across the DTB. However, once *Pdn/Pdn* thalamic axons enter the ventral telecephalon they get completely lost taking several abnormal directions. This is also confirmed both by DiI injections in the *Pdn/Pdn* thalamus described in the previous chapter. This effect is more extreme in the *in vitro* assay. These data correlate with the fact that *Pdn/Pdn* mutants display defects in the distribution of the $Isl1^+$ channel cells within the MGE. Although $Isl1^+$ cells are still migrating ventrally from the LGE to the MGE, they are not organized in a horseshoe shape like structure, and it is more difficult to identify the globus pallidus and the external capsule. The upper branch of the horseshoe, forming the internal capsule, is not as well defined as in the *Pdn/+* ventral telencephalon. This was also confirmed by the

expression of *Nkx2.1,* which is complementary to *Isl1* expression in the ventral telencephalon. *Nkx2.1* expression was shifted ventrally in the *Pdn/Pdn* MGE, resulting in a different shape of the globus pallidus. From these data, it appears that the corridor cells are migrating ventrally forming the internal capsule, but the *Pdn/Pdn* Isl1$^{+}$ area and the globus pallidus are located more ventrally in comparison with control brains. This probably results in an increase in the permeability of the *Pdn/Pdn* MGE to thalamicortical axons. In this way thalamic axons are not repelled by the MGE mantle but are allowed to grow in all directions, without being channelled through the internal capsule. Interestingly, it is likely that *Pdn/Pdn* thalamocortical axons will eventually reach the *Pdn/Pdn* cortex, probably also arriving from alternative ventral telencephalic routes. Indeed, the *Pdn/Pdn* developing cortex still contains some attractive cues for thalamic axons, such as Nrg1-Ig. This is also suggested by DiI injections and NF staining at P0, on *Pdn/Pdn* brains. In addition, it has been recently shown that thalamocortical axons are eventually able to reach their final target from alternative routes (Little et al., 2009). The use of a mouse line, in which thalamic axons are selectively labelled, crossed into the *Pdn* background, would better clarify this possibility (for more details see general discussion, chapter 6).

How *Gli3* controls the formation of the corridor cells and therefore the guidance of thalamocortical axons towards the cortex is unclear. *Gli3* is expressed in ventral telencephalic progenitor cells, and its effect on the development of the thalamocortical tracts and their intermediate guidance cues is more likely to be indirect. Indeed, *Gli3* has been shown to control the patterning of the telencephalon. Therefore, its absence or reduction may affect the patterning of the ventral telencephalon and therefore the

formation of some attractive and repulsive cues along the path of growth of thalamocortical axons, as observed in *Pdn* mutants. This hypothesis will be tested in the following chapter. Surprisingly however, in this study we also found *Gli3* expression for the first time in a small group of cells in the mantle zone of the MGE at E12.5 and E14.5. These cells are probably differentiated neurons and seem to be positioned in the globus pallidus. This could be more accurately checked by the use of double in situ hybridization for *Gli3* and some globus pallidus markers, or with the combination of an in situ hybridization for *Gli3* and immunostaining for globus pallidus markers. Nevertheless, the expression of *Gli3* in neurons suggests novel roles in the developing telencephalon that would need further investigation in the future. Indeed, until now *Gli3* was believed to be expressed and to play a role only in neural progenitor cells, as its expression has never been reported in neurons before. In addition, these neurons upregulating *Gli3* after differentiation are positioned exactly along the path that thalamocortical axons use to navigate in order to reach their final target. This will be further discussed in the general discussion (chapter 6.), in the contest of the experiments shown in the previous and in the following result chapters.

# Chapter 5: Patterning defects in *Pdn* mutants correlate with the failure of corticofugal axons to enter the ventral telencephalon

## 5.1 Introduction

In this chapter possible causes of corticothalamic tract defects are analysed in the *Pdn/Pdn* mutant brains. In chapter 3, it has been observed that the *Pdn* homozygous mutant cortex is able to produce early projecting corticofugal neurons and their axons. However, several guidance mistakes were demonstrated to happen during the development of the *Pdn/Pdn* corticothalamic tract. At E14.5 *Pdn/Pdn* corticothalamic axons do not enter the ventral telencephalon. Only at later developmental stages, some cortical axons penetrate the ventral telencephalon form the PSPB, several others project towards the diencephalon through several abnormal routes, but most cortical axons project along the PSPB towards the amygdaloid region, never entering the ventral telencephalon. These analyses suggested no major defects in the formation of *Pdn/Pdn* corticofugal neurons and their axons. However, at this stage it remained possible that defects in cortical development and in the formation of different cortical layers could underlie cortical axon pathfinding defects (reviewed in (Molyneaux et al., 2007). Alternatively, defects in the formation of guidance cues along the path of

corticothalamic axons in the *Pdn/Pdn* telencephalon could affect the capacity of *Pdn/Pdn* corticothalamic axons to reach their final target. The aim of the following experiments was to investigate the extent to which cortical defects and/or ventral telencephalic abnormalities contribute to the observed corticothalamic axonal phenotype in *Pdn/Pdn* mutant mice. First, cortical lamination was characterized in *Pdn/Pdn* mutants by immunohistochemistry and in situ hybridization for genes expressed in different cortical layers. This analysis showed that the layer identity of P0 *Pdn/Pdn* cortical neurons is not affected. Secondly, DiI injection in the E12.5 cortex revealed the absence of back-labelled pioneer neurons within the *Pdn/Pdn* ventral telencephalon. These pioneers have been suggested to be necessary to guide corticothalamic axons into the ventral telancephalon (Metin and Godement, 1996), and their absence or incapacity to project their axons towards the *Pdn/Pdn* cortex may explain the failure of *Pdn/Pdn* corticothalamic axons to penetrate the subpallium. Subsequent experiments aimed to investigate abnormalities in the development of *Pdn/Pdn* ventral telencephalon that could explain the defects in *Pdn/Pdn* LGE pioneer neurons. Indeed, in situ hybridization and immunoflorescence revealed patterning defects in the *Pdn/Pdn* LGE. These data showed a dorsal shift and an expansion of the *Pdn/Pdn* ventral pallium and a partial ventralization of the *Pdn/Pdn* CGE. This was also confirmed by a reduction in the number of lateral cortical stream cells originating from the dorsal *Pdn/Pdn* LGE. In addition, the mantle region of the *Pdn/Pdn* LGE shows a significant reduction in the total number of differentiated neurons. Analyses of the cell cycle characteristics of *Pdn/Pdn* ventral telencephalic progenitors at E10.5, revealed a significant elongation of the time necessary to complete the S phase and the whole cell cycle, explaining the

reduction of neurons in the *Pdn/Pdn* LGE mantle. Finally, based on the hypothesis that *Gli3* counteracts *Shh* signalling in the developing ventral telencephalon (Rallu et al., 2002; Rash and Grove, 2007), in situ hybridizations and quantitative RT-PCR (qRTPCR) were used to reveal any changes in the expression pattern of the *Shh* target genes *Ptc1* and *Gli1* and in the amount of Shh transcripts. These analyses revealed a dorsal shift of *Ptc1* expression in the *Pdn/Pdn* LGE and an increase in the amount of *Ptc1* and *Gli1* mRNA in *Pdn/Pdn* ventral telencephalic tissue. Altogether, these data showed that the *Pdn* mutation causes an upregulation of *Shh* signalling and patterning defects in *Pdn/Pdn* ventral telencephalon, affecting both the regionalization and the growth of the LGE.

## 5.2 Cortical lamination is not affected in newborn *Pdn/Pdn* mutant brains

Previous studies have reported severe defects in the development of the cerebral cortex in other *Gli3* mutant mice. $Xt^J/Xt^J$ mutants already display defects in the early steps of cortical lamination, which involve the organization of the marginal zone, the cortical plate and the early subplate (Theil, 2005). In addition, $Xt^J/Pdn$ mutants display defects in the E14.5 $Xt^J/Pdn$ cortex displaying clusters of Cajal-Retzius cells and of radial glia fibres that lead to cortical layer abnormalities at P0 (Friedrichs et al., 2008). Therefore, the *Pdn* mutation could also cause cortical lamination defects. To test this possibility, the

lamination process in *Pdn/Pdn* mutant mice at P0 was investigated by immunohistochemistry and in situ hybridization (Fig. 5.1).

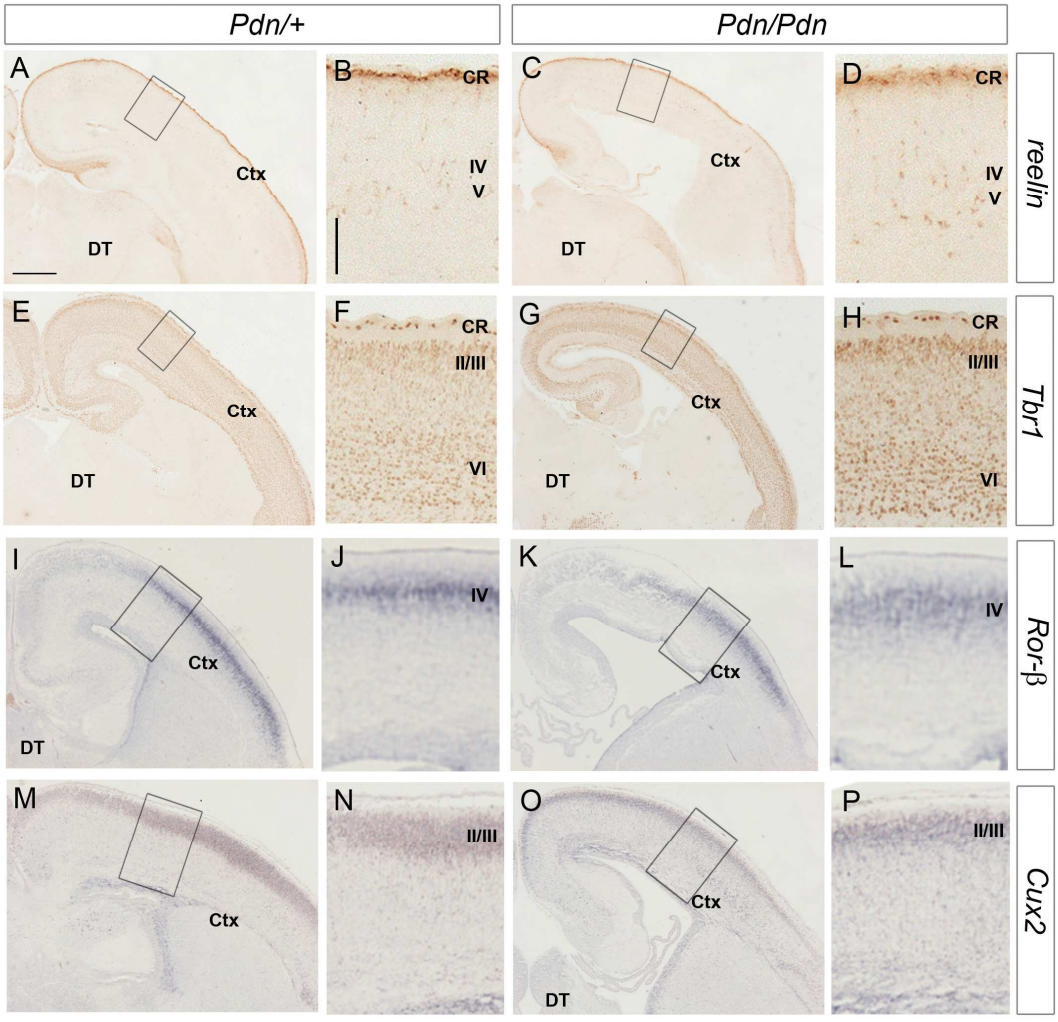

**Figure 5.1.**

**Immunohistochemistry and in situ hybridization analyzing cortical lamination on *Pdn/+* and *Pdn/Pdn* coronal brain sections at P0 (A-P).** B, D, F, H, J, L, N, and P are higher magnifications of A, C, E, G, I, K, M and O, respectively.

Reelin immunohistochemistry revealed the presence of reelin+ cells within the marginal zone (layer I) of the *Pdn/+* cerebral cortex (A, B). These reelin$^{+}$ cells are uniformly organized in a single layer just below the pia surface (B). Higher magnification also showed the presence of reelin$^{+}$ neurons within the cortical layers IV and V (B). The distribution of reelin$^{+}$ cells within the marginal zone of *Pdn/Pdn* mutants seems to be slightly patchier compared to *Pdn/+* (D). However, there are no other major differences in the general organization of reelin+ cells within the *Pdn/Pdn* cerebral cortex (C, D).

Immunohistochemistry on *Pdn/+* sections shows that Tbr1 expression is restricted to post-mitotic neurons within the subplate and cortical layer VI, and to Cajal-Retzius cells within the marginal zone (E, F). In addition, Tbr1 is expressed at low levels in layers II/III (E, F). It is not possible to observe any difference in expression pattern of Tbr1 within the *Pdn/Pdn* cerebral cortex (G, H).

In situ hybridization reveals the expression patterns of *Ror-β* (I, J) and *Cux2* (M, N) in the *Pdn/+* cortex. Both genes are expressed in a gradient of high ventrolateral to low dorsomedial (I, J, M, N). However, *Ror-β* expression was restricted to *Pdn/+* post mitotic neurons in layer IV (I, J), while *Cux2* is a marker for post mitotic neurons of layer II/III (M, N). *Cux2* is also weakly expressed within the cortical ventricular zone (N). Again, it was not possible to detect differences in the expression patterns of *Ror-β* (K, L) and *Cux2* (O, P) within the cerebral cortex *Pdn/Pdn* mutant brains. Abbreviations: CR, Cajal-Retzius cells. (n=3) (Scale bar in A 200 μm; applays to E, I, M and C, G, K, O) (Scale bar in B 100 μm; applays to F, J, N, D, H, L, P).

It is not possible to investigate *Pdn/Pdn* post-natal cortical development because these animals die at birth. Reelin immunohistochemistry on *Pdn/+* coronal brain sections revealed the presence of reelin$^+$ cells within the marginal zone or layer I of the cerebral cortex (Fig. 5.1; A, B). These reelin$^+$ cells are uniformly organized in a single layer just below the pia surface. Higher magnification showed the presence of reelin$^+$ neurons within the cortical layers IV and V (Fig. 5.1; B). These neurons are migrating interneurons, which are also important for cortical lamination (Alcantara et al., 2006; Yoshida et al., 2006). Although the distribution of reelin$^+$ cells within the marginal zone of *Pdn/Pdn* mutants seems to be slightly patchier compared to *Pdn/+* (Fig. 5.1; D), reelin immunostaining does not show other major differences in the general organization of Cajal-Retzius cells within the *Pdn/Pdn* cerebral cortex (Fig. 5.1; C, D).

Subsequently, lamina formation was investigated with the use of specific laminar markers on P0 *Pdn/+* and *Pdn/Pdn* coronal brains sections (Fig. 5.1; E-P). At P0, Tbr1 immunohistochemistry on *Pdn/+* coronal brain sections shows that its expression is restricted to post-mitotic neurons within the subplate and cortical layer VI, but also to Cajal-Retzius cells within the marginal zone (Fig. 5.1; E, F). Tbr1 is also expressed at low levels within the layers II/III (Fig. 5.1; E, F).

The expression patterns of *Ror-$\beta$* and *Cux2* were revealed by in situ hybridization (Fig. 5.1; I, J, M, N). Both genes are expressed in a gradient of high ventrolateral to low dorsomedial within the cerebral cortex. *Ror-$\beta$* expression was restricted to *Pdn/+* post mitotic neurons in layer IV (Fig. 5.1; I, J) (Schaeren-Wiemers et al., 1997). *Cux2* instead is a marker for post mitotic neurons of layer II/III (Nieto et al., 2004; Zimmer et al.,

2004), in the *Pdn/+* cortex (Fig. 5.1; M, N), and is also weakly expressed within the ventricular zone of the P0 cortex (Fig. 5.1; M, N).

Overall, it was not possible to detect differences in the expression patterns of these genes within the cerebral cortex of P0 *Pdn/Pdn* mutant brains (Fig. 5.1; C, D, G, H, K, L, O, P). These analyses suggested that the *Pdn* mutation does not affect the cortical lamination process and the layer identity of different post-mitotic neurons at P0. Although we cannot completely exclude primary defects in corticofugal neurons, these results suggest that the severe guidance mistakes of *Pdn/Pdn* corticofugal axons are more likely to be caused by defects in ventral telencephalic guidance cues. This hypothesis was tested in the following section.

## 5.3 LGE pioneer neurons are missing in the *Pdn/Pdn* ventral telencephalon

At E13.5 corticothalamic axons start to cross the PSPB and to penetrate the ventral telencephalon. *Pdn/Pdn golli τ-GFP* mouse brains show that at E14.5 early projecting cortical neurons and their axons form. In addition, *Pdn/Pdn* cortical neurons acquire the correct layer identity at P0. However, DiI injections in *Pdn/Pdn* E14.5 cortex and GFP immunostaining on *Pdn/Pdn golli τ-GFP* E14.5 coronal brain sections showed a failure of *Pdn/Pdn* corticofugal axons to enter the ventral telencephalon (described in chapter 3).

In this section the formation of ventral telencephalic intermediate guidance cues is investigated in *Pdn/Pdn* brains, since such abnormality may cause the failure of corticofugal axons to enter the LGE. At E12.5 LGE pioneer neurons have been suggested to project axons towards the developing cortex and to guide cortical axons by providing an axonal substrate on which cortical axons grow to pass over the PSPB (Metin and Godement, 1996). However, as with the MGE pioneer neurons pioneering thalamic axons in the MGE (described in the previous chapter), there are no markers available to selectively label the LGE pioneers. To investigate their presence in the developing LGE, DiI was injected into the dorsal telencephalon of E12.5 *Pdn/+* and *Pdn/Pdn* brains (Fig. 5.2). DiI injected in the developing cortex of *Pdn/+* brains diffuses retrogradely along pioneer axons, labelling the cell bodies of pioneer neurons within the mantle zone of the LGE (Fig. 5.2; A, B). At this embryonic stage, no cortical axons have reached the ventral telencephalon, therefore the DiI will only reveal pioneer axons projecting from neurons located within the LGE (Fig. 5.2; A, B). Interestingly, DiI injected in the E12.5 cortex of *Pdn/Pdn* mutant brains did not reveal any pioneer neural cell bodies or axons within the dorsal *Pdn/Pdn* LGE in 4 out of 4 analyzed brains (Fig. 5.2; C, D). These data strongly suggest a failure in the formation of LGE pioneer neurons or in their ability to project axons towards the developing cortex. Such an abnormality could explain why *Pdn/Pdn* corticofugal axons are not able to penetrate the *Pdn/Pdn* ventral telencephalon.

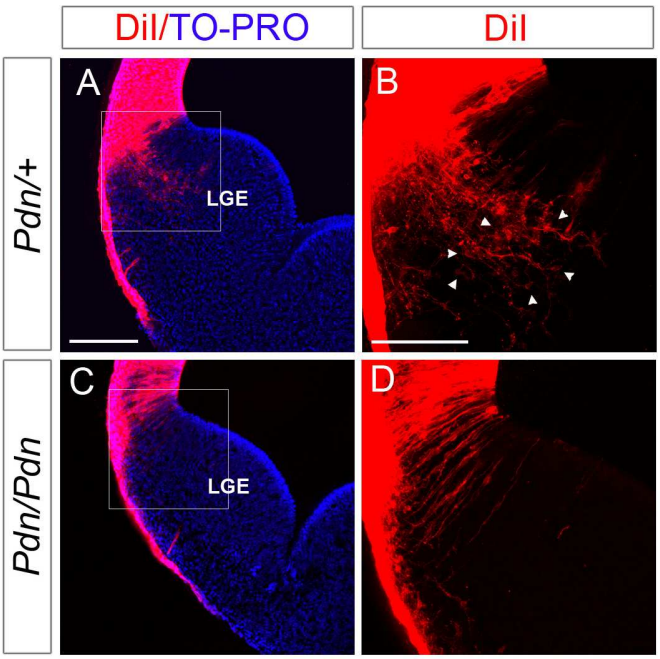


**Figure 5.2.**

**Cortical DiI injections in *Pdn*/+ and *Pdn*/*Pdn* brains at E12.5 (A-D).** B and D are higher magnifications of A and C, respectively. A, C coronal brain sections are contrastained with TO-PRO.

DiI injected in the developing cortex of *Pdn*/+ brains diffuses retrogradely along pioneer axons, labelling the cell bodies of pioneer neurons within the mantle zone of the LGE (A, B). At this embryonic stage, no cortical axons have reached the ventral telencephalon, therefore the DiI will only reveal pioneer axons projecting from neurons located within the LGE (A, B). In addition, higher magnification reveals a conspicuous number of DiI back-labelled neural cell bodies (arrowheads in B).

DiI injected in the cortex of *Pdn/Pdn* mutant brains did not reveal any pioneer neural cell bodies and axons within *Pdn/Pdn* LGE (C, D). This is also confirmed by higher magnification which reveals no DiI back-labelled neural cell bodies (D). (n=4) (Scale bar in A 100 μm; applays to C) (Scale bar in B 50 μm; applays to D).

## 5.4 The *Pdn/Pdn* ventral telencephalon displays regionalization defects within the ventral telencephalon and at the PSPB at early stages of brain development

No specific markers have been found to label ventral telencephalic pioneer neurons, therefore it not possible to know whether they are absent in the *Pdn/Pdn* ventral telencephalon or whether they cannot project towards the developing *Pdn/Pdn* cortex. However, the *Pdn/Pdn* mutation may affect the patterning of the ventral telencephalon, which may lead to defects in the formation of these neurons or to their inability to project towards the developing cortex.

Patterning defects may result in abnormal regionalization of *Pdn/Pdn* ventral telencepholon and/or in proliferation and differentiation defects. In this section the first possibility is analyzed. Regionalization in the *Pdn/Pdn* telencephalon was analyzed by in situ hybridizations and immunohistochemistry at early stages of forebrain development for different regionally expressed markers. Different regions of the telencephalon acquire different identities that are reflected by the molecular expression profiles of these territories (Fig. 5.3).

To discriminate between the dorsal and the ventral telencephalon, *Dlx2* in situ hybridization was performed on E11.5 *Pdn/+* and *Pdn/Pdn* coronal brain sections. These two territories are discriminated by the expression of *Dlx2* within the ventral telencephalon (Fig. 5.3; A). *Dlx2* has a sharp expression boundary at the PSPB, with the

dorsal telencephalon being entirely negative (Fig. 5.3; A). In E11.5 *Pdn/Pdn* brains, *Dlx2* expression is maintained within the ventral telencephalon (Fig. 5.3; B). However, at the *Pdn/Pdn* PSPB some *Dlx2* expressing cells intermingle with *Dlx2*-non-expressing cells suggesting abnormalities in the establishment or maintenance of this boundary (Fig. 5.3; B).

Within the ventral telencephalon *Dlx2* indisciminately labels the LGE and MGE, making it a ventral telencephalic marker (Fig. 5.3; A). Therefore, to further discriminate between LGE and MGE *Nkx2.1* in situ hybridization was performed on E11.5 *Pdn/+* and *Pdn/Pdn* coronal brain sections. *Nkx2.1* in *Pdn/+* E11.5 coronal brain sections is only expressed in the MGE, and stops sharply at the boundary between LGE and MGE (Fig. 5.3; C). No abnormalities were observed in *Nkx2.1* expression in the ventral telencephalon of E11.5 *Pdn/Pdn* brains (Fig. 5.3; D).

The expression of *Dlx2* and *Nkx2.1* shows that at E11.5 the ventral telencephalon is specified correctly in *Pdn/Pdn* mutants, but the PSPB region shows *Dlx2*-expressing cells intermingling with *Dlx2*-non-expressing cells suggesting abnormalities in the formation of this boundary.

The next set of experiments investigated the formation of the appropriate boundaries between the LGE and the surrounding telencephalic territories (the MGE ventrally and the cortex dorsally). Subsequently, the molecular regionalization within the *Pdn/Pdn* LGE was investigated by using markers differentially expressed in dorsal or ventral regions within the LGE.

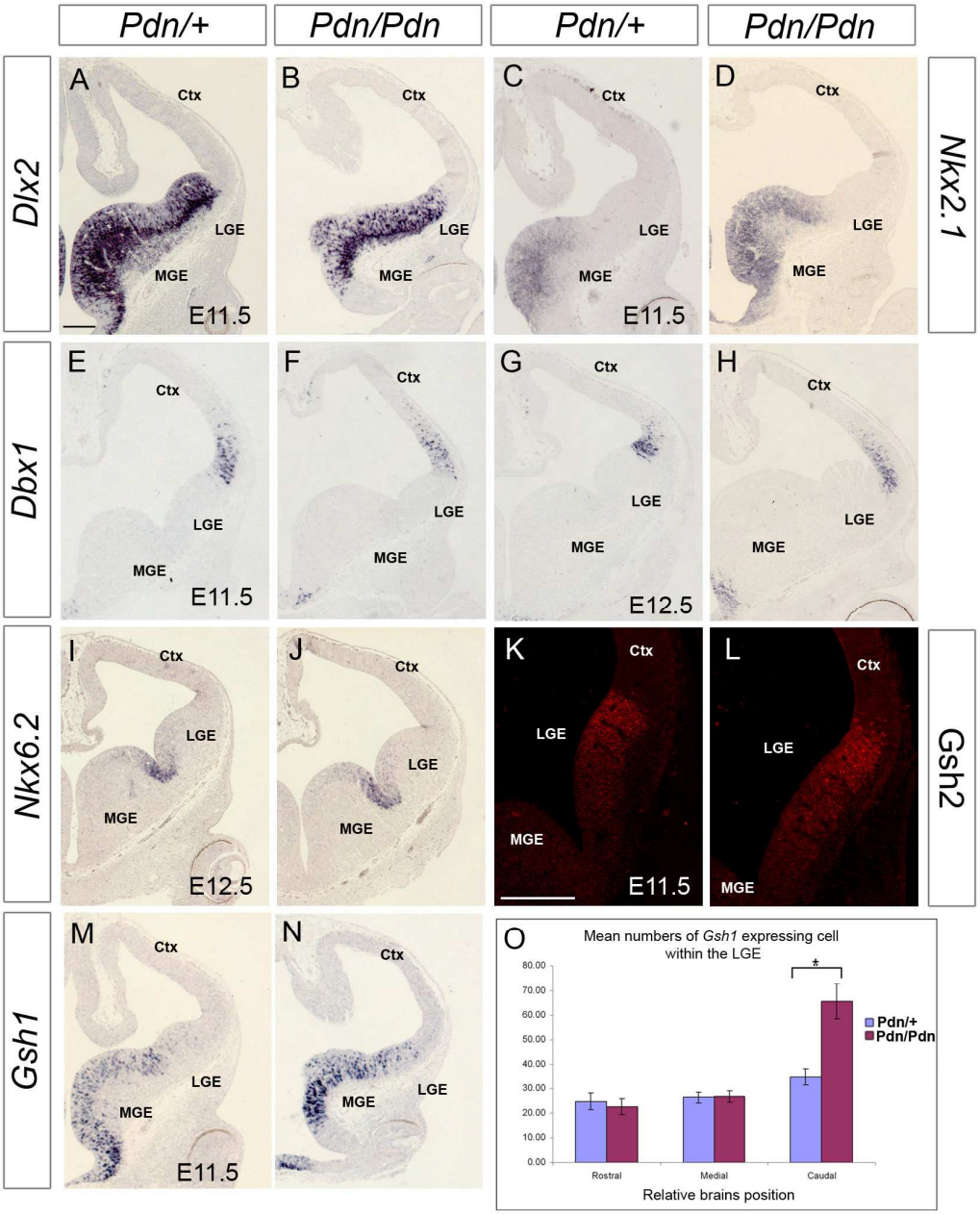
Pdn/+
Pdn/Pdn
Pdn/+
Pdn/Pdn
Dlx2
Nkx2.1
Dbx1
Nkx6.2
Gsh2
Gsh1
A
B
C
D
E
F
G
H
I
J
K
L
M
N
O
Ctx
LGE
MGE
E11.5
E12.5
Mean numbers of Gsh1 expressing cell within the LGE
80.00
70.00
60.00
50.00
40.00
30.00
20.00
10.00
0.00
*
Pdn/+
Pdn/Pdn
Rostral
Medial
Caudal
Relative brains position

**Figure 5.3.**

**In situ hybridization and immunofluorescence analysis of different regionally expressed ventral telencephalic markers on early developing *Pdn/+* and *Pdn/Pdn* coronal brain sections (A-O).** *Dlx2, Nkx2.1* and *Gsh1* in situ hybridization was performed at E11.5 (A-D, M and N); *Dbx1* at E11.5 and E12.5 (E-H); *Nkx6.2* at E12.5 (I-J); Gsh2 immunofluorescence at E11.5 (K-L).In *Pdn/+* brains *Dlx2* in expressed in the whole ventral telenephalon and it has a sharp expression boundary at the PSPB, (A). In *Pdn/Pdn* brains, *Dlx2* expression is maintained within the ventral telencephalon (B). However, at the *Pdn/Pdn* PSPB *Dlx2* expression is not as sharp as in *Pdn/+* (B). In *Pdn/+ Nkx2.1* is only expressed in the MGE, stopping sharply at the boundary between LGE and MGE (C). No differences were observed in *Nkx2.1* expression in the ventral telencephalon of *Pdn/Pdn* brains (D). *Dbx1* is expressed in progenitor cells within the ventral pallium (E, G). In both E11.5 and E12.5 *Pdn/Pdn* telencephali, the ventral limit of *Dbx1* expression is shifted dorsally and expanded into more dorsal cortical regions (F, H). Nkx6.2 is expressed in the ventricular zone of the dorsal most region of the MGE and ventral most regions of the *Pdn/+* LGE (I). No differences were found in *Nkx6.2* expression in *Pdn/Pdn* brains (J).Gsh2 is expressed in a high dorsal to low ventral gradient within the *Pdn/+* LGE (K). A sharp expression boundary was observed at the PSPB (K). No difference was observed in Gsh2 expression within the *Pdn/Pdn* LGE (L). However, Gsh2 expression at the PSPB was not as defined as in *Pdn/+* brains (L). *Gsh1* is expressed in a “salt and pepper” fashion at high levels in the *Pdn/+* MGE ventricular zone (M). Its expression extends until the ventral LGE but it is not expressed within the dorsal LGE (M). Interestingly, *Gsh1* expression expanded dorsally in *Pdn/Pdn* CGE (N, O).This result is quantified in O: *Gsh1* expressing cells within the *Pdn/+* and *Pdn/Pdn* LGE/CGE ventricular zone were counted (these domains were defined as positive for *Dlx2* but negative for *Nkx2.1).* No differences were observed in the number of *Gsh1* expressing cells in rostral and medial sections of *Pdn/+* (Blue) and *Pdn/Pdn* (Purple) LGE. However, the *Pdn/Pdn* CGE displayed a significant increase of about 2-fold in the number of *Gsh1* expressing cells (asterisk in O) (Mann-whitney test, p=0.034, n=3) (Scale bar in A 100 μm; applays to B-J and M-N) (Scale bar in K 100 μm; applays to L).

On E11.5 and E12.5 *Pdn/+* coronal brain sections, *Dbx1* is expressed in progenitor cells within the ventral pallium (Fig. 5.3; E, G). In E11.5 and E12.5 *Pdn/Pdn* telencephali, the ventral limit of *Dbx1* expression is shifted dorsally. Also, *Dbx1* expression expands into more dorsal regions within the *Pdn/Pdn* developing cortex (Fig. 5.3; F). This effect becomes even more obvious at E12.5, where *Dbx1* expression in *Pdn/Pdn* mutant brains display a clear expansion dorsally to the PSPB (Fig. 5.3; H). Similar results have also been found previously in other *Gli3* mutants, such as $Xt^J/Xt^J$ and $Xt^J/Pdn$ (Friedrichs et al., 2008; Hanashima et al., 2007).

A recent report has further divided the LGE and MGE progenitor regions in molecular sub-territories, which are reflected in the expression pattern of genes differentially expressed within the ventral telencephalon (Flames et al., 2007). For example, Nkx6.2 is expressed in the ventricular zone of the dorsal most region of the MGE and ventral most regions of the LGE. *Nkx6.2* clearly shows the transition between *Pdn/+* LGE and MGE, with its expression coinciding with the sulcus anatomically defining the LGE from the MGE bulges (Fig. 5.3; I). These areas have been defined as pMGE1 and pLGE4, respectively (Flames 2007). No differences were found in *Nkx6.2* expression in *Pdn/Pdn* E12.5 brains (Fig. 5.3; J).

Altogether, these marker analyses show defects in the formation of the boundary between the ventral and dorsal telencephalon, with the PSPB becoming less defined and shifted dorsally in the E11.5 and E12.5 *Pdn/Pdn* telencephalon. However, the boundary between the *Pdn/Pdn* LGE and *Pdn/Pdn* MGE did not appear to be affected.

Subsequently, investigation of the regionalization of the proliferating regions within the LGE was carried out. *Gsh1* and *Gsh2* are homeobox genes expressed in progenitor regions of the ventral telencephalon, with their expression pattern largely overlapping. *Gsh2* has been shown to play an important role in patterning the LGE. *Gsh2* knockout mice display a hypoplastic LGE (Szucsik et al., 1997) and the dorsal LGE acquires a ventral pallium-like identity (Yun et al., 2001). No obvious phenotype has been found in the telencephalon of *Gsh1* null mutant mice (Li et al., 1996).

The expression pattern at E11.5 of these two genes is complementary in the ventral telencephalon of *Pdn/+* brains coronal sections (Fig. 5.3; K). Gsh2 immunofluoresence shows its expression in a high dorsal to low ventral gradient within the LGE (Fig. 5.3; K). A sharp expression boundary was observed at the PSPB. No difference compared to control was observed in Gsh2 expression within the *Pdn/Pdn* LGE (Fig. 5.3; L). However, Gsh2 expression at the PSPB was not as defined as in *Pdn/+* brains, and it was possible to observe some $Gsh2^{+}$ cells intermingling with $Ghs2^{-}$ cells within the presumptive ventral pallium (Fig. 5.3; L).

In situ hybridizations on E11.5 *Pdn/+* coronal brain sections showed that *Gsh1* is expressed in a "salt and pepper" fashion at high levels in the MGE ventricular zone (Fig. 5.3; M). Its expression extends until the ventral LGE but it is not expressed within the dorsal LGE (Fig. 5.3; M). Interestingly, in situ hybridization for *Gsh1* on E11.5 *Pdn/Pdn* mutants revealed a dorsal expansion of the *Gsh1* expression in the caudal ganglionic eminence (CGE), but not in more rostral sections (Fig. 5.3; N, O).

To quantify this result, *Gsh1* expressing cells within the *Pdn/+* and *Pdn/Pdn* LGE/CGE ventricular zone were counted. To define the ventral and dorsal limit of the LGE we

used *Dlx2* and *Nkx2.1* staining on adjacent E11.5 brain sections. *Gsh1* expressing cells were counted only within the domain positive for *Dlx2* but negative for *Nkx2.1*. No differences were observed in the number of *Gsh1* expressing cells in rostral and medial sections of *Pdn/+* and *Pdn/Pdn* LGE. However, the *Pdn/Pdn* CGE displayed a significant increase (form 34.7±5.6 cells in *Pdn/+* to 65.7±10 cells in *Pdn/Pdn*) in the number of *Gsh1* expressing cells compared to controls (Mann-whitney test, p=0.034, n=3) (Fig. 5.3; O).

Together with *Dlx2* and *Dbx1* in situ hybridizations, *Gsh2* immunofluorescence also confirmed that the *Pdn/Pdn* PSPB is not as defined as in the *Pdn/+* brains. In addition, a partial ventralization of the *Pdn/Pdn* CGE was revealed by an increase in the number of Gsh1 expressing cells.

To corroborate this result, the formation of cells forming part of the lateral cortical stream originating from the dorsal LGE and/or the ventral pallium was investigated by in situ hybridization and by immunohistochemistry analyses (Fig. 5.4). These cell populations are positive for *Pax6* and *Six3*. Once formed, they migrate ventrally along the corticostriatal boundary and eventually contribute to the piriform cortex, the amygdala and to the olfactory bulbs (Carney et al., 2006). In *Pdn/+* coronal brain sections, *Six3* in situ hybridization clearly labels single cells migrating ventrally along the corticostriatal boundary (Fig. 5.4; A). *Six3* in situ hybridization also labels the ventricular zone of the LGE and MGE, but at lower intensity (Fig. 5.4; A). *Pdn/Pdn* coronal brain sections showed a dramatic reduction of ventrally migrating *Six3* expressing cells (Fig. 5.4; B). Fewer *Six3* expressing cells were present within the mantle region of *Pdn/Pdn* LGE, and very few of them contributed to the lateral cortical

stream (Fig. 5.4; B, C). No difference in *Six3* expression was detected within the ventricular zone of *Pdn/Pdn* MGE and LGE when compared to *Pdn/+* (Fig. 5.4; B).

Pax6 also labelled ventrally migrating cells originating within the dorsal LGE. Pax6 immunohistochemistry on *Pdn/+* coronal brain sections revealed several cells within the mantle region of the LGE migrating along the corticostriatal boundary (Fig. 5.4; D). In addition, it is possible to observe Pax6 expression within the ventricular zone of the dorsal LGE and the ventral pallium (Fig. 5.4; D). Pax6 staining on *Pdn/Pdn* brains sections also showed a reduction in the number of the ventral telencephalic migrating $Pax6^+$ cells (Fig. 5.4; E, F). In addition, *Pax6* ventral telencephalic expression is shifted dorsally.

*Pax6* and *Six3* expression label single migrating cell within the mantle zone of the LGE. The reduction observed by in situ hybridization and immunohistochemistry was quantified counting $Pax6^+$ and *Six3* expressing cells along the *Pdn/+* and *Pdn/Pdn* lateral cortical stream (Fig. 5.4; C, F). This analysis confirmed a significant (for Pax6: Mann-Whitney test p=0.032 n=4 rostral, p=0.034 n=4 medial, p=0.05 n=3 caudal; for *Six3*: Mann-Whitney test p=0.009 n=5 rostral, p=0.009 n=5 medial, p=0.021 n=4 caudal) reduction of about 3 times for *Six3* expressing cells (form 70$\pm$6 cells in *Pdn/+* to 27$\pm$4 cells in *Pdn/Pdn* cells rostrally, form 78$\pm$6 cells to 26$\pm$3 cells medially, form 85$\pm$2 cells to 29$\pm$2 cells caudally) and about 3 times for $Pax6^+$ cells (form 147$\pm$10 cells in *Pdn/+* to 42$\pm$2 cells in *Pdn/Pdn* rostrally, form 155$\pm$10 cells to 38$\pm$3 cells medially, form 109$\pm$16 cells to 24$\pm$1 cells caudally) in the *Pdn/Pdn* ventral telencephalon when compared to *Pdn/+*.

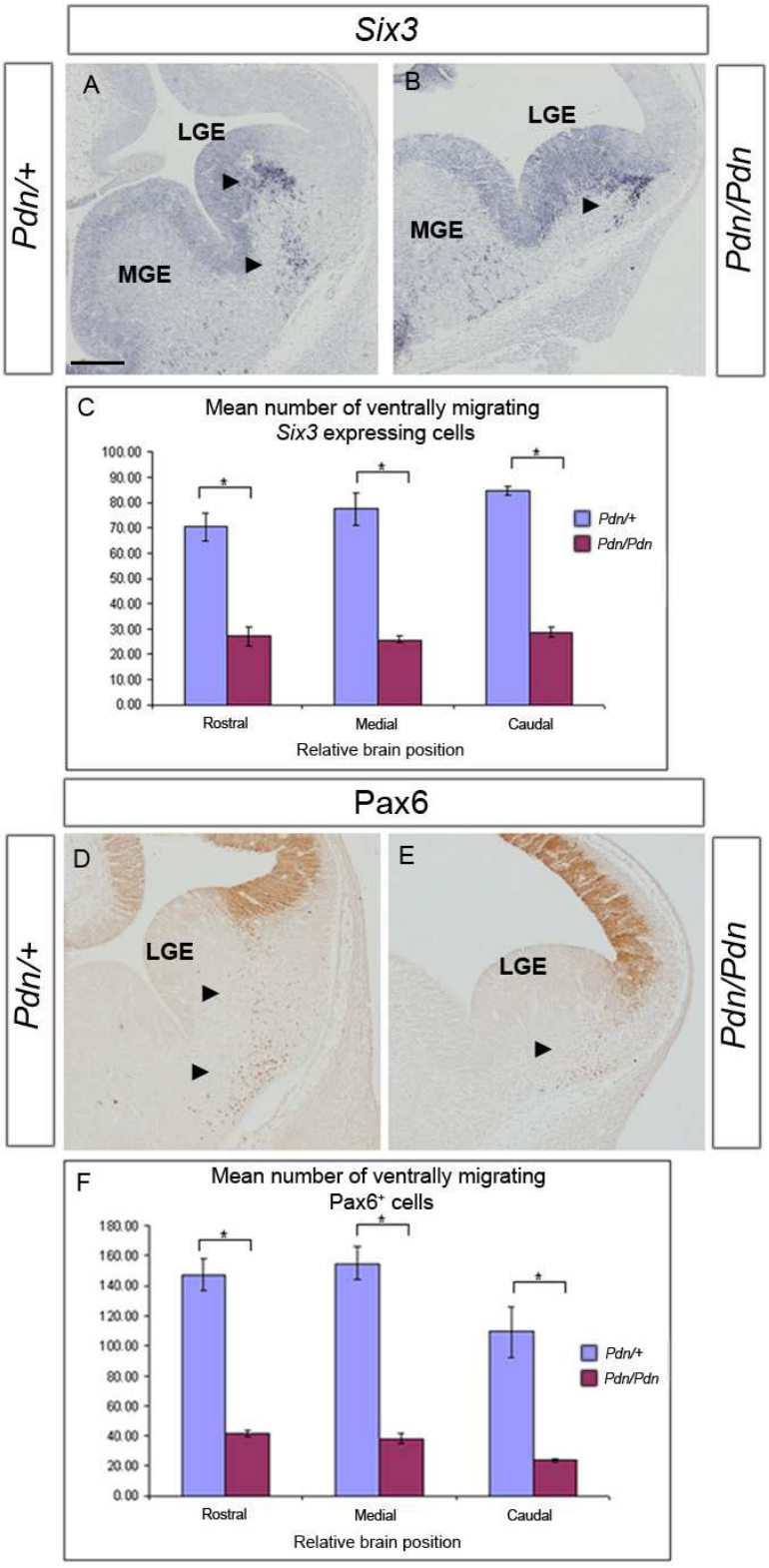
Six3
A
B
LGE
MGE
LGE
MGE
Pdn/+
Pdn/Pdn
C
Mean number of ventrally migrating
Six3 expressing cells
100.00
90.00
80.00
70.00
60.00
50.00
40.00
30.00
20.00
10.00
0.00
Rostral
Medial
Caudal
Relative brain position
Pdn/+
Pdn/Pdn
Pax6
D
E
LGE
LGE
Pdn/+
Pdn/Pdn
F
Mean number of ventrally migrating
Pax6+ cells
180.00
160.00
140.00
120.00
100.00
80.00
60.00
40.00
20.00
0.00
Rostral
Medial
Caudal
Relative brain position
Pdn/+
Pdn/Pdn

**Figure 5.4.**

***Six3* in situ hybridization and *Pax6* immunohistochemistry analyses to reveal the formation of ventrally migrating lateral cortical stream cells originating within the dorsal LGE and/or the ventral pallium (A-F).**

On *Pdn/+* coronal brain sections, cells migrating ventrally along the corticostriatal boundary are positive for *Six3* (arrowheads in A). *Six3* also labels the ventricular zone of the LGE and MGE, but at lower intensity (A). *Pdn/Pdn* coronal brain sections showed a dramatic reduction of ventrally migrating *Six3* expressing cells (arrowhead in B). Fewer *Six3* expressing cells were present within the mantle region of *Pdn/Pdn* LGE, and very few of them contributed to the lateral cortical stream (arrowhead in B, C). No difference in *Six3* expression was detected within the ventricular zone of *Pdn/Pdn* MGE and LGE when compared to *Pdn/+* (A, B).

Pax6 also labelled ventrally migrating cells originating within the dorsal LGE. *Pdn/+* coronal brain sections revealed several cells within the mantle region of the LGE migrating along the corticostriatal boundary (arrowheads in D). In addition, it is possible to observe Pax6 expression within the ventricular zone of the dorsal LGE and the ventral pallium (D). Pax6 staining on *Pdn/Pdn* brains sections also showed a reduction in the number of the ventral telencephalic migrating $Pax6^{+}$ cells (arrowhead in E, F). In addition, *Pax6* ventral telencephalic expression is shifted dorsally (compare D to E).

These results were quantified by counting $Pax6^{+}$ (Mann-Whitney test p=0.032 n=4 rostral, p=0.034 n=4 medial, p=0.05 n=3 caudal) and *Six3* (Mann-Whitney test p=0.009 n=5 rostral, p=0.009 n=5 medial, p=0.021 n=4 caudal) expressing cells along the *Pdn/+* (Blue) and *Pdn/Pdn* (Purple) lateral cortical stream (C and F). This analysis confirmed a significant reduction of about 3 times for *Six3* expressing and $Pax6^{+}$ cells along the antero posterior axes of *Pdn/Pdn* ventral telencephalon when compared to *Pdn/+* (asterisks in C and F). (Scale bar in A 100 μm; applays to all panels).

All together these analyses show a partial ventralization of the LGE and a dorsal shift and expansion of the ventral pallium. This is also confirmed by a reduction of lateral cortical stream cells originating within the dorsal LGE and the ventral pallium. Interestingly, these marker analyses also showed a reduction in the size of the *Pdn/Pdn* LGE, which does not seem to bulge out as much as the *Pdn/+* LGE. However, the size reduction of the *Pdn/Pdn* LGE seemed to be due to a reduction of *Pdn/Pdn* LGE mantle region. This hypothesis is tested in the next section.

## 5.5 The *Pdn/Pdn* LGE displays a reduced number of neurons and an elongation of the S phase and of the cell cycle at E10.5

Patterning defects may affect telencephalic regionalization but also progenitor cell proliferation, differentiation and apoptosis. From the previous marker analyses the *Pdn/Pdn* LGE appeared smaller and less bulged out. Although the *Pdn/Pdn* LGE proliferating region, which is composed of proliferating cells, does not seem to be affected by this size reduction, the *Pdn/Pdn* mantle region, which is composed of post mitotic neurons, seems to be thinner when compared to *Pdn/+*. This is particularly evident with *Dlx2* in situ hybridization and Gsh2 immunofluorescence. Here, the *Pdn/Pdn* ventral telencephalon was tested for its ability to proliferate and produce post mitotic neurons at early steps of forebrain development. To check this, Tuj1 immunostaining was performed on coronal sections of E11.5 *Pdn/+* and *Pdn/Pdn* brains.

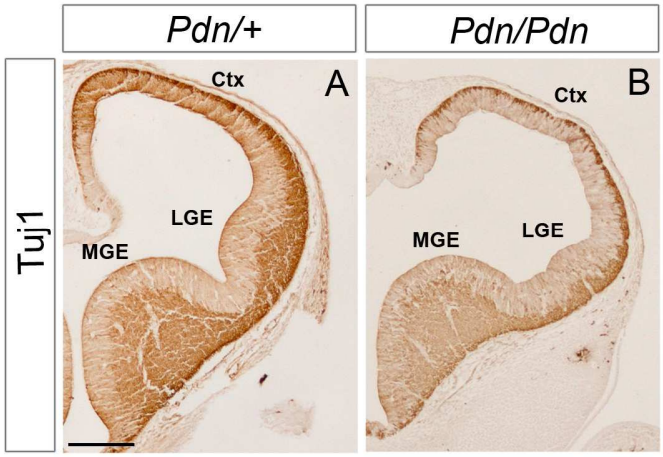


**Figure 5.5.**

**Tuj1 immunostaining showing the structures of the E11.5 *Pdn*/+ (A) and *Pdn*/*Pdn* (B) brain.**

Tuj1 is a pan-neuronal marker staining post mitotic neurons. *Pdn*/+ coronal brain sections reveal thick Tuj1$^{+}$ mantle regions in the MGE and LGE, compared to the developing cortex which only shows a thin layer of Tuj1$^{+}$ cells in the preplate (A).

Tuj1 staining on E11.5 *Pdn/Pdn* coronal brain sections revealed no differences for Tuj1 expression in the MGE mantle and cortical preplate (B). However, from this analysis the *Pdn/Pdn* LGE also appears smaller and less bulged out (B). Although the *Pdn/Pdn* LGE Tuj1-negative proliferating region does not seem to be affected by this size reduction, the *Pdn/Pdn* Tuj1$^{+}$ mantle region is thinner when compared to *Pdn*/+ (B). (Scale bar in A 100 μm; applays to all panels)

Tuj1 is a pan-neuronal marker. Neural progenitor cells proliferate in the ventral telencephalic and cortical ventricular zone and subsequently migrate radially within the MGE and LGE mantle and within the cortical plate respectively, starting their differentiation program. Neural differentiation starts earlier in the ventral telencephalon than in the dorsal region. Indeed, Tuj1 staining at E11.5 on *Pdn/+* coronal brains sections reveals thick $Tuj1^+$ mantle regions in the MGE and LGE, compared to the developing cortex which only shows a thin layer of $Tuj1^+$ cells above the ventricular zone, the preplate (Fig. 5.5; A).

Tuj1 staining on E11.5 *Pdn/Pdn* coronal brain sections revealed no differences for Tuj1 expression in the MGE mantle (Fig. 5.5; B). However, the mantle region of the *Pdn/Pdn* LGE appears thinner when compared to *Pdn/+* (Fig. 5.5; B). This also explains a general reduction in the size of the *Pdn/Pdn* LGE, which results from a reduction of post-mitotic neurons. At E11.5 the $Tuj1^+$ cells within the mantle of the LGE are numerous and densely packed and therefore cannot be resolved form each other. This makes it difficult to quantify the number of post-mitotic neurons within the mantle of the *Pdn/+* and the *Pdn/Pdn* LGE. To define the origin of these defects, earlier stages of development were analyzed. Tuj1 staining was performed on E10.5 coronal brain sections (Fig. 5.6; G-H). At this embryonic stage neural differentiation has just started in the ventral telencephalon, therefore $Tuj1^+$ cells within the LGE and MGE mantle are fewer and less densely packed and can be more easily counted. From this point onwards wild type embryos were used as controls and not *Pdn/+* embryos. Although there were not obvious phenotypical differences observed between wild type and *Pdn/+* embryos, this was done to maximise the differences in the following quantitative analyses and to avoid

an unlikely, but possible, subtle difference between heterozygous and wild type not detectable in the previous experiments. This was particularly important especially in the experiments of qRT-PCR described later.

At E10.5 it is quite difficult to identify anatomically the LGE and the MGE. To do so a combination of molecular markers was used to reveal the extent of the E10.5 LGE, MGE and cortex, similar to that previously described for the quantification of *Gsh1* expressing cells in the ventral telencephalon. In situ hybridization for *Dlx2* and *Nkx2.1* was performed on coronal brain sections (Fig. 5.6; A-D). On these sections, the MGE region is defined as positive for *Dlx2* and *Nkx2.1* and the LGE as positive for *Dlx2* but negative for *Nkx2.1*. Therefore the combination of these two markers clearly defines the +/+ and *Pdn/Pdn* PSPB between LGE and cortex and the boundary between LGE and MGE (Fig. 5.6; A-D). +/+ and *Pdn/Pdn* coronal brain sections, adjacent to those labelled with *Nkx2.1* and *Dlx2* in situ hybridization, were immunostained for Tuj1 (Fig. 5.6; G, H). These immunoreacted sections were conterstained with TO-PRO3, which ubiquitously labels cellular nuclei (Fig. 5.6; E, F). $Tuj1^+$ and $TO\text{-}PRO3^+$ cells were counted within the delineated regions. The number of $Tuj1^+$ cells, within +/+ and *Pdn/Pdn* LGE and MGE, was then calculated as a percentage of the total number of $TO\text{-}PRO^+$ cells in this region according to the formula:

% of $Tuj1^+$ cells = (number of $Tuj1^+$ cells / number of $TO\text{-}PRO3^+$ cells) x 100.

It was not possible to observe significant differences in the percentage of $Tuj1^+$ cells within the MGE of *Pdn/Pdn* coronal brain sections when compared to +/+ (Fig. 5.6; I).

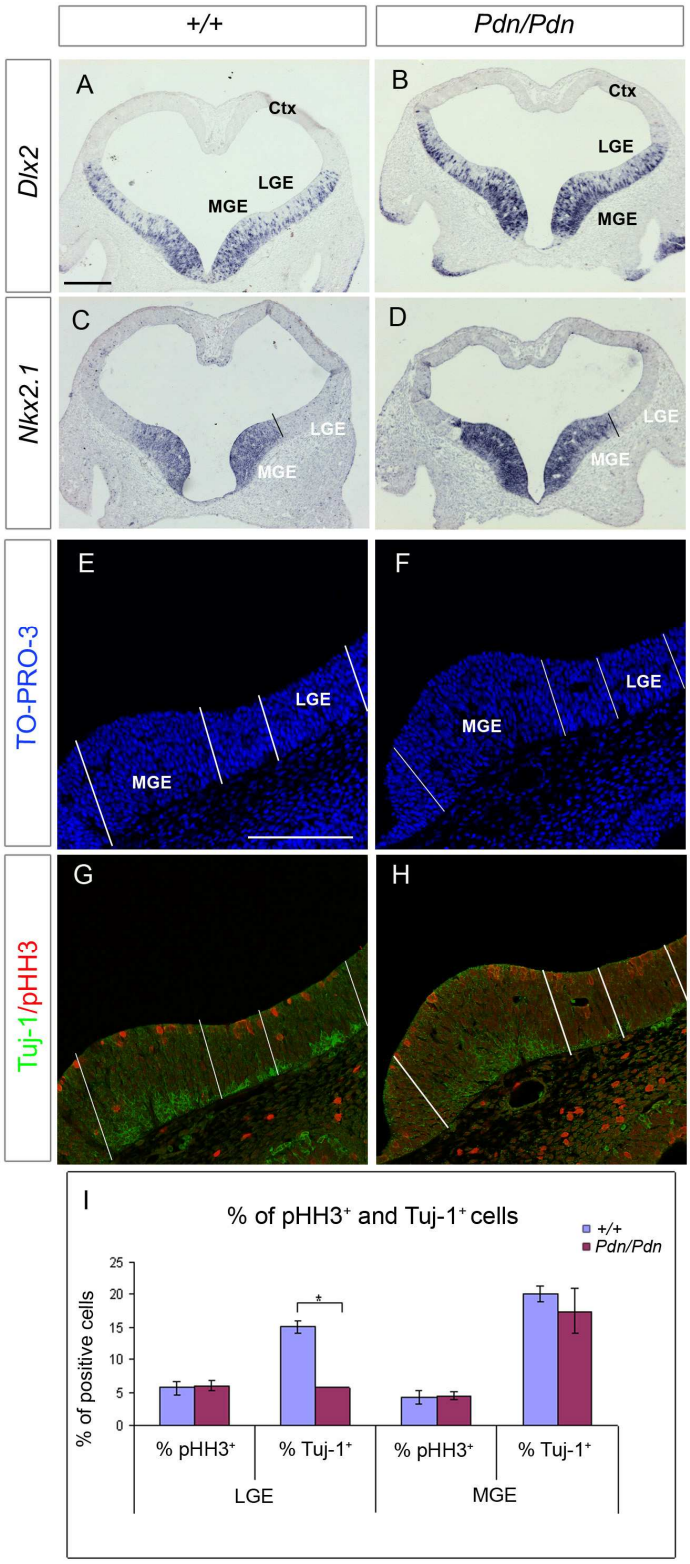
+/+
Pdn/Pdn
Dlx2
Nkx2.1
TO-PRO-3
Tuj-1/pHH3
A
B
C
D
E
F
G
H
I
Ctx
LGE
MGE
% of pHH3⁺ and Tuj-1⁺ cells
+/+
Pdn/Pdn
% of positive cells
25
20
15
10
5
0
*
% pHH3⁺
% Tuj-1⁺
% pHH3⁺
% Tuj-1⁺
LGE
MGE

**Figure 5.6.**

**Quantification of ventral telencephalic post-mitotic neurons Tuj1$^+$ and of cells undergoing mitosis pHH3$^+$ on coronal brain sections of E10.5 +/+ and *Pdn/Pdn* mutants.**

In situ hybridization for *Dlx2* and *Nkx2.1* was performed on coronal brain sections of E10.5 *Pdn/+* and *Pdn/Pdn* mutants (A-D). The MGE region is identified as positive for *Dlx2* and *Nkx2.1* and the LGE as positive for *Dlx2* but negative for *Nkx2.1*. (A-D). In addition, coronal brain sections adjacent to those labelled with *Nkx2.1* and *Dlx2* in situ hybridization, were immunostained for Tuj1 and pHH3 (G, H) and counterstained with the cellular nuclear marker TO-PRO3 (E, F). Lines were drawn to delineate the LGE and MGE territories inside the boundaries given by *Dlx2* and *Nkx2.1* in situ hybridization (E-H). Tuj1$^+$, pHH3 and TO-PRO3$^+$ cells were counted within the delineated regions. The results of the quantification are given in I with +/+ values represented by blue bars and *Pdn/Pdn* values represented by purple bars.

The number of Tuj1$^+$ cells, within +/+ and *Pdn/Pdn* LGE and MGE, was calculated as a percentage of the total number of TO-PRO$^+$ cells in this region according to the formula: % of Tuj1$^+$ cells = (number of Tuj1$^+$ cells / number of TO-PRO3$^+$ cells) x 100. No significant difference was found in the percentage of Tuj1$^+$ cells within the MGE of *Pdn/Pdn* coronal brain sections when compared to +/+ (I). However, the percentage of Tuj1$^+$ cells within the *Pdn/Pdn* LGE is significantly reduced to about a third when compared to the +/+ LGE (asterisk in I) (Mann-Whitney test p=0.05 n=3).

Also, the numbers of pHH3$^+$ cells in the +/+ and *Pdn/Pdn* LGE and MGE were calculated as a proportion of the total number of cells labelled by TO-PRO3 according to the formula: % of pHH3$^+$ cells = (number of pHH3$^+$ cells / number of TO-PRO3$^+$ cells) x 100. It was not possible to detect any differences in the percentage of pHH3$^+$ cells within the ventricular zone of *Pdn/Pdn* LGE and the MGE when compared to +/+ (I). (Scale bar in A 100 μm; applays to B-D) (Scale bar in E 100 μm; applays to F-H)

However, the percentage of $Tuj1^+$ cells within the *Pdn/Pdn* LGE was significantly reduced (form 15.04±1.02 cells in *Pdn/+* to 5.85±0.06 cells in *Pdn/Pdn*) to about a third when compared to the +/+ LGE (Fig. 5.6; I) (Mann-Whitney test p=0.05 n=3).

These data showed an obvious reduction of post mitotic neurons within the mantle region of the *Pdn/Pdn* LGE. This effect may be explained by a reduction of dividing cells within the *Pdn/Pdn* LGE, alternatively increased apoptosis may have reduced the number of proliferating cells and/or differentiating neurons. The same sections immunostained for Tuj1 were also labelled with an antibody against phospho-histone H3 (PHH3) (Fig. 5.6; G, H). pHH3 labels cells undergoing mitoses, histone H3 is a histone protein constituent of chromatin, which is phosphorylated only during mitosis (Tapia et al., 2006). The antibody used here only recognizes the phosphorylated form of histone H3. Within the forebrain, pHH3 labels proliferating cells undergoing mitosis at the ventricular surface of the ventricular zone of MGE, LGE and cortex. The reduction of differentiated neurons could manifest as a direct consequence of a reduction of the proliferating cells within the LGE of *Pdn/Pdn* mutants. The pHH3 positive cells were also counted within the E10.5 LGE and the MGE of +/+ and *Pdn/Pdn* mutant brains (Fig. 5.6; G, H). The numbers of $pHH3^+$ cells in the +/+ and *Pdn/Pdn* LGE and MGE were again calculated as a proportion of the total number of cells labelled by TO-PRO3 according to the formula:

% of $pHH3^+$ cells = (number of $pHH3^+$ cells / number of $TO\text{-}PRO3^+$ cells) x 100.

Surprisingly, it was not possible to detect any differences in the percentage of $pHH3^+$ cells within the ventricular zone of *Pdn/Pdn* LGE and the MGE when compared to +/+ (Fig. 5.6; I).

Taken together these data show a reduction in the proportion of differentiated $Tuj1^+$ neurons in the mantle of the *Pdn/Pdn* LGE at E10.5. However, there was no change in the proportion of mitotic cells in the proliferative zone of the *Pdn/Pdn* LGE, suggesting that the reduction of post-mitotic neurons was not a consequence of a reduced proportion of mitotic cells.

To test any abnormalities in apoptosis, immunostaining for activated caspase3 was performed on coronal brain sections of E10.5 +/+ and *Pdn/Pdn* embryos (Fig. 5.7). caspase3 is an essential protein involved in apoptosis and in order to induce cell death needs to be activated by proteolytic cleavage. Positive immunostaining for activate caspase3 is an indication that programmed cell death is taking place. At E10.5, a small number of $caspase3^+$ cells was observed within the *Pdn/+* forebrain. Apoptotic cells are revealed in the *Pdn/+* dorsal midline, where the two telencephalic hemispheres begin invaginating, and in ventral midline (Fig. 5.7; A and arrow in B). No other apoptotic cells were revealed in any other region of the E10.5 *Pdn/+* telencephalic neuroepithelium (Fig. 5.7; A, B). *Pdn/Pdn* brains display defects in the dorsomedial telencephalic invagination, which are also reflected by the absence of apoptotic cells within the dorsomedial telencephalon (Fig. 5.7; C).

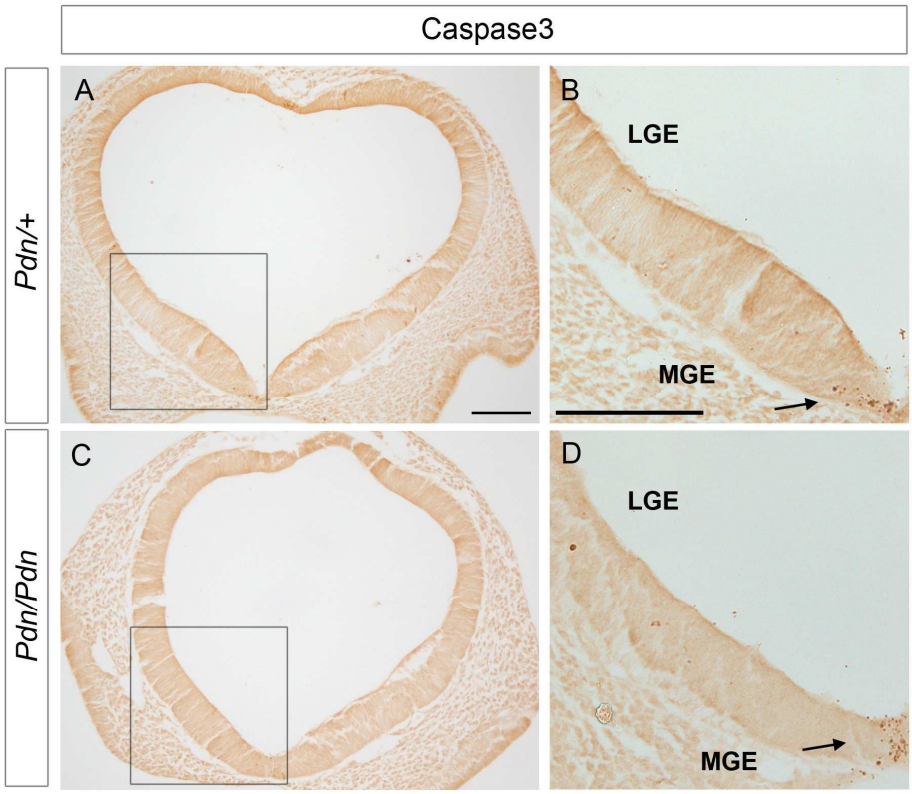


**Figure 5.7.**

**Immunohistochemistry for activated caspase3 analyzing apoptosis on *Pdn/+* and *Pdn/Pdn* coronal brain sections at E10.5.** B and D are higher magnifications of A and C, respectively.At E10.5 very little apoptosis is observed in the *Pdn/+* forebrain. Apoptotic cells are revealed in the *Pdn/+* dorsal midline and in ventral midline (A and arrow in B). No other apoptotic cells were revealed in any other region of the E10.5 *Pdn/+* telencephalic neuroepithelium (A, B). *Pdn/Pdn* brains display absence of apoptotic cells within the dorsomedial telencephalon (C). However, as well as in *Pdn/+* brains, no apoptotic cells were present in any other region of the ventral telencephalic neuroepithelium a part form the ventral midline (C and arrow in D). Although it was not quantified, the number of Caspase3$^{+}$ cells, in the ventral midline, did not seem to differ between *Pdn/+* and *Pdn/Pdn* brains (arrows in B and D). (Scale bar in A 100 μm; applays to C) (Scale bar in B 100 μm; applays to D).

However, similat to *Pdn/+* brains, no apoptotic cells were present in any other region of the ventral telencephalic neuroepithelium apart form the ventral midline (Fig. 5.7; C and arrow in D), revealing that the reduction of $Tuj1^{+}$ cells within the *Pdn/Pdn* LGE was not the result of increasing apoptosis.

In conclusion, neither apoptosis nor a reduction of progenitor cells seemed to be the cause of the reduction of the number of differentiating neurons within the *Pdn/Pdn* LGE mantle. However, another possibility could explain the reduction of these post-mitotic neurons: the *Pdn* mutation may result in a difference in the cell cycle time of proliferating cells in the *Pdn/Pdn* LGE. To test this idea, cell cycle kinetic parameters were analyzed and the total cell cycle length calculated within the ventral telencphalon of *Pdn/+* and *Pdn/Pdn* E10.5 brains (Fig. 5.8).

The measurement of the cell cycle length is based on the paradigm that proliferative cells within the embryonic telencephalic ventricular zone do not cycle synchronously (Takahashi et al., 1993). At any time point it is possible to find cells in mitosis, in DNA synthesis (S phase), G1 or G2. It is possible to label cells in S phase with the use of BrdU and IdU which are halogenated analogues of thymidine and are incorporated into DNA during DNA replication. BrdU and IdU can be injected into pregnant females of E10.5 embryos and circulate within the blood stream, reaching the embryos and incorporating into the DNA of proliferating cells. IdU was injected first at T=0hr, labelling cells in S phase (Fig. 5.8; A). After 1.5hr BrdU is also injected into the pregnant female and cells in S phase will be labelled by both BrdU and IdU (Fig. 5.8; A). However, a proportion of cells that were in S phase at the time of the IdU integration

will have finished DNA synthesis at the time of BrdU injection and will have progressed further through the cell cycle (Fig. 5.8; A). These cells are not labelled by BrdU (Fig. 5.8; A) and are called leaving cells ($L_{cells}$). The female is sacrificed and the embryos isolated 2hr after the first injection. $BrdU^+$ and $IdU^+$ cells are in S phase during both injections ($S_{cells}$). The period that cells can incorporate IdU but not BrdU is 1.5 hr, and is called Ti. The proportion of cells leaving S phase is given by the number of $IdU^+$ cells that are not positive for BrdU, the $L_{cells}$.

The length of the S phase (Ts) was calculated according to the following formula, which is based on the assumption that the proportion of time between any one period of the cell cycle to that of another period is equal to the proportion of cells in the first period to the number of cells in the second period (Nowakowski et al., 1989):

Ts = Ti/( Lcells/Scells).

$L_{cells}$ are $IdU^+$ and $BrdU^-$ and $S_{cells}$ are $IdU^+$ and $BrdU^+$. Positive cells for BrdU and IdU were counted within the LGE and MGE of coronal brain sections of +/+ and *Pdn/Pdn* embryos. Two different antibodies, one recognising IdU as well as BrdU and a second one recognising BrdU only, were used on the IdU and BrdU treated coronal brain sections (Fig. 5.8; D, E). The number of $IdU^+$ $BrdU^-$ cells was given by the number of cells labelled by the IdU/BrdU antibody minus the number of cells labelled by the antibody recognising BrdU only. These brain sections were also counterstained by TO-PRO3 to reveal the total number of cells within the brain sections (Fig. 5.8; B, C). As before, MGE, LGE and cortex were discriminated by *Dlx2* and *Nkx2.1* in situ hybridization on adjacent sections. It was not possible to find any difference in the Ts of proliferating cells in the MGE of *Pdn/+* and *Pdn/Pdn* brains (Fig. 5.8; F).

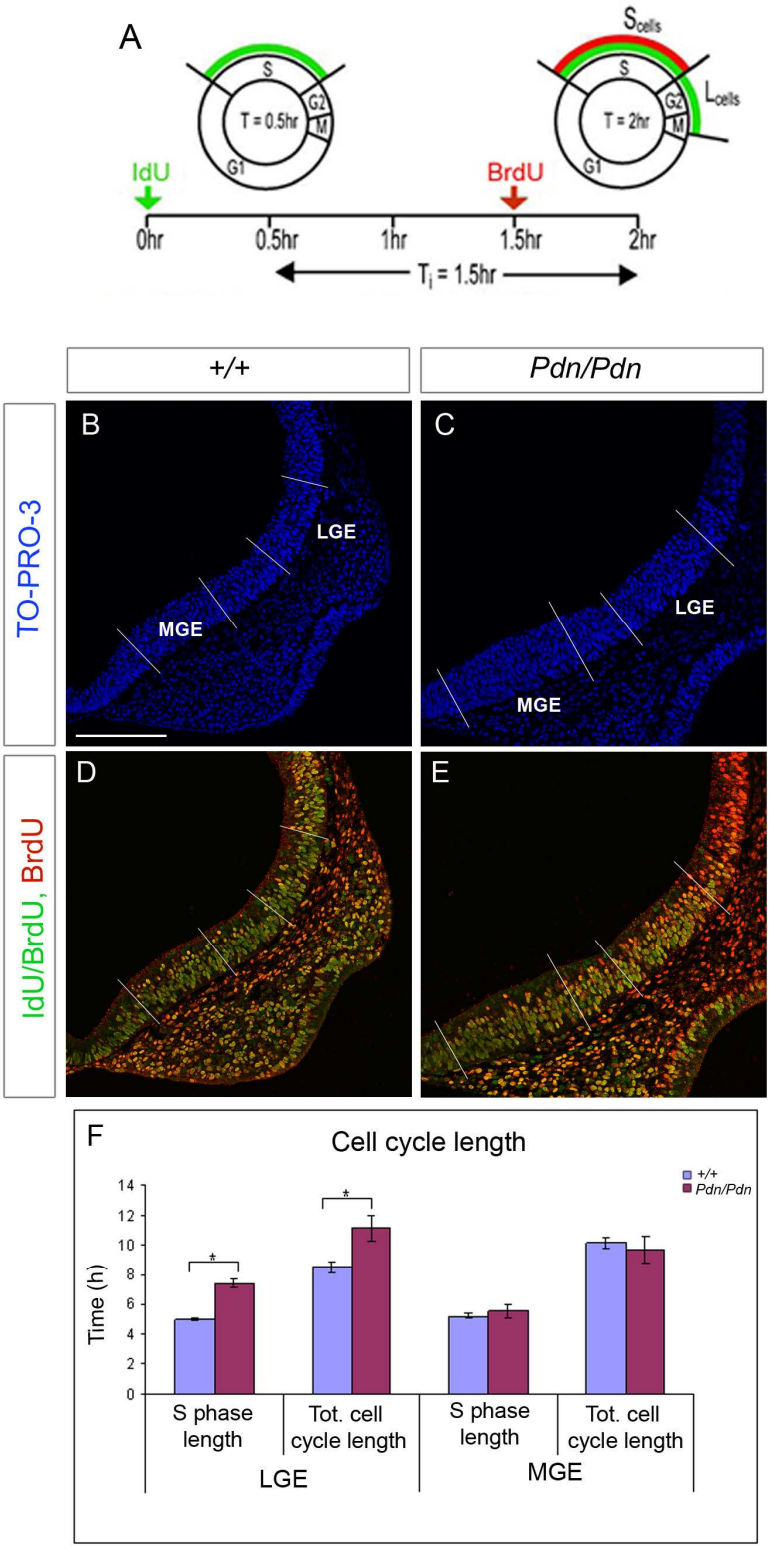
A
S
G2
M
G1
T = 0.5hr
IdU
S cells
T = 2hr
L cells
BrdU
0hr
0.5hr
1hr
1.5hr
2hr
Ti = 1.5hr
+/+
Pdn/Pdn
TO-PRO-3
B
LGE
MGE
C
LGE
MGE
IdU/BrdU, BrdU
D
E
F
Cell cycle length
+/+
Pdn/Pdn
Time (h)
0
2
4
6
8
10
12
14
*
*
S phase length
Tot. cell cycle length
S phase length
Tot. cell cycle length
LGE
MGE

**Figure 5.8.**

**The E10.5 *Pdn/Pdn* LGE displays an elongation of the S phase and of the total cell cycle length.** IdU was injected first at T=0hr (A). After 1.5hr BrdU is also injected into the pregnant female labelling cells in S phase (A). However, a proportion of cells that were in S phase at the time of the IdU integration will have finished DNA synthesis at the time of BrdU injection (A). The female is sacrificed and the embryos isolated 2hr after the first injection. +/+ and *Pdn/Pdn* coronal brain sections are immunostained for BrdU and IdU (D, E) and counterstained with the cellular nuclear marker TO-PRO3 (B, C). Lines were drawn to delineate the LGE and MGE territories (B-E). $BrdU^+$, $IdU^+$ and $TO\text{-}PRO3^+$ cells were counted within the delineated regions. Two different antibodies, one recognising IdU as well as BrdU and a second one recognising BrdU only were used. The number of $IdU^+$ $BrdU^-$ cells was given by the number of cells labelled by the IdU/BrdU antibody (in green) minus the number of cells labelled by the antibody recognising BrdU only (in red). The results of the quantification are given in F with +/+ values represented by blue bars and *Pdn/Pdn* values represented by purple bars. $BrdU^+$ and $IdU^+$ cells are in S phase during both injections ($S_{cells}$). The period that cells can incorporate IdU but not BrdU is 1.5 hr, and is called Ti (A). The proportion of cells leaving S phase is given by the number of $IdU^+$ cells that are not positive for BrdU, the $L_{cells}$. The length of the S phase (Ts) was calculated according to the following formula: Ts = Ti/( Lcells/Scells). Where $L_{cells}$ are $IdU^+$ and $BrdU^-$ and $S_{cells}$ are $IdU^+$ and $BrdU^+$. Applying the same logic it was also possible to calculate the total length of the cell cycle (Tc), which was given by the following formula: Tc = Ts/( Scells/Pcells). In this case, $P_{cells}$ is the total number of proliferating cells within the ventricular zone of MGE and LGE. It was not possible to find any difference in the Ts and in total cell cycle length of proliferating cells in the MGE of *Pdn/+* and *Pdn/Pdn* brains (F). However, the Ts of proliferating cells within the *Pdn/Pdn* LGE was significantly longer by about 2 hours, when compared to +/+ (Mann-Whitney test p=0.05 and n=3). In addition, a significant 2 and half hours increase was found in the total time of cell cycle length of proliferating cells within the *Pdn/Pdn* LGE (Mann-Whitney test p=0.05 and n=3) (asterisks in F). (Scale bar in B 100 μm; applays to all pannels).

However, the Ts of proliferating cells within the *Pdn/Pdn* LGE was significantly longer of about 2 hours (form 5±0.1 hours to 7.5±0.3 hours), when compared to +/+ (Fig. 5.8; F) (Mann-Whitney test p=0.05 and n=3). This revealed that *Pdn/Pdn* LGE proliferating cells were progressing through the phase of DNA synthesis at a slower rate when compared to +/+.

Applying the same logic to calculate the Ts, it was also possible to calculate the total length of the cell cycle (Tc), which was given by the following formula:

Tc = Ts/( Scells/Pcells).

In this case, Pcells is the total number of proliferating cells within the ventricular zone of MGE and LGE. This number was given by the total number of cells in the *Pdn/+* and *Pdn/Pdn* MGE and LGE as labelled by TO-PRO3 minus the number of $Tuj1^+$ neurons. Indeed, at E10.5 neural telencephalic differentiation has just started and, especially within the LGE, only a few differentiating neurons have just formed within the mantle. Therefore it is difficult to discriminate between the mantle region, containing differentiated neurons, and the ventricular zone, containing proliferating cells, only with the TO-PRO3 staining.

This analysis also showed no difference in total cell cycle length of the proliferating cells in the *Pdn/Pdn* MGE when compared to +/+ (Fig. 5.8; F). A significant about 2 and half hours increase (form 8.5±0.4 hours to 11.1±0.8 hours) was found in the total time of cell cycle length of proliferating cells within the *Pdn/Pdn* LGE (Fig. 5.8; I) (Mann-Whitney test p=0.05 and n=3).

Together, these data suggest that the reduction in the size of the LGE is due to a reduction in the number of $Tuj1^+$ post-mitotic neurons within the *Pdn/Pdn* LGE mantle

at E10.5. In addition, the *Pdn* mutation selectively affects the cell cycle length of proliferating cells within the LGE. S phase and the total cell cycle length are significantly longer in *Pdn/Pdn* mutants than in +/+. The elongation of the cell cycle time is likely to contribute to a reduced differentiation rate within the LGE of these mutants.

## 5.6 *Shh* signalling is up-regulated within the ventral telencephalon of *Pdn/Pdn* mutants at early stages of brain development

Gli3 is involved in *Shh* signalling, either as a transcriptional activator or repressor (Aza-Blanc et al., 2000; Ruiz i Altaba, 1998). Gli3 full-length protein is an activator, which needs to be proteolytically cleaved in order to become a transcriptional repressor (Aza-Blanc et al., 2000; Ingham and McMahon, 2001). This happens in the absence of *Shh*, which negatively regulates the proteolytic cleavage of Gli3 protein (Marigo et al., 1996; Wang et al., 2000). In addition, the ration between Gli3 repressor and activator forms changes in different regions of the telencephalon, with the repressor being more abundant within the dorsal telencephalon and the activator more abundant in the ventral telencephalon (Fotaki et al., 2006). Therefore, the Gli3 repressor form has been suggested to play an important role in patterning the dorsal telencephalon in the absence of *Shh* (Ingham and McMahon, 2001; Wang et al., 2000), while evidence has been provided that Shh and Gli3 play complementary roles in patterning the ventral telencephalon (Rallu et al., 2002; Rash and Grove, 2007).

Here, it was hypothesised that *Gli3* might play a role in counteracting *Shh* function within the ventral telencephalon. To test this hypothesis the expression patterns of *Shh* and the mRNA levels of its target genes *Gli1* and *Ptc1* were analyzed in the wild type and *Pdn/Pdn* ventral telencephalon by in situ hybridization and quantitative RT-PCR (qRTPCR), respectively (Fig. 5.9). In situ hybridization on E12.5 wild type coronal brain sections showed that *Shh* is expressed in the mantle zone of the MGE and at a higher level in the ventricular zone of the anterior entopeduncular area/preoptic area, but not within the LGE (Fig. 5.9; A). In situ hybridization on *Pdn/Pdn* coronal brain sections shows no differences in the spatial expression of *Shh* compared to wild type (Fig. 5.9; B).

Although the *Shh* expression pattern did not change in the *Pdn/Pdn* telencephalon, *Gli3* may antagonize *Shh* function by counteracting *Shh* signalling within the ventral telencephalon. If this hypothesis is correct the *Gli3* reduction affecting the *Pdn/Pdn* mutants should result in an up-regulation of *Shh* target genes *Gli1* and *Ptc1* (Pearse et al., 2001; Stamataki et al., 2005). At E12.5 *Gli1* is expressed in the ventricular zone at the boundary between the LGE and MGE of wild type brains (Fig. 5.9; C). E12.5 *Pdn/Pdn* brain coronal sections showed no obvious changes in *Gli1* expression (Fig. 5.9; D). In situ hybridization of *Ptc1* revealed expression within the ventricular zone of the developing MGE on E12.5 wild type coronal sections, but very little *Ptc1* trancripts were detected in the LGE (Fig. 5.9; E). In contrast, E12.5 *Pdn/Pdn* coronal brain sections showed *Ptc1* expression extending from the MGE into the LGE ventricular zone (Fig. 5.9; F).

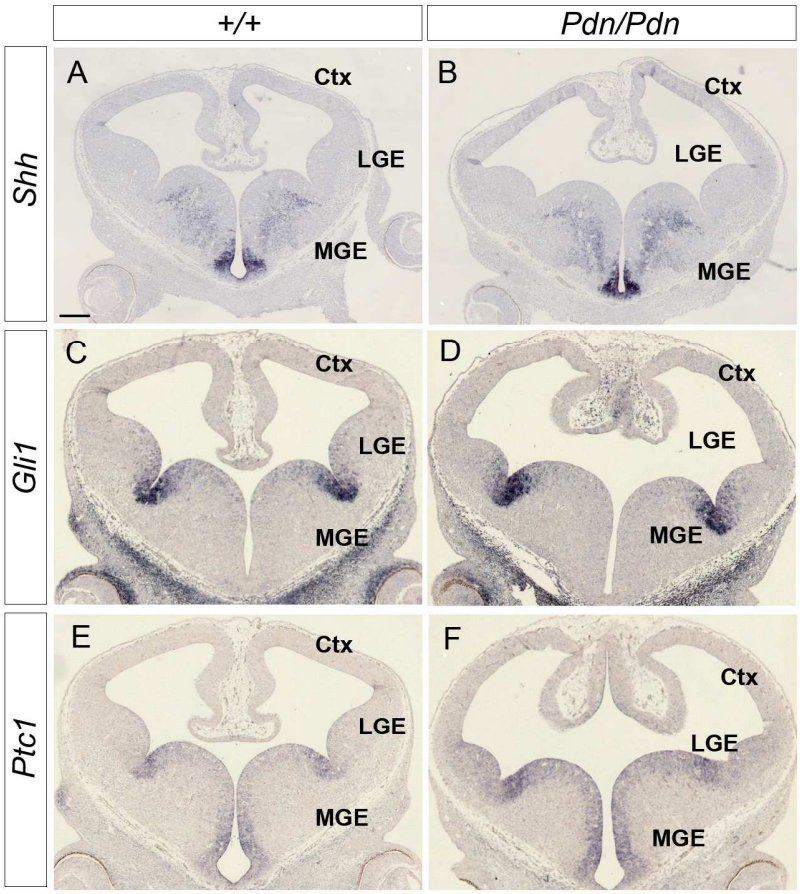
+/+
Pdn/Pdn
Shh
Gli1
Ptc1
A
B
C
D
E
F
Ctx
LGE
MGE

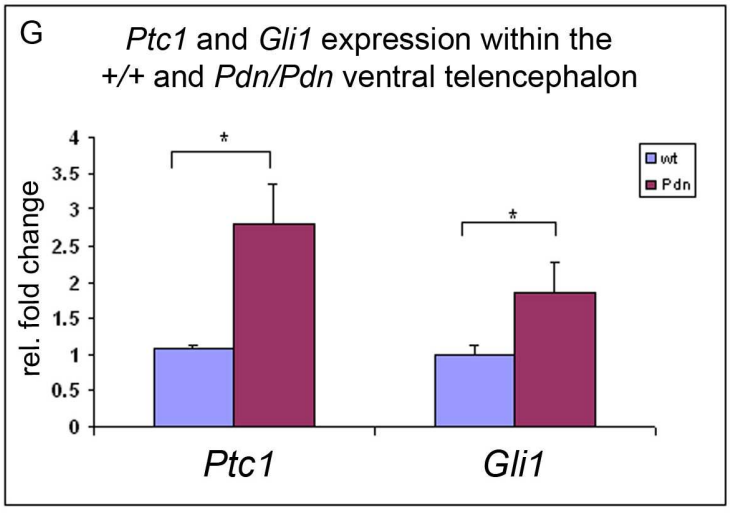
G
Ptc1 and Gli1 expression within the
+/+ and Pdn/Pdn ventral telencephalon
rel. fold change
4
3.5
3
2.5
2
1.5
1
0.5
0
*
*
wt
Pdn
Ptc1
Gli1

**Figure 5.9.**

**In situ hybridizations showing the expression patterns of *Shh* and its target genes *Gli1* and *Ptc1,* and mRNA levels of *Gli1* and *Ptc1* analyzed by quantitative RT-PCR (qRTPCR) in wild type and *Pdn/Pdn* E12.5 ventral telencephali (A-G).**

In situ hybridization on wild type coronal brain sections shows that *Shh* is expressed in the mantle zone of the MGE and at a higher level in the ventricular zone of the anterior entopeduncular area/preoptic area, but not within the LGE (A). No differences are observed in the spatial expression of *Shh* on *Pdn/Pdn* coronal brain sections when compared to wild type (B).

*Gli1* is expressed in the ventricular zone at the boundary between the LGE and MGE of wild type brains (C). Again *Pdn/Pdn* coronal brain sections showed no obvious changes in *Gli1* expression (D). *Ptc1* is expressed in the ventricular zone of the developing MGE, and very little *Ptc1* staining is detected in the ventral region of LGE (E). In contrast, *Pdn/Pdn* coronal brain sections show *Ptc1* expression extending from the MGE into more dorsal region of LGE ventricular zone (F).

qRTPCR was performed on RNA extracted from ventral telencephalic tissues of wild type (Blue) and *Pdn/Pdn* (Purple) brains (G). Interestingly, qRTPCR showed a significantly 3-fold higher *Ptc1* (Mann-Whitney test, p=0.002, n=6) and 2-fold higher *Gli1* (Mann-Whitney test p=0.006, n=8) expression in the *Pdn/Pdn* mutant ventral telencephalon compared to wild type (asterisks in G). (Scale bar in A 100 μm; applays to all pannels).

To quantify this observation qRTPCR was performed on ventral telencephalic tissues of wild type and *Pdn/Pdn* E12.5 brains. To achieve this, forebrains of mutant and wild type embryos were divided into left and right half. From each half, the ventral telencephalon was separated from the dorsal half with a micro-knife. At E12.5, the LGE and MGE are bulging out from the ventral telencephalon, and can easily be distinguished form the dorsal telencephalon. The two half ventral telencephali from the same brain were pooled together and the RNA was extracted before performing qRTPCR. Interestingly, qRTPCR showed a significantly about 2-fold higher *Gli1* (Mann-Whitney test p=0.006, n=8) and about 3-fold higher *Ptc1* (Mann-Whitney test, p=0.002, n=6) expression in the whole *Pdn/Pdn* mutant ventral telencephalon compared to that of wild types (Fig. 5.9; G).

These results indicate that Shh signalling is upregulated in the ventral telencephalon of E12.5 *Pdn/Pdn* mutants. This could explain the regionalization defects described above. The cell cycle defects in *Pdn/Pdn* ventral telencephalon have been observed as early as E10.5. Therefore, to understand whether there was a correlation between cell cycle abnormalities and *Shh* signalling up regulation in *Pdn/Pdn* mutant brains, *Shh, Ptc1* and *Gli1* expression were investigated at E10.5 (Fig. 5.10). At this embryonic age, *Shh* is expressed in the ventricular zone of the MGE and no obvious differences were found in its spatial expression in *Pdn/Pdn* coronal brain sections when compared to wild type (Fig. 5.10; A, B). At E10.5 *Gli1* is expressed in the ventricular zone at the boundary between the LGE and MGE. Again, no differences were found in *Gli1* expression between mutants and wild type (Fig. 5.10; C, D). *Ptc1* is also expressed in the

ventricular zone of the E10.5 MGE of wild type embryos (Fig. 5.10; E). Interestingly, a dorsal expansion of *Ptc1* expression was observed in the *Pdn/Pdn* LGE of E10.5 coronal brain sections, when compared to wild type (Fig. 5.10; F). At this embryonic age, only in situ hybridizations were performed. Proper microdissection of the E10.5 ventral telencephali for qRTPCR analyses was complicated by the absence of obvious morphological landmarks between the developing cortex and the ganglionic eminences. An alternative could have been the use of the whole telencephalon. However, due to time constraints it was not possible to perform this experiment with the number of *Pdn/Pdn* mutant embryos becoming limiting during the course of my PhD program.

Taken together these experiments show an up-regulation of *Shh* targets genes within the ventral telencephalon of *Pdn/Pdn* mutant brains at E10.5 and E12.5. Indeed, in situ hybridization shows an ectopic expansion of *Ptc1* within the *Pdn/Pdn* LGE and qRTPCR reveal a *Ptc1* and *Gli1* up-regulation in the *Pdn/Pdn* ventral telencaphalon. These analyses provide strong support for a role of *Gli3* in counteracting *Shh* signalling within the ventral telencephalon.

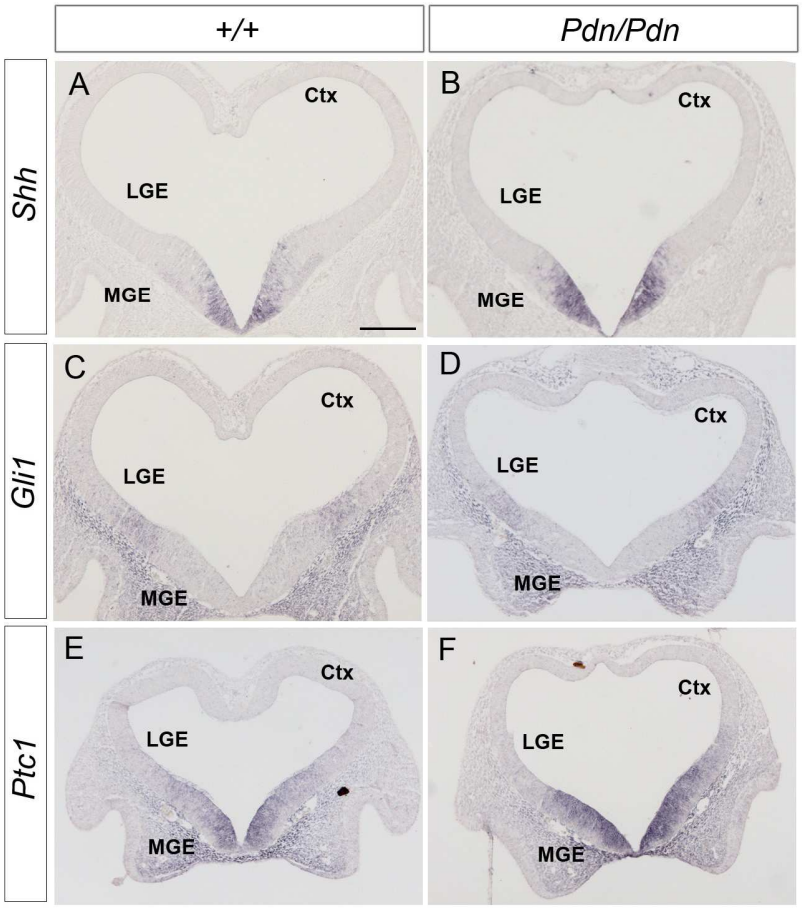


**Figure 5.10.**

**In situ hybridizations showing the expression patterns of *Shh* and its target genes *Gli1* and *Ptc1* on wild type and *Pdn/Pdn* E10.5 ventral telencephali (A-F).**

*Shh* is expressed in the ventricular zone of the MGE (A). A slightly dorsal shift of *Shh* is observed on some (only 1 out of 3) *Pdn/Pdn* coronal brain sections when compared to wild type (compare A to B). *Gli1* is expressed in the ventricular zone at the boundary between the LGE and MGE (C). No differences are found in *Gli1* expression between *Pdn/Pdn* mutants and wild type (compare C to D). *Ptc1* is expressed in the ventricular zone of only the MGE of wild type embryos (E). Interestingly, a dorsal expansion of *Ptc1* expression is observed in the *Pdn/Pdn* LGE coronal brain sections, when compared to wild type (compare E to F). (Scale bar in A 100 μm; applays to all pannels).

## 5.7 Discussion

In chapter 3 it has been shown that the corticothalamic tract fails to form normally in *Pdn/Pdn* brains. Although cortical projecting neurons and their axons are present, *Pdn/Pdn* cortical axons do not enter the *Pdn/Pdn* LGE, but rather project ectopically along the PSPB. However, at later stages of brain development (P0), some *Pdn/Pdn* cortical axons were observed to enter the striatal region and the diencephalon, taking several alternative routes in the *Pdn/Pdn* ventral telencephalon. In addition, they do not reach the *Pdn/Pdn* dorsal thalamus. In this chapter the mechanisms that underlie these defects have been addressed. It has been revealed that cortical lamination normally occurs in *Pdn/Pdn* mutants, suggesting no severe defects in the development of the *Pdn/Pdn* cortex. However, it was not possible to detect the presence of the *Pdn/Pdn* LGE pioneer neurons at E12.5. Between E10.5 and E12.5, patterning of the *Pdn/Pdn* ventral telencephalon is compromised with defects in regionalization and tissue growth. At E11.5 and E12.5 several markers whose expression is normally restricted to specific regions of the ventral telencephalon revealed defects in the establishment of the *Pdn/Pdn* PSPB and a dorsal shift of the ventral pallium, while the *Pdn/Pdn* CGE is partially ventralized. These results are also supported by a reduction in the number of ventrally migrating cells that originate in the *Pdn/Pdn* dorsal LGE. Also, the *Pdn/Pdn* LGE is smaller when compared to *Pdn*/+ and +/+ brains. This is the result of a reduction in the number of post-mitotic neurons in the *Pdn/Pdn* LGE mantle region from E10.5 onwards. The *Pdn/Pdn* LGE progenitors also display an elongation of the S-phase length and of

the total cell cycle length. Finally, at E10.5 and E12.5 the *Pdn/Pdn* ventral telencephalon displays an upregulation of and Shh signalling within the ventral telencephalon.

### 5.7.1 Cortical layer specification is not affected in *Pdn* mutants

Previous studies have reported severe defects in the development of the cerebral cortex (Fotaki et al., 2006; Grove et al., 1998; Quinn et al., 2009; Theil, 2005; Theil et al., 1999b; Tole et al., 2000b)and cortical lamination (Friedrichs et al., 2008) in *Gli3* mutant mice. $Xt^J/Xt^J$ mutants display defects in the early steps of cortical layering (Taglialatela et al., 2004; Theil, 2005), while $Xt^J/Pdn$ mutants display severe abnormalities in the cortical lamination process (Friedrichs et al., 2008).

Previous studies have already shown that the regionalization defects in *Pdn/Pdn* mutants are the mildest of the three different *Gli3* mutants $Xt^J/Xt^J$, $Xt^J/Pdn$ and *Pdn/Pdn* (Kuschel et al., 2003). However, defects in the development of the cerebral cortex and in the cortical lamination process in *Pdn/Pdn* mutants could have been an important cause for defects in the development of the *Pdn/Pdn* corticothalamic tract. To address this possibility it was necessary to analyze cortical development in these mutants.

This work shows that cortical lamination is not disturbed in the *Pdn/Pdn* P0 mouse brains. This has been demonstrated by using several markers for different cortical layers: *reelin* (marginal zone or layer I), *Tbr1* (layer VI, II/III and I), *Ror-β* (layer IV) and *Cux2* (layer II/III) (reviewed in Molyneaux et al., 2007). We also have further evidence to support the absence of cortical lamination defects in *Pdn/Pdn* mutants. Recently, further

progress has been made in the analysis of cortical layer markers in E14.5, E16.5 and P0 *Pdn/Pdn* brains (unpublished data, courtesy of Neil Campbell). Immunofluorescence staining at P0 was performed for Sox5 (layers VI and V), CTIP2 (layer V, corticospinal neurons) and Satb2 (strong expression in layer II/III and low expression in layers IV and V, callosal neurons) (Alcamo et al., 2008; Lai et al., 2008; Molyneaux et al., 2007). These analyses did not show any obvious differences in the expression patterns of these markers between *Pdn/+* and *Pdn/Pdn* brains, at any stages of development. Interestingly, CTIP2 and Satb2 staining shows that corticospinal neurons and callosal neurons, respectively, form normally. Also, $Sox5^{+}$ neurons of layer VI and V, most of which are corticofugal neurons, form normally (unpublished data, courtesy of Neil Campbell). Altogether, the data showed no differences in cortical lamination of *Pdn/Pdn* mutant brains when compared with *Pdn/+*. In addition, the use of *Pdn/Pdn Golli tau-GFP* embryos revealed that the *Pdn* homozygous mutant cortex is able to produce early projecting neurons and their axons in the subplate and cortical plate at E14.5 and corticofugal axons in lower layers and the subplate of the *Pdn/Pdn* P0 cortex.

At this stage it was not possible to completely rule out possible defects in expression of guidance receptors important for the navigation of *Pdn/Pdn* corticothalamic axons. It is therefore necessary to investigate the correct expression of guidance receptors important for corticothalamic axon navigation in *Pdn/Pdn* mutants, such as Robo1 and 2 (Lopez-Bendito et al., 2007). Interestingly indeed, very preliminary data on one *Pdn/Pdn* brain also showed normal expression of the guidance receptor Robo2 in the cortex, suggesting that *Pdn/Pdn* cortical axons also express at least one of the guidance receptors necessary for their navigation towards their final target. Finally, the use of a cortical *Gli3*

conditional knockout would help to investigate the cell-autonomous capacity of *Gli3* mutant cortical axons to navigate, as discussed further in chapter 6.

Altogether, these results suggest that the corticothalamic axon guidance defects in *Pdn/Pdn* mutants are not likely to result of defects in cortical development and cortical layer specification.

### 5.7.2 *Gli3* counteracts *Shh* expression and Shh signalling in the ventral telencephalon

Several ventral telencephalic development defects were observed in *Pdn/Pdn* brains, which could explain the observed cortical axon abnormalities. This hypothesis implies an important role for *Gli3* in the development of the ventral telencephalon. Previous reports have also shown an antagonizing role of *Gli3* and *Shh* in patterning this region (Rallu et al., 2002; Rash and Grove, 2007). In the following section it is discussed how our results are in agreement with this notion, and may even emphasize this counteraction in the ventral telencephalon.

The transcription factor Gli3 is involved in the Shh signalling pathway (Aza-Blanc et al., 2000; Ruiz i Altaba, 1998), functioning either as a transcriptional activator or repressor. Different regions of the Gli3 protein contain different transcriptional activities, with the N-terminal region encoding transcriptional repressor activity and full length encoding transcriptional activator activity (Aza-Blanc et al., 2000; Ingham and McMahon, 2001). Shh controls this transition: Gli3 transcriptional activator form is proteolytically cleaved becoming a transcriptional repressor in the absence of Shh (Marigo et al., 1996; Wang et

al., 2000). The *Gli3* telencephalic phenotype is opposite to defects observed in *Shh* null mutants. Indeed, they play opposite roles in patterning the telencephalon, with Gli3 null mutants displaying a partial ventralization of the dorsal telencephalon (Kuschel et al., 2003; Tole et al., 2000b) and *Shh* null mutants a partial dorsalization of the ventral telencephalon (Chiang et al., 1996; Fuccillo et al., 2004; Kohtz et al., 1998; Rallu et al., 2002). Importantly, patterning of the ventral telencephalon appears to be largely restored in double null mutants for *Gli3* and *Shh* (Rallu et al., 2002). However, the interaction between *Gli3* and *Shh* is more likely to be restricted to the ventral telencephalon close to a *Shh* signalling source. Indeed, the dorsal telencephalic defects of *Gli3* mutants are not restored in *Shh/Gli3* double mutants (Rash and Grove, 2007).

In this study, *Shh* and its signalling was analyzed in the *Gli3* hypomorphic mutant *Pdn*. We found a significant up-regulation of *Shh* target genes of about 3-folds for *Ptc1* and 2-folds for *Gli1* in the *Pdn/Pdn* ventral telencephalon at E12.5 and a dorsal shift of *Ptc1* expression in the *Pdn/Pdn* LGE of E10.5 and E12.5 brains. Recently, the analyses of *Gli1* and *Ptc1* mRNA levels in the telencephalon of 10.5 *Pdn/Pdn* brains became available (unpublished data, courtesy of Dr Kerstin Hasenpusch-Theil). qRTPCRs for *Ptc1* and *Gli1* were performed on total telencephalic extracts of E10.5 *Pdn/+* and *Pdn/Pdn* embryos. These experiments revealed a significant 3-fold increase for *Ptc1,* but not changes for *Gli1* in the telencephalon of E10.5 *Pdn/Pdn* brains when compared to wild type. The mRNA was extracted from the total telencephalon due to the absence of clear anatomical landmarks between dorsal and ventral telencephalon at E10.5 (unpublished data, courtesy of Dr Kerstin Hasenpusch-Theil). However, the use of total telencephali may cause an underestimation of *Ptc1* and *Gli1* upregulation in the *Pdn/Pdn*

mutants. This may be particularly true for *Gli1* since at E10.5 *Ptc1* is expressed in the whole MGE while *Gli1* is only expressed at the boundary between LGE and MGE.

In the limb bud, Gli3 repressor form has been reported to repress *Shh* expression. In the presence of *Gli3, Shh* is expressed in the posterior region of the limb bud (Echelard 1993). However, $Xt^J/Xt^J$ mutants display a duplication of *Shh* expression in anterior regions of the limb bud, leading to polydactyly (reviewed in (Taglialatela et al., 2004; Theil et al., 1999c). Therefore, it would have been interesting to know whether *Gli3* also represses *Shh* expression and not Shh signalling in the developing telencephalon. These data also became available recently. For this purpose qRTPCR was performed to check the level of *Shh* mRNA within the ventral telencephalon of E12.5 and the whole telencephalon of E10.5 wild type and *Pdn/Pdn* mutants (unpublished data, courtesy of Dr Kerstin Hasenpusch-Theil). *Shh* mRNA was significantly increased in the E10.5 brains and E12.5 ventral telencephali of these mutants of about 3-folds. Interestingly, in a recent work increase of *Shh* expression has not been observed at E9.5 in *Pdn/Pdn* mutant brains investigated by real time PCR and whole mount in situ hybridization (Ueta et al., 2008). All together, these analyses show that *Gli3* is necessary to counteract *Shh* expression and Shh signalling in the ventral telencephalon as early as E10.5. A reduction of *Gli3* results in an increase of Shh signalling and in an increase in the level of *Shh* expression itself. *Shh* ventral telencephalic expression is important to maintain ventral telencephalic identity, maintaining the expression of ventral-most telencephalic genes and/or controlling the growth of the ventral telencephalon (reviewed in (Fuccillo et al., 2006a). Therefore *Shh* and *Shh* signalling upregulation may be responsible for the patterning defects observed in the *Pdn/Pdn* ventral telencephalon. Defects in

regionalization and growth in the ventral telencephalon of *Pdn/Pdn* mutants will be discussed separately in the following sections.

### 5.7.3 The *Pdn* mutation causes regionalization defects in the ventral telencephalon and at the PSPB

Regionalization defects were selectively observed in the developing LGE, CGE and at the PSPB, but not in the MGE of *Pdn/Pdn* mutants. The *Pdn* mutation leads to a partial ventralization of the CGE revealed by *Gsh1* expression patterns. *Pax6* expression is shifted dorsally in the *Pdn/Pdn* LGE. This also leads to abnormalities in the establishment of the PSPB with a dorsal shift and an expansion of the ventral pallium domain as revealed by *Gsh2, Dlx2 and Dbx1* expression.

Changes in *Shh* expression and signalling may explain these regionalization defects in the *Pdn* ventral telencephalon. Removal of *Shh* from E8.5 telencephalic primordium using *Foxg1/Cre* results in a loss of ventral telencephalic tissues, suggesting an early requirement for *Shh* in patterning of the ventral telencephalon (Chiang et al., 1996; Fuccillo et al., 2004; Zhang et al., 2001). However, removal of *Shh* between E10.5 and E12.5 using *Nestin/Cre* has only limited effects on the ventral telencephalon, suggesting that ventral telencephalic expression of *Shh* has a role in maintaining the expression of ventral telencephaic genes, rather than promote ventral telencephalic fate, at later stages of development (Machold et al., 2003; Xu et al., 2005).

However, it has been proposed that, in the ventral telencephalon, *Shh* functions to prevent the excessive production of *Gli3* repressor. Indeed, as mentioned before, ventral

patterning is re-established in *Shh/Gli3* double mutants. Moreover, ectopic expression of *Shh* in the dorsal telencephalon results in the induction of ventral markers and in the repression of dorsal markers (Rallu et al., 2002). This suggests that *Shh* may play a role in fate specification of ventral telencephalic structures. Further evidence of the importance of Shh signalling in patterning the ventral telencephalon at later stages of development comes from the analysis on *pan-Gli* mutants in which *Gli2* and *Gli3* have been inactivated (Yu et al., 2009a). *Shh* signalling is mediated by *Gli* transcription factors, including *Gli3*, but also by *Gli1* and *Gli2* (Fuccillo et al., 2006a; Ingham and McMahon, 2001). They can all act to activate *Shh* target genes in the ventral telencephalon (Fuccillo et al., 2006a; Hooper and Scott, 2005; Ingham and McMahon, 2001). Although no obvious defects were previously found in the ventral telencephalon of individual *Gli1* and *Gli2* single or *Gli1/2* double mutatnts (Park et al., 2000), a more accurate look at ventral telencephalic regionalization shows that *Nkx2.1* and *Nkx6.2* expression are lost in two subgroup of progenitors in the sulcus between the LGE and the MGE (Yu et al., 2009a). In addition, the PSPB of *Gli2/3* double mutants, in which Shh signalling is interrupted, displays a dorsal expansion of *Gsh2* and *Dlx2* expression in the ventral pallium and lateral cortex (Yu et al., 2009a).

Recent work has shown that the *Gli3* repressor form is more abundant in the dorsal rather than in the ventral telencephalon, but this analysis did not discriminate between the MGE and the LGE (Fotaki et al., 2006). Our results provide new insights into the role of *Gli3* in the ventral telencephalon and its interaction with *Shh*, showing that *Gli3* is required to repress *Shh* expression and Shh signalling within the ventral telencephalon, and that this interaction is important to repress more ventral fates in the

LGE and at the PSPB. Therefore, the LGE may require a higher activity of the Gli3 repressor form than the MGE to counteract *Shh* for its correct patterning. However, the lack of antibodies distinguishing the Gli3 activator and the Gli3 repressor forms makes this hypothesis difficult to test. The fact that the LGE and PBSP are affected while no defects are found in the MGE of *Pdn* mutants may be explained by the fact that *Gli2* may compensate for a potential reduction of the Gli3 activator form in the *Pdn* mutants (Yu et al., 2009a). It is also possible that although in the *Pdn* mutation *Gli3* is generally reduced, the reduction of the Gli3 activator form in ventral telencephalon is less severe because it is prevented by *Shh* upregulation. Again, a Gli3 western blot may help verify this possibility.

Nevertheless, these data further support an involvement of *Shh* in controlling the specification of distinct progenitors and the regionalization of different progenitor domains in the ventral telencephalon, via the Gli proteins, and not only to maintain ventral gene expression. This also happens in other ventral regions of the neural tube. For example, during spinal cord development 2-fold up regulation of Shh is sufficient to induce cell fate changes (Persson et al., 2002).

The ventral telencephalic regionalization defects in *Pdn/Pdn* mutants are also supported by a reduced number of $Pax6^{+}$ and *Six3* expressing cells of the migratory stream. Because *Pdn/Pdn* $Pax6^{+}$ and *Six3* expressing cells are still able to migrate ventrally, the *Pdn* mutation seems more likely to affect the production of these cells rather than their ability to migrate. In these respects, *Pax6* and *Six3* analyses also suggest differentiation and/or proliferation defects within the *Pdn/Pdn* LGE. The possibilities of growth defects in the *Pdn/Pdn* ventral telencephalon are discussed in the following section.

### 5.7.4 *Pdn* mutation causes growth defects in ventral telencephalon

Patterning defects may also include defects in cell proliferation and neuronal differentiation in the *Pdn/Pdn* LGE. Indeed, at E10.5 and E11.5 the *Pdn/Pdn* LGE mantle displays a reduction in the number of post-mitotic neurons as observed using Tuj1 immunostaining. This abnormality also leads to a reduction in the size of the *Pdn/Pdn* LGE. We therefore explored the causes that may lead to the reduction in the number of neurons within the *Pdn/Pdn* LGE, such as increased apoptosis, abnormal cell proliferation and/or cell cycle defects. Interestingly, we did not observe differences in the number of apoptotic cells in the *Pdn/Pdn* ventral telencephalon that could have led to a reduction of differentiated neurons, nor did we observed a reduction in the number of mitotic cells. However, we observed an elongation of the cell cycle length of proliferating cells specifically in the *Pdn/Pdn* LGE, but not in the MGE. The slower cell cycle rate may explain the reduced number of *Pdn/Pdn* LGE post mitotic neurons.

However, slower progression through the cell cycle and reduced production of neurons not seem to explain the absence of change in the number of cells undergoing mitosis (revealed by pHH3 staining). Indeed, the slower cell cycle should result in a reduction of $Tuj1^{+}$ neurons (which we actually observe), but also in a reduction of $pHH3^{+}$ cells (which we do not observe). This could be solved by assuming that the proportion of proliferating cell is higher in the *Pdn/Pdn* LGE compared to wild type. Therefore, even if LGE proliferating cells progress at a slower rate through the cell cycle, a higher number of them in the *Pdn/Pdn* LGE would produce the same number of mitotic cells,

when compared to wild-type. To verify this hypothesis it would be necessary to know the total number of mitotic cell in the *Pdn/Pdn* LGE. However, this analysis would be extremely complicated, because it would be very difficult to accurately define the dorsal limit of the *Pdn/Pdn* LGE, because of the described regionalization defects. Nevertheless, upregulated *Shh* expression and *Shh* signalling provide a very good explanation for the growth defects in the *Pdn/Pdn* LGE. Indeed, a very recent paper has shown that interrupting *Shh* signalling in the ventral telencephalon by knocking out *Gli2* and *Gli3* results in defects in the production of ventral telencephalic neurons, shown by a reduction in the number of $Tuj^{+}$ and *Lhx6* and *Ebf1* expressing cells in the mantle of *Gli2/3* double mutant MGE and LGE (Yu et al., 2009b). This result is intriguingly similar to what is observed in the ventral telencephalon of *Pdn* mutants.

In addition, *Shh* has been shown to act as a mitogen and to induce proliferation in neural and non-neural tissues (Kenney et al., 2003; Kenney and Rowitch, 2000; Oliver et al., 2003; Rowitch et al., 1999). Another example for a role of *Shh* in regulating proliferation is provided by the fact that uncontrolled activity of *Ptc1* and therefore ectopic activation of *Shh* signalling is a predisposition for basal cell carcinomas and for medulloblastoma in Gorlin's syndrome patients (Goodrich et al., 1997). It seems that the time of exposure to *Shh* can produce different outcomes. This is because the ability of proliferating cells to respond to *Shh* depends on their proliferative state. For example, *Shh* ectopic expression in the E12.5 dorsal spinal cord increases proliferation causing hyperplasia, but does not have any effect at E18.5 (Rowitch et al., 1999). In this work it is also shown that, at E12.5, increased cell proliferation results in an expansion of the spinal cord ventricular region, with proliferating cells being locked in a proliferating

state and failing to undergo differentiation, as revealed by the absence of post-mitotic neurons in the mantle region (Rowitch et al., 1999). Intriguingly, this result is very reminiscent to what was observed in the developing *Pdn/Pdn* LGE, where *Shh* expression and *Shh* signalling upregulation coincides with the decision of neural progenitor cells to preferentially remain in a proliferating state rather than to differentiate.

A recent study has also shown that *Shh* controls cell cycle progression and neural fate specification of neural progenitors in the embryonic mouse retina (Sakagami et al., 2009). In addition, before E9.5, *Shh* is required for proliferation in the mid/hindbrain (Blaess et al., 2006). Recent work has also linked *Shh* activity in the cerebellum with the transcriptional activation of genes implicated in cell cycle processes like *N-myc, cyclin D1, E2f1* and *E2f2* (Kenney et al., 2003; Oliver et al., 2003).

Our study may further emphasize a direct role for *Shh* in controlling the cell cycle of proliferating cells in the telencephalon, which has been previously only indirectly hypothesized by the observation of a size reduction of the telencephalon of $Shh^{-/-}$ mutants. It would be interesting to know if the *Pdn* mutation leads to change in expression of genes controlling the cell cycle progression.

Another role of *Shh* in regulating tissue growth is by controlling cell death. Apoptosis is increased in the spinal cord, diencephalon and midbrain in *Shh* null mutants (Chiang et al., 1996; Ishibashi and McMahon, 2002; Litingtung and Chiang, 2000a). This effect can be repressed by removing *Gli3,* which also suggests that the *Gli3* repressor form can control apoptosis at least in the spinal cord (Babcock, 1984; Blaess et al., 2006; Litingtung and Chiang, 2000b). However, no changes were observed in the number of

apoptotic cells in the *Pdn/Pdn* ventral telencephalon when compared to wild type, showing that this is not the case in the ventral telencephalon, at the ages examined.

A previous studies on $Xt^{j}/Xt^{j}$ mutants investigated the role of *Gli3* within the ventral telencephalon (Yu et al., 2009a). However, the approach and the results differed slightly from the results obtained here. The $Xt^{j}/Xt^{j}$ mutants displaed an increase in the number of differentiated cells within the ventral telencephalon, which was not reflected by defects in the cell cycle time as observed in *Pdn/Pdn* mutants. However, in this study the LGE was not separately analised from the MGE. This and the more severe $Xt^{j}/Xt^{j}$ phenotype may explain the difference between the work of Tian et al. (2009) and the present sudy.

### 5.7.5 LGE pioneer neurons defects may be causing thalamocortical tract abnormalities in *Pdn/Pdn* brains

The *Pdn/Pdn* ventral telencephalon appears to lack retrogradely labelled LGE pioneer neurons. Ventral telencephalic pioneer neurons form transiently in the E12.5 LGE and project axons towards the cortex. At E14.5, soon after corticofugal axons have entered the LGE, it is no longer possible to detect their cell bodies by retrograde labelling in wild type embryos. LGE pioneer neurons are thought to be important to guide corticofugal axons from the developing cortex to enter the ventral telencephalon (Metin and Godement, 1996). However, there is no direct evidence for their role as corticofugal intermediate targets. In addition, the study of ventral telencephalic pioneer neurons is complicated by the fact that there are no markers available that discriminately label them. Consequently, the only way to reveal their presence is to inject carbocyanine dye

within the developing cortex at E12.5. The *Pdn* mutation is the first known mutation to cause the absence of DiI retrogradely labelled LGE pioneer neurons. However, the absence of back-labelled neural cell bodies in *Pdn/Pdn* LGE could be caused either by their absence or by their inability to project axons towards the developing cortex. The lack of markers, however, makes it difficult to distinguish between these possibilities. Further experiments are needed to investigate the nature of LGE pioneer neuron defects in *Pdn/Pdn* brains, but this will be discussed in the next section (chapter 6). Indeed, bases on the experiments described in this thesis both of these hypotheses are still possible. The *Pdn/Pdn* LGE proliferation defects resulting in a reduction of the number of post-mitotic neurons may also result in a reduction of the production, or in the absence of LGE pioneer neurons. This would mean that LGE pioneer neurons originate within the LGE. Experiments necessary to definitively address this possibility will be proposed in the next section (chapter 6). This would also mean that differentiation defects might differentially affect the neural populations originated in the *Pdn/Pdn* LGE. This is true, for example, for corridor cells and for cells of the lateral cortical stream, which both originate in the LGE. However, the *Pdn/Pdn* LGE is largely positive for the corridor cell marker *Ebf1* (chapter 4). In contrast, *Pdn/Pdn* mutants display a reduction in the number of $Pax6^{+}$ and *Six3* expressing lateral cortical stream cells (this chapter).

Alternatively, the *Pdn* mutation may also affect the capacity of pioneer neurons to project their axons towards the developing cortex. Indeed, the *Pdn/Pdn* PSPB is shifted dorsally, and therefore the region in which pioneer axons have to navigate is not immediately adjacent to them. This may increase the distance over which pioneer axons have to navigate and/or may affect the response to hitherto unknown attractive

molecules expressed in the cortex and important to guide pioneer axons across the PSPB.

Finally, the fact that the *Pdn/Pdn* LGE progenitor cells display a slower cell cycle, may lead to a developmental delay in the formation of pioneer neurons, which could still form but at later stages of development. However, this possibility seems to be more unlikely because at E14.5 it is still not possible to detect any retrogradely labelled pioneer cell bodies in the *Pdn/Pdn* LGE. In addition *Pdn/Pdn* corticofugal axons do not enter the ventral telencephalon until after E16.5.

Alternatively, the observed defects in the formation of the *Pdn/Pdn* PSPB may directly affect the navigation of corticofugal axon entering the ventral telencephalon, with *Pdn/Pdn* cortical axons following a 'default pathway' along the PSPB (Molnar & Butler, 2002 and Molnar & Blakemore, 1995).

These two possibilities (the absence of *Pdn/Pdn* LGE pioneer neurons and defects in the formation of the *Pdn/Pdn* PSPB causing the failure of *Pdn/Pdn* cortical axons to enter the venral telencephalon) are not mutually exclusive. However, it is possible that the DiI injected in the E12.5 cortex labelled growth cones of cortical axons (Molnar et al., 1998 and Molnar and Cordery, 1999) and not LGE pioneers, making the 'default pathway' hypothesis the only explanation for the impairment of *Pdn/Pdn* cortical axons to enter the ventral telencephalon. Althought this possibility is unlikely; it would be necessary to stain the E12.5 DiI injected brains with the nuclear marker TO-PRO, to definitively confirm the colocalization of DiI backlabelled cells and TO-PRO$^{+}$ chromatin in the LGE.

Nevertheless, this work emphasizes the importance of LGE pioneer neurons in guiding corticofugal axons towards the ventral telencephalon: defects in their formation and/or in their ability to project axons towards the cortex provide an excellent explanation for the failure of corticofugal axons to pass over the PSPB. These data also suggest novel roles for *Gli3* and *Shh* in the ventral telencephalon: their counteraction is necessary to correctly specify ventral telencephalic intermediate targets for corticofugal axons.

# Chapter 6: General discussion and future work

In this study, I have particularly focused on the mechanisms underlying the defective development of the thalamocortical and corticothalamic tracts in the *Gli3* hypomorphic mutant *Pdn*. Different experimental approaches were combined to dissect the primary defects in the *Pdn/Pdn* thalamocortical and corticothalamic tracts caused by the *Pdn* mutation. The use of the *Gli3* hypomorphic mutant *Pdn* provided the advantage to attenuate the severe regionalization defects observed in the *Gli3* null mutants $Xt^J$. The more subtle anatomical defects in *Pdn* mutants allowed a detailed study of the cellular interactions between *Pdn/Pdn* cortical and thalamic axons and the environment in which they have to navigate.

## 6.1 The *Pdn* mutation does not result in severe defects in the developing cortex and thalamus

*Pdn* mutants do not display severe defects in the formation of the cortical layers and in the patterning of the dorsal thalamus. Corticofugal neurons and their axons form normally in the *Pdn/Pdn* cortex, but their axons only enter the ventral telencephalon with a delay of several days. In contrast, *Pdn/Pdn* thalamic axons make guidance mistakes only after they have entered the *Pdn/Pdn* ventral telencephalon. Primary defects in thalamic and cortical neurons and their axons may cause these defects.

However, we did not observe defects in the patterning of the *Pdn/Pdn* thalamus. In addition, *Pdn/Pdn* thalamic axons behave relatively normally once transplanted in the wild type ventral telencephalon, responding normally to guidance cues and projecting along the internal capsule. This suggests that the great majority of *Pdn/Pdn* thalamic axons are in general able to respond to guidance cues present in the wild-type ventral telencephalon. In some explant experiments, a small population of *Pdn/Pdn* thalamic axons was observed to grow along alternative routes into the wild-type ventral telencephalon. This behaviour was not observed in control experiments, and may indicate that the *Pdn* mutation may affect the ability of a small sub-population of thalamic neurons to correctly project their axons in the ventral telencephalon. It would be interesting to know whether the *Pdn* mutation results in changes of expression in guidance receptors important for thalamic axons to navigate through the ventral telencephalon, such as *Sema6a*. Why *Sema6a* is a good candidate for the thalamocortical defects observed in *Pdn* mutants will be discussed in greater detail later (chapter 6.3). Nevertheless, the analysis of *Gli3* conditional knockouts would help to clarify the cell-autonomous capacity of *Gli3* mutant thalamic axons to navigate towards the cortex. Mutant mice containing a $Gli3^{flox}$ allele became recently available (Blaess et al., 2006). It would be very interesting to cross this line with mouse lines in which the *Cre* enzyme is specifically expressed in the dorsal thalamus, using the *RoR-α/Cre* (unpublished). In *RoR-α/Cre* animals, the expression of the Cre enzyme is driven under the control of regulatory elements of the *RoR-α* gene, which is expressed in most regions of the dorsal thalamus (unpublished).

Nevertheless, our data strongly suggest that *Pdn/Pdn* dorsal thalamic neurons and their axons are not affected and that guidance mistakes are more likely to be caused by abnormalities in the ventral telencephalon. Indeed, in mutant mice in which the development of the dorsal thalamus is affected, thalamic axons transplanted in wild-type ventral telencephalon reproduce their *in vivo* guidance mistakes. This is the case for example in *Pax6*$^{sey/sey}$ mutant mice, in which thalamocortical axons do not enter the ventral telencephalon *in vivo* and *in vitro* when transplanted into the wild-type ventral telencephalon (Pratt et al., 2000a). On the contrary, destruction of ventral telencephalic intermediate guidance cues affects the navigation of wild-type thalamic axons *in vitro* (Lopez-Bendito et al., 2006).

The failure of *Pdn/Pdn* cortical axons in entering the ventral telencephalon could also be caused by defects in *Pdn/Pdn* cortical projecting neurons themselves and/or in *Pdn/Pdn* cortical subplate neurons pioneering the corticothalamic tract. However, the *Pdn/Pdn* cerebral cortex does not display defects in the cortical lamination process, in contrast to more severely affected *Gli3* mutant mice, such as *Xt*$^{J}$*/Pdn* and *Xt*$^{J}$*/Xt*$^{J}$ (Friedrichs et al., 2008; Theil, 2005). In addition, the use of the *Pdn Golli tau-GFP* mouse line revealed that the first projecting *Pdn/Pdn* corticofugal neurons and their axons are formed normally. The *Pdn/Pdn* GFP$^{+}$ cortical axons however, are delayed several days in entering the ventral telencephalon, and cortical axons appear to project along the PSPB. It is still possible that *Pdn/Pdn* early projecting cortical neurons once they form do not express the correct guidance receptors important for their entry into the ventral telencephalon. This hypothesis has not been fully tested yet. To do that it would be

interesting to perform slice culture experiments in which *Pdn/Pdn τ-GFP* cortical explants are transplanted in wild-type cortex.

Therefore, based on the data presented here, it is possible that the failure of early projecting *Pdn/Pdn* cortical axons could be due to a combination of cell-autonomous defects in subplate and cortical plate neurons, but also due to defective LGE pioneer neurons, as discussed in the next section. The analysis of *Gli3* conditional knockouts would help to better clarify these not mutually exclusive possibilities. It would be very interesting to cross $Gli3^{flox}$ line with mouse lines in which the *Cre* enzyme is specifically expressed in the LGE or in the cerebral cortex, using the *Gsh2/Cre* and the *Emx1/Cre* mouse lines, respectively (Kessaris et al., 2006; Young et al., 2007). The causes of *Pdn/Pdn* thalamocortical guidance mistakes in the ventral telencephalon are discussed separately in the section 6.3.

## 6.2 Ventral telencephalic patterning defects in *Pdn* mutants correlate with defects of LGE pioneer neurons, and failure of cortical axons in entering the ventral telencephalon

The ventral telencephalon is now regarded as a source of intermediate guidance cues for the formation of the thalamocortical and corticothalamic tracts and its formation is controlled by a great number of transcription factors expressed in different patterns in the subpallial regions, such us *Pax6, Mash1, Ebf1, Emx2, Nkx2.* and *Dlx2* along the path thalamic and cortical axons have to navigate (Bishop et al., 2000; Hevner et al., 2002;

Jones et al., 2002; Lopez-Bendito et al., 2002; Mallamaci et al., 2000; Pratt et al., 2000b; Tuttle et al., 1999). Some of these genes are also expressed in the cortex and/or thalamus, for example *Pax6, Tbr1, Ngn2, Ebf1, Emx2* while others are only expressed in the thalamus or in the cortex, like *Gbx2* and *Emx1* respectively (Bishop et al., 2000; Hevner et al., 2002; Jones et al., 2002; Lopez-Bendito et al., 2002; Mallamaci et al., 2000; Pratt et al., 2000b; Tuttle et al., 1999). Interestingly, mice mutant for *Gbx2* and *Emx1* display defects in the formation of both the corticothalamic and thalamocortical tracts (reviewed in (Lopez-Bendito and Molnar, 2003). Therefore, cortical and thalamic axons require the correct expression of transcription factors not only in cortex and thalamus but also in territories along which they have to navigate. However, it is difficult to interpret the data coming from the analyses of these mutants. It is not clear yet to which extent defects in the axonal tracts of these mutants are dependent on defects in thalamic and cortical neurons themselves and/or on abnormalities in the territories in which these axons have to navigate. Nevertheless, they have provided precious tools to dissect the cellular and molecular mechanisms underlying the formation of these two tracts.

The *Pdn* mutation results in an upregulation of *Shh* expression and *Shh* signalling in the *Pdn/Pdn* ventral telencephalon, leading to partial ventralization of the *Pdn/Pdn* CGE and a dorsal shift of the *Pdn/Pdn* PSPB. In addition the mantle region of *Pdn/Pdn* LGE is reduced in size. This is due to an elongation of cell cycle length of *Pdn/Pdn* LGE neural progenitors leading to a reduced number of neurons in the *Pdn/Pdn* LGE. *Gli3* has already been proposed previously to antagonize *Shh* function (Rallu et al., 2002). In

addition, *Gli3* can function as a transcriptional activator in the presence of *Shh (Bai et al., 2004; Wang et al., 2007)*, and as a transcriptional repressor in the absence of *Shh* (Aoto et al., 2002; Fotaki et al., 2006; Kuschel et al., 2003; Rallu et al., 2002; Tole et al., 2000b). Indeed, it is probably the ratio between Gli3 repressor and activator forms, which would be higher in the dorsal telencephalon where *Shh* is not expressed and lower in the ventral telencephalon where there is *Shh* expression, which is important for the patterning of the telencephalon (Fotaki et al., 2006). Therefore, it is likely to be the Gli3 repressor form that counteracts *Shh* function. Here we show that Gli3-Shh counteraction in the ventral telencephalon represses ventral fate within the LGE and PSPB. Therefore it possible that the ratio between Gli3 repressor and activator forms is affected in different territories of the *Gli3* hypomorphic mutant *Pdn.* However, the reduction of *Gli3* may not be sufficient to cause severe defects in cortex and thalamus of the *Pdn* mutants, but in the ventral telencephalon this sums up with *Shh* and Shh signalling upregulation making this region the most affected. As mentioned before, the lack of *Gli3* antibodies working in immunohistochemistry makes this hypothesis difficult to verify. However, it would be possible to investigate the ratio of the Gli3 repressor and activator forms in dorsal and ventral telencephalon, and probably even in LGE and MGE, using Gli3 western blot analyses as described in (Fotaki et al., 2006).

Interestingly, patterning abnormalities in the *Pdn/Pdn* LGE correlate with the absence of DiI back-labelled LGE pioneer neurons. Defects in the formation and or projections of the pioneer neurons in the *Pdn/Pdn* LGE may explain why *Pdn/Pdn* corticothalmic axons do not enter the ventral telencephalon. The importance of pioneer neurons is well established in several regions of the forebrain. Pioneer neurons are the first to project

their axons along several axonal pathways, guiding later arriving axons and starting the formation of the tracts. They are transient neurons, and normally disappear at later stages of development once their guidance function has finished. For example, pioneer neurons in the most medial cortical region, the cingulate cortex, are necessary for callosal axons coming from more lateral regions to cross the midline (Koester and O'Leary, 1994; Piper et al., 2009; Rash and Richards, 2001). Also, subplate neurons guide the later projecting corticofugal axons into the internal capsule (De Carlos and O'Leary, 1992; McConnell et al., 1989).

Indeed, chemical ablation of subplate pioneer neurons with the use of the neurotoxin kainic acid results in defects of cortical axons invading their sub-cortical targets without destroying the deep cortical layer neurons (McConnell et al., 1994). Cortical subplate neurons have also been suggested to provide scaffolds and to guide incoming thalamocortical axons, with their ablation resulting in defects in thalamic axons in reaching their cortical target (Blakemore and Molnar, 1990; Ghosh et al., 1990; Ghosh and Shatz, 1993; Molnar and Blakemore, 1995). Finally, a nearly complete absence of back-labeled MGE pioneer neurons has been observed in *Lhx2* mutant mice. This correlates with a failure of $Lhx2^{-/-}$ thalamocortical axons to enter the ventral telencephalon (Lakhina et al., 2007).

However, as discussed in the previous chapter the causes of the absence of back-labelled LGE pioneer neurons are not completely clear. The fact that the *Pdn/Pdn* LGE displays a reduced number of neurons seems to suggest that *Pdn/Pdn* pioneer neurons are reduced too, or do not form at all. Indeed, upregulation of Shh signalling in the *Pdn/Pdn* ventral telencephalon may result in a misspecification of these neurons, as in the spinal

cord, where a 2-fold *Shh* upregulation results in a fate change (Persson et al., 2002). Alternatively, the dorsal shift of the *Pdn/Pdn* PSPB may result in an increased distance between these pioneer neurons and the territory in which they have to project their axons, causing a failure of pioneer axons to enter the *Pdn/Pdn* cortex. The lack of specific molecular markers for these pioneer neurons makes these hypotheses difficult to verify. Another open question concerning the LGE pioneer neurons is their anatomical origin. The analyses of the defects in the *Pdn/Pdn* LGE seem to suggest that they originate from the LGE. However, LGE pioneer neurons could be born in other brain regions, such as the MGE, and subsequently migrate into the LGE. An interesting experiment to investigate they anatomical origin could be done with the use of a *Gsh2/Cre/yellow fluorescent protein (YFP)* reporter mouse line. In *Gsh2/Cre* animals the expression of the Cre enzyme is driven in the LGE from E10.5 under the control of regulatory elements of the *Gsh2* gene. In the YFP reporter mice there is a *stop codon* flanked by two *LoxP* sites upstream of the YFP gene (Srinivas et al., 2001). The expression of Cre removes the *stop codon* and activates expression of the YFP. YFP expression therefore marks all cells derived from the *Gsh2* progenitor region. The injection of DiI in the cortex of E12.5 *Gsh2/Cre/YFP* embryos would reveal whether pioneer neurons originate in the LGE, indicated by the co-localization of the DiI back-label and YFP.

## 6.3 Thalamocortical tract defects in *Pdn* mutants are caused by abnormalities in ventral telencephalic guidance cues

The defects in the *Pdn/Pdn* thalamocortical tracts are more heterogeneous than those observed in *Pdn/Pdn* corticothalamic tract. First, *Pdn/Pdn* thalamocortical axons pass over the DTB entering the ventral telencephalon in accordance with the presence of DiI back-labelled MGE pioneer neurons. Subsequently, however, in the caudal part of the tract *Pdn/Pdn* thalamic axons project ventrally, not entering the internal capsule. Rostrally in the tract, *Pdn/Pdn* thalamic axons navigate through the MGE but they display guidance mistakes in more dorsal regions of the *Pdn/Pdn* ventral telencephalon. Therefore, several different defects may affect the migration of *Pdn/Pdn* thalamic axons through the ventral telencephalon.

The causes of these guidance defects in the rostral part of the tract could be multiple. It is possible for example that thalamocortical axons are not guided towards the *Pdn/Pdn* cortex, because the pathway is not pioneered by *Pdn/Pdn* subplate cortical axons, which, as discussed above, may be defective. Alternatively, because *Pdn/Pdn* cortical axons do not enter the ventral telencephalon they cannot meet incoming *Pdn/Pdn* thalamic axons, and therefore cannot guide them into the cortex. However, it is also possible that the dorsal shift and the expansion of the *Pdn/Pdn* PSPB may affect *Pdn/Pdn* thalamic axons in entering the cortex, in the same way that it could affect the axonal projections of LGE pioneer neurons. Indeed, the PSPB as well as the DTB are critical points for the

navigation of thalamic and cortical axons. Axons approaching or surpassing these boundaries change their growth kinetics and their fasciculation properties. For example thalamic axons strongly fasciculate once they have passed over the DTB in order to enter the internal capsule, while cortical axons pause for few days after they navigate through the PSPB (reviewed in (Lopez-Bendito and Molnar, 2003; Price et al., 2006). Several mice, mutant for genes important in the establishment of these boundaries, display defects in the navigation of thalamocortical and corticothalamic axons (Garel and Rubenstein, 2004; Hammerschmidt et al., 1997; Hevner et al., 2002; Jones et al., 2002; Lopez-Bendito et al., 2002). Defects in the expression of genes around these boundaries do not only cause guidance defects, but may also stop axonal progression over the adjacent territory (reviewed in (Lopez-Bendito and Molnar, 2003; Price et al., 2006). The analysis of the thalamocortical and cortiothalamic tracts in *Gli3* conditional mutants may better clarify these different possibilities. In addition, it would be interestingly to delete *Gli3* expression from the ventral pallium, crossing the $Gli3^{Flox}$ line with a *Dbx1/Cre* mouse line (Fogarty et al., 2005).

The analysis of *Pdn* mutants may help to test the "hand-shake" hypothesis. This hypothesis postulates that cortical axons extend over the PSPB, and later arriving thalamocortical axons contact cortical projections and use them to enter the cortex (Molnar et al., 1998; Molnar and Blakemore, 1995). In E14.5 *Pdn/Pdn* mutants, cortical axons do not pass over the PSPB but project along it. In addition, thalamocortical axons do not project towards the PSPB, but make guidance mistakes in dorsal regions of the *Pdn/Pdn* LGE. Interestingly, however, in the caudal part of the thalamocortical tract, *Pdn/Pdn* thalamic axons project ventrally in the MGE invading the amygdaloid region.

At P0, however, although several *Pdn/Pdn* cortical axons are still projecting along the PSPB, several of them eventually enter the ventral telencephalon, projecting towards the diencephalon. A great number of *Pdn/Pdn* corticothalamic axons also enter the ventral telencephalon from more ventral regions along the PSPB. Finally, several *Pdn/Pdn* cortical axons reach the amygdaloid region and subsequently project towards the diencephalon, entering the ventral telencephalon from very ventral regions. These trajectories of axonal projections seem to coincide with the trajectory mistakes of *Pdn/Pdn* thalamocortical axons. This would also mean that cortical axons are more dependent on the guidance of thalamocortical axons. Indeed, *Pdn/Pdn* thalamic axons are the first to make ventral telencephalic mistakes and are subsequently followed in their alternative route by later arriving *Pdn/Pdn* cortical axons. It would be interesting to further investigate this hypothesis with the use of mouse lines in which cortical and thalamic axons are selectively labelled with GFP and, for example, an alkaline phosphatase enzyme (AP), such as *golli tau-GFP* and *RoR-α/Cre/AP* (a *stop codon* flanked by two *LoxP sites* would be upstream of the AP gene), respectively, generating *Pdn/Pdn Golli tau-GFP RoR-α/Cre* (gift form O' Leary's lab) *AP* embryos at different stages of embryonic development.

Also, the use of *Pdn/Pdn* mutants in a slice culture experiment may provide new insights on the interaction between thalamocortical and corticothalamic projections to guide each other at early steps of brain development. Indeed, at E13.5 it is possible to separate the thalamocortical and corticothalamic tracts in living brain sections, by a $45^{O}$ cut in the ventral telencephalon along the trajectory of thalamic and cortical axons. This results in

the production of two hemi-sections, one containing the whole thalamocortical tract and another containing the whole corticothalamic tract. This is possible because at E13.5 thalamic and cortical axons have not met yet in the ventral telencephalon and they are still growing towards each other. By combining wild-type hemi-sections containing the whole corticothalamic tract with *Pdn/Pdn τ-GFP* hemi-sections containing the whole thalamocortical tract, it would be possible to test whether wild-type cortical axons have the ability to recover the growth of *Pdn/Pdn* thalamic axons into the cortex.

The thalamocortical tract rotates by 90 $^{O}$ during its course from the dorsal thalamus to the cortex. Indeed, thalamic neurons arranged in dorso-ventral fashion in the dorsal thalamus connect their axons with neurons arranged in a caudal-rostral fashion into the cortex. This twist occurs in the ventral telencephalon when thalamic axons navigate through the internal capsule and happens before the differentiation of thalamic nuclei has taken place (Molnar et al., 1998; Molnar and Blakemore, 1995). In addition, in mutant mice in which the antero-caudal organization of the cortex is disrupted or shifted, such as *Emx2* (Hamasaki et al., 2004), *Pax6* (Bishop et al., 2000) and *Fgf8* mutants (Fukuchi-Shimogori and Grove, 2001b; Fukuchi-Shimogori and Grove, 2003), the topographic organization of thalamic axons as they exit the internal capsule is not affected (reviewed in(Garel and Rubenstein, 2004). Altogether, these studies have shown that the early topographic organization of thalamocortical axons happens in the ventral telencephalon, and does not depend on cues within the dorsal thalamus and/or the developing cortex. For example in *Ebf1*-knockout and Dlx1/2-double mutant mice, with no obvious defects in the patterning of the dorsal thalamus and shifts of gene

expression in the cerebral cortex, thalamic axons coming from the dLGN do not reach the putative visual cortex (Garel et al., 2002). Instead, they miss-project ventrally in the ventral telencephalon in the direction of the amygdaloid region, coinciding with a disorganization of ventral telencephalic territories in these mutants (Garel et al., 2002). These defects are strikingly similar to the navigation defects observed in the thalamocortical tracts of *Pdn/Pdn* mutants. In addition, as discussed before (chapter 3) it is very likely that the ectopic ventral branch, in the *Pdn/Pdn* ventral telencephalon, is coming from the dLGE. To test this hypothesis it would be interesting to inject DiI into the amygdaloid region of the *Pdn/Pdn* mutants, back-labeling the neural cell bodies in the dorsal *Pdn/Pdn* thalamus of neurons abnormally projecting their axons in this region and prematurely leaving the internal capsule. This defect is very similar to what happens to thalamocortical axons in *Ebf1* and *Dlx1/2* mutants (Garel et al., 2002). Also, in *Pdn* mutants, these axonal defects coincide with the disorganization of *Pdn/Pdn* ventral telencephalic intermediate guidance cues important for the navigation of thalamic axons. Indeed, the *Pdn/Pdn* ventral telencephalon shows abnormalities in the formation of the permissive $Isl1^{+}$ corridor cells (Lopez-Bendito et al., 2006). Interestingly, *Ebf1* in situ hybridization and Isl1 immunostaining show that the corridor cells form and migrate ventrally from the *Pdn/Pdn* LGE to the MGE. However, their distribution is affected, and $Isl1^{+}$ cells form a broader corridor and show a more diffuse distribution pattern within the *Pdn/Pdn* MGE mantle, globus pallidus and preoptic area. It is conceivable that their migration pattern is not specified correctly, as these cells are derived from the LGE, the patterning of which is severely affected in *Pdn*/*Pdn* embryos.

Interestingly however, in this study a new *Gli3* expression domain was found, which

seems to localize in the globus pallidus in the MGE mantle region. This region contains neurons, suggesting a possible role for *Gli3* in differentiated neurons. Therefore, the MGE mantle may control the correct migration of corridor cells in more ventral regions, and the *Pdn/Pdn* MGE mantle cells may fail in doing that. This may affect the correct navigation of *Pdn/Pdn* thalamic axons in the internal capsule as well as their topographic organization. Again, a conditional-knockout strategy may help to clarify these different possibilities, by crossing for example the $Gli3^{flox}$ mouse line with a *Nkx2.1/Cre* line, and selectively inactivating *Gli3* in MGE (Fogarty et al., 2005; Kessaris et al., 2006)

*Gli3* may also have a role in controlling the expression of thalamocortical guidance molecules in the mantle region of the MGE. A number of guidance molecules have been shown to be important for the guidance of thalamocortical axons in the ventral telencephalon, including cadherins, ephrins and Eph receptors, neurotrophins, netrin 1 and semaphorins (reviewed by(Lopez-Bendito and Molnar, 2003). As it would be time consuming to test the expression pattern of all these different guidance molecules in the *Pdn/Pdn* telencephalon, some of them are good candidates to explain the thalamic axonal defects in *Pdn/Pdn* brains, and are worth further investigations. Recently, interesting defects heve been reported in the development of the thalamocortical tract of *Sema6a* mutant mice (Leighton et al., 2001; Little et al., 2009). In these embryos, a great fraction of dLGN axons project ventrally in the ventral telencephalon in the direction of the amygdaloid region (Leighton et al., 2001). This effect is very reminiscent of the thalamocortical phenotype observed in *Pdn* mutant brains. In addition, the expression pattern of *Sema6a* in ventral telencphalon seems to coincide with the *Gli3* MGE mantle expression domain. This would still need to be checked with the combination of an in

situ hybridization for *Gli3* together with an immunostaining for *Sema6a*.

This study also shows the enormous plasticity of the thalamocortical tract (Little et al., 2009). Because *Sema6a*$^{-/-}$ mutant mice survive, it was possible to observe that thalamic axons coming from the dLGN eventually reach their target area and form appropriate connections with the visual cortex but get to the cortex along abnormal routes in the ventral telencephalon, which they have taken at early stages of their development. In addition, by injecting DiI into the amygdaloid region of *Sema6a*$^{-/-}$ mutants it was possible to observe back-labelled cortical neurons in the visual cortex. This suggests that visual cortical axons and their reciprocal dLGN thalamic axons intermingle in the amygdaloid region (Little et al., 2009). Once again this phenotype seems to be very similar to what is hypothesized to happen to the thalamocortical and corticothalamic axons in *Pdn/Pdn* brains. Unfortunately, *Pdn/Pdn* animals die at birth, and the extent of which the *Pdn/Pdn* thalamocortical and corticothalamic tracts recover their connections cannot be investigated. However, the use of a *Gli3* ventral telencephalic conditional knockout may again provide a good tool to further investigate this possibility.

## 6.4 Synopsis

In this last section I would like to propose a model to explain the thalamocortical and corticothalamic axon pathfinding defects observed in the *Pdn/Pdn* mutants (see Fig 6.1). I will describe how patterning defects in the *Pdn/Pdn* ventral telencephalon may cause defects in the formation of intermediate guidance cues and lead to abnormal axonal

connections between the *Pdn/Pdn* cortex and thalamus. This model is not definitive and some aspects of it need to be further investigated as discussed in the previous section. Nevertheless, the aim of this model is to provide a general picture of the *Pdn* axonal phenotype, unifying the different findings on the defects in ventral telencephalic patterning and in the development of the thalamocortical and corticothalamic tracts.

The earliest alteration I observed in *Pdn* mutants was the upregulation of *Shh* and Shh signalling in the ventral telencephalon, at E10.5 and E12.5. This causes patterning defects in the *Pdn/Pdn* ventral telencephalon and in the region immediately dorsal to it, the ventral pallium. These patterning defects include regionalization defects, such as partial ventralization of the *Pdn/Pdn* CGE and a dorsal shift and expansion of the *Pdn/Pdn* PSPB region. In addition, the proliferating cells in the *Pdn/Pdn* LGE ventricular zone display an increase in cell cycle time, which causes a reduced production of neurons. Regionalization and growth defects contribute to the failure of *Pdn/Pdn* LGE pioneer neurons to form and/or project axons normally at E12.5 and to subsequently guide *Pdn/Pdn* corticothalamic axons into the ventral telencephalon. The absence of cortical axons in the ventral telencephalon and/or the dorsal shift of the PSPB may also cause a delay in the entry of incoming thalamic axons into the cortex. However, *Pdn/Pdn* thalamic axons also make guidance mistakes before their interaction with *Pdn/Pdn* corticothalamic axons. This defect is probably due to abnormalities in the arrangement of the *Pdn/Pdn* “corridor cells” and/or the *Pdn/Pdn* MGE mantle region has lost its repulsive effects on thalamic axons. Despite several abnormal routes, some of *Pdn/Pdn* thalamic axons eventually reach the *Pdn/Pdn* cortex. Similar to this partial recovery of the *Pdn/Pdn* thalamocotical tract at P0, cortical axons eventually project in

the direction of the thalamus. Interestingly, these axons take reciprocal routes as thalamocortical axons, enphasizing a close interaction and reciprocal guidance between thalamic axons and coticofucal axons.

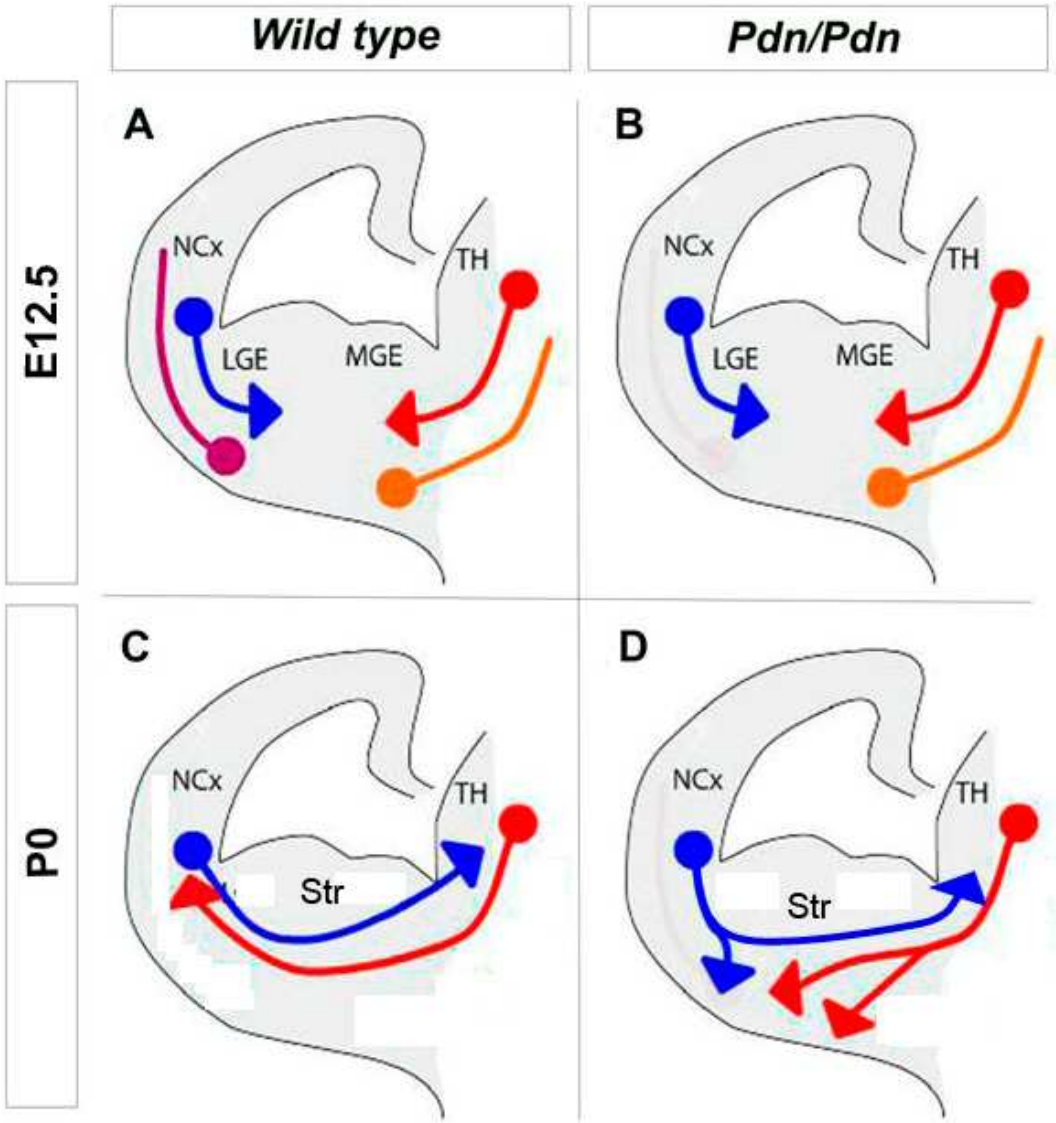

**Figure 6.1.**
**Diagram explaining the axonal phenotype observed in *Pdn/Pdn* mutants.**

The failure of *Pdn/Pdn* LGE pioneer neurons to form normally at E12.5 result in a failure of *Pdn/Pdn* corticothalamic axons to enter the ventral telencephalon. The absence of cortical axons in the ventral telencephalon may also cause a delay in the entry of incoming thalamic axons into the cortex (compare A with B).

*Pdn/Pdn* thalamic axons also make guidance mistakes before their interaction with *Pdn/Pdn* corticothalamic axons (compare C with D, more ventro-medial branch) projecting ventrally in a complete opposite direction to their normal route. However, later arriving thalmic axons take reciprocal routes as cortical axons (compare C with D, more dorso-lateral branch), enphasizing a close interaction and reciprocal guidance between thalamic axons and coticofucal axons.

# Bibliography


Alcamo, E. A., Chirivella, L., Dautzenberg, M., Dobreva, G., Farinas, I., Grosschedl, R., and McConnell, S. K. (2008). Satb2 regulates callosal projection neuron identity in the developing cerebral cortex. *Neuron* **57,** 364-77.

Alcantara, S., Pozas, E., Ibanez, C. F., and Soriano, E. (2006). BDNF-modulated spatial organization of Cajal-Retzius and GABAergic neurons in the marginal zone plays a role in the development of cortical organization. *Cereb Cortex* **16,** 487-99.

Anderson, S. A., Marin, O., Horn, C., Jennings, K., and Rubenstein, J. L. (2001). Distinct cortical migrations from the medial and lateral ganglionic eminences. *Development* **128,** 353-63.

Aoto, K., Nishimura, T., Eto, K., and Motoyama, J. (2002). Mouse GLI3 regulates Fgf8 expression and apoptosis in the developing neural tube, face, and limb bud. *Dev Biol* **251,** 320-32.

Assimacopoulos, S., Grove, E. A., and Ragsdale, C. W. (2003). Identification of a Pax6-dependent epidermal growth factor family signaling source at the lateral edge of the embryonic cerebral cortex. *J Neurosci* **23,** 6399-403.

Aza-Blanc, P., Lin, H. Y., Ruiz i Altaba, A., and Kornberg, T. B. (2000). Expression of the vertebrate Gli proteins in Drosophila reveals a distribution of activator and repressor activities. *Development* **127,** 4293-301.

Babcock, D. S. (1984). The normal, absent, and abnormal corpus callosum: sonographic findings. *Radiology* **151,** 449-53.

Bachy, I., Failli, V., and Retaux, S. (2002). A LIM-homeodomain code for development and evolution of forebrain connectivity. *Neuroreport* **13,** A23-7.

Bagnard, D., Lohrum, M., Uziel, D., Puschel, A. W., and Bolz, J. (1998). Semaphorins act as attractive and repulsive guidance signals during the development of cortical projections. *Development* **125,** 5043-53.

Bagri, A., Marin, O., Plump, A. S., Mak, J., Pleasure, S. J., Rubenstein, J. L., and Tessier-Lavigne, M. (2002). Slit proteins prevent midline crossing and determine the dorsoventral position of major axonal pathways in the mammalian forebrain. *Neuron* **33,** 233-48.

Bai, C. B., Stephen, D., and Joyner, A. L. (2004). All mouse ventral spinal cord patterning by hedgehog is Gli dependent and involves an activator function of Gli3. *Dev Cell* **6,** 103-15.

Bayer, S. A., Altman, J., Russo, R. J., Dai, X. F., and Simmons, J. A. (1991). Cell migration in the rat embryonic neocortex. *J Comp Neurol* **307,** 499-516.

Biesecker, L. G. (2006). What you can learn from one gene: GLI3. *J Med Genet* **43,** 465-9.

Biesecker, L. G., and Johnston, J. (2005). Syndromic and non-syndromic GLI3 phenotypes. *Clin Genet* **68,** 284; author reply 285.

Bisgrove, B. W., and Yost, H. J. (2006). The roles of cilia in developmental disorders and disease. *Development* **133,** 4131-43.

Bishop, K. M., Garel, S., Nakagawa, Y., Rubenstein, J. L., and O'Leary, D. D. (2003). Emx1 and Emx2 cooperate to regulate cortical size, lamination, neuronal differentiation, development of cortical efferents, and thalamocortical pathfinding. *J Comp Neurol* **457,** 345-60.

Bishop, K. M., Goudreau, G., and O'Leary, D. D. (2000). Regulation of area identity in the mammalian neocortex by Emx2 and Pax6. *Science* **288,** 344-9.

Blaess, S., Corrales, J. D., and Joyner, A. L. (2006). Sonic hedgehog regulates Gli activator and repressor functions with spatial and temporal precision in the mid/hindbrain region. *Development* **133,** 1799-809.

Blakemore, C., and Molnar, Z. (1990). Factors involved in the establishment of specific interconnections between thalamus and cerebral cortex. *Cold Spring Harb Symp Quant Biol* **55,** 491-504.

Bolz, J., Uziel, D., Muhlfriedel, S., Gullmar, A., Peuckert, C., Zarbalis, K., Wurst, W., Torii, M., and Levitt, P. (2004). Multiple roles of ephrins during the formation of thalamocortical projections: maps and more. *J Neurobiol* **59,** 82-94.

Bonatz, E., Descartes, M., and Tamarapalli, J. R. (1997). Acrocallosal syndrome: a case report. *J Hand Surg [Am]* **22,** 492-4.

Bose, J., Grotewold, L., and Ruther, U. (2002). Pallister-Hall syndrome phenotype in mice mutant for Gli3. *Hum Mol Genet* **11,** 1129-35.

Braisted, J. E., Catalano, S. M., Stimac, R., Kennedy, T. E., Tessier-Lavigne, M., Shatz, C. J., and O'Leary, D. D. (2000). Netrin-1 promotes thalamic axon growth and is required for proper development of the thalamocortical projection. *J Neurosci* **20,** 5792-801.

Briscoe, J., and Ericson, J. (1999). The specification of neuronal identity by graded Sonic Hedgehog signalling. *Semin Cell Dev Biol* **10,** 353-62.

Bulfone, A., Puelles, L., Porteus, M. H., Frohman, M. A., Martin, G. R., and Rubenstein, J. L. (1993). Spatially restricted expression of Dlx-1, Dlx-2 (Tes-1), Gbx-2, and Wnt-3 in the embryonic day 12.5 mouse forebrain defines potential transverse and longitudinal segmental boundaries. *J Neurosci* **13,** 3155-72.

Bumcrot, D. A., Takada, R., and McMahon, A. P. (1995). Proteolytic processing yields two secreted forms of sonic hedgehog. *Mol Cell Biol* **15,** 2294-303.

Butts, S. C., Liu, W., Li, G., and Frenz, D. A. (2005). Transforming growth factor-beta1 signaling participates in the physiological and pathological regulation of mouse inner ear development by all-trans retinoic acid. *Birth Defects Res A Clin Mol Teratol* **73,** 218-28.

Cang, J., Kaneko, M., Yamada, J., Woods, G., Stryker, M. P., and Feldheim, D. A. (2005). Ephrin-as guide the formation of functional maps in the visual cortex. *Neuron* **48,** 577-89.

Carney, R. S., Alfonso, T. B., Cohen, D., Dai, H., Nery, S., Stoica, B., Slotkin, J., Bregman, B. S., Fishell, G., and Corbin, J. G. (2006). Cell migration along the lateral cortical stream to the developing basal telencephalic limbic system. *J Neurosci* **26,** 11562-74.

Caspary, T., Larkins, C. E., and Anderson, K. V. (2007). The graded response to Sonic Hedgehog depends on cilia architecture. *Dev Cell* **12,** 767-78.

Chen, L., Guo, Q., and Li, J. Y. (2009). Transcription factor Gbx2 acts cell-nonautonomously to regulate the formation of lineage-restriction boundaries of the thalamus. *Development* **136,** 1317-26.

Cheng, B., Dong, Y., He, L., Tang, W., Yu, H., Lu, J., Xu, L., Zheng, B., Li, K., and Xiao, C. (2006). Crossed polydactyly type I caused by a point mutation in the GLI3 gene in a large Chinese pedigree. *J Clin Lab Anal* **20,** 133-8.

Chiang, C., Litingtung, Y., Lee, E., Young, K. E., Corden, J. L., Westphal, H., and Beachy, P. A. (1996). Cyclopia and defective axial patterning in mice lacking Sonic hedgehog gene function. *Nature* **383,** 407-13.

Corbin, J. G., Gaiano, N., Machold, R. P., Langston, A., and Fishell, G. (2000). The Gsh2 homeodomain gene controls multiple aspects of telencephalic development. *Development* **127,** 5007-20.

Corbin, J. G., Nery, S., and Fishell, G. (2001). Telencephalic cells take a tangent: non-radial migration in the mammalian forebrain. *Nat Neurosci* **4 Suppl,** 1177-82.

Corbin, J. G., Rutlin, M., Gaiano, N., and Fishell, G. (2003). Combinatorial function of the homeodomain proteins Nkx2.1 and Gsh2 in ventral telencephalic patterning. *Development* **130,** 4895-906.

Curran, T., and D'Arcangelo, G. (1998). Role of reelin in the control of brain development. *Brain Res Brain Res Rev* **26,** 285-94.

D'Arcangelo, G., Miao, G. G., Chen, S. C., Soares, H. D., Morgan, J. I., and Curran, T. (1995). A protein related to extracellular matrix proteins deleted in the mouse mutant reeler. *Nature* **374,** 719-23.

De Carlos, J. A., and O'Leary, D. D. (1992). Growth and targeting of subplate axons and establishment of major cortical pathways. *J Neurosci* **12,** 1194-211.

Ding, Q., Motoyama, J., Gasca, S., Mo, R., Sasaki, H., Rossant, J., and Hui, C. C. (1998). Diminished Sonic hedgehog signaling and lack of floor plate differentiation in Gli2 mutant mice. *Development* **125,** 2533-43.

Dou, C. L., Li, S., and Lai, E. (1999). Dual role of brain factor-1 in regulating growth and patterning of the cerebral hemispheres. *Cereb Cortex* **9,** 543-50.

Echelard, Y., Epstein, D. J., St-Jacques, B., Shen, L., Mohler, J., McMahon, J. A., and McMahon, A. P. (1993). Sonic hedgehog, a member of a family of putative signaling molecules, is implicated in the regulation of CNS polarity. *Cell* **75,** 1417-30.

Elson, E., Perveen, R., Donnai, D., Wall, S., and Black, G. C. (2002). De novo GLI3 mutation in acrocallosal syndrome: broadening the phenotypic spectrum of GLI3 defects and overlap with murine models. *J Med Genet* **39,** 804-6.

Ericson, J., Muhr, J., Placzek, M., Lints, T., Jessell, T. M., and Edlund, T. (1995). Sonic hedgehog induces the differentiation of ventral forebrain neurons: a common signal for ventral patterning within the neural tube. *Cell* **81,** 747-56.

Fernandes, M., Gutin, G., Alcorn, H., McConnell, S. K., and Hebert, J. M. (2007). Mutations in the BMP pathway in mice support the existence of two molecular classes of holoprosencephaly. *Development* **134,** 3789-94.

Flames, N., Pla, R., Gelman, D. M., Rubenstein, J. L., Puelles, L., and Marin, O. (2007). Delineation of multiple subpallial progenitor domains by the combinatorial expression of transcriptional codes. *J Neurosci* **27,** 9682-95.

Fogarty, M., Richardson, W. D., and Kessaris, N. (2005). A subset of oligodendrocytes generated from radial glia in the dorsal spinal cord. *Development* **132,** 1951-9.

Fotaki, V., Yu, T., Zaki, P. A., Mason, J. O., and Price, D. J. (2006). Abnormal positioning of diencephalic cell types in neocortical tissue in the dorsal telencephalon of mice lacking functional Gli3. *J Neurosci* **26,** 9282-92.

Friedrichs, M., Larralde, O., Skutella, T., and Theil, T. (2008). Lamination of the cerebral cortex is disturbed in Gli3 mutant mice. *Dev Biol* **318,** 203-14.

Fuccillo, M., Joyner, A. L., and Fishell, G. (2006a). Morphogen to mitogen: the multiple roles of hedgehog signalling in vertebrate neural development. *Nat Rev Neurosci* **7,** 772-83.

Fuccillo, M., Rallu, M., McMahon, A. P., and Fishell, G. (2004). Temporal requirement for hedgehog signaling in ventral telencephalic patterning. *Development* **131,** 5031-40.

Fuccillo, M., Rutlin, M., and Fishell, G. (2006b). Removal of Pax6 partially rescues the loss of ventral structures in Shh null mice. *Cereb Cortex* **16 Suppl 1,** i96-102.

Fukuchi-Shimogori, T., and Grove, E. A. (2001a). Neocortex patterning by the secreted signaling molecule FGF8. *Science* **294,** 1071-4.

Fukuchi-Shimogori, T., and Grove, E. A. (2001b). Neocortex patterning by the secreted signaling molecule FGF8. *Science* **294,** 1071-4.

Fukuchi-Shimogori, T., and Grove, E. A. (2003). Emx2 patterns the neocortex by regulating FGF positional signaling. *Nat Neurosci* **6,** 825-31.

Furuta, Y., Piston, D. W., and Hogan, B. L. (1997). Bone morphogenetic proteins (BMPs) as regulators of dorsal forebrain development. *Development* **124,** 2203-12.

Gal, J. S., Morozov, Y. M., Ayoub, A. E., Chatterjee, M., Rakic, P., and Haydar, T. F. (2006). Molecular and morphological heterogeneity of neural precursors in the mouse neocortical proliferative zones. *J Neurosci* **26,** 1045-56.

Garel, S., Huffman, K. J., and Rubenstein, J. L. (2003). Molecular regionalization of the neocortex is disrupted in Fgf8 hypomorphic mutants. *Development* **130,** 1903-14.

Garel, S., and Rubenstein, J. L. (2004). Intermediate targets in formation of topographic projections: inputs from the thalamocortical system. *Trends Neurosci* **27,** 533-9.

Garel, S., Yun, K., Grosschedl, R., and Rubenstein, J. L. (2002). The early topography of thalamocortical projections is shifted in Ebf1 and Dlx1/2 mutant mice. *Development* **129,** 5621-34.

Ghosh, A., Antonini, A., McConnell, S. K., and Shatz, C. J. (1990). Requirement for subplate neurons in the formation of thalamocortical connections. *Nature* **347,** 179-81.

Ghosh, A., and Shatz, C. J. (1993). A role for subplate neurons in the patterning of connections from thalamus to neocortex. *Development* **117,** 1031-47.

Gonchar, Y., and Burkhalter, A. (1997). Three distinct families of GABAergic neurons in rat visual cortex. *Cereb Cortex* **7,** 347-58.

Goodrich, L. V., Johnson, R. L., Milenkovic, L., McMahon, J. A., and Scott, M. P. (1996). Conservation of the hedgehog/patched signaling pathway from flies to mice: induction of a mouse patched gene by Hedgehog. *Genes Dev* **10,** 301-12.

Goodrich, L. V., Milenkovic, L., Higgins, K. M., and Scott, M. P. (1997). Altered neural cell fates and medulloblastoma in mouse patched mutants. *Science* **277,** 1109-13.

Gotz, M., and Huttner, W. B. (2005). The cell biology of neurogenesis. *Nat Rev Mol Cell Biol* **6,** 777-88.

Gradwohl, G., Fode, C., and Guillemot, F. (1996). Restricted expression of a novel murine atonal-related bHLH protein in undifferentiated neural precursors. *Dev Biol* **180,** 227-41.

Grove, E. A., Tole, S., Limon, J., Yip, L., and Ragsdale, C. W. (1998). The hem of the embryonic cerebral cortex is defined by the expression of multiple Wnt genes and is compromised in Gli3-deficient mice. *Development* **125,** 2315-25.

Gutin, G., Fernandes, M., Palazzolo, L., Paek, H., Yu, K., Ornitz, D. M., McConnell, S. K., and Hebert, J. M. (2006). FGF signalling generates ventral telencephalic cells independently of SHH. *Development* **133,** 2937-46.

Hamasaki, T., Leingartner, A., Ringstedt, T., and O'Leary, D. D. (2004). EMX2 regulates sizes and positioning of the primary sensory and motor areas in neocortex by direct specification of cortical progenitors. *Neuron* **43,** 359-72.

Hammerschmidt, M., Brook, A., and McMahon, A. P. (1997). The world according to hedgehog. *Trends Genet* **13,** 14-21.

Han, Y. G., Spassky, N., Romaguera-Ros, M., Garcia-Verdugo, J. M., Aguilar, A., Schneider-Maunoury, S., and Alvarez-Buylla, A. (2008). Hedgehog signaling and primary cilia are required for the formation of adult neural stem cells. *Nat Neurosci* **11,** 277-84.

Hanashima, C., Fernandes, M., Hebert, J. M., and Fishell, G. (2007). The role of Foxg1 and dorsal midline signaling in the generation of Cajal-Retzius subtypes. *J Neurosci* **27,** 11103-11.

Hartfuss, E., Galli, R., Heins, N., and Gotz, M. (2001). Characterization of CNS precursor subtypes and radial glia. *Dev Biol* **229,** 15-30.

Hayasaka, I., Nakatsuka, T., Fujii, T., Naruse, I., and Oda, S. (1980). Polydactyly Nagoya, Pdn: A new mutant gene in the mouse. *Jikken Dobutsu* **29,** 391-5.

Hebert, J. M., Mishina, Y., and McConnell, S. K. (2002). BMP signaling is required locally to pattern the dorsal telencephalic midline. *Neuron* **35,** 1029-41.

Hevner, R. F., Miyashita-Lin, E., and Rubenstein, J. L. (2002). Cortical and thalamic axon pathfinding defects in Tbr1, Gbx2, and Pax6 mutant mice: evidence that cortical and thalamic axons interact and guide each other. *J Comp Neurol* **447,** 8-17.

Hevner, R. F., Neogi, T., Englund, C., Daza, R. A., and Fink, A. (2003). Cajal-Retzius cells in the mouse: transcription factors, neurotransmitters, and birthdays suggest a pallial origin. *Brain Res Dev Brain Res* **141,** 39-53.

Hill, R. E., Jones, P. F., Rees, A. R., Sime, C. M., Justice, M. J., Copeland, N. G., Jenkins, N. A., Graham, E., and Davidson, D. R. (1989). A new family of mouse homeo box-containing genes: molecular structure, chromosomal location, and developmental expression of Hox-7.1. *Genes Dev* **3,** 26-37.

Hooper, J. E., and Scott, M. P. (2005). Communicating with Hedgehogs. *Nat Rev Mol Cell Biol* **6,** 306-17.

Houde, C., Dickinson, R. J., Houtzager, V. M., Cullum, R., Montpetit, R., Metzler, M., Simpson, E. M., Roy, S., Hayden, M. R., Hoodless, P. A., and Nicholson, D. W. (2006). Hippi is essential for node cilia assembly and Sonic hedgehog signaling. *Dev Biol* **300,** 523-33.

Hsieh-Li, H. M., Witte, D. P., Szucsik, J. C., Weinstein, M., Li, H., and Potter, S. S. (1995). Gsh-2, a murine homeobox gene expressed in the developing brain. *Mech Dev* **50,** 177-86.

Huangfu, D., and Anderson, K. V. (2005). Cilia and Hedgehog responsiveness in the mouse. *Proc Natl Acad Sci U S A* **102,** 11325-30.

Huangfu, D., Liu, A., Rakeman, A. S., Murcia, N. S., Niswander, L., and Anderson, K. V. (2003). Hedgehog signalling in the mouse requires intraflagellar transport proteins. *Nature* **426,** 83-7.

Hui, C. C., and Joyner, A. L. (1993). A mouse model of greig cephalopolysyndactyly syndrome: the extra-toesJ mutation contains an intragenic deletion of the Gli3 gene. *Ciba Found Symp* **181,** 118-34; discussion 134-43.

Hui, C. C., Slusarski, D., Platt, K. A., Holmgren, R., and Joyner, A. L. (1994). Expression of three mouse homologs of the Drosophila segment polarity gene cubitus interruptus, Gli, Gli-2, and Gli-3, in ectoderm- and mesoderm-derived tissues suggests multiple roles during postimplantation development. *Dev Biol* **162,** 402-13.

Ingham, P. W., and McMahon, A. P. (2001). Hedgehog signaling in animal development: paradigms and principles. *Genes Dev* **15,** 3059-87.

Ishibashi, M., and McMahon, A. P. (2002). A sonic hedgehog-dependent signaling relay regulates growth of diencephalic and mesencephalic primordia in the early mouse embryo. *Development* **129,** 4807-19.

Ishibashi, M., Saitsu, H., Komada, M., and Shiota, K. (2005). Signaling cascade coordinating growth of dorsal and ventral tissues of the vertebrate brain, with special reference to the involvement of Sonic Hedgehog signaling. *Anat Sci Int* **80,** 30-6.

Jacob, J., and Briscoe, J. (2003). Gli proteins and the control of spinal-cord patterning. *EMBO Rep* **4,** 761-5.

Jacobs, E. C., Campagnoni, C., Kampf, K., Reyes, S. D., Kalra, V., Handley, V., Xie, Y. Y., Hong-Hu, Y., Spreur, V., Fisher, R. S., and Campagnoni, A. T. (2007). Visualization of corticofugal projections during early cortical development in a tau-GFP-transgenic mouse. *Eur J Neurosci* **25,** 17-30.

Johnson, D. R. (1967a). Extra-toes: a new mutant gene causing multiple abnormalities in the mouse. *J Embryol Exp Morphol* **17,** 543-81.

Johnson, D. R. (1967b). Extra-toes: anew mutant gene causing multiple abnormalities in the mouse. *J Embryol Exp Morphol* **17,** 543-81.

Johnston, J. J., Olivos-Glander, I., Turner, J., Aleck, K., Bird, L. M., Mehta, L., Schimke, R. N., Heilstedt, H., Spence, J. E., Blancato, J., and Biesecker, L. G. (2003). Clinical and molecular delineation of the Greig cephalopolysyndactyly contiguous gene deletion syndrome and its distinction from acrocallosal syndrome. *Am J Med Genet A* **123,** 236-42.

Jones, L., Lopez-Bendito, G., Gruss, P., Stoykova, A., and Molnar, Z. (2002). Pax6 is required for the normal development of the forebrain axonal connections. *Development* **129,** 5041-52.

Kang, S., Graham, J. M., Jr., Olney, A. H., and Biesecker, L. G. (1997). GLI3 frameshift mutations cause autosomal dominant Pallister-Hall syndrome. *Nat Genet* **15,** 266-8.

Kawaguchi, Y. (1997). Neostriatal cell subtypes and their functional roles. *Neurosci Res* **27,** 1-8.

Kenney, A. M., Cole, M. D., and Rowitch, D. H. (2003). Nmyc upregulation by sonic hedgehog signaling promotes proliferation in developing cerebellar granule neuron precursors. *Development* **130,** 15-28.

Kenney, A. M., and Rowitch, D. H. (2000). Sonic hedgehog promotes G(1) cyclin expression and sustained cell cycle progression in mammalian neuronal precursors. *Mol Cell Biol* **20,** 9055-67.

Kessaris, N., Fogarty, M., Iannarelli, P., Grist, M., Wegner, M., and Richardson, W. D. (2006). Competing waves of oligodendrocytes in the forebrain and postnatal elimination of an embryonic lineage. *Nat Neurosci* **9,** 173-9.

Koester, S. E., and O'Leary, D. D. (1994). Axons of early generated neurons in cingulate cortex pioneer the corpus callosum. *J Neurosci* **14,** 6608-20.

Kohtz, J. D., Baker, D. P., Corte, G., and Fishell, G. (1998). Regionalization within the mammalian telencephalon is mediated by changes in responsiveness to Sonic Hedgehog. *Development* **125,** 5079-89.

Komuta, Y., Hibi, M., Arai, T., Nakamura, S., and Kawano, H. (2007). Defects in reciprocal projections between the thalamus and cerebral cortex in the early development of Fezl-deficient mice. *J Comp Neurol* **503,** 454-65.

Kuschel, S., Rüther, U., and Theil, T. (2003). A disrupted balance between Bmp/Wnt and Fgf signaling underlies the ventralization of the Gli3 mutant telencephalon. *Developmental Biology* **260,** 484-95.

Lai, T., Jabaudon, D., Molyneaux, B. J., Azim, E., Arlotta, P., Menezes, J. R., and Macklis, J. D. (2008). SOX5 controls the sequential generation of distinct corticofugal neuron subtypes. *Neuron* **57,** 232-47.

Lakhina, V., Falnikar, A., Bhatnagar, L., and Tole, S. (2007). Early thalamocortical tract guidance and topographic sorting of thalamic projections requires LIM-homeodomain gene Lhx2. *Dev Biol* **306,** 703-13.

Lazzaro, D., Price, M., de Felice, M., and Di Lauro, R. (1991). The transcription factor TTF-1 is expressed at the onset of thyroid and lung morphogenesis and in restricted regions of the foetal brain. *Development* **113,** 1093-104.

Lee, K. J., and Jessell, T. M. (1999). The specification of dorsal cell fates in the vertebrate central nervous system. *Annu Rev Neurosci* **22,** 261-94.

Lee, S. M., Tole, S., Grove, E., and McMahon, A. P. (2000). A local Wnt-3a signal is required for development of the mammalian hippocampus. *Development* **127,** 457-67.

Leighton, P. A., Mitchell, K. J., Goodrich, L. V., Lu, X., Pinson, K., Scherz, P., Skarnes, W. C., and Tessier-Lavigne, M. (2001). Defining brain wiring patterns and mechanisms through gene trapping in mice. *Nature* **410,** 174-9.

Li, H., Zeitler, P. S., Valerius, M. T., Small, K., and Potter, S. S. (1996). Gsh-1, an orphan Hox gene, is required for normal pituitary development. *Embo J* **15,** 714-24.

Litingtung, Y., and Chiang, C. (2000a). Control of Shh activity and signaling in the neural tube. *Dev Dyn* **219,** 143-54.

Litingtung, Y., and Chiang, C. (2000b). Specification of ventral neuron types is mediated by an antagonistic interaction between Shh and Gli3. *Nat Neurosci* **3,** 979-85.

Litingtung, Y., Dahn, R. D., Li, Y., Fallon, J. F., and Chiang, C. (2002). Shh and Gli3 are dispensable for limb skeleton formation but regulate digit number and identity. *Nature* **418,** 979-83.

Little, G. E., Lopez-Bendito, G., Runker, A. E., Garcia, N., Pinon, M. C., Chedotal, A., Molnar, Z., and Mitchell, K. J. (2009). Specificity and plasticity of thalamocortical connections in Sema6A mutant mice. *PLoS Biol* **7,** e98.

Liu, A., Wang, B., and Niswander, L. A. (2005). Mouse intraflagellar transport proteins regulate both the activator and repressor functions of Gli transcription factors. *Development* **132,** 3103-11.

Lopez-Bendito, G., Cautinat, A., Sanchez, J. A., Bielle, F., Flames, N., Garratt, A. N., Talmage, D. A., Role, L. W., Charnay, P., Marin, O., and Garel, S. (2006). Tangential neuronal migration controls axon guidance: a role for neuregulin-1 in thalamocortical axon navigation. *Cell* **125,** 127-42.

Lopez-Bendito, G., Chan, C. H., Mallamaci, A., Parnavelas, J., and Molnar, Z. (2002). Role of Emx2 in the development of the reciprocal connectivity between cortex and thalamus. *J Comp Neurol* **451,** 153-69.

Lopez-Bendito, G., Flames, N., Ma, L., Fouquet, C., Di Meglio, T., Chedotal, A., Tessier-Lavigne, M., and Marin, O. (2007). Robo1 and Robo2 cooperate to control the guidance of major axonal tracts in the mammalian forebrain. *J Neurosci* **27,** 3395-407.

Lopez-Bendito, G., and Molnar, Z. (2003). Thalamocortical development: how are we going to get there? *Nat Rev Neurosci* **4,** 276-89.

Lopez-Bendito, G., Shigemoto, R., Kulik, A., Vida, I., Fairen, A., and Lujan, R. (2004a). Distribution of metabotropic GABA receptor subunits GABAB1a/b and GABAB2 in the rat hippocampus during prenatal and postnatal development. *Hippocampus* **14,** 836-48.

Lopez-Bendito, G., Sturgess, K., Erdelyi, F., Szabo, G., Molnar, Z., and Paulsen, O. (2004b). Preferential origin and layer destination of GAD65-GFP cortical interneurons. *Cereb Cortex* **14,** 1122-33.

Machold, R., Hayashi, S., Rutlin, M., Muzumdar, M. D., Nery, S., Corbin, J. G., Gritli-Linde, A., Dellovade, T., Porter, J. A., Rubin, L. L., Dudek, H., McMahon, A. P., and Fishell, G. (2003). Sonic hedgehog is required for progenitor cell maintenance in telencephalic stem cell niches. *Neuron* **39,** 937-50.

Machon, O., Backman, M., Machonova, O., Kozmik, Z., Vacik, T., Andersen, L., and Krauss, S. (2007). A dynamic gradient of Wnt signaling controls initiation of neurogenesis in the mammalian cortex and cellular specification in the hippocampus. *Dev Biol* **311,** 223-37.

MacKay, G. E., Keighren, M. A., Wilson, L., Pratt, T., Flockhart, J. H., Mason, J. O., Price, D. J., and West, J. D. (2005). Evaluation of the mouse TgTP6.3 tauGFP transgene as a lineage marker in chimeras. *J Anat* **206,** 79-92.

Malatesta, P., Hack, M. A., Hartfuss, E., Kettenmann, H., Klinkert, W., Kirchhoff, F., and Gotz, M. (2003). Neuronal or glial progeny: regional differences in radial glia fate. *Neuron* **37,** 751-64.

Mallamaci, A., Muzio, L., Chan, C. H., Parnavelas, J., and Boncinelli, E. (2000). Area identity shifts in the early cerebral cortex of Emx2-/- mutant mice. *Nat Neurosci* **3,** 679-86.

Mangale, V. S., Hirokawa, K. E., Satyaki, P. R., Gokulchandran, N., Chikbire, S., Subramanian, L., Shetty, A. S., Martynoga, B., Paul, J., Mai, M. V., Li, Y., Flanagan, L. A., Tole, S., and Monuki, E. S. (2008). Lhx2 selector activity specifies cortical identity and suppresses hippocampal organizer fate. *Science* **319,** 304-9.

Marigo, V., Johnson, R. L., Vortkamp, A., and Tabin, C. J. (1996). Sonic hedgehog differentially regulates expression of GLI and GLI3 during limb development. *Dev Biol* **180,** 273-83.

Marin, O., and Rubenstein, J. L. (2001). A long, remarkable journey: tangential migration in the telencephalon. *Nat Rev Neurosci* **2,** 780-90.

Martynoga, B., Morrison, H., Price, D. J., and Mason, J. O. (2005). Foxg1 is required for specification of ventral telencephalon and region-specific regulation of dorsal telencephalic precursor proliferation and apoptosis. *Dev Biol* **283,** 113-27.

Matise, M. P., Epstein, D. J., Park, H. L., Platt, K. A., and Joyner, A. L. (1998). Gli2 is required for induction of floor plate and adjacent cells, but not most ventral neurons in the mouse central nervous system. *Development* **125,** 2759-70.

May, S. R., Ashique, A. M., Karlen, M., Wang, B., Shen, Y., Zarbalis, K., Reiter, J., Ericson, J., and Peterson, A. S. (2005). Loss of the retrograde motor for IFT disrupts localization of Smo to cilia and prevents the expression of both activator and repressor functions of Gli. *Dev Biol* **287,** 378-89.

Maynard, T. M., Jain, M. D., Balmer, C. W., and LaMantia, A. S. (2002). High-resolution mapping of the Gli3 mutation extra-toes reveals a 51.5-kb deletion. *Mamm Genome* **13,** 58-61.

McCann, E., Fryer, A. E., Craigie, R., Baillie, C., Ba'ath, M. E., Selby, A., and Biesecker, L. G. (2006). Genitourinary malformations as a feature of the Pallister-Hall syndrome. *Clin Dysmorphol* **15,** 75-79.

McConnell, S. K., Ghosh, A., and Shatz, C. J. (1989). Subplate neurons pioneer the first axon pathway from the cerebral cortex. *Science* **245,** 978-82.

McConnell, S. K., Ghosh, A., and Shatz, C. J. (1994). Subplate pioneers and the formation of descending connections from cerebral cortex. *J Neurosci* **14,** 1892-907.

Metin, C., Deleglise, D., Serafini, T., Kennedy, T. E., and Tessier-Lavigne, M. (1997). A role for netrin-1 in the guidance of cortical efferents. *Development* **124,** 5063-74.

Metin, C., and Godement, P. (1996). The ganglionic eminence may be an intermediate target for corticofugal and thalamocortical axons. *J Neurosci* **16,** 3219-35.

Meyer, G., Perez-Garcia, C. G., Abraham, H., and Caput, D. (2002). Expression of p73 and Reelin in the developing human cortex. *J Neurosci* **22,** 4973-86.

Miyashita-Lin, E. M., Hevner, R., Wassarman, K. M., Martinez, S., and Rubenstein, J. L. (1999). Early neocortical regionalization in the absence of thalamic innervation. *Science* **285,** 906-9.

Mo, Z., Moore, A. R., Filipovic, R., Ogawa, Y., Kazuhiro, I., Antic, S. D., and Zecevic, N. (2007). Human cortical neurons originate from radial glia and neuron-restricted progenitors. *J Neurosci* **27,** 4132-45.

Molnar, Z., Adams, R., and Blakemore, C. (1998). Mechanisms underlying the early establishment of thalamocortical connections in the rat. *J Neurosci* **18,** 5723-45.

Molnar, Z., and Blakemore, C. (1995). How do thalamic axons find their way to the cortex? *Trends Neurosci* **18,** 389-97.

Molnar, Z., and Butler, A. B. (2002). The corticostriatal junction: a crucial region for forebrain development and evolution. *Bioessays* **24,** 530-41.

Molyneaux, B. J., Arlotta, P., Menezes, J. R., and Macklis, J. D. (2007). Neuronal subtype specification in the cerebral cortex. *Nat Rev Neurosci* **8,** 427-37.

Monuki, E. S., Porter, F. D., and Walsh, C. A. (2001). Patterning of the dorsal telencephalon and cerebral cortex by a roof plate-Lhx2 pathway. *Neuron* **32,** 591-604.

Murcia, N. S., Richards, W. G., Yoder, B. K., Mucenski, M. L., Dunlap, J. R., and Woychik, R. P. (2000). The Oak Ridge Polycystic Kidney (orpk) disease gene is required for left-right axis determination. *Development* **127,** 2347-55.

Murone, M., Rosenthal, A., and de Sauvage, F. J. (1999). Hedgehog signal transduction: from flies to vertebrates. *Exp Cell Res* **253,** 25-33.

Muzio, L., DiBenedetto, B., Stoykova, A., Boncinelli, E., Gruss, P., and Mallamaci, A. (2002). Conversion of cerebral cortex into basal ganglia in Emx2(-/-) Pax6(Sey/Sey) double-mutant mice. *Nat Neurosci* **5,** 737-45.

Muzio, L., and Mallamaci, A. (2003). Emx1, Emx2 and Pax6 in Specification, Regionalization and Arealization of the Cerebral Cortex. *Cereb. Cortex* **13,** 641-647.

Muzio, L., and Mallamaci, A. (2005). Foxg1 confines Cajal-Retzius neuronogenesis and hippocampal morphogenesis to the dorsomedial pallium. *J Neurosci* **25,** 4435-41.

Nakagawa, Y., and O'Leary, D. D. (2001). Combinatorial expression patterns of LIM-homeodomain and other regulatory genes parcellate developing thalamus. *J Neurosci* **21,** 2711-25.

Naruse, I., Kato, K., Asano, T., Suzuki, F., and Kameyama, Y. (1990). Developmental brain abnormalities accompanied with the retarded production of S-100 beta protein in genetic polydactyly mice. *Brain Res Dev Brain Res* **51,** 253-8.

Nery, S., Fishell, G., and Corbin, J. G. (2002). The caudal ganglionic eminence is a source of distinct cortical and subcortical cell populations. *Nat Neurosci* **5,** 1279-87.

Nieto, M., Monuki, E. S., Tang, H., Imitola, J., Haubst, N., Khoury, S. J., Cunningham, J., Gotz, M., and Walsh, C. A. (2004). Expression of Cux-1 and Cux-2 in the subventricular zone and upper layers II-IV of the cerebral cortex. *J Comp Neurol* **479,** 168-80.

Nowakowski, R. S., Lewin, S. B., and Miller, M. W. (1989). Bromodeoxyuridine immunohistochemical determination of the lengths of the cell cycle and the DNA-synthetic phase for an anatomically defined population. *J Neurocytol* **18,** 311-8.

Ogawa, M., Miyata, T., Nakajima, K., Yagyu, K., Seike, M., Ikenaka, K., Yamamoto, H., and Mikoshiba, K. (1995). The reeler gene-associated antigen on Cajal-Retzius neurons is a crucial molecule for laminar organization of cortical neurons. *Neuron* **14,** 899-912.

Ohkubo, Y., Chiang, C., and Rubenstein, J. L. (2002). Coordinate regulation and synergistic actions of BMP4, SHH and FGF8 in the rostral prosencephalon regulate morphogenesis of the telencephalic and optic vesicles. *Neuroscience* **111,** 1-17.

Oliver, G., Mailhos, A., Wehr, R., Copeland, N. G., Jenkins, N. A., and Gruss, P. (1995). Six3, a murine homologue of the sine oculis gene, demarcates the most anterior border of the developing neural plate and is expressed during eye development. *Development* **121,** 4045-55.

Oliver, T. G., Grasfeder, L. L., Carroll, A. L., Kaiser, C., Gillingham, C. L., Lin, S. M., Wickramasinghe, R., Scott, M. P., and Wechsler-Reya, R. J. (2003). Transcriptional profiling of the Sonic hedgehog response: a critical role for N-myc in proliferation of neuronal precursors. *Proc Natl Acad Sci U S A* **100,** 7331-6.

Orenic, T. V., Slusarski, D. C., Kroll, K. L., and Holmgren, R. A. (1990). Cloning and characterization of the segment polarity gene cubitus interruptus Dominant of Drosophila. *Genes Dev* **4,** 1053-67.

Paek, H., Gutin, G., and Hebert, J. M. (2009). FGF signaling is strictly required to maintain early telencephalic precursor cell survival. *Development* **136,** 2457-65.

Panchision, D. M., Pickel, J. M., Studer, L., Lee, S. H., Turner, P. A., Hazel, T. G., and McKay, R. D. (2001). Sequential actions of BMP receptors control neural precursor cell production and fate. *Genes Dev* **15,** 2094-110.

Park, H. L., Bai, C., Platt, K. A., Matise, M. P., Beeghly, A., Hui, C. C., Nakashima, M., and Joyner, A. L. (2000). Mouse Gli1 mutants are viable but have defects in SHH signaling in combination with a Gli2 mutation. *Development* **127,** 1593-605.

Parr, B. A., Shea, M. J., Vassileva, G., and McMahon, A. P. (1993). Mouse Wnt genes exhibit discrete domains of expression in the early embryonic CNS and limb buds. *Development* **119,** 247-61.

Paul, L. K., Brown, W. S., Adolphs, R., Tyszka, J. M., Richards, L. J., Mukherjee, P., and Sherr, E. H. (2007). Agenesis of the corpus callosum: genetic, developmental and functional aspects of connectivity. *Nat Rev Neurosci* **8,** 287-99.

Pearse, R. V., 2nd, Vogan, K. J., and Tabin, C. J. (2001). Ptc1 and Ptc2 transcripts provide distinct readouts of Hedgehog signaling activity during chick embryogenesis. *Dev Biol* **239,** 15-29.

Persson, M., Stamataki, D., te Welscher, P., Andersson, E., Bose, J., Ruther, U., Ericson, J., and Briscoe, J. (2002). Dorsal-ventral patterning of the spinal cord requires Gli3 transcriptional repressor activity. *Genes Dev* **16,** 2865-78.

Piper, M., Plachez, C., Zalucki, O., Fothergill, T., Goudreau, G., Erzurumlu, R., Gu, C., and Richards, L. J. (2009). Neuropilin 1-Sema signaling regulates crossing of cingulate pioneering axons during development of the corpus callosum. *Cereb Cortex* **19 Suppl 1,** i11-21.

Pleasure, S. J., Anderson, S., Hevner, R., Bagri, A., Marin, O., Lowenstein, D. H., and Rubenstein, J. L. (2000). Cell migration from the ganglionic eminences is required for the development of hippocampal GABAergic interneurons. *Neuron* **28,** 727-40.

Polleux, F., Giger, R. J., Ginty, D. D., Kolodkin, A. L., and Ghosh, A. (1998). Patterning of cortical efferent projections by semaphorin-neuropilin interactions. *Science* **282,** 1904-6.

Powell, A. W., Sassa, T., Wu, Y., Tessier-Lavigne, M., and Polleux, F. (2008). Topography of thalamic projections requires attractive and repulsive functions of Netrin-1 in the ventral telencephalon. *PLoS Biol* **6,** e116.

Pratt, T., Sharp, L., Nichols, J., Price, D. J., and Mason, J. O. (2000a). Embryonic stem cells and transgenic mice ubiquitously expressing a tau-tagged green fluorescent protein. *Dev Biol* **228,** 19-28.

Pratt, T., Vitalis, T., Warren, N., Edgar, J. M., Mason, J. O., and Price, D. J. (2000b). A role for Pax6 in the normal development of dorsal thalamus and its cortical connections. *Development* **127,** 5167-78.

Price, D. J., Kennedy, H., Dehay, C., Zhou, L., Mercier, M., Jossin, Y., Goffinet, A. M., Tissir, F., Blakey, D., and Molnar, Z. (2006). The development of cortical connections. *Eur J Neurosci* **23,** 910-20.

Puelles, L., Kuwana, E., Puelles, E., Bulfone, A., Shimamura, K., Keleher, J., Smiga, S., and Rubenstein, J. L. (2000). Pallial and subpallial derivatives in the embryonic chick and mouse telencephalon, traced by the expression of the genes Dlx-2, Emx-1, Nkx-2.1, Pax-6, and Tbr-1. *J Comp Neurol* **424,** 409-38.

Quinn, J. C., Molinek, M., Mason, J. O., and Price, D. J. (2009). Gli3 is required autonomously for dorsal telencephalic cells to adopt appropriate fates during embryonic forebrain development. *Dev Biol* **327,** 204-15.

Rakic, P. (1972). Mode of cell migration to the superficial layers of fetal monkey neocortex. *J Comp Neurol* **145,** 61-83.

Rakic, P. (2003a). Developmental and evolutionary adaptations of cortical radial glia. *Cereb Cortex* **13,** 541-9.

Rakic, P. (2003b). Elusive radial glial cells: historical and evolutionary perspective. *Glia* **43,** 19-32.

Rallu, M., Machold, R., Gaiano, N., Corbin, J. G., McMahon, A. P., and Fishell, G. (2002). Dorsoventral patterning is established in the telencephalon of mutants lacking both Gli3 and Hedgehog signaling. *Development* **129,** 4963-74.

Rash, B. G., and Grove, E. A. (2007). Patterning the dorsal telencephalon: a role for sonic hedgehog? *J Neurosci* **27,** 11595-603.

Rash, B. G., and Richards, L. J. (2001). A role for cingulate pioneering axons in the development of the corpus callosum. *J Comp Neurol* **434,** 147-57.

Richards, L. J. (2002). Axonal pathfinding mechanisms at the cortical midline and in the development of the corpus callosum. *Braz J Med Biol Res* **35,** 1431-9.

Richards, L. J., Plachez, C., and Ren, T. (2004). Mechanisms regulating the development of the corpus callosum and its agenesis in mouse and human. *Clin Genet* **66,** 276-89.

Rowitch, D. H., B, S. J., Lee, S. M., Flax, J. D., Snyder, E. Y., and McMahon, A. P. (1999). Sonic hedgehog regulates proliferation and inhibits differentiation of CNS precursor cells. *J Neurosci* **19,** 8954-65.

Ruiz i Altaba, A. (1998). Combinatorial Gli gene function in floor plate and neuronal inductions by Sonic hedgehog. *Development* **125,** 2203-12.

Ruppert, J. M., Vogelstein, B., Arheden, K., and Kinzler, K. W. (1990). GLI3 encodes a 190-kilodalton protein with multiple regions of GLI similarity. *Mol Cell Biol* **10,** 5408-15.

Sakagami, K., Gan, L., and Yang, X. J. (2009). Distinct effects of Hedgehog signaling on neuronal fate specification and cell cycle progression in the embryonic mouse retina. *J Neurosci* **29,** 6932-44.

Sasaki, H., Nishizaki, Y., Hui, C., Nakafuku, M., and Kondoh, H. (1999). Regulation of Gli2 and Gli3 activities by an amino-terminal repression domain: implication of Gli2 and Gli3 as primary mediators of Shh signaling. *Development* **126,** 3915-24.

Schaeren-Wiemers, N., Andre, E., Kapfhammer, J. P., and Becker-Andre, M. (1997). The expression pattern of the orphan nuclear receptor RORbeta in the developing and adult rat nervous system suggests a role in the processing of sensory information and in circadian rhythm. *Eur J Neurosci* **9,** 2687-701.

Schimmang, T., Lemaistre, M., Vortkamp, A., and Ruther, U. (1992). Expression of the zinc finger gene Gli3 is affected in the morphogenetic mouse mutant extra-toes (Xt). *Development* **116,** 799-804.

Schimmang, T., van der Hoeven, F., and Ruther, U. (1993). Gli3 expression is affected in the morphogenetic mouse mutants add and Xt. *Prog Clin Biol Res* **383A,** 153-61.

Seibt, J., Schuurmans, C., Gradwhol, G., Dehay, C., Vanderhaeghen, P., Guillemot, F., and Polleux, F. (2003). Neurogenin2 specifies the connectivity of thalamic neurons by controlling axon responsiveness to intermediate target cues. *Neuron* **39,** 439-52.

Shimamura, K., Hartigan, D. J., Martinez, S., Puelles, L., and Rubenstein, J. L. (1995). Longitudinal organization of the anterior neural plate and neural tube. *Development* **121,** 3923-33.

Shimamura, K., Martinez, S., Puelles, L., and Rubenstein, J. L. (1997). Patterns of gene expression in the neural plate and neural tube subdivide the embryonic forebrain into transverse and longitudinal domains. *Dev Neurosci* **19,** 88-96.

Shimamura, K., and Rubenstein, J. L. (1997). Inductive interactions direct early regionalization of the mouse forebrain. *Development* **124,** 2709-18.

Shu, T., Li, Y., Keller, A., and Richards, L. J. (2003). The glial sling is a migratory population of developing neurons. *Development* **130,** 2929-37.

Shu, T., and Richards, L. J. (2001). Cortical axon guidance by the glial wedge during the development of the corpus callosum. *J Neurosci* **21,** 2749-58.

Shu, W., Jiang, Y. Q., Lu, M. M., and Morrisey, E. E. (2002). Wnt7b regulates mesenchymal proliferation and vascular development in the lung. *Development* **129,** 4831-4842.

Silver, J., Edwards, M. A., and Levitt, P. (1993). Immunocytochemical demonstration of early appearing astroglial structures that form boundaries and pathways along axon tracts in the fetal brain. *J Comp Neurol* **328,** 415-36.

Silver, J., Lorenz, S. E., Wahlsten, D., and Coughlin, J. (1982). Axonal guidance during development of the great cerebral commissures: descriptive and experimental studies, in vivo, on the role of preformed glial pathways. *J Comp Neurol* **210,** 10-29.

Simeone, A., Gulisano, M., Acampora, D., Stornaiuolo, A., Rambaldi, M., and Boncinelli, E. (1992). Two vertebrate homeobox genes related to the Drosophila empty spiracles gene are expressed in the embryonic cerebral cortex. *Embo J* **11,** 2541-50.

Simpson, T. I., Pratt, T., Mason, J. O., and Price, D. J. (2009). Normal ventral telencephalic expression of Pax6 is required for normal development of thalamocortical axons in embryonic mice. *Neural Dev* **4,** 19.

Smart, I. H. (1973). Proliferative characteristics of the ependymal layer during the early development of the mouse neocortex: a pilot study based on recording the number, location and plane of cleavage of mitotic figures. *J Anat* **116,** 67-91.

Smith, K. M., Ohkubo, Y., Maragnoli, M. E., Rasin, M. R., Schwartz, M. L., Sestan, N., and Vaccarino, F. M. (2006). Midline radial glia translocation and corpus callosum formation require FGF signaling. *Nat Neurosci* **9,** 787-97.

Srinivas, S., Watanabe, T., Lin, C. S., William, C. M., Tanabe, Y., Jessell, T. M., and Costantini, F. (2001). Cre reporter strains produced by targeted insertion of EYFP and ECFP into the ROSA26 locus. *BMC Dev Biol* **1,** 4.

Stamataki, D., Ulloa, F., Tsoni, S. V., Mynett, A., and Briscoe, J. (2005). A gradient of Gli activity mediates graded Sonic Hedgehog signaling in the neural tube. *Genes Dev* **19,** 626-41.

Stenman, J., Toresson, H., and Campbell, K. (2003a). Identification of two distinct progenitor populations in the lateral ganglionic eminence: implications for striatal and olfactory bulb neurogenesis. *J Neurosci* **23,** 167-74.

Stenman, J. M., Wang, B., and Campbell, K. (2003b). Tlx controls proliferation and patterning of lateral telencephalic progenitor domains. *J Neurosci* **23,** 10568-76.

Storm, E. E., Garel, S., Borello, U., Hebert, J. M., Martinez, S., McConnell, S. K., Martin, G. R., and Rubenstein, J. L. (2006). Dose-dependent functions of Fgf8 in regulating telencephalic patterning centers. *Development* **133,** 1831-44.

Stoykova, A., Fritsch, R., Walther, C., and Gruss, P. (1996). Forebrain patterning defects in Small eye mutant mice. *Development* **122,** 3453-65.

Stoykova, A., Gotz, M., Gruss, P., and Price, J. (1997). Pax6-dependent regulation of adhesive patterning, R-cadherin expression and boundary formation in developing forebrain. *Development* **124,** 3765-77.

Stoykova, A., Treichel, D., Hallonet, M., and Gruss, P. (2000). Pax6 modulates the dorsoventral patterning of the mammalian telencephalon. *J Neurosci* **20,** 8042-50.

Sussel, L., Marin, O., Kimura, S., and Rubenstein, J. L. (1999). Loss of Nkx2.1 homeobox gene function results in a ventral to dorsal molecular respecification within the basal telencephalon: evidence for a transformation of the pallidum into the striatum. *Development* **126,** 3359-70.

Szucsik, J. C., Witte, D. P., Li, H., Pixley, S. K., Small, K. M., and Potter, S. S. (1997). Altered forebrain and hindbrain development in mice mutant for the Gsh-2 homeobox gene. *Dev Biol* **191,** 230-42.

Taglialatela, P., Soria, J. M., Caironi, V., Moiana, A., and Bertuzzi, S. (2004). Compromised generation of GABAergic interneurons in the brains of Vax1-/- mice. *Development* **131,** 4239-4249.

Taipale, J., Cooper, M. K., Maiti, T., and Beachy, P. A. (2002). Patched acts catalytically to suppress the activity of Smoothened. *Nature* **418,** 892-7.

Takahashi, T., Nowakowski, R. S., and Caviness, V. S., Jr. (1993). Cell cycle parameters and patterns of nuclear movement in the neocortical proliferative zone of the fetal mouse. *J Neurosci* **13,** 820-33.

Tao, W., and Lai, E. (1992). Telencephalon-restricted expression of BF-1, a new member of the HNF-3/fork head gene family, in the developing rat brain. *Neuron* **8,** 957-66.

Tapia, C., Kutzner, H., Mentzel, T., Savic, S., Baumhoer, D., and Glatz, K. (2006). Two mitosis-specific antibodies, MPM-2 and phospho-histone H3 (Ser28), allow rapid and precise determination of mitotic activity. *Am J Surg Pathol* **30,** 83-9.

Tarabykin, V., Stoykova, A., Usman, N., and Gruss, P. (2001). Cortical upper layer neurons derive from the subventricular zone as indicated by Svet1 gene expression. *Development* **128,** 1983-93.

Theil, T. (2005). Gli3 is required for the specification and differentiation of preplate neurons. *Dev Biol* **286,** 559-71.

Theil, T., Alvarez-Bolado, G., Walter, A., and Ruther, U. (1999a). Gli3 is required for Emx gene expression during dorsal telencephalon development. *Development* **126,** 3561-71.

Theil, T., Alvarez-Bolado, G., Walter, A., and Rüther, U. (1999b). Gli3 is required for Emx gene expression during dorsal telencephalon development. *Development* **126,** 3561-71.

Theil, T., Aydin, S., Koch, S., Grotewold, L., and Rüther, U. (2002). Wnt and Bmp signalling cooperatively regulate graded Emx2 expression in the dorsal telencephalon. *Development* **129,** 3045-54.

Theil, T., Kaesler, S., Grotewold, L., Bose, J., and Rüther, U. (1999c). Gli genes and limb development. *Cell Tissue Res* **296,** 75-83.

Thien, H., and Rüther, U. (1999). The mouse mutation Pdn (Polydactyly Nagoya) is caused by the integration of a retrotransposon into the Gli3 gene. *Mamm Genome* **10,** 205-9.

Tissir, F., and Goffinet, A. M. (2003). Reelin and brain development. *Nat Rev Neurosci* **4,** 496-505.

Tole, S., Goudreau, G., Assimacopoulos, S., and Grove, E. A. (2000a). Emx2 is required for growth of the hippocampus but not for hippocampal field specification. *J Neurosci* **20,** 2618-25.

Tole, S., Ragsdale, C. W., and Grove, E. A. (2000b). Dorsoventral patterning of the telencephalon is disrupted in the mouse mutant extra-toes(J). *Dev Biol* **217,** 254-65.

Toresson, H., Potter, S. S., and Campbell, K. (2000a). Genetic control of dorsal-ventral identity in the telencephalon: opposing roles for Pax6 and Gsh2. *Development* **127,** 4361-71.

Toresson, H., Potter, S. S., and Campbell, K. (2000b). Genetic control of dorsal-ventral identity in the telencephalon: opposing roles for Pax6 and Gsh2. *Development* **127,** 4361-71.

Torii, M., and Levitt, P. (2005). Dissociation of corticothalamic and thalamocortical axon targeting by an EphA7-mediated mechanism. *Neuron* **48,** 563-75.

Tuttle, R., Nakagawa, Y., Johnson, J. E., and O'Leary, D. D. (1999). Defects in thalamocortical axon pathfinding correlate with altered cell domains in Mash-1-deficient mice. *Development* **126,** 1903-16.

Ueta, E., Kurome, M., Teshima, Y., Kodama, M., Otsuka, Y., and Naruse, I. (2008). Altered signaling pathway in the dysmorphogenesis of telencephalon in the Gli3 depressed mouse embryo, Pdn/Pdn. *Congenit Anom (Kyoto)* **48,** 74-80.

Valerius, M. T., Li, H., Stock, J. L., Weinstein, M., Kaur, S., Singh, G., and Potter, S. S. (1995). Gsh-1: a novel murine homeobox gene expressed in the central nervous system. *Dev Dyn* **203,** 337-51.

Vortkamp, A., Franz, T., Gessler, M., and Grzeschik, K. H. (1992). Deletion of GLI3 supports the homology of the human Greig cephalopolysyndactyly syndrome (GCPS) and the mouse mutant extra toes (Xt). *Mamm Genome* **3,** 461-3.

Vortkamp, A., Gessler, M., and Grzeschik, K. H. (1991). GLI3 zinc-finger gene interrupted by translocations in Greig syndrome families. *Nature* **352,** 539-40.

Wang, B., Fallon, J. F., and Beachy, P. A. (2000). Hedgehog-regulated processing of Gli3 produces an anterior/posterior repressor gradient in the developing vertebrate limb. *Cell* **100,** 423-34.

Wang, C., Ruther, U., and Wang, B. (2007). The Shh-independent activator function of the full-length Gli3 protein and its role in vertebrate limb digit patterning. *Dev Biol* **305,** 460-9.

Wassarman, K. M., Lewandoski, M., Campbell, K., Joyner, A. L., Rubenstein, J. L., Martinez, S., and Martin, G. R. (1997). Specification of the anterior hindbrain and establishment of a normal mid/hindbrain organizer is dependent on Gbx2 gene function. *Development* **124,** 2923-34.

Whitfield, J. F. (2004). The neuronal primary cilium--an extrasynaptic signaling device. *Cell Signal* **16,** 763-7.

Wichterle, H., Garcia-Verdugo, J. M., Herrera, D. G., and Alvarez-Buylla, A. (1999). Young neurons from medial ganglionic eminence disperse in adult and embryonic brain. *Nat Neurosci* **2,** 461-6.

Wichterle, H., Turnbull, D. H., Nery, S., Fishell, G., and Alvarez-Buylla, A. (2001). In utero fate mapping reveals distinct migratory pathways and fates of neurons born in the mammalian basal forebrain. *Development* **128,** 3759-71.

Wild, A., Kalff-Suske, M., Vortkamp, A., Bornholdt, D., Konig, R., and Grzeschik, K. H. (1997). Point mutations in human GLI3 cause Greig syndrome. *Hum Mol Genet* **6,** 1979-84.

Willaredt, M. A., Hasenpusch-Theil, K., Gardner, H. A., Kitanovic, I., Hirschfeld-Warneken, V. C., Gojak, C. P., Gorgas, K., Bradford, C. L., Spatz, J., Wolfl, S., Theil, T., and Tucker, K. L. (2008). A crucial role for primary cilia in cortical morphogenesis. *J Neurosci* **28,** 12887-900.

Xu, Q., Wonders, C. P., and Anderson, S. A. (2005). Sonic hedgehog maintains the identity of cortical interneuron progenitors in the ventral telencephalon. *Development* **132,** 4987-98.

Xuan, S., Baptista, C. A., Balas, G., Tao, W., Soares, V. C., and Lai, E. (1995). Winged helix transcription factor BF-1 is essential for the development of the cerebral hemispheres. *Neuron* **14,** 1141-52.

Yoshida, M., Assimacopoulos, S., Jones, K. R., and Grove, E. A. (2006). Massive loss of Cajal-Retzius cells does not disrupt neocortical layer order. *Development* **133,** 537-45.

Yoshida, M., Suda, Y., Matsuo, I., Miyamoto, N., Takeda, N., Kuratani, S., and Aizawa, S. (1997). Emx1 and Emx2 functions in development of dorsal telencephalon. *Development* **124,** 101-11.

Young, K. M., Fogarty, M., Kessaris, N., and Richardson, W. D. (2007). Subventricular zone stem cells are heterogeneous with respect to their embryonic origins and neurogenic fates in the adult olfactory bulb. *J Neurosci* **27,** 8286-96.

Yu, T., Fotaki, V., Mason, J. O., and Price, D. J. (2009a). Analysis of early ventral telencephalic defects in mice lacking functional Gli3 protein. *J Comp Neurol* **512,** 613-27.

Yu, W., Wang, Y., McDonnell, K., Stephen, D., and Bai, C. B. (2009b). Patterning of ventral telencephalon requires positive function of Gli transcription factors. *Dev Biol*.

Yun, K., Garel, S., Fischman, S., and Rubenstein, J. L. (2003). Patterning of the lateral ganglionic eminence by the Gsh1 and Gsh2 homeobox genes regulates striatal and olfactory bulb histogenesis and the growth of axons through the basal ganglia. *J Comp Neurol* **461,** 151-65.

Yun, K., Potter, S., and Rubenstein, J. L. (2001). Gsh2 and Pax6 play complementary roles in dorsoventral patterning of the mammalian telencephalon. *Development* **128,** 193-205.

Zaki, P. A., Quinn, J. C., and Price, D. J. (2003). Mouse models of telencephalic development. *Curr Opin Genet Dev* **13,** 423-37.

Zhang, J., Rosenthal, A., de Sauvage, F. J., and Shivdasani, R. A. (2001). Downregulation of Hedgehog signaling is required for organogenesis of the small intestine in Xenopus. *Dev Biol* **229,** 188-202.

Zimmer, C., Tiveron, M. C., Bodmer, R., and Cremer, H. (2004). Dynamics of Cux2 expression suggests that an early pool of SVZ precursors is fated to become upper cortical layer neurons. *Cereb Cortex* **14,** 1408-20.